Imperial College London

MRC Clinical Sciences Centre

A window on the ageing brain:

Imaging synapses and their dynamics *in vivo*

Federico William Grillo

Neuroplasticity and Disease group

Clinical Sciences Centre

Imperial College London

2013

Thesis submitted for the degree of Doctor of Philosophy

Declaration of originality

All performed experiments and data analysis, unless explicitly stated, were part of my own work carried out at the Clinical Sciences Centre. No part of this degree has been submitted for any other degree or qualification.

The majority of this work was published as a scientific article in the journal *Proceedings of the National Academy of Sciences of the United States of America*.

Grillo, F. W. et al. Increased axonal bouton dynamics in the aging mouse cortex. Proc Natl Acad Sci U S A, doi:10.1073/pnas.1218731110 (2013).

Copyright declaration

Age is an issue of mind over matter.

If you don't mind, it doesn't matter.

Mark Twain

Abstract

The ageing process has an enormous impact on the human body and it represents a major risk factor for a number of diseases. Ageing is also associated with a progressive cognitive decline mainly involving the memory domain. Up to date many studies have investigated the structural and functional changes that occur in the ageing brain. Rather than neuronal loss, it is now widely accepted that synaptic impairments underlie the decreased cognitive performance. Such studies point to reduced synaptic density and plasticity, in specific brain regions, during ageing. However, most studies so far made use of either post-mortem or *ex vivo* preparations. Thus, the key question addressed in this thesis is to what extent synaptic elements are dynamic in the intact aged brain. A combination of *in vivo* two-photon imaging, correlated two-photon-electron microscopy and novel computational tools was used to study synaptic boutons in the aged mouse somatosensory cortex. Unexpectedly, circuit-specific increased rates of bouton formation, elimination, and destabilization were found. Age related increased dynamics greatly affected large (i.e., strong) boutons, thought to encode long-term memory, as opposed to smaller ones. The rigorous measurement of the size and location of axonal boutons, achieved for the first time *in vivo,* showed that while the average density and size of boutons was not affected by ageing, bouton size changes were greater in the aged animals. Such increased size fluctuations were again confined to larger, persistent boutons., Long-term memory impairment, as assessed in a novel behavioural task, was therefore associated with increased, rather than decreased, synaptic destabilization and dynamics, suggesting the existence of a novel mechanism underlying age related cognitive decline.

Table of Contents

List of figures and tables

1. Introduction

Social and scientific advances in the industrialized world have greatly improved human life expectancy over the past few centuries. The gradual increase of hygienic conditions and the abundance of food supply are major contributing factors. In parallel the development of medicine and social healthcare has been crucial for tackling infant death rates as well as early and middle life diseases. On the other hand, the success of such progress has generated a larger population with a much older average age. As life expectancy keeps growing, the percentage in the total population of the elderly grows dramatically (Figure 1). This disproportion of age groups brings new challenges to society. Besides life expectancy, the active working life of individuals will need to increase to sustain the modern lifestyle and social welfare. To work longer people will have to be healthier for longer. In this sense ageing represents a major risk factor for a variety of diseases, from heart conditions, to cancer and neurodegenerative pathologies. Not only disease contrasts with a productive lifestyle – hopefully a happy one too – but it also represents a considerable cost to modern healthcare. In view of these considerations, understanding the process of ageing and the intrinsic alterations it causes in the organism becomes a key goal for the scientific community. Indeed over the past few decades research in the ageing field has grown constantly and more resources and attention are given to this crucial subject.

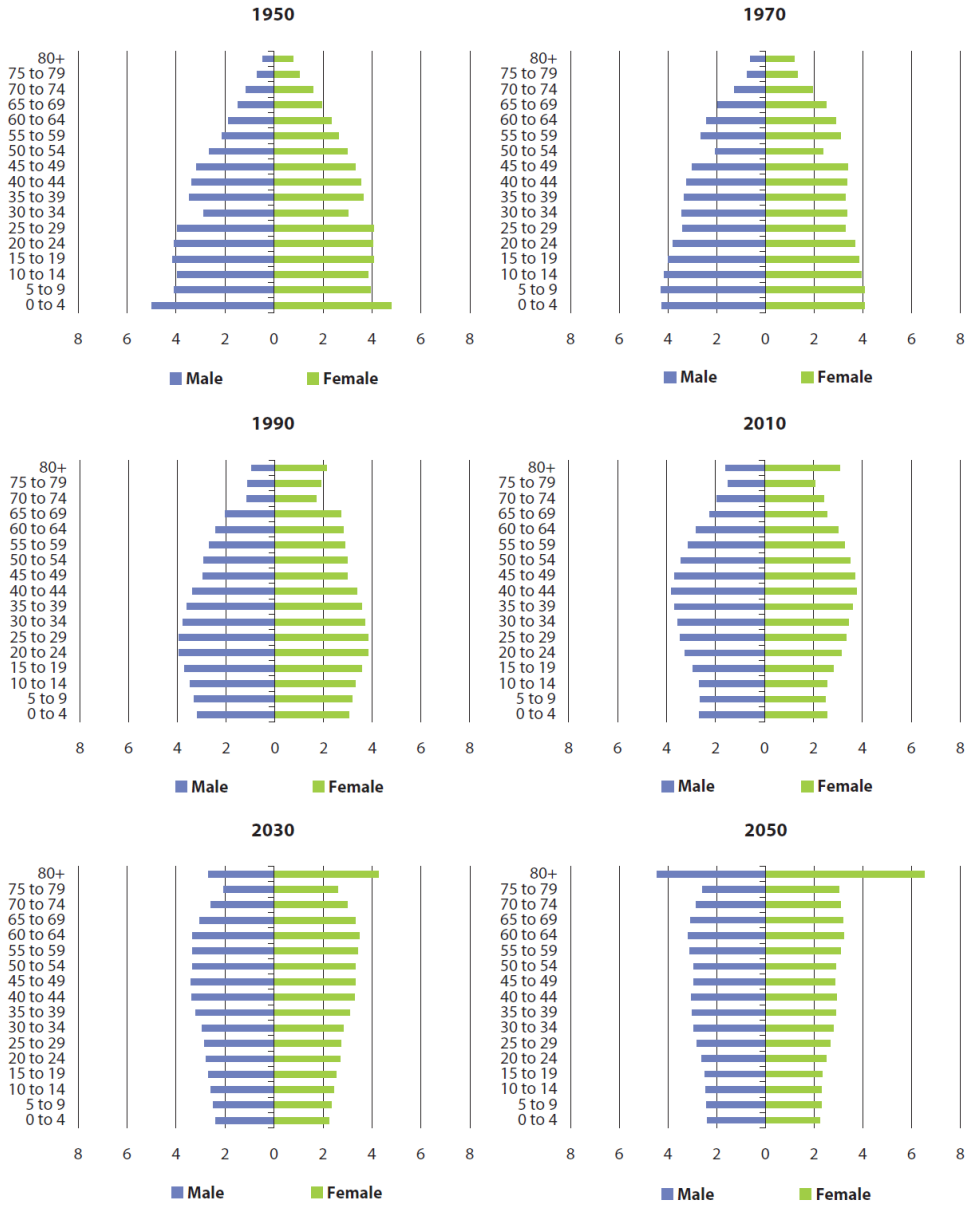

Figure 1 Age pyramids in the European Union from 1950 to future projections in 2050. In the near future the older age groups will grow considerably in proportion. The *x* axis shows age groups, the *y* axis shows the percentage relative to the total population. Source: Eurostat, EUROPE IN FIGURES – Yearbook 2009.

Ageing presents itself as a progressive deterioration of the tissues in the body affecting the structure and function of the entire organism (Kenessary et al., 2012; Yeoman et al., 2012) increasing susceptibility to disease and death (Fontana et al., 2010). Ageing is a common trait in the great majority of animals and it determines for each species the maximum lifespan, which is widely variable (Holliday, 2006), ranging from the 2 weeks of

Caenorhabditis elegans (Kenyon et al., 1993) to the over 5 centuries of *Arctica Islandica* (Ridgway et al., 2011). The variability of the speed of ageing for different species suggests that it is a process governed via genetic factors. Indeed extensive evidence has shown the involvement of specific genes in the regulation of maximum lifespan and maximum health span in worms (Kenyon et al., 1993), flies (Clancy et al., 2001; Tatar et al., 2001) and mice (Bluher et al., 2003; Holzenberger et al., 2003). Functionally, the majority of these genes are involved in nutrient sensing and metabolic regulation (Kenyon, 2005; Kenyon, 2010) and are highly conserved in humans, where they have been associated with longevity (Fontana et al., 2010). The answer to why organisms age and how ageing evolved, is still a matter of debate. Ageing might be the result of accumulative faults in mitotic and post-mitotic tissues as a result of antagonistic pleiotropy[1] (Williams, 1957; Yeoman et al., 2012). This view favours a non-programmed emergence of the ageing process arising from the fact that genes that facilitate reproduction in early life (when the selective pressure is stronger) could result in negative effects in later life (when the selective pressure is weaker). Others refer to a positive selection of longevity, where mutations that favour maintenance and tissue damage control, confer greater fitness (Kenyon, 2005; Kenyon, 2010). That ageing is caused by macromolecular damage has a wider consensus (Yeoman et al., 2012), but how this damage arises is still not clear. Multiple mechanisms of the ageing process have been described (Holliday, 2006; Yeoman et al., 2012). Oxidative stress (Harman, 1991), cell senescence, the process that limits cell division cycles, (Baker et al., 2011) and the failure to replace and repair damaged molecules, dubbed green theory, (Iqbal et al., 2009) are all proposed causes of ageing. Each one is likely to take part in the gradual loss of homeostasis that ageing involves (Kenyon, 2010).

The work presented here is a study devoted to the ageing rodent brain. In particular, attention is focused on cortical circuits and the physical contacts between neurons,

[1] A gene that affects multiple phenotypic traits is said to be pleiotropic. Antagonistic pleiotropy refers to the hypothetical existence of genes being beneficial to the individual fitness in early life (promoting reproduction) and detrimental in later life, causing senescence to be adaptive.

synapses. Before describing in detail the results section, a comprehensive overview of the current knowledge regarding the ageing brain is given in this introduction. The section describes how ageing alters cognition in humans and the most studied animal models: monkeys, rats and mice. Furthermore it looks at what structural and physiological changes are most likely causing altered cognitions. Finally, because *in vivo* imaging is central to the project described below, it presents the field of structural synaptic plasticity and its advanced techniques that allow *in vivo* imaging of synaptic structures.

1.1 The ageing brain

A familiar trait of ageing is the ensemble of age related changes that affect cognition during the life of individuals (Burke and Barnes, 2010). All adults have either direct or indirect experience of episodes of "forgetfulness" or the colloquially known "senior moments". Many of such changes are detrimental, for example 38% of subjects between 60 and 78 years old perform 1 standard deviation below young adults in a standard memory function task (Koivisto et al., 1995). Though it is also clear that ageing affects people (and animals) differently, the cognitive changes are highly variable and often aged subjects do as good or outperform their younger counterparts (Glisky, 2007; Yeoman et al., 2012). Both neural and cognitive functions are complex and could allow for compensatory action. An obvious candidate would be the role of experience and the capacity of storing and recognizing patterns. Nevertheless, the ageing process gradually decreases the power of cognitive memory domains including working, episodic, spatial and implicit memory (Yeoman et al., 2012), as well as processing speed and executive function (Hedden and Gabrieli, 2004). Associating cognitive changes with normal ageing has proven difficult especially in humans, being hard to verify the advancement of pathologies such as Alzheimer's, Parkinson's, cerebrovascular disease and also hypertension and diabetes for which ageing represents

the major risk factor (Hedden and Gabrieli, 2004). Other confounding factors, difficult to account for, are changes in mental states and practice in longitudinal studies, historical, socio-economical and educational differences in cross-sectional studies (Hedden and Gabrieli, 2004). Besides these challenges, there is wide agreement that the underlying, unavoidable, ageing process has profound effects on human (and animal) cognition (Burke and Barnes, 2006, 2010; Dickstein et al., 2007; Glisky, 2007; Grady, 2012; Hedden and Gabrieli, 2004; Morrison and Baxter, 2012).

1.2 Cognitive changes in aged humans and animal models

1.2.1 Age related cognitive decline in humans

As people age, they change both physically and psychologically. The ageing brain entails cognitive changes, some of which may be for the better. For example semantic memory, the store of general knowledge about the world, is usually extended in older people, simply because living longer allows learning more facts (Glisky, 2007; Park et al., 2002). However, many changes are less positive and affect a wide range of cognitive processes.

Attention is a basic cognitive function that can be divided in different subgroups. Many other cognitive processes rely on some form of attention; therefore declines in attention can have profound effects on different cognitive tasks (Glisky, 2007). There is evidence that divided attention is significantly impaired in older subjects. Divided attention tasks require the monitoring and processing of two or more information sources at one time. Older adults are slower and perform worse than young adults especially when the tasks get harder and more complex (Tsang and Shaner, 1998). Attention switching, the ability to prioritize alternatively different stimuli, is also impaired in the aged subjects which have a slower response in

switching from one task to another when multiple tasks are involved (Verhaeghen and Cerella, 2002). Limited and declining resources for processing information may be at the basis of deficits in attention seen in aged humans. Other forms of attention are not affected in an age related manner. Selective attention, focusing on one stimulus and disregarding the others, is preserved in older adults (Verhaeghen and Cerella, 2002). Older adults perform well also in vigilance tasks that involve sustained attention (Glisky, 2007).

Working memory is a fundamental cognitive block that can be highly affected by normal ageing (Glisky, 2007; Jagust, 2013; Morrison and Baxter, 2012). It is involved in the correct function of long-term memory, language, problem solving and decision making. Working memory is the function that allows the manipulation of the information maintained in focal attention (short-term memory). For example, short-term memory can be tested by asking subjects to keep in mind a series of numbers (e.g. a phone number). Aged adults have generally no problem remembering 7 ± 2 digits as long as the numbers are being rehearsed. Repeating the same numbers backwards requires active reorganization of the information held in short-term memory and is dependent on intact working memory. In this case aged adults have on average more difficulties than young adults (Glisky, 2007). Different theories have been proposed of how working memory is affected in the ageing brain, although neurophysiological correlates of these processes are still lacking. Attentional resources[2], limited by forms of mental energy, could be involved in working memory decline which is effectively a divided attention task, as it requires contemporary maintenance of current information and its active elaboration. Therefore deficits in divided attention could help explain working memory impairments (Craik and Byrd, 1982). The speed at which the information is processed might be the key resource affected by normal ageing (Salthouse, 1996). A large amount of evidence shows that older adults are slower than young adults in a variety of cognitive tests suggesting that a declined processing speed may account for many

[2] The expression “attentional resources” refers to the limited ability of an individual to dedicate its attention to a multiple set of stimuli. Therefore the amount of information processed is limited by the individual’s attentional resources.

age related cognitive deficits. Finally, an interesting theory involves inhibitory control. More precisely, aged subjects might fail to correctly suppress irrelevant information to the advantage of what is relevant in a specific moment. In other words they are less able to erase prior information that is no longer needed from the working memory domain therefore reducing the capacity for new stimuli to be correctly processed (May et al., 1999). Whatever the mechanism, ageing undeniably affects working memory. The resulting effects are extensive as working memory is involved in many day to day complex tasks such as decision making, planning, and goal directed behaviours (Glisky, 2007). Neuroimaging experiments have shown that the brain area that displays increased activity during working memory tasks is the prefrontal cortex (Wager and Smith, 2003).

One of the most investigated cognitive domains in the ageing context is long-term memory. Unlike short-term memory and working memory, long-term memory requires the retrieval of information that has been acquired in the past and no longer maintained in an active state. A perfectly functioning long-term memory system needs correct memory encoding, storage and retrieval. The ageing process appears to affect all three functions, leading to long-term memory decline in the elderly.

Episodic memory is a form of long-term memory that refers to the personal experience of an individual. It allows people to think back and remember past events. At the input level, the encoding stage, it might be that older adults tend to elaborate the acquired information less, so that the resulting memory trace is less distinctive and harder to retrieve (Glisky, 2007). It might also be that older individuals acquire the central core of the information but fail to add the details of the context that would normally help future retrieval. The process of elaborating and encoding information for memory storage is dependent on the prefrontal cortex, an area susceptible to age related functional decline (Glisky et al., 2001). The processes of consolidation and storage instead depend greatly on the hippocampus and the medial temporal lobe. The binding of different aspects of the experience are thought to play a major role in the consolidation of a composite memory trace. In aged individuals the binding

between the event and its temporal and spatial context may be weaker (Glisky, 2007). Problems in retrieval depend on bad encoding but could also be directly caused by ageing, especially when recollection is not helped by cues. Recognition memory on the other hand is minimally affected in aged individuals (Jennings and Jacoby, 1997). Retrieval of episodic memories and their details functionally depends on the prefrontal cortex and the hippocampus (Nolde et al., 1998). Older people generally think they have strong memories of their past, however it is likely that the general core information is preserved whilst the details, spatial and temporal context above all, are more vulnerable compared to the young adults. This makes remembering the context and the source of such memory more problematic for older adults to the point that they are not sure that an event actually took place or was imagined (Glisky, 2007). Other forms of memory are less affected by the ageing process, like semantic memory and procedural memory, the knowledge of skills such as riding a bicycle or reading (Glisky, 2007).

The executive control is a multicomponent structure encompassing different processes involved in the planning, organization, coordination, implementation and evaluation of non-routine tasks. It plays a major role in allocating attentional resources, inhibiting irrelevant information in the working memory domain, producing strategies for encoding and retrieving long-term memories and planning goal directed behaviours. It is fundamental for successful completion of novel tasks, ones for which no automatic strategy has yet been learned (Glisky, 2007). Executive function is dependent on the prefrontal cortex which in turn is anatomically affected during the ageing process (Morrison and Baxter, 2012). The involvement of the executive control in a wide variety of high cognitive functions provides an economic explanation of its causal role in ageing related cognitive decline.

The picture that emerges in human cognitive ageing is that age related cognitive changes vary greatly across individuals and cognitive domains. The two main areas on which research has focused are changes in memory and attention during ageing. Subtle age related changes in these general domains may account for large differences in the specific

tasks tested. Recently, a compensatory mechanisms of brain activity has been proposed, where older subjects tend to recruit larger brain areas compared to young adults in order to solve the same task (Grady, 2012). It is not clear if this compensation results in a more successful response or if it is detrimental to the task performance.

1.2.2 Age related cognitive decline in monkeys

The study of ageing in humans has obvious ethical and practical limitations. In most cases it is difficult to collect from human subjects behavioural, physiological and pathological data in a short period of time. Animal models have proven very valuable to overcome such limitations. Rhesus monkeys are a suited model of ageing as they have a well characterised behavioural repertoire and they do not show signs of Alzheimer's and dementia (Peters et al., 2008). Moreover, working with animals allows the experimenter to collect behavioural, physiological, anatomical and molecular data in a short time frame making use of invasive investigations (Moss et al., 2007).

Among the cognitive systems most affected and described in the ageing monkey are the executive function and different forms of memory (Morrison and Baxter, 2012). Two key components of executive control have been found to be impaired in aged monkeys: abstraction (extracting relevant information from an object) and set-shifting (ability to display flexibility in response to changing patterns of reinforcement). Aged monkeys make more perseverative errors in a task that requires identifying a specific object property (shape or colour) which changes when the previous task has been successfully completed (10 consecutive correct answers) (Moore et al., 2006). Among others two tests have typically been used to study memory in aged monkeys: the delayed non-matching to sample test (DNMS) and the delayed recognition span test (DRST). The DNMS is a recognition memory test dependent on an intact medial temporal lobe (Morrison and Baxter, 2012). The animal is first presented with a baited sample object. After a temporal delay (usually 10 seconds) the

animal is shown the sample object and a novel object, to get the reward the monkey must pick the novel object. Aged monkeys need more trials to learn the task and their performance is worse, compared to younger animals, when the delay increases (Dumitriu et al., 2010; Herndon et al., 1997). The DRST is a short-term / working memory test that requires identifying the new stimulus among a growing set of previously experienced stimuli. The task is dependent on the hippocampus and dorsolateral prefrontal cortex (*dl*PFC). The performance is measured by the average number of correct responses before the animal makes a mistake over multiple trials (i.e. 100 trials). Rhesus monkeys show an age related impairment in performing this task especially in the spatial dimension (Herndon et al., 1997). In the aged monkey, defects have mainly been highlighted in the short-term memory domain. The difference in performance with younger individuals though increases when the response delay is longer, implicating long-term memory deficits as seen in humans. This view is further strengthened by growing evidence that the acquisition phase of the DNMS is reliant on the *dl*PFC, an area associated with short-term and working memory, whilst the performance in the extended delay trials (once the task has been learned) is dependent on the medial temporal lobe, an area associated with long-term memory storage (Dumitriu et al., 2010).

1.2.3 Age related cognitive decline in rodents

Rodents are the preferred animal model in many areas of biomedical research and the ageing field is no exception. The advantages of using rats or mice are their relatively short lifespan, the wide range of behavioural assays developed to test their cognitive abilities, the anatomical homology of brain areas with those of primates, the possibility of genetic manipulation (mainly in mice) and the apparent absence of neurodegenerative phenotypes that could confound conclusions on normal ageing (Rodefer and Baxter, 2007).

Spatial memory, which is related to episodic long-term memory, has been widely studied in rodents and different tasks have been devised to test their relative cognitive abilities (Burke and Barnes, 2006). Aged rats and mice are impaired in a wide range of spatial tasks which rely on hippocampal function and integrity (Geinisman et al., 1995). Most notably memory impairments have been described in the Barnes circular maze and the Morris water maze, two behavioural tasks that avoid motivating the animals with strong aversive stimuli such as electric shocks and food deprivation which could differentially affect the aged animals. The Barnes maze consists of a circular board fully exposed to bright light, on which the animal is placed, with many holes at the periphery. Only one of the holes provides an escape to a dark box away from the direct illumination which rodents naturally tend to avoid. Using external spatial cues, young adult rats easily relocate the correct hole over different trials while aged rats perform poorly making more mistakes and retaining the memory for a shorter period (Barnes, 2011; Burke and Barnes, 2006, 2010; Markowska et al., 1989). Aged mice are also found to be impaired in the circular maze test compared to young mice (Bach et al., 1999), though the spatial memory deficit is reduced with training (Barreto et al., 2010). The Morris water maze test is a spatial memory task where rodents have to find a submerged, not visible, platform in a large deep water pool, relying on external visual cues. Finding the platform is the only way to stop swimming in deep water, it provides the motivation to perform the task. In a number of studies it has been shown that aged rats (Frick et al., 1995; Gage et al., 1984; Markowska et al., 1989; Rapp et al., 1987) and aged mice (Frick et al., 2000; Peleg et al., 2010) have impaired spatial memory, taking longer to learn the platform location, failing to accurately localise the platform in the final probe trial and performing worse in a reversal memory test when the platform is relocated.

A hippocampus dependent associative learning paradigm that has often been used to study memory formation and retention in rodents is the fear conditioning test. The animal has to associate a conditioned stimulus, classically a sound tone, to an aversive unconditioned stimulus, an electrical foot shock. Successful memory formation is measured, at different

time intervals, via the fear induced freezing response generated by the conditioned stimulus alone (Rodefer and Baxter, 2007). Aged mice (Blank et al., 2003; Peleg et al., 2010) and aged rats have impaired fear responses when the tone and the foot shock are separated a few seconds apart (trace conditioning procedure) but not when the shock immediately follows the tone (delay conditioning). Middle aged (18 months old) and aged (30 months old) rats were shown to be impaired in associating a noise (conditioned stimulus) with an electrical shock on the eye that causes a blinking response, when compared to younger rats (12 months and 3 months old groups) that learned the task (Weiss and Thompson, 1991). Mice were shown to have a similar impairment in the early sessions of conditioning where an audible tone was paired to an air puff directed to the eye (Vogel et al., 2002). In this case the older mice were able to learn the cerebellum dependent association task in later sessions. Associative memory can also be tested without a stress inducing aversive stimulus but with an appetitive reward as a motivation. Young adult rats can learn to associate a context (the testing chamber) with a specific odour in order to find the reward. The animals were tested in either of two different contexts, characterised by visual patterns and floor textures, being presented two scented containers one of which contained the reward under a layer of sand. In context 1 the food reward was in the container with odour A, whilst in context 2 the correct odour was B. Aged rats only reached 60% of correct responses while the younger group outperformed them with 80% successful responses (Luu et al., 2008). This is an interesting result given the similarity with the episodic memory of humans, for which remembering a context is required.

Behaviours that involve typically the frontal areas in humans and primates have been shown to be particularly prone to age related decline, though well-established models of such behaviours are limited in rodents (Rodefer and Baxter, 2007). To some extent behaviours relating to prefrontal cortex function have been assessed in the ageing rodent brain context. A longitudinal study, where animals had to monitor five different locations in order to receive a reward, revealed that rats suffer from an age related attention decline as early as 13-14

months of age, the difference with younger rats progresses with further ageing (Muir et al., 1999). Moreover when the attentional demand of the task was increased the performance gap was wider between aged and younger rats (Grottick and Higgins, 2002). Some studies have been able to assess the executive function deficits in aged rats using attentional set-shifting tasks that require the animal to suppress previously learned responses that no longer predict the location of the reward. For example in (Barense et al., 2002) animals were allowed to dig in only one of two pots presented to them in order to find a food reward. The discrimination the rats had to do was based on either an odour or the medium they had to dig through. If the cue to find the food reward was a new stimulus (new odour) in the same perceptual field as in previous trials (odour recognition), the attention shift was intra-dimensional. In intra-dimensional discrimination, aged rats performed as well as the young adult rats. Aged rats were significantly impaired when the shift was extra-dimensional requiring attention to a new perceptual dimension, switching from odour to digging medium or vice versa, as they displayed more perseverative errors. Interestingly, although aged animals were impaired in the spatial memory related Morris water maze, these two measures did not correlate indicating that frontal and hippocampal dysfunction might be dissociable. It appeared that in all discrimination tasks aged rats needed more trials to reach the acquisition criterion of six consecutive correct responses, for initial simple discrimination, for the intra-dimensional shift, for its reversal and the extra-dimensional shift, compared to younger adults. Though only the extra-dimensional shift reached significance, indicating that the higher degree of difficulty was acting on an underlying deficit (Barense et al., 2002; Rodefer and Nguyen, 2008). More perseverance errors by aged rats were observed in an olfactory discrimination task when the correct response is reversed, indicating that a central inhibitory function is defective (Schoenbaum et al., 2002). Visual discrimination has been used to study object recognition in rats and mice. Rodents tend to spend more time exploring a novel object rather than a familiar one, this natural behaviour has been exploited to test memory formation in a variety of experimental paradigms (Bevins and Besheer, 2006; Ennaceur and Delacour, 1988). There is evidence that aged rats have on average more

difficulties recognising the familiar object as such when tested over long retention periods (e.g. 24 hours)(Wallace et al., 2007). The recognition memory can be better consolidated in aged rats with more sampling trials (Platano et al., 2008) of the familiar object or by reducing the retention interval (Dellu et al., 1992). The deficit in long-term memory consolidation is consistent with what seen in humans. Recognition memory has also been used to test short-term memory in rats, unsurprisingly age related deficits were highlighted in this cognitive domain too (Dunnett et al., 1988). Here rats were trained to press one of two levers to receive a food reward. The test required the animals to remember for varying short delay intervals which lever was first presented in a sample trial. In the subsequent choice trial animals had to press the correct lever following either a matching to sample rule or non-matching to sample rule. In both young and aged rats the performance was dependent on the delay between sample and choice, but the performance of the aged rats was greatly reduced by increasing delays, especially in the non-matching to sample version, indicating they found it harder to retain the previously provided information.

Similarities in the effects of ageing on cognitive function can be found in the species described. In all a striking characteristic of ageing emerges: the high degree of performance variability found within aged individuals, indicating that age related cognitive decline is highly subjective. Understanding the neurophysiology behind these differences might open the way to future intervention.

1.3 Age related brain structural changes

1.3.1 Age related neuronal death

A common belief associates brain ageing with a global neuronal loss in cortical and subcortical areas. This simplistic view is the legacy of primordial stereological studies, in human and animal tissues comparing young and aged brains, which claimed a reduction of up to 60% of neocortical neurons in the human brain (Brody, 1955; Coleman and Flood, 1987) and a profound loss of neurons in the hippocampus and prefrontal cortex (PFC) of rhesus monkeys (Brizzee et al., 1980). Gradual and global neuronal loss seemed an easy and fitting explanation for gradual age related cognitive decline, given that neurons are post-mitotic cells incapable of self-renewal, unlike many other cell types. However these early results were refuted in the nineties, by the development of more rigorous stereological methods for counting nerve cells (West, 1993). A series of studies confirmed that generalized neuronal loss is not a prevalent characteristic of ageing. In the human hippocampus neuronal loss was found to be confined to Alzheimer's patients but not the case for healthy age matched controls (West et al., 1994). A comprehensive cross-sectional study on human brains, ranging from 20 to 90 years old subjects, found that only 10% of the total neurons are lost in the entire cortex as a result of ageing (Pakkenberg and Gundersen, 1997) compared to a 16% difference between sexes. A follow up study showed that no significant change occurs in the number of glial cells in the same regions (Pakkenberg et al., 2003).

Further studies have confirmed these findings in non-human primates and rodents. A key advantage of these animal models is that they do not suffer from ageing related neurodegenerative diseases (Peters et al., 2008). In rhesus monkeys area 46[3] of the cortex does not show neuronal loss in aged individuals (Peters et al., 1994). No neuronal loss

[3] Brodmann area 46 is a region of the frontal cortex, in humans and primates, involved in working memory, attention and inhibitory control.

related to ageing was found in *lamina* II neurons, the cells projecting via the perforant pathway to the hippocampus (Gazzaley et al., 1997), nor in laminae III, V and VI (Merrill et al., 2000) of the entorhinal cortex. Finally in the hippocampus of aged monkeys no neuronal death occurs in the Cornus Ammonis 1 (CA1), CA2, CA3, subiculum, hilus nor in the dentate gyrus (Keuker et al., 2003). Similar findings were confirmed in aged rats where neuronal cell loss was not detected in the hippocampus (Rapp and Gallagher, 1996; Rasmussen et al., 1996) and in any entorhinal cortex layer (Merrill et al., 2001), despite variable performances in the Morris water maze, a classic spatial memory test, in which around half of the aged rats were impaired. All these works point to a marginal role of neuronal death in the cognitive decline development. Nevertheless region specific ageing related neuronal death and atrophy cannot be discounted. A considerable reduction has been reported in the *dl*PFC region in area 8A of the rhesus monkey (Smith et al., 2004). In particular, a 30% reduction in neuron number in area 8A and a 50% neuron reduction in the subcortical nucleus basalis that projects to the cortical region were observed. The gravity of the cellular loss positively correlated to the impairment in a working memory task, specifically when the required response (manually choosing the correct location) was delayed by 10 seconds or more to receive a food reward. Moreover the neighbouring regions were unaffected by ageing, area 46 (also related to working memory function) and the corresponding projecting nucleus basalis did not show evidence of neuronal death.

Though interneuron numbers are preserved, in the aged rat hippocampus, compared to the young, the number of cells positively labelled for GAD67 (Glutamate decarboxylase – isoform 67) is decreased during ageing. Given that GAD is responsible for the production of the γ-aminobutyric acid (GABA) neurotransmitter suggests that while no neurodegeneration of interneurons is taking place, these are losing their phenotype and their functionality (Stanley and Shetty, 2004). Furthermore ageing appears to differentially affect interneuron subtypes, with cells expressing parvalbumin and calretinin generally being preserved while

cells expressing neuropeptide Y and somatostatin preferentially lose their GAD (GAD65 and GAD67) labelling (Vela et al., 2003).

During healthy ageing, as opposed to pathological neurodegeneration, it appears that neuronal cells are generally preserved in the brain of humans, as in animal models. A moderate reduction of neuron numbers has been reported in some brain areas, though more subtle morphological changes are likely to underlie age related cognitive decline.

1.3.2 Age related structural changes of dendritic morphology

Besides contained region specific loss of neurons, most studies suggest that neuronal number is preserved in healthy ageing. On the other hand a widespread region dependent volume reduction has been reported in longitudinal Magnetic Resonance Imaging (MRI) studies (Raz et al., 2005). Notably the hippocampus, the cerebellum, the caudate and the prefrontal cortex were among the most susceptible regions whilst the entorhinal cortex was only mildly affected and the primary visual cortex not at all. If cellular death is not causing such shrinkage, or at least not entirely, neuronal morphological changes might be a major contributor to the age related volume reduction of the brain. Early studies on dendritic arbors in ageing claimed extensive retraction of dendrites in the entorhinal cortex and hippocampus (Scheibel et al., 1976) and in the prefrontal and temporal cortices (Scheibel et al., 1975). The data though included healthy subjects and dementia patients so that the findings may relate more to a disease state rather than the general normal ageing process (Burke and Barnes, 2006). Interestingly, others have reported a growth of dendrites in specific brain areas in healthy ageing. In the parahippocampal gyrus of humans, *lamina* II pyramidal neurons had longer and more branched apical dendrites and longer basal dendrites in healthy aged subjects than both adults or patients with senile dementia landmarks (Buell and Coleman, 1979, 1981). An age related extension of dendritic branching was also found in granule cells of the dentate gyrus in aged human subjects (Flood et al., 1987a) but not in other

hippocampal sub regions. In the CA1 (Hanks and Flood, 1991), CA3 (Flood et al., 1987b) and the subiculum (Flood, 1991), dendritic arbor extent did not change in relation to the subjects' age, but it was diminished in the case of Alzeheimer's disease subjects. Dendritic branching alterations have been described in many cortical areas, where neuronal morphology seems to be more vulnerable. In the motor cortex a reduction in the length of dendritic branches was noted in aged subjects on *lamina* V cells and to a lesser extent on *lamina* III cells (Nakamura et al., 1985). In the aged superior temporal gyrus supragranular (above the granule cell layer – lamina IV) pyramidal cells have shorter dendrites (Jacobs and Scheibel, 1993). In the PFC, specifically areas 9 and 46, *lamina* IIIc pyramids have been shown to be morphological resilient to age with no reduction in dendritic branching, *lamina* V neurons instead display considerable decreases in their basal dendrites branch number and length (de Brabander et al., 1998). Contrasting evidence comes from supragranular cells in area 10 (medial PFC) which show a mild reduction in length of their dendrites (Jacobs et al., 1997), alongside area 18 (occipital secondary cortex) supragranular neurons. The generalized picture that emerges in humans is that dendritic branching is reduced in older age only in specific regions and sub-regions (cortical layers), associative cortical regions are most affected while primary sensory regions (somatosensory and visual cortex) do not show age related differences (Uylings and de Brabander, 2002). Although invaluable, studies on human tissues remain of controversial interpretation due to the small sample sizes, differences in the experiences of the subjects (including education), effects of hypoxia, delay of tissue fixation and the high degree of variability that occurs between individuals (Jacobs et al., 1997). For instance a high degree of variability has been described even in the cortical gyral patterns of monozygotic twins (Bartley et al., 1997).

In the rhesus monkey, as in humans, region specific alterations have been described regarding changes in age related dendritic branching (Dickstein et al., 2007). In *lamina* I of area 46 (PFC) a reduction of the density of dendrites (presumably apical dendrites from *lamina* II neurons) has been reported in an Electron Microscopy (EM) study (Peters et al.,

1998b). Cortical neurons projecting to area 46 (located in *lamina* III of the superior temporal cortex) have also been shown to suffer from apical dendrite branch retractions in relation to old age (Duan et al., 2003).

Age related dendritic branching changes have been the subject of research also in rodents, especially in rats. Pyramidal neurons in the CA1 of aged male rats have been reported to have longer dendritic processes (Pyapali and Turner, 1996). Controversially, a reduction of the dendritic extent has also been reported for aged male rats in a sex comparative study, where aged females were found to have less extended dendrites that did not retract during ageing (Markham et al., 2005). In the medial frontal cortex a specific effect of ageing on dendritic branching has been described. In this area both the basal and apical dendrites of *lamina* II/III neurons actively extend until 18 months of age, the same cells undergo a reduction in dendritic total length thereafter, measured at 28 months of age. No such development of dendritic arbors is observed on *lamina* V pyramidal cells (Grill and Riddle, 2002). In the anterior cingulate (part of the medial frontal cortex and arguably the homologue of the primate PFC) a reduction of basal and apical dendritic arborisation of lamina V neurons has been observed in aged rats, both in males and females, but more prominent in males (Markham and Juraska, 2002). Overall the retraction of dendrites and their branches seems to be an important factor in the ageing of the brain that could contribute, to a certain degree, to the declining cognitive functions. As for neuronal loss also the extent of dendritic debranching appears not to be as vast as initially thought. Rather, dendrites display a retraction in specific cell types in confined brain regions (mainly the PFC), whereas in other regions a continuous age related growth is possible. The findings have been corroborated in rats, monkeys and humans with small differences, though in humans difficulties arise when having to distinguish between normal ageing and forms of senile dementia.

1.3.3 Age related changes in dendritic spines

To date, the prevailing view is that the cognitive deficits that ageing entails are mostly due to alterations in synaptic connectivity rather than neuronal loss and the shrinkage of neuronal arbors (Burke and Barnes, 2006, 2010; Dickstein et al., 2007; Hof and Morrison, 2004; Morrison and Baxter, 2012), though the anatomical changes that lead to such cognitive impairment have not yet been directly proven (Yeoman et al., 2012). The nervous tissue is densely packed with synapses (Holtmaat and Svoboda, 2009), the connections between neurons. Most excitatory synapses occur on dendritic spines (Holtmaat and Svoboda, 2009; Nimchinsky et al., 2002) that make contact with presynaptic boutons on the axon. Structural plasticity of neural networks, the process that allows neurons to modify their connections and circuits, is believed to be fundamental for the formation of new memory traces (Holtmaat and Svoboda, 2009). Indeed the formation and stabilization of spines has been linked to the process of learning and memory storage (Fu et al., 2012; Lai et al., 2012; Roberts et al., 2010; Xu et al., 2009; Yang et al., 2009). There is extensive evidence that the density of synaptic spines decreases with ageing (Burke and Barnes, 2006; Morrison and Baxter, 2012). A reduction of the density of postsynaptic spines has been documented in human ageing, on apical dendrites of *lamina* III neurons of the motor cortex (Nakamura et al., 1985), on supragranular neurons of the superior temporal gyrus (Anderson and Rutledge, 1996), and in the CA1 of patients with mild cognitive impairment (Scheff et al., 2007). Interestingly in (Jacobs et al., 1997) the authors described a 50% decrease in spine density on lamina III neurons of cortical areas 10 (PFC) and 18 (occipital cortex) in subjects over 40 years old but the density was not further reduced in older ages. Furthermore, an EM study found a slight age related reduction in the thickness of area 9, in the human frontal cortex, but no decrease in synapse density in *laminae* III and V (Scheff et al., 2001). Though no distinction was made for synaptic types, it points to synaptic preservation in healthy ageing.

More evidence has been gathered in monkeys and rodents. In aged rhesus monkeys a ~ 25% decrease in spine density was reported on pyramidal neurons of the subiculum

(Uemura, 1985). Spine density was reduced in *lamina* I of cortical area 46 (PFC) (Peters et al., 1998b; Uemura, 1980). The gravity of the reduction in spine density and the thinning of layer I showed a strong negative correlation with the performance in cognitive tests, involving recognition and working memory (delayed non-matching to sample test) and spatial memory (delayed recognition span test) (Peters et al., 1998b). Neurons projecting to area 46, from the temporal cortex, have been shown to suffer dendritic spine reduction related to ageing, in both supragranular and infragranular pyramidal neurons (Duan et al., 2003; Page et al., 2002). Further investigation of the PFC area 46 showed that excitatory (asymmetric, axospinous), as opposed to inhibitory (symmetric, axodendritic), synapses are the most affected by ageing. The density of such synapses is 30% less in *lamina* II/III and 20% less in *lamina* V. The decrease in synaptic density in *lamina* III, but not in *lamina* V, negatively correlates with the cognitive index of the individual animals (Peters et al., 2008). In the *dl*PFC, which contains area 46, it has been shown that thin spines were the most affected by the ageing process on *lamina* III neurons (Hao et al., 2007). Behavioural impairment and thin spines density reduction can be successfully reversed with oestrogen treatment. Spine size is of great importance because it strongly correlates to synaptic efficacy (Cheetham et al., 2012; Kasai et al., 2010a; Matsuzaki et al., 2001; Zito et al., 2009), suggesting that smaller thin spines are involved in learning and memory formation when stabilized and strengthened (Holtmaat and Svoboda, 2009; Kasai et al., 2003). Thin spines were also found to be greatly affected in another study, on *lamina* III pyramidal neurons of the aged *dl*PFC (Dumitriu et al., 2010). Here the researchers were able to confirm that axospinous synapses number decreased in the *dl*PFC of older monkeys, along with spine density. The decrease in spine density was entirely due to the decrease in thin spines, and aged animals had an increased spine head volume of thin spines. Finally the volume of thin spines highly correlated with the difficulty to learn a delayed non-matching to sample task, suggesting that the ageing process has a selective negative effect on synaptic structure, reducing the most plastic elements in the circuit and preserving the least plastic.

Extensive anatomical studies of synaptic spines have been carried out on aged rodents. Ageing related spine loss (~ 30% reduction in apical and basal dendrites) was described in *lamina* V pyramidal neurons in auditory and visual cortex of the rat, using Golgi preparations (Feldman and Dowd, 1975). In the mouse a decrease in spine density was described in *laminae* III and V neurons of the visual cortex, a 50% reduction was observed at 540 days of age (18 months) that did not progress in 720 days (24 months) old animals (Leuba, 1983). Aged female rats were found to suffer a mild spine density reduction specifically in the apical dendrites, but not on the basal arborisation, of *lamina* II/III of the PFC, the same animals were shown to badly perform in an object recognition task (Wallace et al., 2007). However, larger reductions in spine density caused by ageing have been described in male rats when directly compared to females (Markham and Juraska, 2002) in the anterior cingulate cortex on *lamina* V cells. It appeared that younger males had a higher density of spines, and the density of spines in both sexes is reduced to similar levels at older ages. On the other hand, in the CA1 region of the hippocampus no spine density reduction was observed in either sex, although males suffered age related dendritic retraction (Markham et al., 2005). Interestingly synaptic loss has also been described in the cerebellum of aged rats, a brain region important for motor function that appears to have been neglected in the ageing literature. In particular Purkinje cells are affected in their number, dendritic branching and synaptic density (Rogers et al., 1984). The molecular layer of the cerebellum was thinner in the aged rat, with less synapses occurring between the granule cells and the Purkinje neurons. Furthermore it was reported that the remaining synapses were larger, with larger spine and bouton volume which was accompanied by larger synaptic vesicle pools (Chen and Hillman, 1999). Contrasting data has been gathered in the hippocampus of aged rodents, suggesting region and layer specific effects of the ageing process. In the molecular layer of the dentate gyrus, no reduction in the number of synaptic contacts was found and the size of spines was comparable between young and aged rats (Curcio and Hinds, 1983). In contrast, a decline in synaptic density in aged rats compared to young adults has been reported (Bondareff and Geinisman, 1976; Geinisman et al., 1977) in the middle molecular layer of the dentate gyrus.

Furthermore, a selective loss of axospinous perforated synaptic contacts was found in the dentate gyrus of aged rats that were cognitively impaired in the radial maze task, a hippocampus dependent spatial memory test, but not in unimpaired aged rats and young animals (Geinisman et al., 1986), corroborating the importance of synaptic spines in cognition. Subsequently the age related decrease of synaptic density was confirmed, selectively for axospinous contacts (opposed to axodendritic), in the dentate gyrus inner and medial molecular layers with unbiased sampling techniques (Geinisman et al., 1992). The reduction was noted for perforated (interrupted post synaptic densities) as well as non-perforated (continuous post synaptic densities) synapses. The same investigators assessed the total number of synaptic contacts in the CA1 stratum radiatum layer of aged rats, finding that there was no difference compared to the total number scored in the young adult controls (Geinisman et al., 2004). More recently, besides age related spine density reduction, experience dependent spine structural plasticity has been suggested to be lowered in the aged brain of the rat (Bloss et al., 2011). The authors found that spine density, compared to young rats (3 months old) is lower on *lamina* III neurons of the pre-limbic cortex (part of the medial PFC) in middle age rats (12 months old) and spine loss progresses in aged rats (20 months old). They also highlight a differential effect of ageing on density depending on the morphology of spines. Thin spines are the most affected, drastically reduced in middle age and even more so in the aged cohorts. Interestingly, large mushroom like spines (likely to be the physical substrate of long term memories) are only slightly reduced in the middle age group but not in the aged group. In addition the average size of the spine heads were found to be larger in the aged cohort. In the same study the researchers were able to show that structural remodelling of dendritic spines is impaired in aged and middle age rats when these are forced in a stress paradigm known to induce structural plasticity in the mPFC (Radley et al., 2006). Compared to young rats, which display stress induced reduction of spines and subsequent recovery, older rats fail to show spine plasticity in terms of spine density and morphology. Though not a direct demonstration, because the PFC is an associative area strongly linked to higher cognitive functions, such as working memory and executive

function, a reduction in structural plasticity in this region could help explain ageing related cognitive decline. To make matters more complicated, in an *in vivo* two-photon imaging study, which shares many similarities with the work presented in the following chapters, spine density was found to be heightened in the later stages of life in *lamina* V cells of the intact mouse somatosensory cortex (Mostany et al., 2013). For the first time spine density development could be checked over one year in the same animals on the same apical dendrites. This approach showed that in these cells spine density increased from middle age (8 to 15 months old) to old age (20 months or older). Moreover, spine volume was found to be increased in the middle age group but not in aged mice and no difference in the distribution of spine morphologies was found in any age group. Surprisingly the spine dynamics were also increased in the older age groups compared to the young adults (3 to 5 months old), with more spines turning over. In addition spines in the old group were more likely to stabilize a month later compared to the ones in the middle age group. Such unexpected results suggest that the ageing brain is a complex environment that is not just resisting degradation (neuronal loss, dendritic retraction, synaptic loss) but it might be actively compensating specific dysfunctions.

Overall it is clear that synaptic loss is a major candidate for age related cognitive decline, though not a global effect with many exceptions throughout the brain. Focal points of age related morphological changes are the PFC and the hippocampus both involved in high order cognitive functions. Many of the controversies arise from the difficulty to distinguish healthy ageing from pathological states, especially in humans, though hidden pathological states cannot be ruled out in monkey brains either. Furthermore a general limitation of Golgi preparation studies and EM imaging is that it is not possible to compare the same structures in the same subjects over time. Though the development of new stereological techniques have proven valuable tools to investigate age related neuronal changes, the possibility of imaging neurons *in vivo* might represent a key step forward in understanding the underlying age related neuronal mechanisms.

1.3.4 Age related changes on the presynaptic side, axons and boutons

In comparison to the post-synaptic side, a lot less is known on presynaptic changes during the ageing process. Because axons project over great distances it is not easy to study discrete populations arising from a confined group of cells, unlike dendrites which are always in the proximity of the soma. In addition synaptic boutons are sparsely distributed along axonal processes compared to the densely packed synaptic spines, a feature that makes spines preferable when large numbers are needed. Axon regeneration is regarded as a form of plasticity in response to injury. In aged rats it has been shown that the ability of adrenergic fibres in the septum to proliferate was reduced, compared to younger rats, when the area was denervated (Scheff et al., 1978). Further evidence was provided in the peripheral nervous system where ageing was associated to reduced end-plate sprouting and reduced sensory and motor axon regeneration (Pestronk et al., 1980). The structure of nerve fibre tracts in the central nervous system is affected during the ageing process, these alterations affect both the myelin sheaths and the axons themselves (Peters, 2007). The first evidence of degenerating nerve fibres in aged systems was obtained by light microscopy studies. In the visual cortex of older humans, compared to young adults, it was found with myelin stainings that there is a reduction of the fibre myelination in the line of Gennari. This structure is a tract of myelinated fibres typical of the human primary visual cortex (Lintl and Braak, 1983). A reduction in myelin labelling has been reported in other parts of the human aged brain, especially in association areas such as the frontal lobes, however some controversies still exist owing to the fact that it is not clear if these effects are due to reduction of myelin or to a reduction to its dye binding properties (Peters, 2007). Electron microscopy studies on the monkey corpus callosum and on the prefrontal and visual cortices have revealed that a common feature of ageing myelin sheaths are the formation of dense cytoplasm splits between the *lamellae*. These formations are more frequent as age advances (Peters, 2009; Peters et al., 2000). The dense cytoplasm formations have been shown, in human samples, to contain accumulations of ubiquitinated proteins that are not

being degraded by the proteosomes, possibly leading to toxic effects (Dickson et al., 1992). The extent of such inclusions, however, does not correlate with the cognitive performance of the subjects, though there is a correlation between the amount of myelin basic protein labelling in frontal white matter and performance (Wang et al., 2004). Besides alterations of the myelin structure in the central nervous system also nerve fibre loss has been documented in human brains, where the reduction of the white matter has been reported to be around 27% in older adults (above 65 years of age) compared to younger adults (Pakkenberg and Gundersen, 1997; Tang et al., 1997). Other studies indicate that between 20 and 80 years of age the white matter is reduced by over 20% and that up to 45% of the total fibre length is lost, mostly caused by the loss of thinner fibre tracts (Marner et al., 2003). In a structural Magnetic Resonance Imaging study white matter lesions were analysed in aged patients that were also tested on cognitive performance (de Groot et al., 2000). In particular the researchers focused on periventricular fibres (deeper tracts close to the cerebral ventricle) and subcortical fibres. A correlation with poor cognitive scores was found with lesions in the periventricular fibres, which interconnect distant cortical areas or subcortical nuclei with the cortex, but no correlation was found between performance and subcortical fibres lesions which connect adjacent cortical regions, indicating that degeneration of association fibres plays a major role in cognitive decline.

Further confirmation of this view comes from light and electron microscopy analysis of the anterior commissure of the rhesus monkey brain (Sandell and Peters, 2003). The anterior commissure is a white matter bundle that connects the temporal lobes and part of the orbitofrontal cortices, piriform cortices and the amygdala between hemispheres. In aged monkeys (25 – 35 years old) this structure was found to have a reduced cross-sectional area compared to young adults (5 – 10 years old). Furthermore the number of nerve fibres decreased and the number of abnormal axons (degenerating axons or with altered myelin sheaths) increased in relation to age. Interestingly, the reduction in number of the nerve

fibres correlated with the cognitive performance (DNMS, DRS tests) of the individual animals.

Axon terminals and axonal boutons, the presynaptic compartment of neural contacts, are also prone to age related alterations in specific circuits of the mammalian brain. By labelling synaptophysin, a synaptic vesicle component, it was demonstrated that in the hippocampus of rats there is an age related decline of presynaptic contacts. In particular the areas most affected were the outer and middle molecular layers of the dentate gyrus and the stratum lacunosum moleculare of the CA3 region. These regions receive their input from *lamina* II of the entorhinal cortex through the perforant path fibres. The decrease in synaptophysin labelling in the boutons of these axons well correlated with impaired spatial memory ability in the Morris water maze task (Smith et al., 2000). The number of synaptophysin puncta detected in the dentate gyrus has also been successfully correlated to the performance in a spatial working memory task (the T-Maze test) in aged (18 - 22 months old) rats (Slutsky et al., 2010). Contradictory results have also been reported, in aged mice (18 – 20 months old) where synaptophysin labelling increases compared to younger adults (3 – 12 months old) in the hippocampal regions CA1, CA3 and Dentate Gyrus as well as the Entorhinal cortex and Amygdala (Benice et al., 2006). Though these results might have been influenced by extensive behavioural training suggesting an age related compensatory effect. Moreover, confocal laser scanning microscopy cannot resolve the presence of a fully equipped synapse on an axonal bouton. An EM study in the rhesus monkey hippocampus revealed that in the dentate gyrus outer molecular layer the number and size of presynaptic boutons is preserved in aged animals (Hara et al., 2011). However in aged monkeys more non-synaptic boutons (i.e., boutons with no apparent synaptic contact) were found and less multiple-synapse boutons (i.e., boutons forming two or more synaptic contacts) were detected compared to the younger adult monkeys. The percentage of non-synaptic boutons strongly correlated with the number of trials that the monkey needed to acquire the delayed non-matching to sample task and negatively correlated to the average accuracy in the test

phase, indicating that the amount of non-synaptic boutons relates to poor performance. Moreover the average number of synapses made by single multiple-synapse boutons positively correlated with cognitive performance in the same test, suggesting that multi-synaptic contacts are reinforcing the coupling of the presynaptic neurons in the Entorhinal cortex with the postsynaptic neurons in the Dentate Gyrus. Bouton number and size have also been studied in a recently published study that shares many affinities with the work presented in the following chapters. By imaging *in vivo*, synaptic boutons density was found to be higher on axons in aged mice (over 20 months old) compared to young adults (3 – 5 months old). The size of axonal boutons also grew from young to middle age (8 – 15 months old) but did not significantly progress in the older group. Interestingly the level of bouton turnover, the rate at which synaptic elements are replaced, did not significantly vary in the different age cohorts while it is generally thought that synaptic dynamics and plasticity should decrease with ageing. Furthermore new boutons formed in the aged brain were three times more likely to stabilize over a period of 30 days compared to the middle age group (Mostany et al., 2013), a surprising result that goes against the general view that consolidating synapses represent long-term memory traces which are expected to be affected in the ageing brain.

1.4 Physiological changes in the aged brain

The biophysical and physiological properties of neurons are affected by the ageing process (Burke and Barnes, 2006, 2010; Kumar and Foster, 2007; Morrison and Baxter, 2012; Yeoman et al., 2012). The anatomical changes described above are likely to alter the biophysical characteristics of a neuron, for example damaged myelin will reduce motor and sensory information speed and reliability (Kumar and Foster, 2007). On the other hand altered firing might influence the formation and elimination rates of synaptic structures,

hence affecting neural anatomy. Besides structure, the function of ageing neurons and their circuits is most likely affected by changes in the molecular composition and mechanisms that accompany the ageing process. Despite these links not being clear yet there is extensive evidence for specific alteration in neuronal and synaptic function in the ageing brain, with many of such parameters having been associated or correlated to cognitive performance (Burke and Barnes, 2010; Kumar and Foster, 2007).

1.4.1 Electrophysiological age related changes in the Prefrontal cortex

The prefrontal cortex is a key structure in the emergence of age related cognitive decline. Indeed alterations in the physiology of the neurons residing in this region could underlie such impairment. *Lamina* II/III neurons, recorded in slices taken from the monkey prefrontal cortex, were found to have an increased input resistance, increased firing rates, lower action potentials amplitude and increased after-hyper-polarisation (AHP) potentials in aged animals compared to younger adults. The increased firing rates and input resistance were correlated to the cognitive impairment, assessed in DRST and DNMS tests (Chang et al., 2005). The same neurons were described to have a decreased excitatory synaptic input and increased inhibitory synaptic input (Luebke et al., 2004). In contrast the biophysical properties of *lamina* V neurons were described as largely unchanged by the ageing process. In this cortical layer the only significant alteration that was detected in relation to ageing was an increased AHP potential amplitude, whereas the excitability and firing were comparable in aged and young adult monkeys (Luebke and Chang, 2007). In a more recent study increased AHP potential amplitude was found to negatively correlate with behavioural cognitive score. In particular pyramidal neurons of *lamina* II/III had larger AHP potentials in aged impaired monkeys compared to unimpaired aged monkeys and young adults (Luebke and Amatrudo, 2012). In *macaca mulatta* neurons in the *dl*PFC have been recorded *in vivo* while the monkeys were performing a delayed response task that tested working memory. In aged monkeys, which

were less effective in the behavioural task, the neurons that fired during the delay period (possible mechanism for memory retention) displayed a loss of persistent firing. The inconsistent firing during the delay retention period started in middle aged monkeys and worsened in fully aged animals (Wang et al., 2011). Persistent firing was recovered by inhibiting cyclic adenosine monophosphate (cAMP) signalling. It had been previously shown that the drug guanfacine (α_{2A} receptor agonist, used in Attention-deficit hyperactivity disorder) reduces cAMP levels and has a positive effect on working memory.

In rodents the presence of an equivalent structure to the *dl*PFC is controversial, though some suggest the same functions might be mediated by medial Prefrontal Cortex (mPFC) (Morrison and Baxter, 2012). For this reasons the electrophysiological properties of aged neurons in rodents have mainly been explored in the hippocampus. In contrast the characterization of the electrophysiological properties of hippocampal aged neurons is lacking in monkeys. Possibly because this region is not directly accessible *in vivo* and preparations have been preferably studied on an anatomical level.

1.4.2 Electrophysiological age related changes in the Hippocampus

The hippocampus has been extensively investigated in the ageing context because of its relatively simple circuitry and because of the prominent age related cognitive impairments associated with hippocampal function. The anatomical observations of reduced synaptic contacts in the dentate gyrus are supported by the electrophysiological analysis of the perforant path. Stimulating the entorhinal cortex fibres has revealed that the excitatory postsynaptic potential (EPSP) and the presynaptic fibre potential measured in aged rats are reduced compared to younger animals (Barnes and McNaughton, 1980). The ratio, though, between pre- and postsynaptic amplitude is greater in aged rats indicating the presence of stronger synapses. This finding is confirmed by an increased quantal size of synaptic transmission at the same synapse in the aged rat (Foster et al., 1991). Because age related

neuronal loss in the entorhinal cortex has been excluded, it has been speculated that during ageing there is a reduction in the perforant path axon collaterals (Burke and Barnes, 2010). The increased synaptic strength of single synapses is likely to be due to an increased presence of the α-amino-3-hydroxy-5-methylisoxazole-4-proprionate (AMPA) receptors and the concurrent reduction of the N-methyl-D-aspartate (NMDA) receptors that has been documented on the perforant path synapses in the aged rat brain (Yang et al., 2008). The recorded EPSP upon Schaffer collateral stimulation also suffers an age related reduction in rats (Barnes et al., 1992) though, in this case, the presynaptic fibre potential has been shown to not change with increasing age and the unitary synaptic strength is also unchanged (Barnes et al., 1997). These results suggest that an increasing number of synapses become silent with advancing age in this specific region (Burke and Barnes, 2010). Similar for what seen in prefrontal neurons, ageing consistently increases the AHP potential amplitude and its duration in hippocampal CA1 neurons. Spatially impaired aged rats, tested in the Morris water maze, had larger AHP potentials compared to unimpaired aged and young rats. Both the acquisition and the probe performance in the Morris water maze test inversely correlated to the amplitude of AHP potentials (Tombaugh et al., 2005). This increase in AHP potential amplitude and duration, which lowers neuron excitability, is dependent on age related increased levels of intracellular Ca^{2+} (Kumar and Foster, 2007). In the presence of kainate (specific agonist of the kainate receptor), used as an exogenous stimulation, CA3 interneurons display reduced AHP potentials in aged compared to young rats (Lu et al., 2011). The larger depolarization was accompanied by increases in the intracellular Ca^{2+} concentration in aged interneurons compared to young ones. On the other hand, such differences in inhibitory neurons were not detectable in the absence of the drug, unlike aged pyramidal excitatory cells, pointing to cell specific physiological variations during brain ageing.

Neurons in the aged brain generally appear to be less excitable than those found in younger brains. It seems that such a decrease is generated by changes in the neuronal functional

response to synaptic transmission, larger AHPs and increased intracellular Ca^{2+} concentrations. These alterations are further magnified by the decrease in synaptic contacts and by the imbalance of the excitatory and inhibitory inputs, with the latter relatively spared by the ageing process.

1.4.3 Age related changes in synaptic plasticity, LTP and LTD

Long term potentiation (LTP) is a widely studied mechanism of functional synaptic plasticity, which induces synaptic strengthening through high frequency electrical stimulation, regarded as the synaptic basis of learning and memory (Bliss and Collingridge, 1993). Early-phase LTP and late-phase LTP are respectively involved in LTP induction and maintenance. LTP induction requires NMDA receptors activation with the consequent increase in postsynaptic Ca^{2+} (Bliss and Collingridge, 1993). LTP maintenance refers to sustained synaptic efficacy persisting after LTP induction, insertion of AMPA receptors and changes in gene expression mediate this process (Malinow and Malenka, 2002).

LTP induction is equally achieved at the perforant path – granule cell synapse in the hippocampus of aged as well as young adult rats (Burke and Barnes, 2010; Diana et al., 1994a; Diana et al., 1994b). Similarly LTP induction is preserved at the Schaffer collateral – CA1 (Bodhinathan et al., 2010; Landfield et al., 1978) and the perforant path – CA3 (Dieguez and Barea-Rodriguez, 2004) synapses in the aged rat hippocampus. However LTP induction is protocol dependent, the use of peri-threshold electrical stimulation resulting in LTP induction in the dentate gyrus of young rat hippocampal slices fails to induce LTP in the aged rat (Barnes et al., 2000) indicating that LTP induction threshold is raised in these aged neurons. In the aged CA1 the induction threshold is not raised, rather the level of LTP induced is lower compared to what observed in younger animals (Deupree et al., 1991; Kelly et al., 2011; Moore et al., 1993; Tombaugh et al., 2002). Ageing appears to be detrimental to late-phase LTP, in the CA3 (Dieguez and Barea-Rodriguez, 2004) and dentate gyrus

(Barnes and McNaughton, 1980) LTP maintenance is deficient in aged rats compared to younger controls. Moreover in the aged brain LTP reversal is facilitated (Foster and Norris, 1997). Consistent with this result, long-term depression (LTD), the activity dependent reduction in synaptic efficacy mediated by low frequency electrical stimulation, is facilitated in aged neurons (Norris et al., 1996). Importantly, deficits in LTP induction and maintenance correlate with impaired learning (Burke and Barnes, 2006, 2010). In particular, spatial memory impairments have been linked, via correlative analysis, with late phase LTP defects in the CA1 region of aged rats (Bach et al., 1999). Though the role of LTP like mechanisms in memory formation and consolidation has not yet been clearly demonstrated, extensive evidence suggests that LTP and LTD are required for learning and are at the same time defective in aged neurons (Rosenzweig and Barnes, 2003). In general, the magnitude of LTP is not diminished during ageing, however LTP induction is less effective compared to the young adult brain. Moreover ageing is associated with a functional synaptic plasticity shift, which reduces LTP and favours LTD induction and LTP reversal (Kumar, 2011).

1.5 Mechanisms of brain ageing

1.5.1 Oxidative stress

A prevalent explanation of what causes the ageing process is the oxidative damage theory. Reactive oxygen species (ROS) are the source of oxidative stress which would be able to cause ageing and age related pathological states. Reacting with endogenous molecules ROSs, mainly a by-product of the respiratory chain, can cause damage to lipid layers, proteins and DNA. The accumulation of oxidative damage can kill cells or alter their phenotype, for example by affecting gene expression (Yeoman et al., 2012). Though many

studies have correlated reduced oxidative damage to an increased lifespan in the worm, fly, and mouse, direct experimental evidence of the role of oxidative stress in ageing is still controversial (Perez et al., 2009). While knocking out antioxidant genes, which encode for enzymes that limit oxidative damage, has shown a reduction in lifespan, the overexpression of antioxidant factors has failed to extend maximum lifespan (Perez et al., 2009; Yeoman et al., 2012). Though the role of oxidative stress might be complex in the general ageing of the whole organism, oxidative stress might have a major impact on the brain. The CNS has a high metabolic demand and mature neurons are post-mitotic cells that live as long as the individual's life (Wang and Michaelis, 2010). Moreover oxidative stress has been shown to increase in the ageing brain and linked to a parallel up-regulation of genes involved in stress response (Yankner et al., 2008). Superoxide dismutase (SOD) is an enzyme responsible for superoxide scavenging, overexpression of SOD in the aged brain was found to improve LTP induction and spatial learning (Hu et al., 2006). An important consequence of oxidative stress in the ageing brain appears to be its contribution to the dysregulation of intracellular Ca^{2+}, which is responsible for altered excitability and LTP/LTD functionality (Foster, 2007). In this respect oxidative stress has been shown to increase the release of Ca^{2+} from intracellular stores affecting NMDA receptor function through the activation of calcineurin (Kamsler and Segal, 2004). Blocking Ca^{2+} release from intracellular stores ameliorates NMDA receptor function in aged animals (Kumar and Foster, 2004). Extracellular oxidative damage has been shown to result in the increased influx of extracellular Ca^{2+} through L-type channels and at the same time reduced calcium influx through NMDA receptors (Foster, 2007). Such shifts in the source of intracellular Ca^{2+} may lead to activation of different pathways, causing functional differences in neuronal transmission (see below). The hypothesis that age related changes in Ca^{2+} regulation affect neuronal physiology, hence cognitive function, is a tissue specific (i.e. neuronal) proposed mechanism of the ageing process (Yeoman et al., 2012).

1.5.2 Ageing and neuronal Ca^{2+} concentration

Fine tuning of the levels and fluctuations of intracellular and subcellular Ca^{2+} concentration is needed to regulate the physiological functioning of nerve cells. At the synaptic level rises in Ca^{2+} concentration mediate synaptic plasticity phenomena, altering synaptic transmission and inducing LTP and LTD events (Foster, 2007). The Ca^{2+} hypothesis of neuronal ageing implies that the regulation of Ca^{2+} is altered in aged neurons and that this affects neural circuit transmission. As described above, AHP potentials are increased and last longer in aged neurons. Local increases in Ca^{2+} concentration are known to activate K^{+} outward currents that contribute to excessive hyperpolarization in aged neurons reducing excitability (Landfield and Pitler, 1984). Ca^{2+} homeostasis is altered by an increased density of L-type Ca^{2+} channels on the membranes of aged CA1 pyramidal neurons, increasing Ca^{2+} conductance (Thibault and Landfield, 1996). Ca^{2+} induced Ca^{2+} release from internal stores has also been shown to increase with ageing, facilitating AHP currents and favouring LTD and decreasing the probability of LTP induction in the case of weak electrical stimulation. LTD induction was reduced when inhibiting the ryanodine receptor mediated Ca^{2+} release from internal stores (Kumar and Foster, 2005). While Ca^{2+} cell entry is increased via increased storage release and voltage dependent Ca^{2+} channels conductance, the NMDA receptor contribution of Ca^{2+} entry is decreased (Foster and Norris, 1997), suggesting a further alteration for LTP induction. Furthermore there is evidence of a correlation between altered Ca^{2+} levels and cognitive impairments in rodents (Burke and Barnes, 2010). An age related increase of L-type Ca^{2+} channels was found to correlate with the number of errors aged rats made in a working memory task. Moreover the age related detrimental effect on cognition was counteracted by nimodipine treatment, a voltage gated calcium channel blocker. The drug also reduced the expression levels of a specific channel subunit, the alpha (1D) (Ca(v)1.3), protein which is up-regulated in the aged hippocampus leading to increased Ca^{2+} conductance (Veng et al., 2003).

Intracellular Ca^{2+} signalling is central to neuronal function, playing a major role in synaptic transmission and plasticity. It is therefore expected that disturbances in such an important and highly regulated process can lead to alterations to neuronal physiology and eventually structure.

1.6 Structural plasticity in the brain

Processes of memory formation and consolidation are the cognitive elements that suffer the major impact during healthy and pathological ageing. Classically the phenomena of learning and memory have been interpreted as the ability of neurons to modify their synaptic weights in response to specific activity patterns, the so called Hebbian theory (Caroni et al., 2012). Neural circuits throughout life are shaped by experience. The action of experience is not simply affecting synaptic efficacy, it is promoting the elimination, the formation and stabilization of synapses, therefore continuously changing neuronal structure and circuit connectivity (Holtmaat and Svoboda, 2009). Synapses are densely packed on neuronal processes. They are defined by the presence of neurotransmitter-containing vesicles and an active zone on the presynaptic side, a synaptic cleft and the postsynaptic density containing the neurotransmitter receptors. Most excitatory synapses occur between *en passant boutons* (EPBs), synaptic specializations along the axon shaft, and dendritic spines. A subset of axonal boutons, *terminaux boutons* (TBs), protrude from the axon and more frequently make contact with the dendritic shaft (*lamina* VI to *lamina* IV synapse) (McGuire et al., 1984), though others have reported an equal proportion of spine vs. shaft synapses for EPBs and TBs (*laminae* II/III and IV neurons – synapses in *lamina* III) (Anderson and Martin, 2001). The ability of synapses to form and remodel in response to a wide range of stimuli has brought them to be regarded as the main anatomical contribution to the acquisition,

consolidation and storage of memory traces, in species ranging from worms to mammals (Hubener and Bonhoeffer, 2010).

Structural plasticity can alter brain circuitry in different ways on different scales. Fine structural changes can occur at the synapse level, where an existing excitatory or inhibitory neuronal connection is enlarged or made smaller, changing synaptic strength. New synapses can be formed, and existing ones lost, between adjacent neuronal processes, adding or eliminating a transmission site in the network. An active growth of processes, or indeed their retraction, can reach out to recruit new cells in the circuit by forming new synapses on distant neurons. Finally, new neurons are generated in confined brain areas and these cells gradually integrate in the circuit replacing neurons. Through such strategies structural plasticity provides a cellular basis for learning and memory, where physically shaping brain connectivity allows the formation of long lasting memory traces that can be recruited for future retrieval (Caroni et al., 2012). Though these events happen throughout the life of high order organisms, the general view is that large scale remodelling is characteristic of the development stage. During adult life the extent of such remodelling is reduced in favour of local synaptic remodelling. Relatively little is known on what happens during ageing, the general view is that the reduction in structural plasticity in adulthood is further reduced in the latter stages of life.

1.6.1 Structural remodelling of synaptic morphology

Synapses in the brain display a range of different morphologies; their structure is not fixed but changes over time (Kasai et al., 2010b). Importantly, the variation in size of a synapse determines changes in synaptic strength (Cheetham et al., 2012; Knott et al., 2006), a process dependent on activity (Matsuzaki et al., 2004). Synapse size further correlates with presynaptic probability release (Tokuoka and Goda, 2008) and with the probability of the synapse to persist over relatively long periods of time (Holtmaat et al., 2006). Sensory

experience can drive synaptic growth, enlarging the spine head, increasing the number of postsynaptic receptors and increasing the pool of docked vesicles in the presynaptic bouton (Yuste and Bonhoeffer, 2001). Furthermore, increased synaptic size may reflect the recruitment of organelles or cellular machinery to the site, promoting synaptic stability (Caroni et al., 2012). At the level of the postsynaptic spine, it has been shown that fast repeated glutamate uncaging was sufficient to elicit spine growth and synaptic strengthening (Matsuzaki et al., 2004), whereas low frequency glutamate activity could promote spine shrinkage and synaptic weakening (Oh et al., 2013). Song learning in zebra finches was found to result in spine enlargement *in vivo,* correlated with stronger synaptic activity (Roberts et al., 2010). On the other hand deafening the birds caused dendritic spines in the auditory cortex to shrink (Tschida and Mooney, 2012). Enlargement and shrinkage of spines represent LTP and LTD like phenomena that are tightly linked to experience suggesting that existing synapses play a role in memory formation. Indeed the enlargement and stabilization of thin dendritic spines has been proposed as a major contributor to memory consolidation (Kasai et al., 2003).

1.6.2 Structural plasticity, synapse formation, stabilization and elimination

Early studies have examined synaptic plasticity at an EM level *post mortem*, following environmental enrichment or sensory stimulation *in vivo*. In both cases synaptogenesis was promoted and more synapses were detected in the plasticity induced animals compared to controls (Knott et al., 2002; Turner and Greenough, 1985).

Over the past decade structural plasticity studies have greatly benefitted from the development of techniques that have allowed the live, time-lapse imaging of synapses in the intact animal (Holtmaat and Svoboda, 2009). In particular the development of two-photon laser scanning microscopy has given the possibility to image deep (up to 0.5 mm) in the brain through localized excitation and low power infrared excitation wavelengths (Helmchen

and Denk, 2005). Coupling two-photon microscopy with the development of transgenic animal lines that express fluorescent proteins in neuronal subsets has opened the way to synaptic *in vivo* imaging. Furthermore a few techniques have been devised to gain chronic optical access to the brain by thinning or removing a portion of the skull in order to repeatedly collect data from the same animals over time (Drew et al., 2010; Holtmaat et al., 2009; Yang et al., 2010). These new techniques enabled researchers to follow neuronal process over extended periods of time in their intact environment. Thanks to genetically encoded sparse labelling of excitatory neurons (Feng et al., 2000) it has been possible to visualize synaptic spines *in vivo* in the neocortex. Both in the visual cortex and somatosensory cortex spines on *lamina* V neurons were found to be highly stable over a period of up to three months, though a small but considerable fraction of spines were lost and gained in the adult mouse (Grutzendler et al., 2002; Trachtenberg et al., 2002). These changes appeared to be greater in the developing brain and could be enhanced in the adult following manipulation of the sensory input trimming the mystacial whiskers of the animals. Importantly dendritic spines carry excitatory synapses; it has been shown that it takes about a day for a newly formed spine to form a complete synapse (Knott et al., 2006) *in vivo* as well as *in vitro* (Nagerl et al., 2007). Conversely the loss of a spine has been shown to result in the loss of a synapse (Becker et al., 2008). Alternatively, spine disappearance could underlie the transformation to a shaft synapse (i.e., where the neurotransmitter release site is directly on the dendritic shaft). Though possible, such eventuality is likely to be infrequent given that existing excitatory shaft synapses are greatly outnumbered by the observed retracting spines (Trachtenberg et al., 2002). Furthermore a spine or a bouton, in the great majority of cases, corresponds to one synapse (Harris et al., 1992; Shepherd and Harris, 1998). Few spines (~ 4%) and boutons (~ 10%) do not form complete synapses (Arellano et al., 2007; Knott et al., 2006; Shepherd and Harris, 1998) and a small proportion of boutons (~ 14%) make multiple contacts with different spines (Knott et al., 2006). On this basis, observing dendritic spines and their dynamics is a fair approximation of observing synaptic sites directly (Hubener and Bonhoeffer, 2010).

Structural remodelling of dendritic spines has been found to be enhanced in the developing brain of rodents. Through *in vivo* imaging it has been shown that during the first weeks of life spine turnover (the sum of spines that appear and disappear) is rapid and the density of spines is higher than what seen in adults (Grutzendler et al., 2002; Holtmaat et al., 2005; Lendvai et al., 2000; Mostany et al., 2013; Zuo et al., 2005). A period of spine pruning (spine elimination is greater than spine formation) follows the initial stages confirming the view that brain maturation is accompanied by a selection of synapses (De Felipe et al., 1997). In adult life, synaptic dynamics are slowed down, though plastic synaptic responses can be elicited through peripheral lesions, sensory stimulation and learning paradigms (Caroni et al., 2012; Holtmaat and Svoboda, 2009; Hubener and Bonhoeffer, 2010).

Neuronal activity in the cortex can be altered by partially ablating the source of sensory information. Trimming the whiskers of rodents in a chessboard fashion is known to cause functional plasticity in the somatosensory cortex (Glazewski and Fox, 1996). *In vivo* imaging experiments have shown that following clipping of the whiskers in adult mice spine turnover is enhanced (Holtmaat et al., 2006; Trachtenberg et al., 2002). In particular the overall density of spines was not altered but more spines were formed and more existing spines were lost on *lamina* V pyramidal neurons. Moreover, newly formed spines were more likely to be stabilized when the whiskers were trimmed than in control condition in a cell specific manner (Holtmaat et al., 2006). When all whiskers were ablated from one side of the animals face spine elimination was reduced in the contralateral somatosensory cortex, conversely spine formation was preserved (Zuo et al., 2005). In the visual cortex the input to a specific area can be interrupted by focal retinal lesions. In this case the lesion is permanent and peripheral input is not recovered. Eventually though the initially silenced region returns to respond to visual stimuli denoting a functional reorganization of the cortex that had lost sensory input (Keck et al., 2008). During such reorganization the net spine density was found to remain stable, on the other hand spine turnover increased greatly, to the extent that nearly all pre-lesion spines had been replaced after two months. The same effect did not

occur when the peripheral input was completely ablated, removing the whole retina highlighting the importance of neighbouring activity as a means of function recovery. The monocular deprivation (MD) is a well-established plasticity paradigm. MD requires the temporary closure of one eye, which results in a functional shift of neurons in the binocular region of the visual cortex causing neurons to respond more to the open eye. If the animal had experienced MD earlier in life, a second deprivation was found to elicit a faster plastic response (Hofer et al., 2006). Two-photon *in vivo* imaging revealed that spine changes during the first MD were limited to *lamina* V neurons in the binocular zone of the visual cortex, producing an increase in spine density (Hofer et al., 2009). Reopening the eye brought spine dynamics back to basal levels, though spine density remained elevated. During the second MD spine turnover did not increase from basal levels and the spines previously formed during the first MD persisted. Furthermore these spines increased their size following the second MD, indicating that they might serve as a physical substrate for the memory trace that is readily activated when the experience is repeated. The increased size may underlie the rapid functional shift following the second MD.

Sensory stimulation, as opposed to peripheral lesions, has been shown to elicit plastic responses in dendritic spines. Environmental enrichment was reported to cause an increase in spine turnover within two days, causing elevated spine formation and spine loss (Yang et al., 2009) in *lamina* V neurons of the barrel cortex (cortical region that receives inputs from the whiskers) of the mouse. On *laminae* V and II/III neurons, spine density increased and was sustained over time in the somatosensory cortex of mice that were placed in an enriched environment containing motor and sensory features of stimulation (Jung and Herms, 2012). Spine formation and spine elimination were also higher in the enriched condition compared to control. Furthermore, similar results were obtained when raising the animals in enriched conditions or when introducing the enrichment in adulthood.

Learning has been involved in the formation and stabilization of spines in the auditory cortex of birds (zebra finches), increases in spine density and turnover were induced by learning to

sing from a tutor (Roberts et al., 2010). The degree of spine turnover prior to the tutoring predicted how well the birds would learn to sing, indicating a role in cognitive performance for baseline synaptic turnover. Learning skills required by specific motor tasks has been linked to spine formation and stabilization in the mouse motor cortex. Learning to run on the rotarod (a rotating rod device used for motor skill assessment) or learning to grasp a seed with fine paw movements elicited in the mice a rapid formation of new spines on *lamina* V neurons (Xu et al., 2009; Yang et al., 2009). Moreover the newly formed spines were preferentially stabilized by training. Motor performance was strongly correlated with both the amount of spines induced by motor learning and the number of pre-existing spines (prior to learning) that were eliminated. Repeated motor learning leads to the formation of spines close to previously formed spines induced by training on the same task (Fu et al., 2012). Learning induced spine clusters are more likely to persist compared to unrelated spines. Furthermore the average size of clustered spines increases over four days of training; whilst on average non-clustered spines do not grow in size. A location specific effect on dendritic spines of *lamina* V cells was also observed in a different behavioural paradigm. During fear conditioning (pairing a foot shock with an auditory cue) it was reported that spines are eliminated in the frontal cortex of the mouse (Lai et al., 2012). Extinction of the fear memory, obtained by continuous exposure to the conditioned stimulus, caused formation of new spines on the same dendrites where spines were previously lost. Extinction induced spine formation was cue and location specific, a larger proportion of new spines were within 2 µm of fear conditioning eliminated spines relevant to the extinguished cue compared to a non-extinguished fear trace. Together with the motor learning clustering of spines, these results suggest that neighbouring spines encode for similar memory traces (Caroni et al., 2012).

Dendritic spines have been at the focus of the experience dependent structural plasticity research. Comparably little attention has been given to the presynaptic side, axonal boutons. However with classical techniques it has been shown that axons respond to sensory deprivation, especially in the visual cortex. Subcortical and intra-cortical projections grow or

retract in spared and deprived cortical areas respectively (Hubener and Bonhoeffer, 2010). Few studies have looked at bouton dynamics *in vivo* in the mammalian cortex. At basal conditions different bouton dynamics of morphologically different axons were observed in the adult mouse somatosensory cortex (De Paola et al., 2006). It was found that axons originating from *lamina* VI neurons, typically rich in *terminaux boutons*, display a higher degree of basal synaptic turnover compared to other axonal morphologies. The *en passant bouton* rich axons, originating from *lamina* V, *lamina* II/III and from the thalamus, were instead found to have a remarkably stable synaptic population. Furthermore, in basal conditions it appeared that axonal branches were very stable extending and retracting minimally over time. Similar results were obtained in the visual cortex of the *macaca fascicularis* monkey (Stettler et al., 2006), where synaptic boutons displayed a baseline turnover while the overall bouton density was unchanged. Following retinal lesion, axonal boutons in the macaque visual cortex were found to increase in numbers and collateral branches were observed sprouting from axons (Yamahachi et al., 2009). Sensory deprivation in the mouse (plucking the whiskers) caused extensive axonal remodelling in the barrel cortex of deprived as well as non-deprived regions, involving excitatory and inhibitory axons and their boutons (Marik et al., 2010). Together the sensory deprivation studies suggest that axonal sprouting is a structural response to a functional recovery of the input in deprived cortical areas. Crucially though these studies have employed viral vectors to label cortical neurons. The fact that they have not followed individual neurites poses the question of whether the increased total axonal length does not derive from subsequent viral activation of the fluorescent reporter expression. In transgenic mice stably expressing GFP focal retinal lesions were not reported to cause axonal sprouting in the visual cortex (Keck et al., 2011). On the other hand inhibitory circuits were shown to respond to the lesion faster than excitatory neurons. Within a few hours, the number of spines and subsequently the amount of boutons decreased on inhibitory neurons following the retinal lesion. The result suggested that changes caused by altered sensation on interneurons precede changes on excitatory cells in the relevant cortical areas. A recent chronic two-photon *in vivo* imaging study

considered axonal bouton morphological and dynamic properties during different stages of life in mice (Mostany et al., 2013). Surprisingly an increase in bouton size and density was reported. Moreover, newly formed boutons were more likely to stabilize in the aged (over 20 months old) brain compared to a middle age (between 8 and 15 months old) stage.

1.6.3 Structural plasticity of axonal arbors

As reported above, axons have been shown to grow in the adult brain following peripheral lesions that interrupt sensory input to the relevant cortical areas (Marik et al., 2010; Yamahachi et al., 2009). Conversely, trimming the rat vibrissae has been shown to cause retraction of thalamocortical fibres, but not the density of synapses on the axons, from the deprived barrel cortex (Oberlaender et al., 2012). Indeed axonal plasticity was observed as a response to more serious injuries. Limb amputation in the macaque caused intracortical, but not thalamocortical, axonal sprouting in somatosensory cortex (Florence et al., 1998). This result was obtained using retrograde tracers and comparing the axonal length of injured versus control animals. The mechanism of axons extending in the deprived cortical areas has been proposed to cause the phantom limb phenomenon. Axonal sprouting has also been observed as a consequence of central lesions. An ischemic injury, which destroyed the hand representation area in the squirrel monkey primary motor cortex, induced extensive axon growth from neighbouring regions towards the infarcted area (Dancause et al., 2005). In the rat barrel cortex axonal arbor extension was observed in response to partial vibrissectomy, a procedure that requires full removal of the vibrissal follicle (Kossut and Juliano, 1999). In the hippocampus of rats experience dependent axonal sprouting has been described. It has been reported in different rat strains that spatial learning in the water maze (but not swimming alone) causes mossy fibre terminals to remodel and extend (Holahan et al., 2006). Interestingly, environmental enrichment was found to increase the complexity and volume of mossy fibre terminals in the CA3 (Galimberti et al., 2006). In the absence of a

direct manipulation of experience, axonal arbors are relatively stable when imaged *in vivo* and followed over multiple time points (De Paola et al., 2006) in the mouse somatosensory cortex. Elongation and retraction events, associated with synapse formation and elimination, were observed over tens of µm, though the overall large scale structure of axons did not change in adult mice. In the cerebellum a similar behaviour was observed, where a subset of climbing fibres arising from the same cell body, were found to be motile in basal conditions (Nishiyama et al., 2007). Because large scale axonal remodelling is frequent in the developing cortex (Portera-Cailliau et al., 2005) it would be interesting to know whether such processes are further reduced during ageing.

1.6.4 Differences in synaptic structure scoring analysis

The *in vivo* imaging field has produced a considerable amount of studies looking at synaptic dynamics over the past decade. The general findings are that spines and boutons are relatively dynamic at basal conditions and these dynamic rates can be influenced by experience and learning. There are though some striking differences between studies when comparing quantifications of synaptic turnover rates (Holtmaat and Svoboda, 2009). Differences can be partially explained by different experimental conditions. Different studies have looked at different cortical regions: frontal, motor, somatosensory, auditory, visual cortices. At least two different techniques have been employed to gain optical access to the cortex, the cranial window implant (Holtmaat et al., 2009) and the thinned skull preparation (Yang et al., 2010). Furthermore different mouse lines have been used which express different fluorescent proteins (GFP or Yellow Fluorescent Protein - YFP) in different expression patterns, sparse labelling versus dense labelling of neurons. Sampling could vary in different studies, sparse labelling allows the experimenter to acquire longer tracts of the same neurite, whereas following a process is more complex in densely labelled tissue. In addition to these variables a large contribution to such discrepancies is provided by

differences in the methodology of the analysis of two-photon image stacks. Indeed, ~75% difference in spine turnover was detected in the same set of images by two different groups of investigators (Holtmaat et al., 2009). Differences in the criteria adopted in identifying synaptic structures and the fact that current analysis methods are still manual (i.e., user dependent), may explain such discrepancy. Different interpretations of subtle morphological changes (e.g. persistent spine motility, drifting on the dendrite) may also lead to differences in the result outputs. Importantly though keeping strict criteria when analysing images within a study can highlight important relative variations in a specific experimental condition. Better ways of analysing images should include the implementation of automated algorithms able to consistently score spines and boutons from *in vivo* and *in vitro* acquired images. In summary, true synaptic turnover estimation will be possible when reliable techniques will be developed to track the presynaptic and the postsynaptic compartments simultaneously, possibly with super-resolution microscopy, which allows imaging at the nanoscale.

1.7 Aims

The primary aim of this work was to investigate axonal bouton dynamics in a healthy ageing mammalian model. Rodents have extensively been used for ageing studies, a major reason for this being rats and mice have a very short lifespan compared to other mammals (Yeoman et al., 2012). For example, male C57BL/6 background mice have an average lifespan of 800 days [26.7 months (Selman et al., 2009)]. Experiments were performed using two age groups of male C57BL/6 mice comprising a Young Adult cohort aged between 4 and 6 months old and an Aged cohort ranging between 22 and 24 months old. In addition, a small group of an intermediate age were also studied, ranging between 12 and 14 months of age. Two-photon *in vivo* imaging of cortical structures is a powerful tool to study axonal and synaptic dynamics in the intact brain of living animals, especially when coupled with a sparse

neuronal expression of a fluorescent protein. The Thy1-GFP mouse lines have subsets of excitatory neurons labelled in cortical and subcortical structures making them an ideal tool for this purpose (De Paola et al., 2003; Feng et al., 2000). The brain area considered here is the somatosensory cortex (S1) which includes the barrel fields, an area well characterized in previous studies concentrating on synaptic dynamics in adult mice (De Paola et al., 2006; Holtmaat et al., 2006; Trachtenberg et al., 2002).

1.7.1 Experimental outline

To study synaptic bouton dynamics in the living intact brain in the context of ageing, two transgenic mouse lines were employed: the Thy1-GFP M line (Feng et al., 2000) and the Thy1-GFP L15 (De Paola et al., 2003). In both lines Green Fluorescent Protein (GFP) is expressed in a subset of excitatory neurons under the control of the Thymocyte differentiation antigen 1 (Thy-1) promoter (Figure 2). The two lines, which share the same genetic background (i.e., C57BL/6), differ by the GFP form they express: the GFP M line expressing a cytosolic form (Figure 2 a) and the L15 expressing a plasma membrane bound form (Figure 2 b) of the reporter protein. In both lines labelling in the neocortex is sparse, the majority of labelled soma are found in *lamina* V and consist of pyramidal excitatory neurons; consistent cell labelling is found also in *lamina* VI and *lamina* II/III (De Paola et al., 2003; Feng et al., 2000). In *lamina* I, the most superficial cortical layer, labelled cell bodies are very rare while relatively sparse labelling of axons and dendrites allows extensive axonal imaging. Such GFP labelled axons (in somatosensory cortex S1) arise from cell bodies residing in *laminae* II/III, V, VI and in the thalamus. In superficial layers of S1 in terms of morphology two different types of axons can be found: *En Passant Bouton* (EPB) rich axons and *Terminaux Bouton* (TB) rich axons (De Paola et al., 2006). The GFP M line was used to look at EPB rich axons and the L15 line was used to look at the protruding boutons that are found on TB rich axons. Importantly these axons have been shown to originate from different

neuronal populations that reside in different cortical and subcortical regions, TB rich axons originate from *lamina* VI and EPB rich axons from *laminae* II/III, V and thalamic nuclei (De Paola et al., 2006).

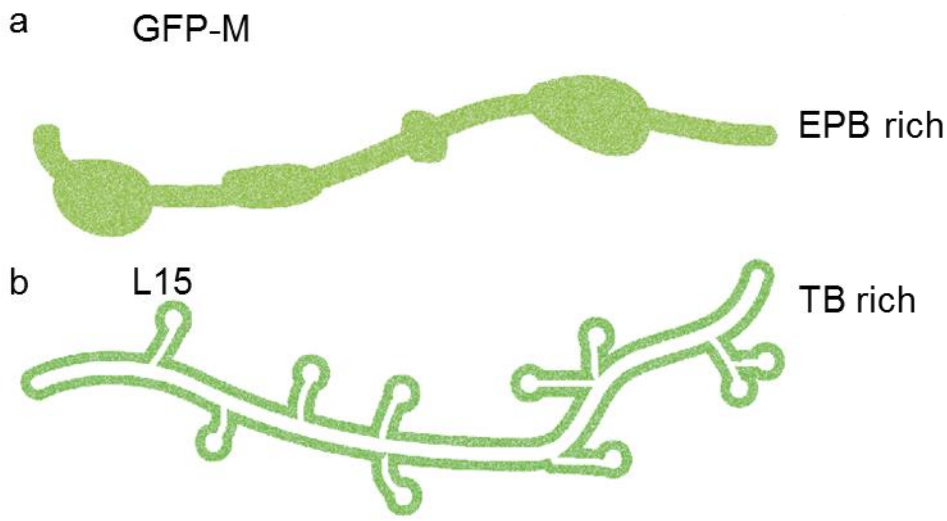

Figure 2 Thy1-GFP lines label different cellular compartments. (a) The GFP-M line was used for the EPB dataset. In this mouse line the cytosol of a subset of excitatory neurons is labelled. The labelling is usually sparse, allowing axon traceability. (b) In the L15 a similar subset of neurons, is labelled, though GFP is bound to the plasma membrane allowing reliable imaging of small protrusions such as the TBs.

The animals underwent a surgical procedure in order to optically expose the brain surface above somatosensory cortex S1 and barrel fields. The *dura,* the outer membrane that protects the brain, is left intact. A cranial window is implanted and sealed to give chronic optical access for long term imaging experiments (Holtmaat et al., 2009). The technique is well established but was never carried out on aged animals before. This meant extra care had to be taken when handling animals from the Aged group and lowering the anaesthetic dose to the minimum necessary. Animals were allowed a two week recovery period after the surgery before the two-photon imaging protocol started. Such recovery period is needed to

allow for the post-surgical inflammation to completely wear out. Repeated two-photon *in vivo* imaging of axonal processes would then begin, every four days for a maximum span of twenty-four days, totalling 7 imaging sessions (Figure 3).

Imaged axons were mainly in *lamina* I and possibly in *lamina* II/III of the cortex, up to 150 μm deep from the *pia mater*, the innermost layer of the meninges covering the brain. Axons were chosen based on the length that could be followed, including side branches. The maximum traceable length is normally limited by the window area, local opacity, the axon going deep in the tissue, the axon disappearing beneath a blood vessel or by excessive density of the GFP labelled neuropil. Boutons on both EPB rich or TB rich axons were classified in two major groups and one subgroup according to their dynamic behaviour: boutons that were stably present for the whole duration of the imaging paradigm were defined as Persistent; on the contrary boutons that were not stable throughout the imaging sessions and that appeared or disappeared at least once were defined as Non-persistent. Within this second group a specific subset of boutons were identified as Destabilized: these were boutons that were found during all the first three imaging time points and were subsequently lost before the last day of imaging (Figure 3). The fact that these boutons were present for at least eight days (day 0 - day 4 - day 8) means that they are very likely to form stable functioning synapses. Previous electron microscopy work has shown how synaptic structures form complete synapses within four days of their appearance (Knott et al., 2006) and other studies have considered a similar relatively stable population of dendritic spines (Holtmaat et al., 2006).

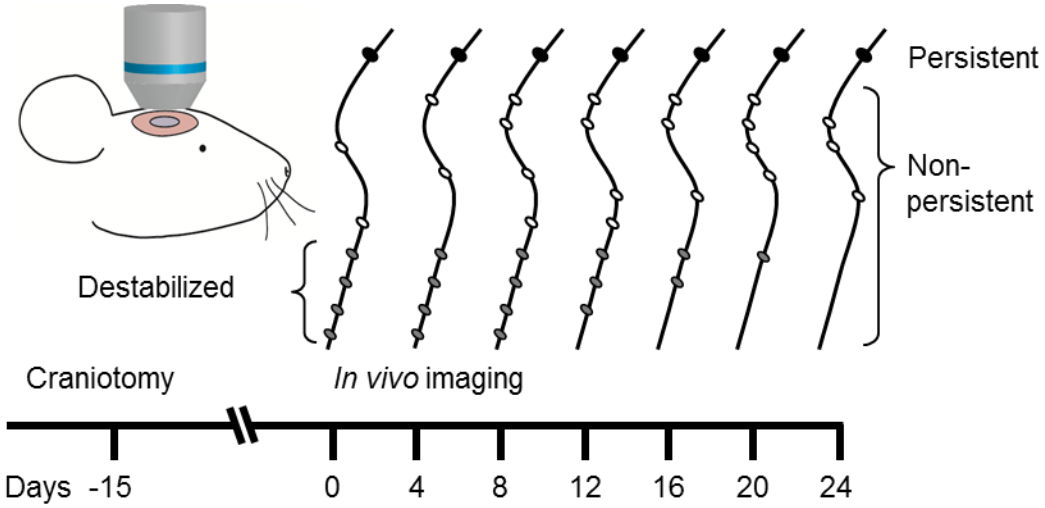

Figure 3 Imaging time line and bouton classification. After the surgical procedure to implant the cranial window the mice were allowed 15 days recovery. Imaging of the same axons was repeated every four days for a maximum 24 days (7 sessions). Axonal boutons were classified according to their dynamic behaviour. Persistent = present at every time point. Non-persistent = absent in at least one session. Destabilized = present on day 0, 4 and 8 (i.e., stable first 3 sessions) and subsequently lost.

Crucially, ageing is associated with cognitive decline (Burke and Barnes, 2006), (Barnes, 1979), (Morrison and Baxter, 2012), thus an important section of the study was dedicated to characterize the learning ability of the aged mice. To do so a behavioural task was designed to test the ability of the animals to recognize objects using their whiskers up to a day after having first experienced them. The tactile novel object recognition test was devised for the purpose of testing the animal's memory in the context of whisker sensation given that the *in vivo* imaged area is the primary sensory area for tactile and whisker sensation.

2. Materials and Methods

2.1 Animals

In this study male mice on a C57BL/6 background were used and housed in groups with at least one littermate, ranging from 2 to 4 mice per cage. Mice were housed in individually ventilated cages (IVC) containing wood chip bedding, nesting material, a wooded stick for chewing, a small cardboard tunnel and access to food and water *ad libitum*. In addition, a long maintenance diet was employed (R05-10 from SAFE, Scientific Animal Food & Engineering) to limit obesity for all mice. All cages were maintained in a 12 hour light-dark cycle. For the purpose of this study, two different age groups of animals were used: a Young and an Aged adult group. Young Adult mice were between 4 and 5 months old whilst Aged mice were between 22 and 24 months of age, approaching the average lifespan of C57BL/6 male mice (Selman et al., 2009). In addition to the two main age groups used, an extra cohort was employed in a small set of experiments with ages ranging between 12 and 14 months.

In order to visualize neuronal processes and synaptic elements, two distinct transgenic mouse lines were used, both expressing GFP in excitatory neurons under the Thy1 promoter. The Thy1-GFP-M (Feng et al., 2000) line was used to image *En Passant Boutons* (EPBs) which expresses a cytosolic form of EGFP (Enhanced Green Fluorescent Protein) in excitatory neurons, making it ideal for intensity related volume measurements of axonal varicosities. For the *Terminaux Boutons* (TBs) dataset the Thy1-GFP-L15 (De Paola et al., 2003) was employed which expresses a membrane bound form of EGFP ideal for tracing small protrusions (such as TBs). Both transgenic lines label the same neuronal populations, subsets of excitatory neurons in cortical (*laminae* 2/3, 5 and 6) and subcortical areas (e.g. thalamocortical projecting neurons).

All experiments were carried out, and measures to limit pain and discomfort were adopted, in accordance to the United Kingdom Animals Scientific Procedures Act of 1986. In addition all procedures were authorized and listed on a personal licence conducted within a project licence document.

2.2 Craniotomy

Cranial windows were implanted according to previously published protocols (Holtmaat et al., 2009) with a few modifications. Firstly, the mouse was anaesthetized in a chamber containing oxygen and 2% isofluorane and was subsequently given an intraperitoneal (I.P.) injection comprising a mix of ketamine (Ketaset – Fort Dodge Animal health) and xylazine (Rompun – Bayer) (0.083mg/g ketamine, 0.0078 mg/g xylazine) to induce general anaesthesia lasting just over an hour. The animal was then placed in a stereotaxic frame resting on a heated pad to maintain body temperature and eye ointment (Lacrilube - Allergan) applied to prevent dehydration. An intramuscular (I.M.) injection of Dexamethasone [Organon (~ 2 µg/g)], an anti-inflammatory agent, was administered into the quadriceps to reduce cortical stress during the surgery and limit potential cerebral oedema (Holtmaat et al., 2009). Finally, a subcutaneous (S.C.) injection of the anaesthetic bupivacaine [Taro pharmaceuticals (~ 1 µg/g)] was administered just below the ears. Bupivacaine exerts its effects via binding to the intracellular portion of sodium channels present on pain fibres (Wolfe and Butterworth, 2011) hence reducing post-surgical pain for up to 24 hours. Before surgery began, full anaesthesia and analgesia were verified by paw pinch. Next, the head was carefully washed with ethanol using cotton swabs to disinfect the area. Using surgical tools sterilized in a hot glass-bead sterilizer, an incision was made and a large portion of scalp removed to expose the skull above both brain hemispheres (Figure 4 a). The area exposed was enlarged by stretching the skin both sideways and long ways using cotton

swabs dampened with cortex buffer (see cortex buffer composition). The periosteum, a thin membrane covering the skull bones, was then removed by using dry swabs and eventually gently using a scalpel blade. A few drops of the local anaesthetic lidocaine [Hamlen pharmaceuticals (1% w/v)] (Wolfe and Butterworth, 2011), was added directly to the skull to reduce acute pain before displacing the right temporalis muscle using a sterile blunt-end dissecting tool. Next, a thin layer of n-butyl cyanoacrylate glue (Vetbond – 3M) was applied to seal the skin edges to the bone, to fill the gap resulting from displacing the temporalis muscle and also to cover the exposed bone area excluding the portion of the skull directly above the right barrel cortex (interaural – 1.5 mm from bregma, 3.5 mm lateral Figure 2 a). Once the cyanoacrylate layer had dried, using an air driven high speed dental drill, the region of interest was drawn out by incising a circular groove (Figure 4 b). This action was slowly repeated deepening the groove with cortex buffer regularly applied to limit overheating and clean away bone debris from the area. The drilling continued until the circular bone island (diameter ~ 3-4 mm) moved under slight pressure and, using sterile tissue forceps, was removed very carefully so as not to injure the *dura mater*, the outer most membrane of the meninges that protect the brain. The exposed *dura* was then cleaned with cortex buffer (see Table 1) and dried using small blocks of an absorbing gelatine sponge (Gelfoam) which also served to soak up any superficial bleeding. At this point a sterile circular glass coverslip (diameter ~5 mm) was placed over the exposed brain, with the overlapping edges lying on the bone. Care was taken to ensure cortex buffer filled the gap between the glass and the *dura* to avoid the cyanoacrylate glue to enter beneath the coverslip. Next, the surrounding skull was dried with cotton swabs and the window edges sealed to the skull using cyanoacrylate glue (Figure 4 c). Once the glue dried, the window was sealed with a thick layer of acrylic dental cement to cover the whole skinless area. The dental cement also provides a protective head-cap that includes a fixed titanium head-bar by which the animal can be attached to the microscope stage during subsequent imaging sessions (Figure 4 d). Once the dental cement started to solidify the animal was removed from the stereotaxic frame and placed in a heated (37° C) recovery box and continuously

monitored until recovery. Mice were allowed 15 days to recover from the procedure before imaging experiments were performed (Figure 4 e and f).

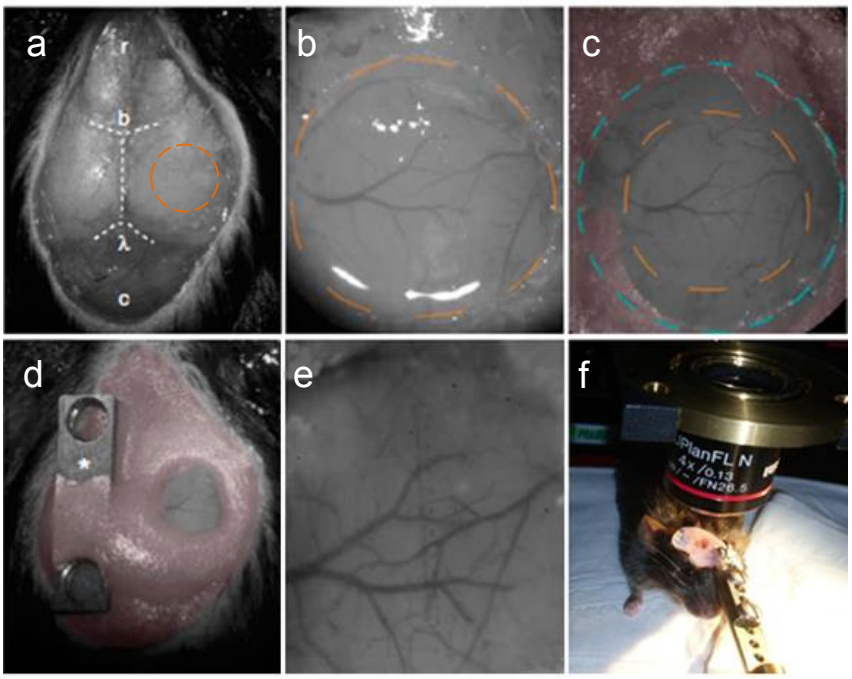

Figure 4 Chronic cranial window procedure. (a) The skull was exposed and a thin layer of cyanoacrylate glue was used to seal the skin edges and reposition the right temporalis muscle. The orange circle indicates where the window will be drilled. Dashed white lines indicate cranial structures b (bregma) and λ (lambda). (r, rostral; c, caudal). (b) After drilling (orange line) the bone flap was removed and the *dura* exposed, giving optical access to the cortex. (c) A circular cover glass (blue circle) was placed covering the window and was cemented. (d) The entire wound was covered with dental cement leaving the window clear. A titanium head bar (*) was positioned. (e) Bright field view of the blood vessels on the brains surface through the glass covered window. (f) The mouse was immobilised on the microscope stage through the head bar for *in vivo* imaging. Figure adapted from Holtmaat et al. 2009.

cortex buffer composition	
components	concentration in H_2O
NaCl	125 mM
KCl	5 mM
Glucose	10 mM
Hepes	10 mM
$CaCl_2$	2 mM
$MgSO_4$	2 mM

Table 1. Chemical composition of the Cortex buffer.

2.3 *In vivo* imaging

Imaging experiments in this study were performed using a commercially available two-photon laser scanning microscope (Prairie Technologies, Inc.) equipped with a tuneable Ti:Sapphire laser (Coherent, Inc.) and all images were acquired using the PraireView acquisition software. Similar to what occurs prior to surgery, each mouse was anaesthetised initially using an isofluorane chamber, followed by an I.P. injection containing a mixture of ketamine/xylazine (0.083 mg/g ketamine, 0.0078 mg/g xylazine). Once anaesthetised, the mouse was placed on a heat pad (37° C) under the microscope and fixed to a support via the head bar that was bound to the head cap during surgery. As described previously, the eyes of the mouse were coated with Lacrilube to prevent dehydration. Each imaging session lasted up to 1 hour, during which, the depth of anaesthesia was closely monitored. In the first imaging session a reference point using the blood vessel pattern was chosen, typically at the centre of the window. This was done using a 4X Olympus objective with a 0.13 numerical aperture and an easily recognizable blood vessel was picked, often a large vessel with a side branch. After taking a picture at low magnification the objective was replaced by a long working distance 40X Olympus objective with 0.80 numerical aperture. The blood vessel was centred and another bright field picture was taken. Finally a two-photon image was acquired of the same region as a reference for future sessions to reliably relocate the starting point.

The coordinates system implemented in the acquisition software were always reset to zero in this specific region in every subsequent session. The imaged axons were then picked on the basis of traceability, aiming to image the longest possible axons (360 μm ± 27 on average). All images of axons were acquired using a 910 nm wavelength laser beam never exceeding 70 mW of power at the back focal plane, to minimise photodamage. Image stacks were acquired at 4 times zoom factor (75.3 x 75.3 μm field of view, 512 x 512 pixels) and 1 μm step size in the z plane. Up to 40 image stacks per animal were acquired per session with the number of axons ranging from 1 to 8. Axons were followed for as long as possible including areas devoid of boutons. Typically, axon tracing during imaging was limited by a number of factors including image quality, density of GFP processes, reaching the window edge or by an axon going deep in the cortical tissue. Mice were then imaged every four days, up to and including twenty-four days (seven imaging time points).

2.4 Behaviour

In this study, the classical version of the visual object recognition test, as described in (Bevins and Besheer, 2006), was adapted so it would rely on tactile sensation, more related to somatosensory cortex. Experiments were performed in a 35 x 45 x 40 cm open field apparatus with opaque walls. The two object categories employed differed by surface texture only, which was either rough or smooth, whilst colour, size and shape were kept the same. The objects were custom made using 60 ml sample cylinders filled with salt and sealed, to increase their weight. The lateral area of the cylinders was covered with a sandpaper sheet using double-sided adhesive tape. Coarse P80 sandpaper (purchased at the local hardware shop) was used for the rough objects and superfine P1000 sandpaper for the smooth category. Two objects at a time were placed in the open field in a symmetrical position. The

behavioural test was then systematically performed following rigorous steps with some variants (Figure 5).

2.4.1 24 hour latency test

This trial consisted of three separate stages consisting of 1) familiarization, 2) presentation of sample and 3) the test phase, which was performed 24 hours after the initial two (Figure 5). The mice were collected from the animal house and transported to the behavioural room where they were left to acclimatise for at least 1 hour in individually housed cages before beginning the experiment. During the initial 5 minute familiarization trial, a single animal was placed in an empty open field free to explore the enclosed environment. After 5 minutes, the mouse was returned to its cage for a 3 minutes inter-trial period. Next, the sample stage was performed which consisted of three repeated trials, 6 minutes long and separated by 3 minute inter-trial periods. In each sample trial, each animal was presented with the same two identical objects and was free to explore them. These objects were either rough or smooth and alternated between mice to reduce bias. At the end of each sample trial and, prior to the next, the animal was returned to its individual cage for a 3 minute inter-trial period. At the end of the third sample trial, the animal was once again returned to its cage where it stayed for 1 hour before being placed back in the transport box. Between animals tested the equipment was thoroughly cleaned with 70% ethanol, to minimise contaminating odours that could bias the experiment. During the interim stages of the sample trials, the objects were removed and the open field floor was wiped with dry tissue paper to clean urine and faecal droppings. Following this, the objects were repositioned for the next sample trial. When all animals had completed their sample trials, they were returned to the animal facility and housed overnight in their home cages. 24 hours later, the mice underwent a test trial. Once again the animals were allowed 1 hour acclimatisation in individually housed cages prior to testing. During this test trial the animal was presented with two objects: the familiar object

and the novel object. To avoid olfactory recognition of the familiar object both objects placed in the open field during the test trial were brand new. The familiar object was identical to the objects experienced in the sample stages, either rough or smooth accordingly. The novel object had a different texture to the former. The fact that the familiar object is also new (but identical to the ones previously experienced) restricts discrimination to the tactile dimension. The test trial lasted 6 minutes after which the animal was returned to its cage. All trials were performed in the dark, to avoid visual recognition of the objects. In each trial the animal entered the open field from the same corner.

2.4.2 1 hour latency test

The 1 hour latency test was performed in a similar manner to the previous task where differing only in that the animals were tested 1 hour after completing the sample stage (rather than 24 hours). As before, mice were kept in their individual cages between the sample stage and the test trial.

2.4.3 Whisker trimmed animals

These animals were exposed to the standard 24 hour latency; however, their whiskers were depleted bilaterally prior to undertaking the sample stage.

To eliminate any visual cue all trials were performed in dark conditions, forcing the mice to rely on tactile discrimination to explore the objects. All trials were recorded using an infrared CCD camera suspended above the open field and illuminated with infrared light using an infrared LED lamp. The animals were tracked with AnyMaze software specifically designed for behavioural tasks. The exploration time was scored manually and recorded by the software by pressing assigned keys when the mouse's nose was in contact with the object and not when either they made contact using their paws or when they climbed on top of the

object. The discrimination index (DI) was calculated as: DI = ((novel exploration time/ total exploration time) – (familiar exploration time/ total exploration time)) x 100.

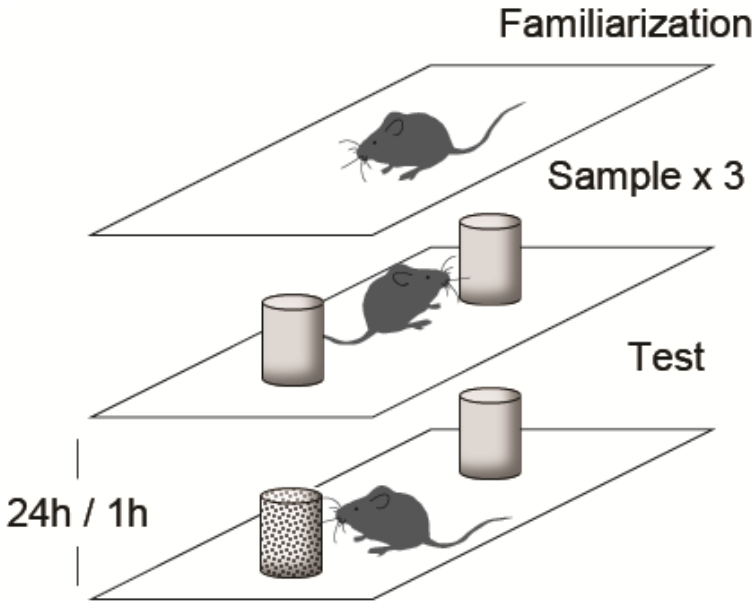

Figure 5 Tactile novel object recognition protocol. The behavioural task is divided in 3 different phases: 1) Familiarization, 2) Sample, 3) Test. In the familiarization phase the animal explores the empty open field. In the Sample phase the mouse explores the open field and 2 identical objects in it. The sample phase is repeated 3 times. The test phase can be delayed by 1 hour or 24 hours from the final sample trial. During the test trial the animal is presented with a familiar and a novel object that has a different texture (either rough or smooth).

2.5 Image analysis

In vivo two-photon images were processed and analysed using custom made software based on the Matlab (Mathworks) platform.

2.5.1 *Terminaux Bouton* rich axon analysis

The TB rich axon data set was analysed using the spine analysis software used previously (Holtmaat et al., 2009). All images were converted to 8 bit multi tiff stacks with the same region of interest (ROI) analysed simultaneously for each imaging time point. Before beginning, the lookup tables for each image were set so all time points are comparable in brightness and contrast. With this software, TBs were manually traced from the centre of the axonal shaft, from which they protrude, to the protrusion tip. The tracing followed the vectorial length of the TB without considering twists and turns, rather simply a straight line. The tracing was done in the planes that contain the brightest signal of the base and the tip of the TB meaning the tracing could start in one plane where the base and the axonal area around it were brighter and end on a different plane where the tip of the TB was brighter. Although, in this way, the tracing was effectively performed in 3 dimensions the software only counted the two dimensional length projections. The length was calculated in pixels which were converted to micrometres by setting the conversion rate depending on the size of the image field of view. All images in this study were acquired with a 75.3 x 75.3 µm field of view and a 512 x 512 pixel resolution, hence each pixel corresponded to 75.3/512 = 0.147 µm. Once all TBs had been traced in all time points they were correlated between sessions if they were retained, scored as gains when new ones appeared and scored as losses if previously present ones had disappeared. Because of the subjectivity involved in TB (or spine) analysis, a strict list of criteria was followed when performing annotations (see Figure 6). All protrusions or swellings along the axonal backbone of interest were annotated, whereby such structures had to be visible in at least two consecutive Z planes of the image

stacks. Whenever a new bouton was scored, i.e. a potential gain, extra care was taken to make sure that no pre-existing protrusion or swelling could have been missed in the previous image at the same location. The same principles were applied to any potential bouton loss, i.e. a previously present TB had to be lost beyond any doubt in the session of interest. After all protrusions of a particular region of interest for all time points were annotated, they were correlated between sessions to determine whether they were stable, gained or lost. Such procedure was based on the location of the structures and, whilst it is normally straightforward, a few particular cases apply (see Figure 6) such as a) Transitions between a TB protrusion and an EPB varicosity and vice versa were considered as stable, b) Two or more TBs could share their protruding point making it difficult to tell when a new bouton was added or removed, to be as conservative as possible these cases were considered as stable, c) if a new TB grew outwards from an existing TB it was considered individually, hence as a gain, the same applied for an existing TB branching off from another TB being lost, finally d) a TB found pointing outwards on the opposite side of the axonal shaft, but at the same axonal location, was considered as stable.

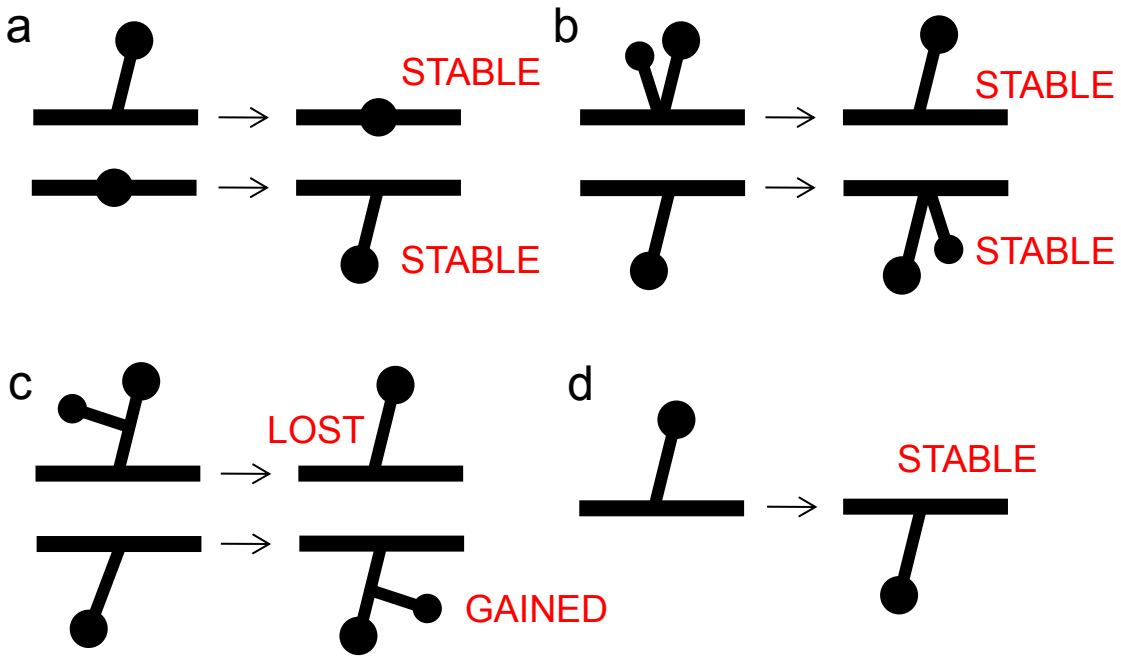

Figure 6 Schematic illustration of TB annotation criteria. (a) TB to EPB conversions, and vice versa, were considered as stable boutons. (b) TBs sharing the same base on the axonal shaft were considered stable when appearing or disappearing. (c) TBs arising from other TBs were considered separately hence their appearance or disappearance were counted as gains or losses. (d) TBs that appeared on the same axonal site but pointing in different directions were considered stable.

Once all the annotations were correlated, the axon was traced with a built-in polyline tool to extract the overall length of the axon of interest. The results expressed in length (μm) over time points (four-day intervals) were saved as a comma separated file (*.csv) and post-processed with Matlab to calculate the bouton dynamics parameters used in this study. The following criteria were applied to classify TBs as stable, gained or lost (Figure 7); a) to be included a TB had to be longer than 1 μm in length in at least one imaging session, b) if at any time point a TB exceed 5 μm in length it would be excluded and considered as an axonal branch, c) once included a TB would be considered stable as long as it were present in the annotations regardless of its length, d) a gain was assigned at the first time point of appearance, although a TB could reach its inclusion length of 1 μm only later on, e) a loss was assigned at the time point where the bouton ceased to be annotated, regardless of

length in the previous session and f) for density measurements all boutons were counted for each time point as long as they were present in that given time point regardless of length.

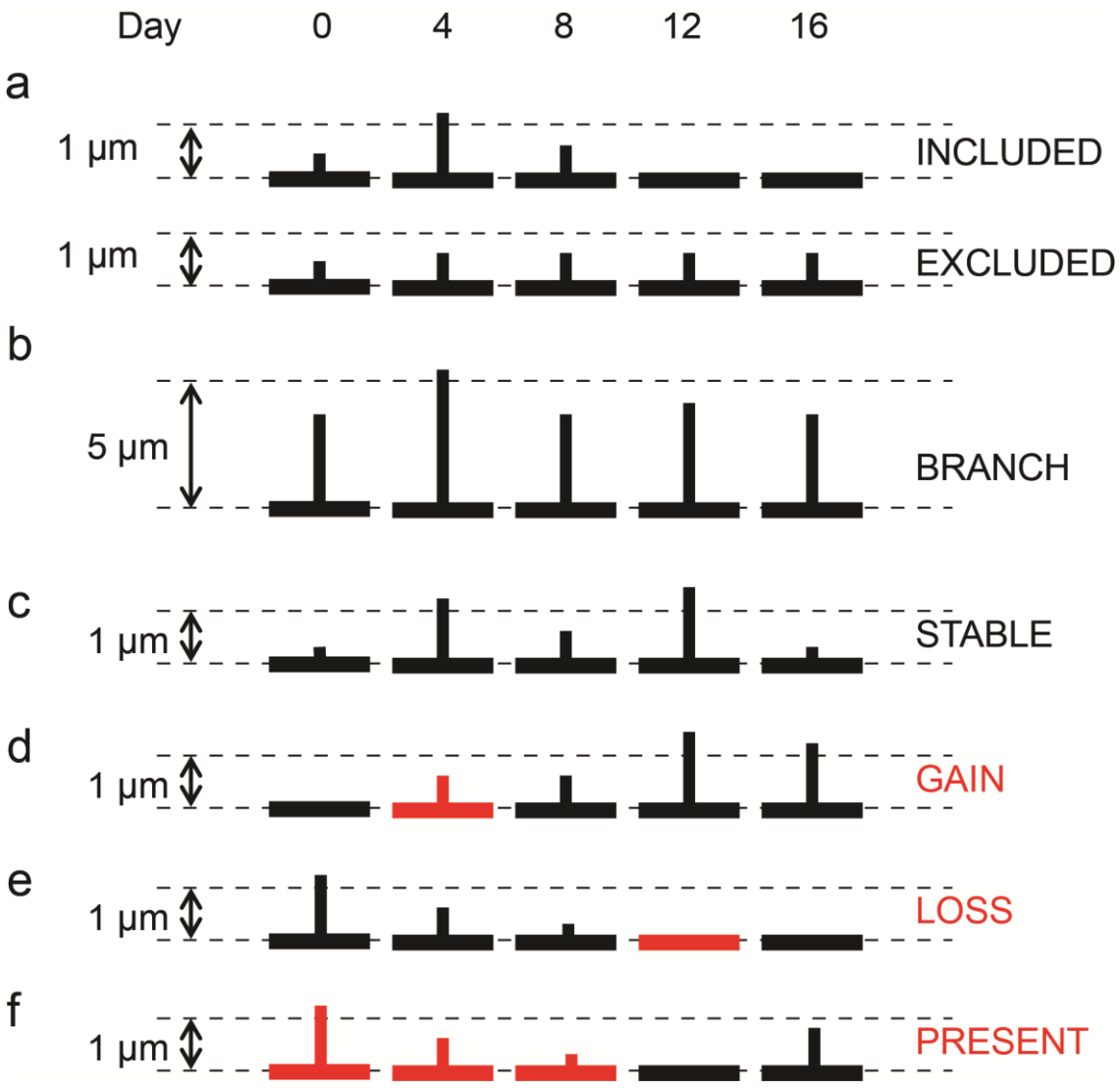

Figure 7 Schematic illustration of the criteria to score TBs. (a) Included TBs had to reach 1 µm in length in at least 1 session. The presence of the bouton was then "backdated" to the first session in which it was annotated regardless of its length. (b) If a protrusion exceeded 5 µm in length at any time point it was considered as a branch and included in the branch dataset. (c) TBs were considered stable provided they were included (over 1 µm at least once) and they were annotated in all sessions. (d) A gain was assigned when a previously not present TB reached 1 µm in length. The gain is scored when the TB first appeared. (e) A loss was assigned when a previously present TB disappeared completely. (f) TBs were considered present in a specific session provided they reached 1 µm in length in any session and that they were annotated in the session of interest regardless of length. Once lost a TB had to reach the 1 µm threshold again to be considered present. If it is lost and it does not reach the threshold subsequently the TB is not scored (as in the last two sessions).

2.5.2 Branch analysis

Branch data was extracted from the TB rich axon data and separately analysed in Excel (Microsoft Office 2010). The following criteria applied; 1) side protrusions had to be longer than 5 µm at any time point, 2) branches to be considered dynamic had to fulfil one of two previously published requirements based on elongation noise level estimation, a) the largest elongation or retraction event exceeded by 2 times the largest change in the noise measurement (2 x 3 µm = 6 µm), b) the average absolute length change was larger than 3 x the root-mean-square (σx) of the mean displacement (x) of 2 fiducial points (3 * σx = 1.6 µm) (De Paola et al., 2006).

2.5.3 *En Passant Bouton* rich axon analysis

Two-photon images of *en passant bouton* rich axons were analysed using a newly developed matlab based application, termed EPBscore, and developed in collaboration with Professor Sen Song's team (Beijing University). The software was designed to increase automation and decrease subjectivity. Images were initially grouped by ROI within a single folder containing all imaging time points of a specific axonal segment. All images were loaded in their original 16bit multi tiff (image stack) format, median filtered (radius = 7) and saved. The images were then displayed on the users screen in consecutive pairs as filtered maximum intensity projections whilst retaining full 3 dimensional information. At this point the axon of interest was automatically traced, either by manual editing for adjustments or completely manually traced if the result was unsatisfying. The software then shifted the linear tracing along the brightest pixels of the axonal extension obtaining an axon intensity profile. From such a profile, an estimation of the axonal backbone intensity could be extracted using the median intensity value of all pixels. The backbone intensity could then be used to normalize the intensity profile. The software recognized boutons by analysing the peaks in the intensity profile with the detection criteria previously set by the user to be, in this

study, fixed at twice the value of backbone intensity and at least 10 pixels in width for a bouton to be included. Once all these steps were completed for both images the user set a number of reference points (at least 2) to allow the program to align the two intensity profiles and correlate boutons between sessions. Both images and relative analysis were saved, with the first image closed and the second reopened to serve as the first image of the next pair and so on until all time points were analysed. The results are then displayed in the Matlab command line and exported to an Excel (Microsoft Office) data sheet for post-processing. All boutons were double checked to ensure that alignment issues did not arise, and the correct values were related to the correct individual bouton over time. Any mistakes detected were manually corrected. A second Matlab application was devised (also in collaboration with Professor Sen Song) to analyse the collected EPB data (normalized brightness over time) and calculate EPB dynamics parameters. The following criteria were employed (Figure 8); a) to be included an EPB had to be 2 times brighter than the backbone intensity in at least 2 consecutive imaging sessions, b) varicosities below the intensity threshold of 2 were not considered to be boutons, c) a gain was assigned at the time point when the EPB reached a normalized intensity value of 2, d) an EPB was considered lost when the intensity in its location dropped below the threshold of 2, and e) an EPB was considered stable when continuously detected at the same axonal location with a 2 μm shift tolerance on either side. EPB rich axon length measurements were performed in ImageJ using the NeuronJ plugin, a Java based neurite tracing tool available to download from www.imagescience.org.

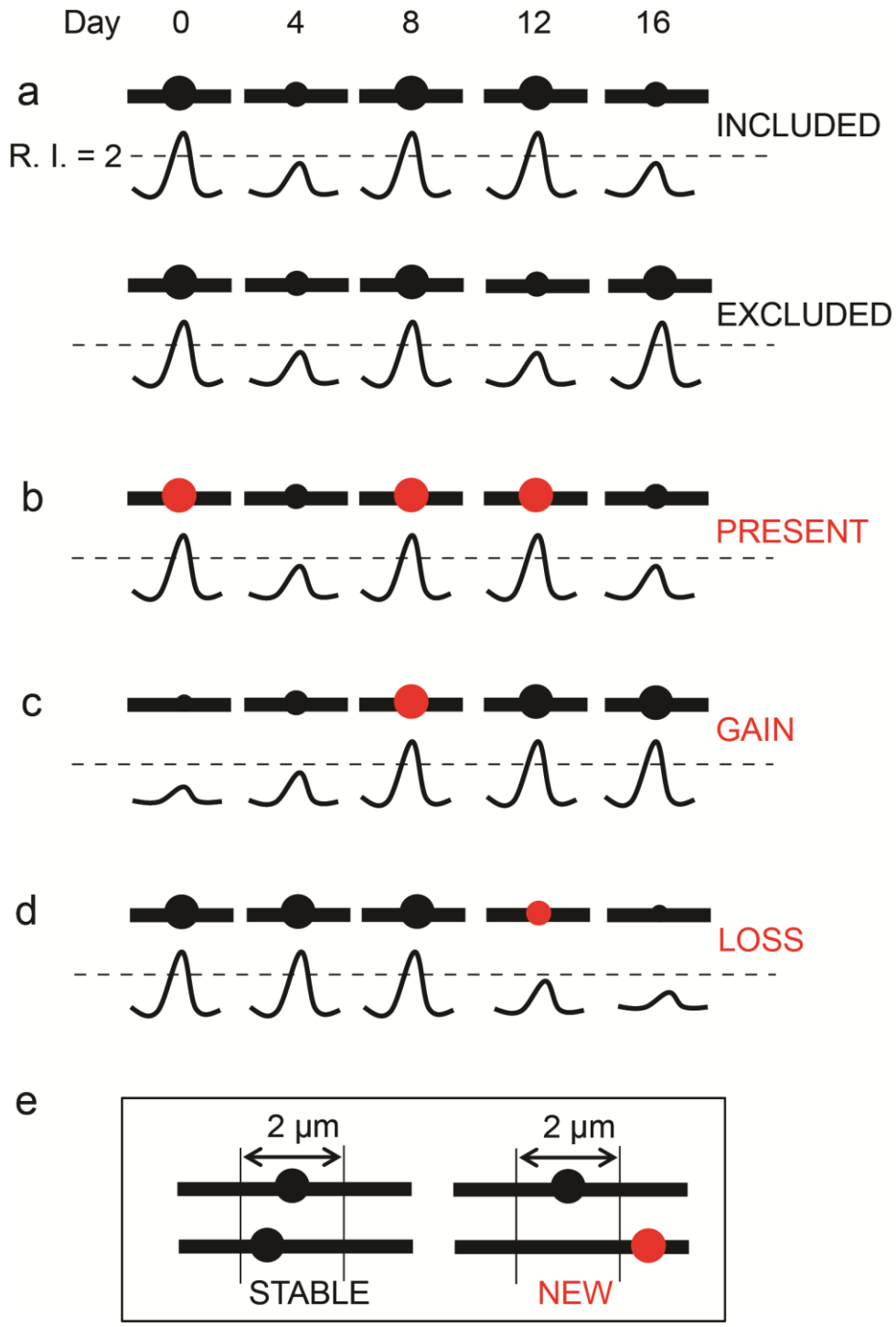

Figure 8 Schematic illustration of the criteria applied to all EPBs found with EPBscore to meet inclusion. (a) At any point an EPB had to reach the threshold of 2 backbone intensity units. Moreover this criterion had to be met in at least 2 consecutive sessions. (b) EPBs were considered present if they were above the intensity threshold (i.e. > 2 backbone units) and if they were present in at least 2 consecutive sessions at any time point in the same axonal location. (c) Provided the bouton is included, a gain is assigned when an EPB reaches the intensity threshold. (d) A loss is assigned whenever a previously present EPB drops below the intensity threshold. (e) A 2 µm shift tolerance threshold on the axonal shaft was applied to consider EPBs stable over time.

2.5.4 Definitions of dynamic parameters

- In order to study the behaviour of synaptic boutons and axonal branches a number of parameters were employed:
- Survival Fraction (SF): considers boutons imaged and scored on the first day of imaging (day 0), i.e., the initial boutons. $SF_{(t)} = N_{(t)}/N_{(0)}$, where $N_{(0)}$ is the number of boutons at t = 0 (initial boutons) and $N_{(t)}$ is the number of initial boutons surviving after time = t.
- Destabilization probability (DP): considers a relatively stable population, i.e., boutons imaged and scored in the first three imaging sessions (days 0 to 8) and then lost by the end of the imaging protocol. DP = SB_L / SB, where SB is the total number of boutons that were stable the first 8 days and SB_L is the number of SBs lost by day 24.
- Destabilization density (Dd): considers the same boutons as above but normalizes the number of destabilization events by unit length of axon. Dd = SB_L / µm.
- Stabilization rate (SR): considers the boutons that were gained in the day 4 to day 16 window still present at the final time point (day 24). SR = GB_{ST} / $GB_{(4\text{-}16)}$, where $GB_{(4\text{-}16)}$ is the total number of boutons gained (day 4 to 16) and GB_{ST} is the number of $GB_{(4\text{-}16)}$ stable at day 24.
- Persistence rate (PR): considers all boutons gained and how many of these persist for at least two further sessions (8 days). PR = $GB_{(8d)}$ / GB, where GB are all gained boutons and $GB_{(8d)}$ the number of GBs that persisted for at least 8 days.
- Gains fraction (GF): considers the proportion of new boutons that appear between consecutive time points. $GF_{(a\text{-}b)} = nG_{(b)} / nT_{(a)}$, where $nT_{(a)}$ is the total number of boutons in the previous session (a) and $nG_{(b)}$ is the number of boutons gained in session b.
- Losses fraction (LF): considers the proportion of boutons that disappear between consecutive time points. $LF_{(a\text{-}b)} = nL_{(b)} / nT_{(a)}$, where $nT_{(a)}$ is the total number of boutons in the previous session (a) and $nL_{(b)}$ is the number of boutons lost in session b.
- Turnover Rate (TOR): considers both gains and losses at a given time point. $TOR_{(a\text{-}b)} = nG_{(b)} + nL_{(b)} / 2nT_{(a)}$. It is a measure of bouton replacement.

- Gains density (Gd): considers the number of bouton gains normalized per unit length of the axon. $Gd_{(a\text{-}b)} = nG_{(b)}$ / µm.
- Losses density (Ld): considers number of bouton losses normalized per unit length of the axon. $Ld_{(a\text{-}b)} = nL_{(b)}$ / µm.
- TOR density (TORd): considers the sum of gains and losses normalized per unit length of the axon. $TORd_{(a\text{-}b)} = nG_{(b)} + nL_{(b)}$ / µm.
- Intensity Ratio (IR): measures the intensity variation of individual EPBs between consecutive time points regardless of direction; i.e., the largest intensity value divided by the smallest. $IR_{(a\text{-}b)} = \exp|Log_{(int\ a)} - Log_{(int\ b)}|$, where Log is the natural logarithm of intensities at session a (int a) and b (int b).
- Absolute Intensity Difference (ID): measures the absolute change in intensity of an individual EPB between consecutive time points regardless of direction. $ID = |I_{(a)} - I_{(b)}|$, where I is the intensity in sessions a and b.
- Dynamic fraction (DF): expresses the proportion of branches that undergo structural remodelling, beyond the noise level of length measurements, at any imaging time point. DF = *n*DBr / *n*Br, where *n*Br is the total number of branches and *n*DBr is the number of branches that displayed either elongation or retraction during the imaging
- Absolute length change (AL): Asses the change in length of the dynamic fraction of branches between sessions (four day interval) regardless of the direction (retraction/elongation). $AL = |L_{(a)} - L_{(b)}|$, where L is the length in µm of an individual branch at time points a and b.

2.6 Transcardial perfusion

Transcardial perfusion was performed when animals completed the imaging paradigm and the behavioural protocol, in order to collect and store the fixed brain. In some cases the cranial window clarity would deteriorate impeding two-photon imaging and, in such cases, these animals were perfused earlier and used for the immunohistochemistry experiments to assess astrocytic reaction during the imaging period (Figure 42). Mice were first anaesthetized with isofluorane followed by an I.P. injection of ketamine / xylazine (0.3 mg/g and 0.04 mg/g respectively) for terminal surgery. Deeply anaesthetized mice were immobilized to the operating surface and the pulsating heart was exposed by opening the ribcage. The perfusion needle was placed into the left ventricle to deliver the fixative solution (4% PFA w/v dissolved in PBS and sterile filtered pH 7.4) and the right atrium was punctured to allow exchange of blood from the circulatory system with fixative. Between 20 and 30 ml of fixative were delivered per animal at a constant rate of 5 ml per minute. Next, the brain was extracted and placed in a 20 ml tube filled with fixative solution where it was post-fixed overnight at 4 °C gently shaking. The following day the brain was washed with Phosphate Saline Buffer (PBS) and stored in PBS with 0.01% w/v azide at 4 °C.

2.7 Immunohistochemistry

Brains were immersed in 30% w/v sucrose PBS solution overnight for cryoprotection. The following day the brains were embedded in OCT (Optimal Cutting Temperature) embedding media (R A Lamb) and frozen with dry ice. 20 μm thick frozen coronal sections were cut using a cryostat (Leica), mounted on glass slides and stored at -20 °C. The sections collected included the cortical regions immediately below the cranial window with the opposing contralateral regions on the left hemisphere. The next day, sections were washed

3 times with PBS for 5 minutes and subsequently incubated overnight at 21 °C with the primary antibody solution (Triton-X 0.1% and Azide 0.01% in PBS). Sections were washed three times with PBS for 5 minutes to remove the primary antibody before the addition of secondary antibody solution (Triton-X 0.1% and Azide 0.01% in PBS) followed by incubation for 2h in the dark at 21 °C. Later the sections were washed as described previously (3 times in PBS) and finally a DAPI staining was performed by briefly applying a 1:1000 DAPI solution in PBS for a few seconds, before washing with PBS. The sections were then mounted with Dako mounting media and covered with a glass coverslip that was sealed with nail varnish. The antibodies employed were: primary rabbit anti Glial Fibrillary Acidic Protein (GFAP - DakoCytomation, Denmark) diluted 1:1000; secondary Cy3.5 anti-rabbit diluted 1:500 (Genetex, USA).

2.8 Confocal imaging

A Leica SP5 confocal microscope was used to image labelled astrocytes (GFAP positive cells). Images were acquired using a 10x objective with a 1.55 mm x 1.55 mm field of view for a general image of the ipsilateral and contralateral region of interest. The sampling images were acquired using a 20x lens with a zoom factor of 2, for a resulting field of view of 387.5 x 387.5 µm (surface 0.15 mm^2). All images were acquired with a 1024x1024 pixel resolution. The sampled images were chosen to include the cortical surface and to fall in the middle of the window area, where *in vivo* imaging would take place, avoiding the window edges where more damage was likely to have occurred. For each image collected in the area of the viewing window, a comparable image was taken on the contralateral side. Two ipsilateral and two contralateral images were acquired per section consisting of four focal planes 0.5 µm apart. A sequential scan was adopted to better separate the signal coming from the DAPI and the Cy3.5 fluorophore. These images were then analysed by an

automated routine implemented in CellProfiler with cells identified by the presence of the DAPI nuclear staining. The number of nuclei that colocalized with the red fluorescent signal were counted as astrocytes.

2.9 Statistics

Statistical analysis was carried out using either Microsoft Excel 2010 or Matlab 2010a. The novel object recognition test analysis was performed in Excel, and a two-way analysis of variance (ANOVA) was used within groups to determine whether the novel object was preferentially explored during the test. The discrimination indexes (see above) were calculated for Aged and Young Adult groups and compared with an unpaired t-test. Axon dynamics parameters were found to have a non-normal distribution, therefore non parametric tests were employed using Matlab. All parameters presented (i.e., absolute intensity ratios, turnover rate, destabilization probability, bouton density, bouton intensity, branch density, branch length, branch dynamic fraction, branch absolute length change), except for the survival fraction curves, which were analysed with a log rank test, were analysed with the Wilcoxon Rank-Sum test. The immunohistochemistry data were analysed using unpaired t-tests. Data are shown as mean ± standard error of the mean unless otherwise stated.

2.10 Electron Microscopy

Electron Microscopy (EM) imaging of axonal boutons was carried out in the laboratory of Dr. Graham Knott in the Centre of Interdisciplinary Electron Microscopy at the École Polytechnique Fédérale in Lausanne. Nine boutons imaged *in vivo* in the Young Adult brain were reconstructed using Serial Section Electron Microscopy (SSEM). Animals were perfused soon after the imaging session with 200 ml of 0.2% v/v gluteraldehyde and 2% w/v paraformaldehyde in a 0.1 M Phosphate Buffer (PB) solution with a pH of 7.4. Following fixation the brains were sectioned tangentially to the imaging window in 60 µm thick slices, which were cryoprotected in 2% v/v glycerol and 20% v/v Dimethyl sulfoxide (DMSO) diluted in 0.1 M PB. The sections were subsequently freeze-thawed in liquid nitrogen. In order to identify two-photon imaged axons at the EM level a GFP immunostaining protocol was employed to associate the fluorescent protein with an electron dense precipitate visible in light microscopy as well as in transmission EM. Sections were incubated over night with the primary antibody (rabbit anti-GFP, Chemicon) in PBS 1:600 at 4 °C. The sections were then incubated for 2 hours at 21 °C with the biotinylated secondary antibody (goat anti-rabbit (F)ab fragment, Jackson Laboratories) diluted 1:500 in PBS. Labelling was then revealed by precipitation of 3, 3'-diaminobenzidine tetrachloride (DAB – Fluka) through reaction with avidin biotin peroxidase complex (ABC Elite, Vector Laboratories) in 0.015% v/v hydrogen peroxide in PBS. The sections were then washed in PBS and postfixed in osmium tetroxide and embedded in Epson resin (Fluka). The axons that were imaged *in vivo* were localized in the sections with the aid of anatomical features such as blood vessels and adjacent labelled dendrites. Once the region of interest was located, 60 nm thick serial sections were cut and collected on carbon coated pioloform membranes. Serial images were acquired in a Philips CM12 transmission electron microscope.

The two boutons reconstructed at the ultra-structural level from Aged brains were obtained with the Focused Ion Beam Scanning Electron Microscopy (FIBSEM) technique (Knott et al., 2011), coupled with the Near Infrared Branding (NIRB – Figure 9) of the region of interest

(Bishop et al., 2011). The two boutons (Figure 9) were adjacent on the axon imaged in the intact brain of an aged mouse. On post-natal day 768 (25.6 months old) the animal was imaged and subsequently perfused with 200 ml of a 2.5% v/v gluteraldehyde and 2% paraformaldehyde w/t PBS solution (0.1 M), at a rate of ~ 10 ml per minute. Once perfused the brain was allowed to postfix at room temperature without being extracted. The brain was then extracted and washed three times in 20 ml PBS 0.1 M. Sections were then obtained cutting tangentially (Figure 9 a) to the cortical surface in correspondence of the craniotomy using a vibratome (Leica). 60 μm thick sections were collected; images of each section were acquired on a dissection scope (Leica) at a low magnification (~ 6-7 X). The images were then overlaid, in the correct order, and aligned to reconstruct the cortical area below the imaging window (Figure 9 a). The blood vessel picture taken during the *in vivo* experiment as a reference for the two-photon imaging was used to align the two-photon images with the sliced brain images (Figure 9 a). By doing so it is possible to locate the imaged axons on the cut slices. Once the correct slice is identified (Figure 9 b and c) the axon and boutons of interest were found using the two-photon microscope (Figure 9 d and e). To aid the localization and reconstruction at the EM level the area around the synaptic boutons of interest was branded with the laser. A large NIRB mark was induced using repeated laser line scans (~ 1000 repetitions) at high power using a 60x lens with a digital zoom factor of 2 (Figure 9 d). This first mark was on a different focal plane of the axon of interest, roughly 10 μm above the imaged structures. A second NIRB mark was induced with a higher zoom factor (zoom 6) and at the same focal plane of the axon to precisely locate the structures of interest (Figure 9 e). The NIRB marks were designed to be asymmetric (indent in the top right corner) to avoid confusion in orientation. The marks are visible both in bright field and at the EM level; they constitute reliable fiducial points in order to correlate two-photon and EM imaging of synaptic structures. The section was then sent to Lausanne where Dr. Graham Knott and colleagues embedded the sample and prepared it for the FIBSEM setup (NVision 40 FIBSEM, Zeiss NTS). Serial images in a FIBSEM setup are acquired by scanning the top

surface of a tissue block. The acquired surface is then removed by an ion beam revealing the next plane to be acquired.

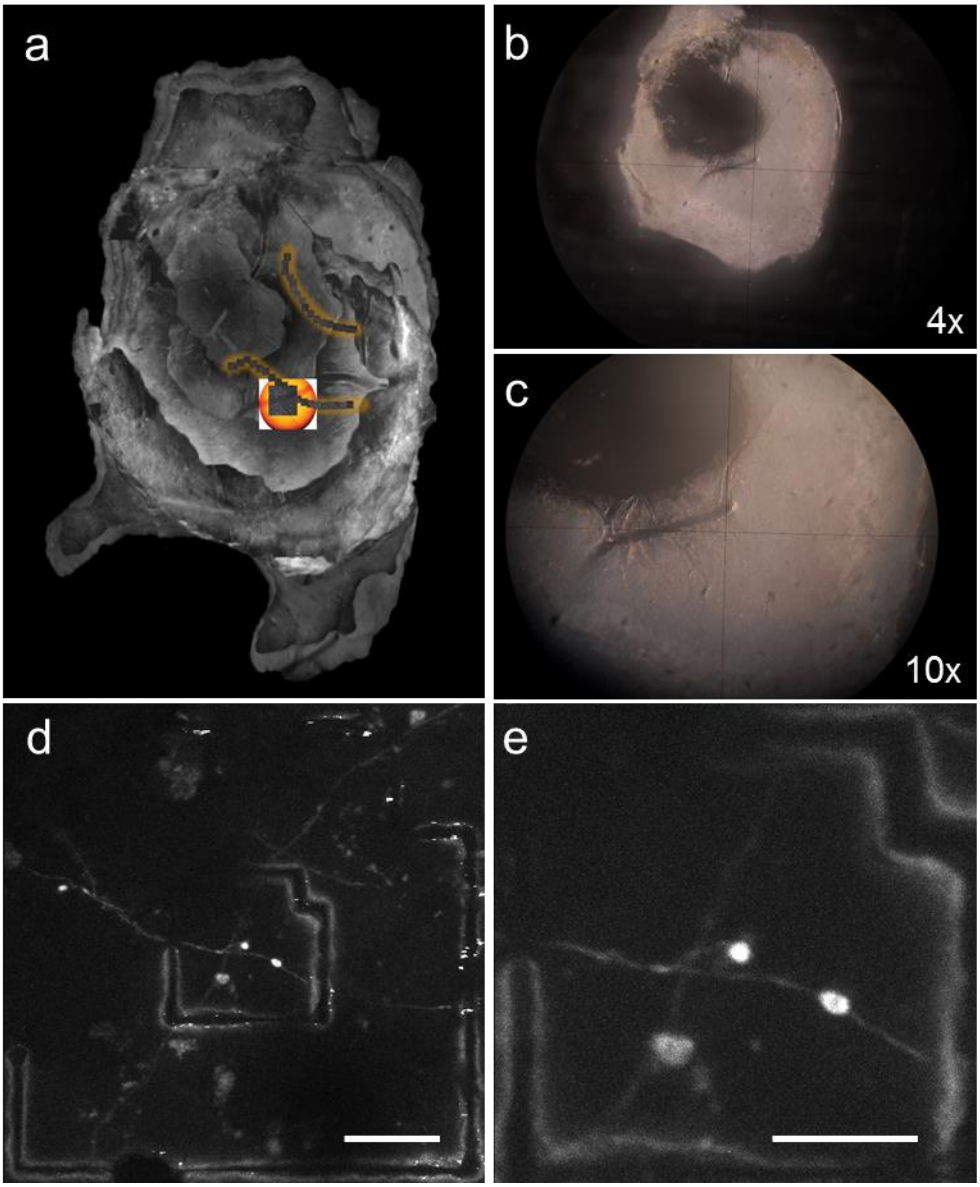

Figure 9 NIRBing protocol steps. (a) Tangential slices (60 µm thick) of the *in vivo* imaged cortical area. The slices were overlaid using Adobe Photoshop and aligned with the blood vessel reference picture (taken *in vivo*) and the two-photon ROIs. (b) The slice containing the ROI is selected, and a picture taken with a 4x lens. (c) The blood vessel provides a cue for the ROI location (centre of the cross). This image was taken with a 10x lens. (d) Two-photon image (60x lens, zoom 2) of the NIRBed (large and small marks) area containing the ROI with the two boutons, scale bar 20 µm. (e) Higher magnification (60x lens, zoom 6) with small NIRB mark used for subsequent fine location of the structures of interest, scale bar 10 µm.

All 11 boutons were reconstructed in three dimensions using the TrakEM2 ImageJ plugin directly from the EM micrographs. The volume of each bouton was calculated in cubic micrometres. The volume of mitochondria was also calculated when present, in order to exclude it from the total bouton volume calculations. The reconstructed models were rendered in the Blender software (version 2.57; Blender Foundation, http://www.blender.org).

3. Terminaux bouton rich axons

3.1 Introduction

TB rich axons are characterized by the presence of many spine-like protrusions emanating from a thin (compared to a dendrite) axonal shaft. TB rich axons are a minority when compared to EPB rich axon numbers in *lamina* I. TBs and EPBs can be found on the same axons, though TB rich axons are characterized by a high density of TBs (> 70 TBs per mm), while EPB rich axons present few TBs (De Paola et al., 2006). It has been proposed that TBs on *lamina* VI pyramidal cell axons preferentially form dendritic shaft synapses, to reduce axonal tortuosity (McGuire et al., 1984). However, a more recent report has challenged this view, showing that TBs and EPBs, on *lamina* II/III and IV cell axons, form similar proportions of spine and shaft synapses (Anderson and Martin, 2001). In previous studies in the adult mouse, TB rich axons have been described to be highly dynamic in terms of bouton turnover [> 50% over one month (De Paola et al., 2006)]. The same study showed evidence that, in the Thy1-GFP transgenic mouse lines, these axons observed in *lamina* I derive from neurons that have the cell body in cortical *lamina* VI, the deepest layer of the cortex. Because of the high degree of bouton remodelling, this axon class represented a possible target for ageing related bouton plasticity dysfunction. The data presented in this section was collected from 6 Young Adult animals and from 7 Aged animals. Because most of the Aged group did not reach the final imaging time point, the data presented considers only the first 6 imaging sessions, from day 0 to day 20.

3.2 Comparable branch dynamics in Young Adult and Aged mice

The first axonal structures taken into consideration were side branches of TB rich axons (Figure 10). Although it is well established that axonal arbors are relatively stable in the adult cortex in the absence of peripheral input depletion (De Paola et al., 2006; Stettler et al., 2006), a subset of these branches undergoes significant elongation or retraction over tens of microns, over a few days, in baseline conditions (De Paola et al., 2006). Based on previous work (De Paola et al., 2006) the length threshold to consider a side protrusion a branch was set at 5 μm, and such length had to be reached in at least one imaging session. This classification is based on the fact that branches longer than 5 μm are unlikely to be replaced, while shorter TBs are replaced frequently at high rates (De Paola et al., 2006).

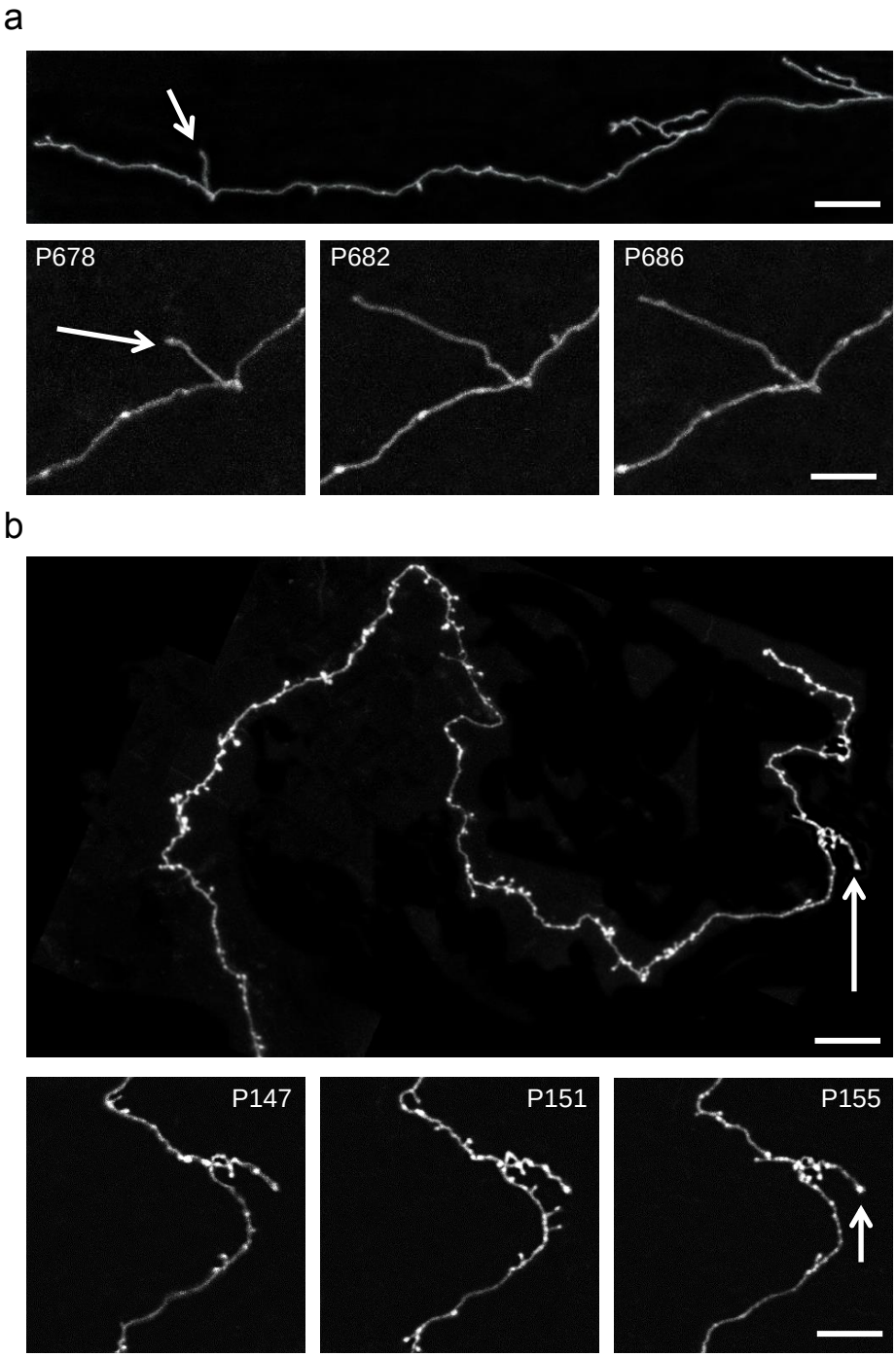

Figure 10 Representative axonal branches present on layer 6 TB rich axons imaged in layer 1 of somatosensory cortex. (a) Low magnification (above, scale bar 20 μm) of an axon in the Aged brain with a branch indicated by the white arrow. Below, higher magnification (scale bar 10 μm) time series (postnatal day indicated) of the branch showing active elongation in an Aged animal. (b) TB rich axon in the Young Adult brain with a side branch. In the time series the branch appears to be static over the indicated time points. (scale bars 20 μm above and 10 μm below.

Surprisingly, the branch density (number of branches per unit length) and the average length were found to be comparable between Aged and Young Adult mice (Figure 11; n = 72 branches, 7 axons, 7 Young Adult mice and n = 109 branches, 10 axons, 7 Aged mice; Young Adult average branch density = 0.014 ± 0.004 branch/µm, Aged average branch density = 0.018 ± 0.002 branch/µm; *P* = 0.22; Figure 11 a). The average length of branches in the two age groups was not significantly different (Young Adult = 5.42 ± 0.28 µm, Aged = 5.31 ± 0.28 µm; *P* = 0.44; Figure 11 b).

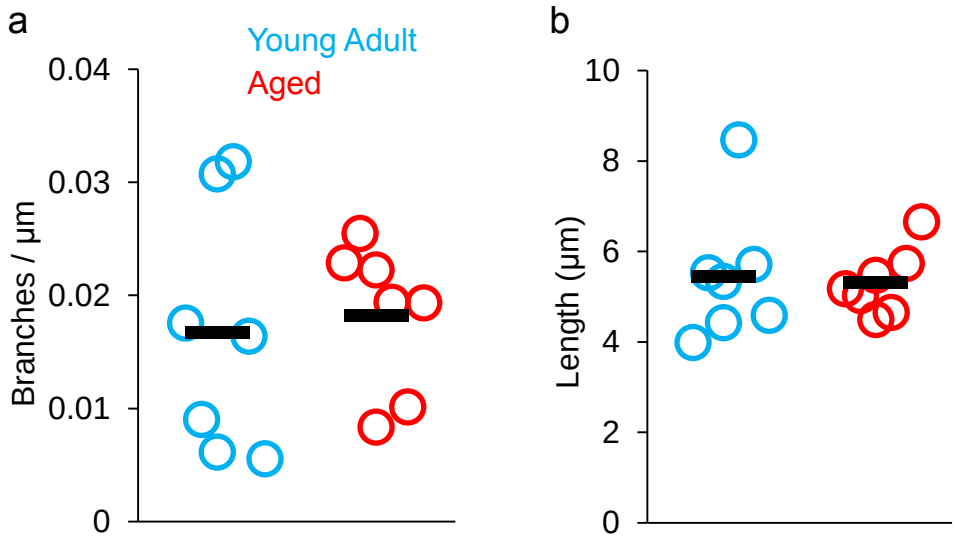

Figure 11 Layer 6 TB rich axons have similar branch density and average branch length in Young Adult (n = 7) and Aged (n = 7) mice. (a) Density of side protrusions (longer than 5 µm at any time) is comparable between age groups. (b) Average length per animal of side branches in TB rich axons is similar in both age groups. Blue markers (left) YA, red markers (right) Ag, Black markers are mean values for the corresponding group.

Besides branch density and branch length, two dynamic parameters were considered: the fraction of dynamic branches and the average absolute length change of dynamic branches (see methods for definition). A subset of branches was dynamic in baseline conditions. The proportion of dynamic branches is represented by branches that actively retract or elongate.

A previously published criterion, based on the calculation of the average noise level in the neuronal processes length measurements (see methods section), was used to score dynamic branches (De Paola et al., 2006). The dynamic fraction of branches on TB rich axons in Aged and Young Adult animals was comparable (Young Adult = 0.48 ± 0.13 dynamic branches / total branches, Aged = 0.45 ± 0.06 dynamic branches / total branches; *P* = 0.56; Figure 12 a). Interestingly, these branches actively elongated or retracted at similar rates in both age groups. Over a four-day period, the Young Adult cohort exhibited an average absolute length change (absolute difference of length between sessions, |a-b|) similar to the average length variation seen in the Aged animals (Young Adult = 3.03 ± 0.27 µm; Aged = 3.09 ± 0.33 µm; *P* = 0.94; Figure 12 b).

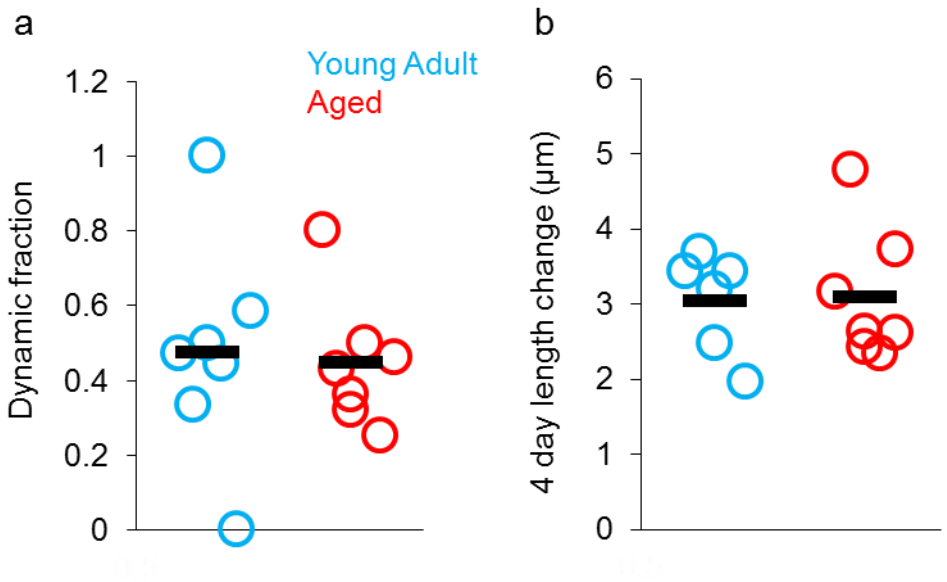

Figure 12 Side branches in the Aged (n = 7) mouse brain retain basal active dynamics found in the Young Adult (n = 7) brain. (a) The fraction of dynamic branches (those that actively elongate or retract beyond random noise levels) is comparable in Young Adult and Aged animals. (b) Average length change of side branches per animal between imaging sessions (absolute length difference). Young Adults and Aged mice have similar rates of active elongation and retraction of side branches. Blue markers (left) YA, red markers (right) Ag, Black markers are mean values for the corresponding group.

Surprisingly, these results provide evidence that active elongation and retraction are still taking place in the ageing brain in a specific subset of axons in *lamina* I of the somatosensory cortex. These changes occur at similar rates when compared to brains from younger adult mice, with balanced growth and retraction resulting in constant average length in both age groups (Figure 13). In Young Adults, the average branch length was 5.5 ± 0.48 µm on day 0, 5.4 ± 0.49 µm on day 4, 5.1 ± 0.48 µm on day 8, 4.8 ± 0.42 µm on day 12, 5.2 ± 0.52 µm on day 16, 5.9 ± 0.9 µm on day 20; in Aged mice the average branch length was 5.1 ± 0.26 µm on day 0, 5.2 ± 0.28 µm on day 4, 5.4 ± 0.20 µm on day 8, 5.6 ± 0.52 µm on day 12, 5.1 ± 0.37 µm on day 16, 5.3 ± 0.47 µm on day 20; (P = 0.78 and P = 0.91 for Young Adult and Aged groups respectively, one way ANOVA).

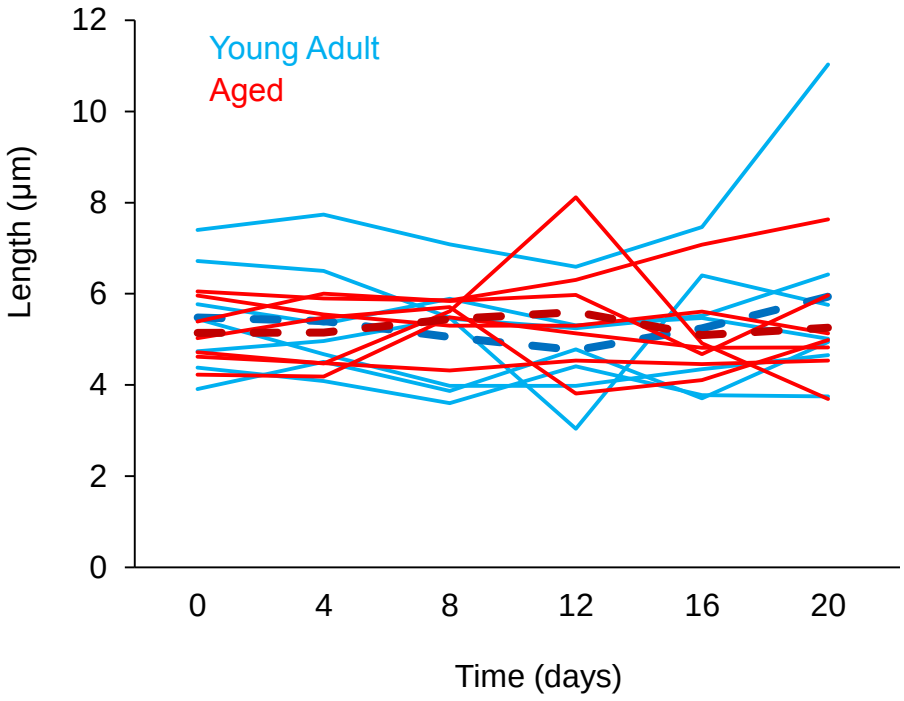

Figure 13 The average length of side branches on TB rich axons in Aged (n = 7, red lines) and Young Adult (n = 7, blue lines) mice is comparable and constant over time (20 days, 6 imaging sessions). Dashed lines represent the average length of branches across age groups, red Aged, blue Young Adult.

3.3 Similar TB density in Aged and Young adult mice

TB rich axons are characterized by a relatively high proportion of TBs [typically with density > 0.07 TBs per micron, (De Paola et al., 2006)]. Bouton densities can vary greatly between regions of the same axon, with some portions completely void of boutons and others densely packed. Because of such dis-homogenous distribution of boutons, it is important to image relatively long segments of the axon (> 300 µm). For the TB rich axon dataset a total of 13 animals were imaged: 7 Young Adults with 7 axons spanning 4.2 mm and comprising 692 TBs, 7 Aged mice with 10 axons for a total length of 5.1 mm and 720 TBs. The TB density on axons imaged in *lamina* I of somatosensory cortex was comparable between age groups (Young Adults = 0.17 ± 0.02 TB/µm, Aged = 0.14 ± 0.01 TB/µm; $P = 0.58$; Figure 14 a). Furthermore, these values remain constant over time (Figure 14 b) for both age groups. No net bouton gain or loss was detected over time: in Young Adults, the TB density was 0.16 ± 0.02 µm on day 0, 0.17 ± 0.02 µm on day 4, 0.17 ± 0.2 µm on day 8, 0.17 ± 0.2 µm on day 12, 0.17 ± 0.2 µm on day 16, 0.16 ± 0.1 µm on day 20; in Aged mice the average TB density was 0.14 ± 0.1 µm on day 0, 0.14 ± 0.01 µm on day 4, 0.15 ± 0.1 µm on day 8, 0.15 ± 0.1 µm on day 12, 0.14 ± 0.1 µm on day 16, 0.14 ± 0.1 µm on day 20; ($P = 0.99$ and $P = 0.98$ for Young Adult and Aged groups respectively, one way ANOVA).

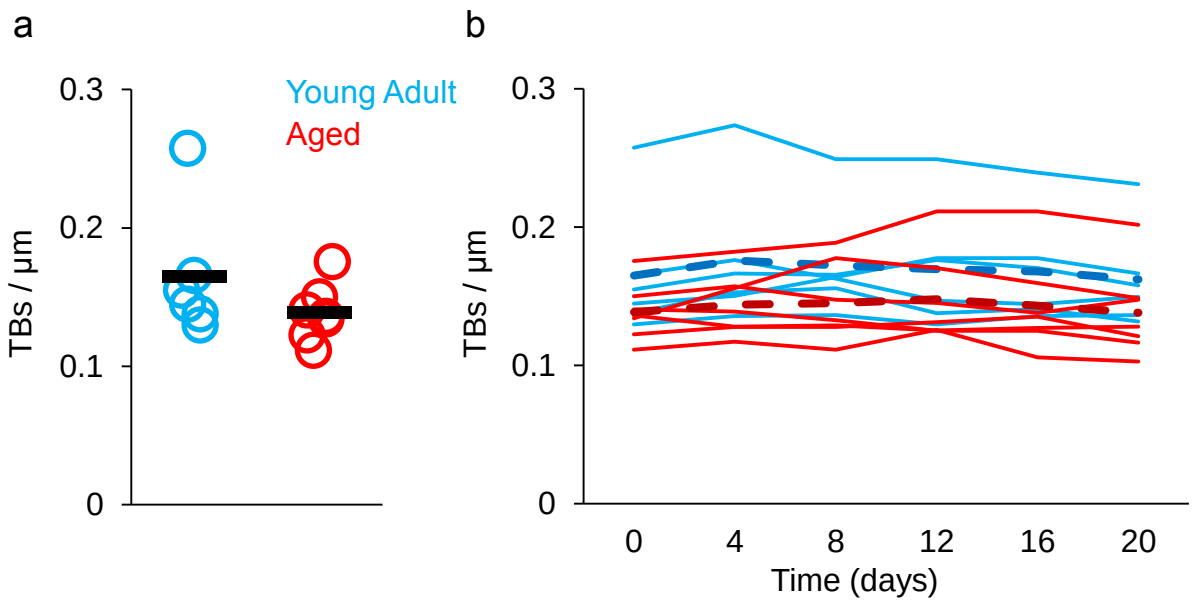

Figure 14 TB density is similar and constant over time in the Aged (n = 7) and in the Young Adult (n = 7) cortex. (a) The average density per animal is comparable between age groups. Blue markers (left) YA, red markers (right) Ag. Black markers are mean values for the corresponding group. (b) The average density is constant over time (20 days, 6 imaging sessions) for both age cohorts. Aged animals red lines, Young Adult animals blue lines, dashed lines are mean values for each group.

3.4 Similar TB dynamics in the Aged and Young Adult cortex

TB rich axons have been described as highly dynamic, with TBs potentially undergoing an almost complete turnover within 2 or 3 months (De Paola et al., 2006). These fast structural rearrangements (Figure 15) appear to be unaffected by the ageing process since there were no major differences between Young Adult and Aged mice.

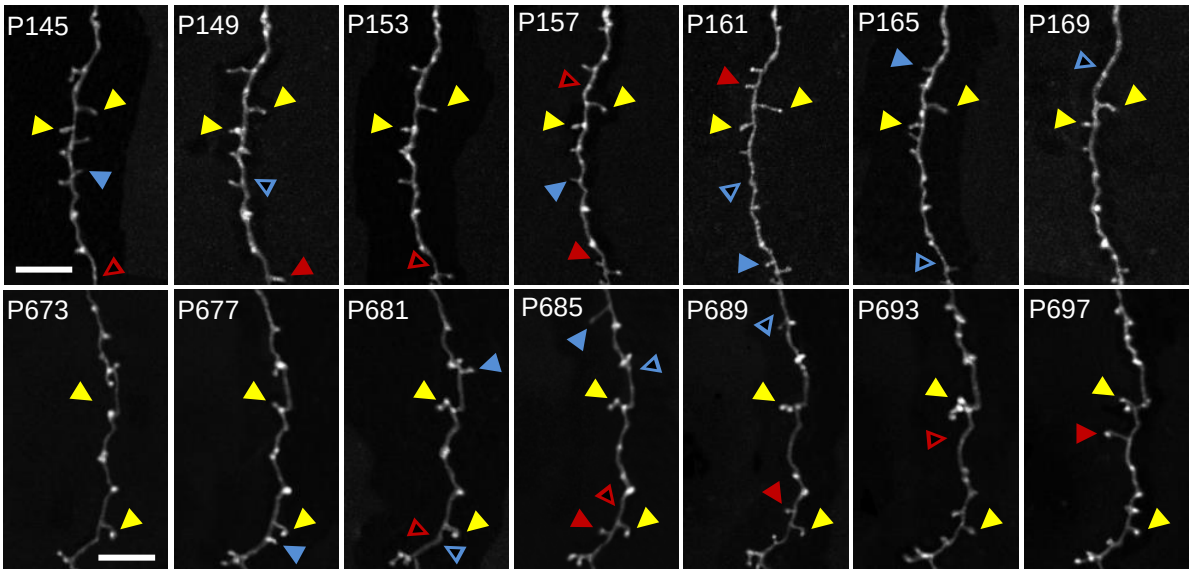

Figure 15 Time series (6 imaging sessions over 20 days) of two representative TB rich axons in the Young Adult (upper row) and Aged (lower row) brain. In the top left corner of each panel the post natal (P) day of the mouse is indicated, scale bars are 10 µm. Yellow arrowheads point to persistent (always present) TBs. Blue arrowheads highlight TB losses, solid blue TBs that will be lost in the following sessions and open blue the location of previously present TBs. Red arrowheads point to TB gains, open red the location of TBs gained in the following time point, solid red TBs gained.

The survival fraction (SF: initial boutons surviving / total number of boutons imaged at the first time point) is a useful parameter to show what proportion of boutons persists from the first imaging session at multiple time points and at what rate they are lost. Normally more boutons will be lost at earlier time intervals than at later ones. Eventually depending on the axon type, the survival curve reaches a lower plateau (limit) which represents boutons that persist for long time scales [i.e. for the whole life of the animal (De Paola et al., 2006)]. The two survival fraction curves for Aged and Young Adult animals in the case of TB rich axons were overlapping, meaning that TBs were lost at a similar rate (Figure 16). The number of initial TBs, imaged on day 0, decreased at similar rates over time in the Young Adult and in the Aged cortex (Young Adult = 100% TBs on day 0, 89 ± 3% on day 4, 81% ± 3% on day 8, 72% ± 5% on day 12, 65% ± 6% on day 16, 60.6% ± 6% on day 20; Aged = 100% on day 0,

89% ± 1% on day 4, 80% ± 1% on day 8, 73% ± 2% on day 12, 66% ± 3% on day 16, 62% ± 3% on day 20; *P* = 0.66; Figure 16 a).

The similar SFs suggested that TBs are lost at comparable rates in both age cohorts. By definition the SF only looks at boutons present at day 0 and does not take into account the stability of this initial pool of boutons (i.e., between day 0 and day 8). Looking at the survival of relatively stable TBs might be important in identifying a subset of boutons that take part in the formation of complete synaptic structures (Holtmaat and Svoboda, 2009). Relatively stable boutons were identified on the basis of a minimum eight days stability period during the first three imaging sessions, from day 0 to day 8. The greater part of these boutons was maintained throughout the imaging period, from the first imaging session to the last. A smaller but considerable part of such relatively stable boutons were lost before the end of the imaging window. The latter group were defined as destabilized boutons and the Destabilization Probability (see methods) was defined as the fraction given by the number of destabilized boutons divided by the total number of initially stable boutons (i.e., boutons present on day 0 to 8). In the case of TB rich axons the destabilization probability was not significantly altered by the ageing process (Young Adult: total initially stable TBs = 392, destabilized TBs = 109, destabilization probability = 0.28 ± 0.04; Aged: total initially stable TBs = 564, destabilized TBs = 124, destabilization probability = 0.22 ± 0.02; *P* = 0.23; Figure 16 b).

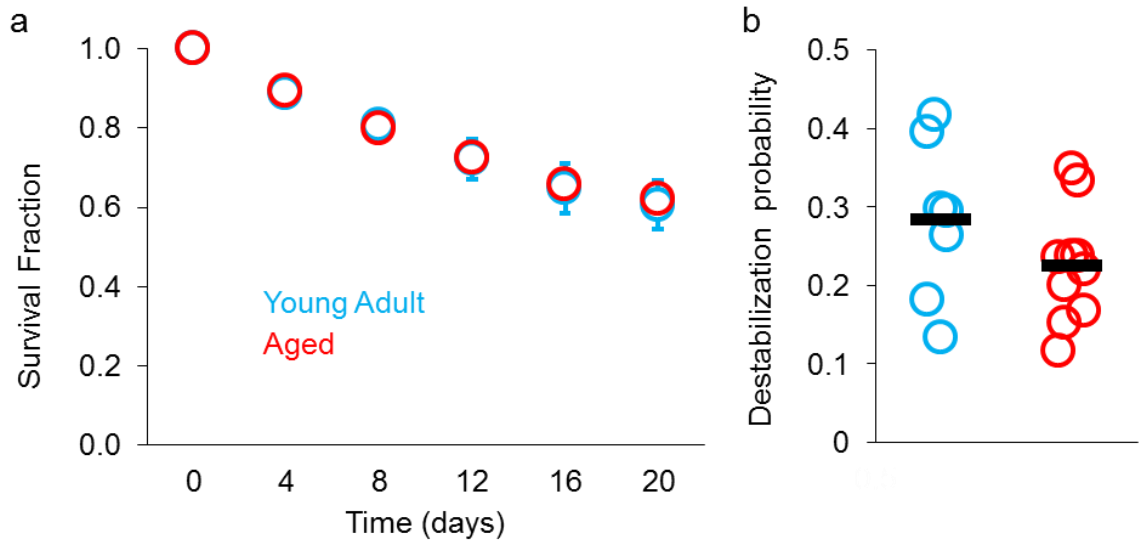

Figure 16 Initial and stable TBs are lost at comparable rates in Young Adult (n = 7) and Aged (n = 7) animals. (a) The survival fraction (SF) curves of the 2 age groups are undistinguishable. Blue markers average Young Adult SF, red markers average Aged SF, error bars are S.E.M. Error bars in Aged group are smaller than the circular marker. (b) Destabilization probability of TBs that are present during the first 8 days (3 time points) is comparable in Young Adult and Aged mice. Blue markers (left) YA, red markers (right) Ag, Black markers are mean values for the corresponding group.

In addition to measures of bouton loss, where Aged and Young Adult mice did not show significant differences on their TB rich axon population, parameters of bouton replacement were assessed. Four-day bouton turnover rates (TOR) were calculated for both age groups and compared. TOR is a measure of bouton replacement accounting for gains and losses at the same time and is expressed as a fraction (or percentage) given by the sum of gains and losses in a specific session divided by twice the total number of boutons present in the previous session (i.e. [*n* Gains + *n* Losses] / 2*n* Boutons, see methods; Figure 17). There was no significant difference in the average TOR between Young Adult and Aged animals (TOR Young Adult = 0.14 ± 0.01, TOR Aged = 0.125 ± 0.01; *P* = 0.36; Figure 17 a). In addition, no difference was observed by separating the contribution to TOR of gains and losses of boutons (Figure 17 c and d). The fraction of boutons gained over a four-day period was similar in both age groups (Fraction of gains Young Adult = 0.074 ± 0.004, Fraction of gains Aged = 0.066 ± 0.01; *P* = 0.37; Figure 17 c). Similarly the fraction of losses was also

comparable between the two different age groups (Fraction of losses Young Adult = 0.061 ± 0.01, Fraction of losses Aged = 0.057 ± 0.01; *P* = 0.63; Figure 17 d). Bouton turnover can also be expressed as a function of the axon length, i.e., as density of turnover (gains + losses) events ([*n* Gains + *n* Losses] / µm, see methods). By normalizing TB turnover with the length of the imaged axons rather than the total number of boutons the previous results are confirmed (Figure 17 b, e and f). Such confirmation was expected because the number of boutons per unit length on TB rich axons was found to be comparable between the Aged and Young Adult group (Figure 14) and at the same time TOR rates (calculated on the total number of boutons present) were also similar (Figure 17 a). Nevertheless the fact that the densities of turnover events for TBs in Aged and Young Adult animals were comparable further validates the solidity of the result. The overall density of turnover events was not significantly different comparing age groups (Young Adult = 0.048 ± 0.007 nG+nL/µm, Aged = 0.035 ± 0.003 nG+nL/µm; *P* = 0.18; Figure 17 b). No significant difference was found when considering the density of gains and losses separately (Density of TB gain events: Young Adult = 0.26 ± 0.003 nG/µm, Aged = 0.019 ± 0.003 nG/µm; *P* = 0.2; Figure 17 e. Density of loss events: Young Adult = 0.022 ± 0.005 nL/µm, Aged = 0.016 ± 0.001 nL/µm; *P* = 0.42; Figure 17 f).

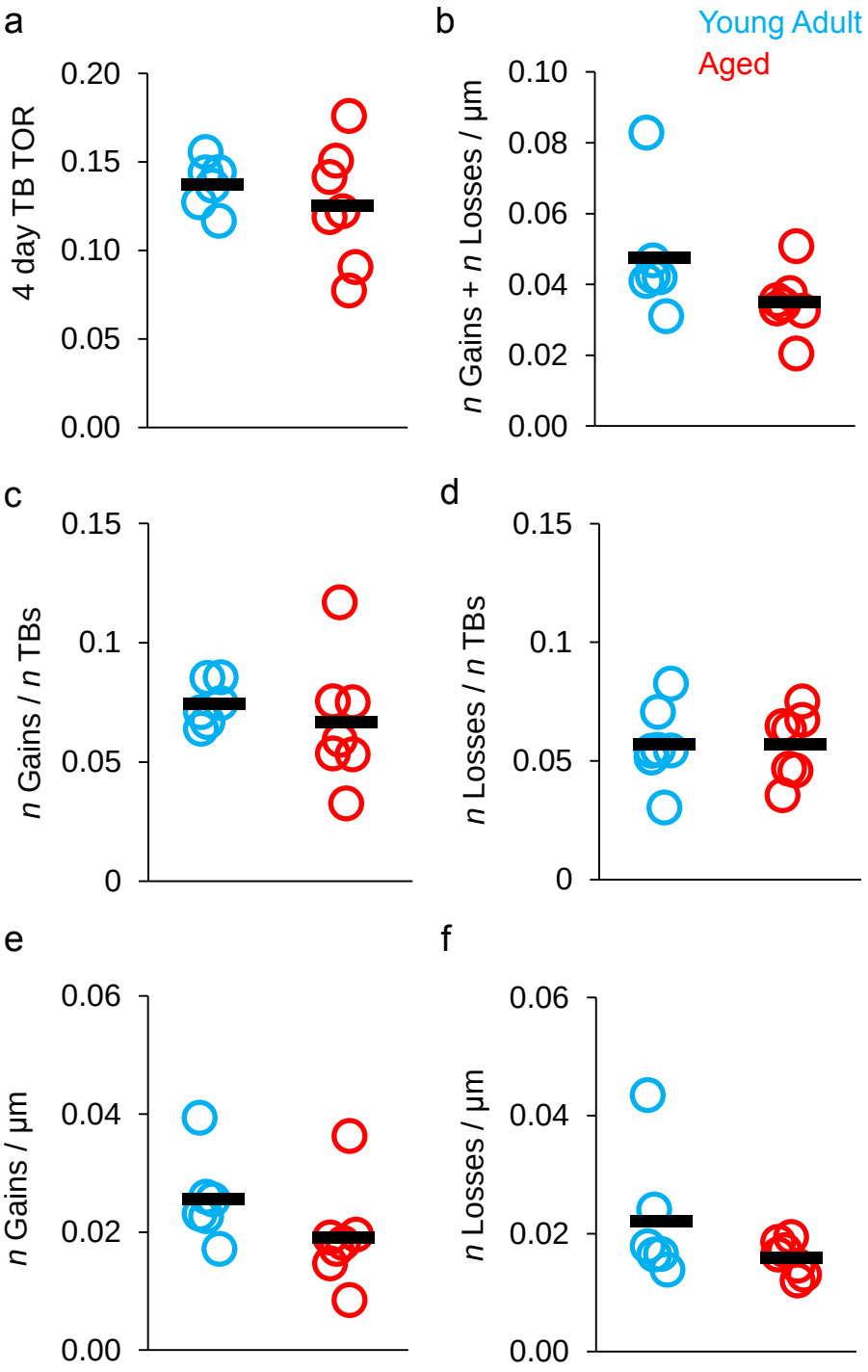

Figure 17 TBs are added and eliminated every four days at similar rates in Young Adult (n = 7) and Aged (n = 7) animals. (a) The average four-day TOR is comparable for both age groups. (b) TOR expressed as density (TOR events per µm) is comparable in both groups. (c - f) No significant difference is found when TOR is broken down in TB gains and losses. (c) Fractions of TB gains, (d) fraction of TB losses, (e) density of TB gains, (f) density of TB losses. Blue markers (left) YA, red markers (right) Ag. Black markers are mean values for the corresponding group.

The average turnover data, including the rates of TB gains and losses, did not highlight any substantial difference between the Aged and Young Adult animals. It was then important to analyse how the TOR develops over time and if any differences emerged from this comparison between the two age cohorts. For instance, it could be argued that over time these parameters were affected, perhaps the imaging protocol has different effects on TOR depending on the age of the animal. By looking at the time course (every four days for twenty total days) of TB TOR for each individual animal no significant difference was observed. The average TOR did not vary and the two age groups means did not diverge (Figure 18). In each time point comparison (day 0 vs. day 4, day 4 vs. day 8, day 8 vs. day 12, day 12 vs. day 16, day 16 vs. day 20) TOR averages remained comparable between age groups [Young Adult TB TOR = (0.14 ± 0.01, 0.14 ± 0.02, 0.11 ± 0.04, 0.13 ± 0.04, 0.11 ± 0.03, one way ANOVA P = 0.45), Aged TB TOR = (0.13 ± 0.03, 0.12 ± 0.02, 0.12 ± 0.04, 0.12 ± 0.02, 0.11 ± 0.03, one way ANOVA P = 0.85)].

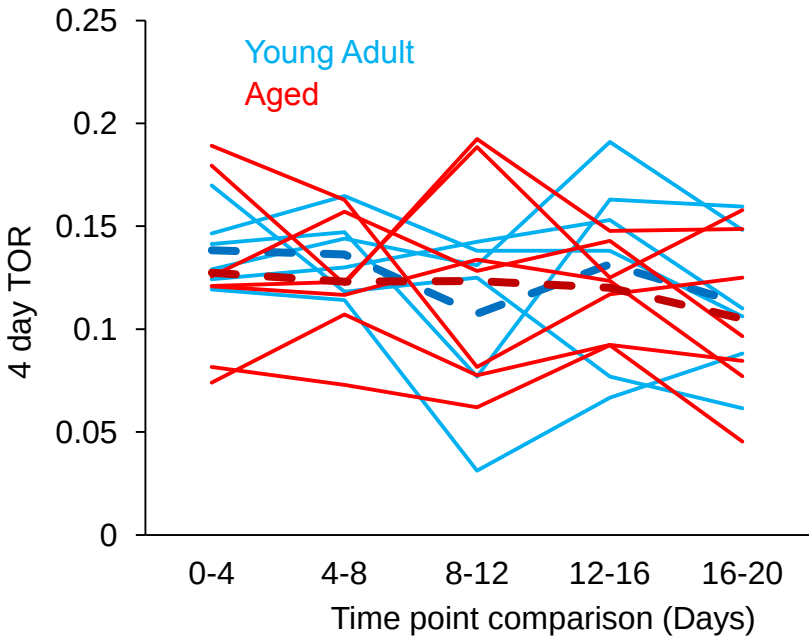

Figure 18 The average four-day TOR of TBs on layer 6 TB rich axons in Aged (n = 7, red lines) and Young Adult (n = 7, blue lines) mice is comparable and constant over time (20 days, 6 imaging sessions). Dashed lines are means, red Aged, blue Young Adult.

3.5 Conclusions

The work described in this chapter provides a detailed description of the structure and dynamic properties of *terminaux bouton* rich axons and their presynaptic terminals in Young Adult and Aged animals. In the first section of the chapter the focus is on axonal branches, defined as protrusions that exceed 5 μm in length in at least a single imaging session. The attention then moves on to the static and dynamic properties of TBs. TBs are defined as spine-like side protrusions that reach 1 μm in length at least in one imaging session. TB rich axons are characterised by a relatively high TB density (ranging from 70 to over 200 TBs per millimetre of axon) as opposed to EPB rich axons. De Paola et al. in 2006 have shown evidence that Thy1-GFP labelled TB rich axons imaged in cortical *lamina* I originate from *lamina* VI pyramidal neurons. The clear morphological distinction and the fact that these axons originate from a defined cortical region, make these axons of particular interest as they arguably represent a homogenous population. TBs on TB rich axons (originating from *lamina* VI) supposedly form shaft synapses preferentially (McGuire et al., 1984). These synapses have been shown to mediate a weak postsynaptic response with high facilitation (Lee and Sherman, 2009). Moreover, they have been described as highly plastic cortical elements with up to 60% of their boutons being replaced over a period of a month in the adult mouse brain (De Paola et al., 2006). It must be said that it is not easy to compare dynamic rates between EPBs and TBs because of the different strategies that are adopted to analyse the respective images, differences that are described in detail in this thesis (see methods). Undoubtedly, though, TBs on TB rich axons undergo profound remodelling in the adult brain as boutons could potentially be completely replaced over 2 – 3 months (De Paola et al., 2006). Such striking dynamic behaviour in baseline conditions could have made TB rich axons and their boutons ideal targets of the ageing process, a condition that is expected to slow down plastic and dynamic neuronal properties (Burke and Barnes, 2006), (Bloss et al., 2011) (Morrison and Baxter, 2012). Surprisingly, these axons appear unaffected in terms of morphology and dynamic behaviour of their branches and pre-synaptic structures in the

aged cortex of mice. In the case of axonal branches it is interesting to note that not only the density and length (Figure 11) of such structures were similar in both ages but, more importantly, branches in aged animals were still able to elongate and retract at similar rates to those seen in the young adults (Figure 12). Moreover, such activity was not confined to retraction only but by equal elongation and retraction events, shown by the fact that the overall average length remains constant over time (Figure 13). The unexpected dynamic behaviour of axons imaged in *lamina* VI of the ageing brain extends to *terminaux boutons* as well. TBs were found in equal numbers (i.e. density) on Aged and Young Adult axons (Figure 14 a). This density was stable over time (twenty days of imaging) thus it was unaffected by neither age nor imaging itself (Figure 14 b). Strikingly the dynamic properties of TBs appeared intact in the aged mouse brain. The survival fraction of TBs in Young Adult animals resembled what previously published confirming their highly plastic nature. The survival curve generated by the data collected in the Aged group was virtually overlapping the Young Adult curve (Figure 16 a). TBs retain their intrinsic dynamic properties throughout the lifetime of these mice as initial boutons were lost at comparable speeds. Further confirmation comes from all other dynamic parameters presented. The probability that a bouton stable for eight days was eliminated (destabilization probability) was similar between age groups (Figure 16 b). Not only the likelihood of TB destabilization was similar between age groups, all other dynamic TB parameters in the Aged pool were comparable to the Young Adult counterpart: the TB four-day TOR was comparable (Figure 17 a), which should be expected at this point because, as previously stated, boutons were being lost at the same rate but the densities in both cases were stable. Again the density of TOR events is not different (Figure 17 b), also an expected result being the density and the turnover fraction similar in both age groups. In further detail, no difference could be detected across groups when splitting turnover rates in bouton gains and bouton losses. The number and the density of gains were similar in Young Adult and Aged mice (Figure 17 c and e), just as the losses were (Figure 17 d and f). Finally, it was shown that the four-day turnover fraction of TBs was constant throughout the imaging window (Figure 18). Overall these results show that in the

Thy1-GFP mouse the ageing process had little or no effect on TB rich axons, both considering their branches and bouton dynamics. Such results went against the initial expectation of reduced structural remodelling during the ageing process.

4. *En Passant Bouton* rich axons

4.1 Introduction

The major class of cortical presynaptic structures are *en passant boutons* (EPBs), classically described as spheroid swellings or varicosities of the axonal compartment hosting the presynaptic machinery. EPB rich axons are characterized by the prevalence of EPBs along their shaft with a comparatively lesser occurrence of TBs. Such prevalence of EPBs makes them morphologically distinguishable from TB rich axons. EPB rich axons represent the majority of axons visible in the superficial layers of the cortex. In the S1 cortex of Thy1-GFP animal lines, EPB rich axons observed in *lamina* I originate from neural somas residing within the cortex in *laminae* II/III and V, and sub-cortically in thalamic nuclei (De Paola et al., 2006; Holtmaat and Svoboda, 2009) such as the posteriomedial nucleus (POm) and the ventral posteromedial nucleus (VPM). In previous studies EPBs found on EPB rich axon have been described as relatively more stable than spines on dendrites and TBs on TB rich axons (De Paola et al., 2006; Holtmaat and Svoboda, 2009; Majewska et al., 2006), with ~20% average bouton turnover over one month in baseline conditions. It should be noted that such turnover estimations are strongly dependent on the way that image analysis is performed, which in turn is influenced by the nature of the analysed structures (i.e. varicosities vs. side protrusions). So the study and description of turnover rates of spines, TBs and EPBs, although it can produce solid and useful relative information within each group, should be compared across groups taking these issues into account. Such direct comparisons could therefore induce to misleading interpretations on how differently spines and boutons behave at basal conditions. Nevertheless, highly plastic TBs were expected to have reduced dynamics during ageing, while more stable EPBs were expected to be less

affected by ageing. However, a reduction in number and overall EPB size might be expected (Burke and Barnes, 2010; Smith et al., 2000).

4.2 EPBscore analysis tool

Because of their shape, EPB analysis poses a far greater challenge to the experimenter compared to structures such as TBs or dendritic spines (Canty and De Paola, 2011), which one can easily measure in length units as they protrude from the main shaft of the axon or dendrite. EPB size, instead, cannot reliably be measured geometrically because their diameter is often around or below the resolution limits of the two-photon microscope (Holtmaat and Svoboda, 2009; Svoboda, 2004) especially in the Z plane (> 1 µm). So far EPBs have been counted manually or relying on the intensity integral of the axonal portion of interest. This produces a high user dependency, making it difficult to consistently decide what is a synaptic bouton and what is not. In this work a lot of effort went into the development of a tool that could reliably analyse EPB rich axons and that given a fixed set of parameters would be able to reproduce the same results independently from the user. The software was named EPBscore and developed in collaboration with Professor Sen Song at MIT, Boston (currently at Tsinghua University, Beijing, China). The program was based on the Matlab environment and it was designed to extract an intensity profile of *in vivo* imaged axons and estimate bouton volume over multiple time points (Figure 19). The mouse line used for the EPB dataset was the Thy1 GFP-M line (Feng et al., 2000) which induces cytosolic GFP expression in targeted neurons. GFP molecules therefore fill the axon and its boutons evenly. As EPBs are effectively swellings of the axonal backbone, more GFP molecules collect inside the boutons compared to the adjacent axon backbone itself. Such GFP accumulation makes boutons brighter and the acquired intensity signal larger (Figure 19 a). Because EPBs are normally below the point spread function of the microscope (Knott

et al., 2006), especially in the Z plane, the detected intensity is effectively an integration of the local intensity signal proportional to the size of the compartment (Svoboda, 2004). Consequently, the maximum intensity can be used as a predictor of bouton size.

EPBscore is a semi-automated software that is able to trace axonal segments in three dimensions. It then positions the trace over the line of most intense pixels, along the axon of interest. EPBscore then estimates the intensity value of the axonal backbone using the median intensity value of all the pixels in the intensity profile. The extracted median value is then used to normalize the whole pixel intensity profile; in other words it offsets the backbone to 1 relative intensity unit (Figure 19 b). This way the brighter spots, supposedly EPBs, are represented by peaks in the profile that are expressed in backbone units, a measure of relative intensity. Peaks that are larger than twice the backbone value (relative intensity of 2) are scored as axonal boutons (Figure 19 c). Finally, the intensity profiles of the same region of interest imaged over multiple time points are overlaid (Figure 19 b). This way EPBs are correlated over different sessions so that their appearance, disappearance and size fluctuations are individually tracked over the imaging period (for more details see methods).

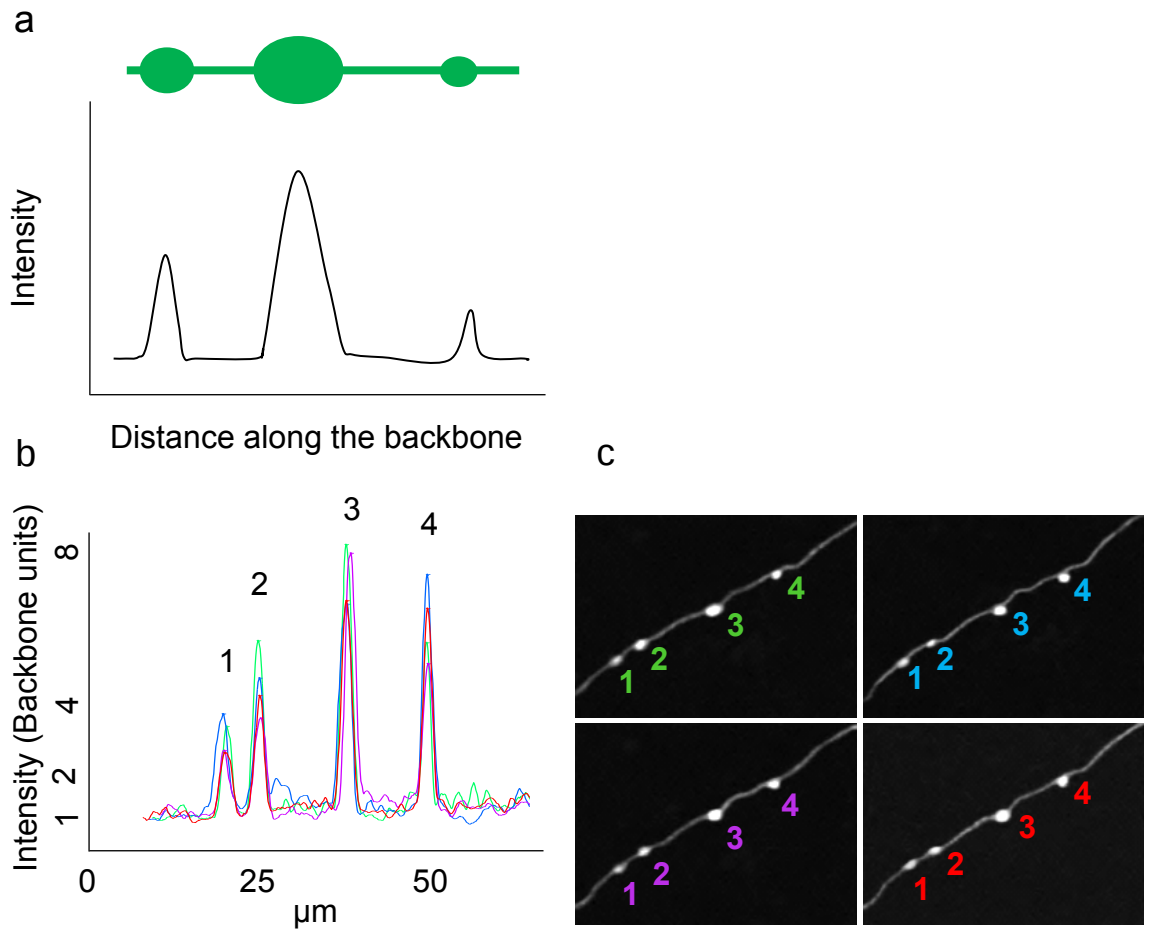

Figure 19 Principles of the EPBscore analysis software. (a) Under the assumption that GFP fills the imaged axons homogenously, larger axonal compartment (EPBs) will contain more fluorophore than the thin adjacent backbone. Plotting the maximum intensity along the axon returns an intensity profile where EPBs are represented by intensity peaks. (b) Overlaid intensity profiles obtained with multiple imaging of the same region of interest. The 4 peaks correspond to the 4 boutons in (c) and the colours correspond to the 4 different time points at which images were taken (i.e., 0-4-8-12 days).

4.3 Validation of EPBscore and bouton volume estimation noise

As EPBscore provides an indirect measure of bouton size through intensity it is important to show that these relative measurements are accurate and precise volume estimations. Two strategies were adopted: 1) relate the two-photon intensity measurements to the measurements made from electron microscopy (EM) reconstruction of the same *in vivo*

imaged boutons; 2) compare four-day *in vivo* imaging sessions of individual boutons with imaging conditions in which boutons should not alter their size, i.e. *in vivo* over short periods of time (minutes and seconds) and by imaging fixed tissue preparation.

4.3.1 Correlated two-photon – electron microscopy

EM represents so far the only, well established, way of having accurate direct volume measurements of subcellular compartments such as spines and boutons (Cheetham et al., 2012; Harris and Stevens, 1989; Knott et al., 2006; Murthy et al., 2001). Also, EM can provide important structural information to establish that boutons actually form synaptic contacts. In the near future super-resolution optical techniques, such as stimulated emission depletion (STED) microscopy, may be able to give precise size measurements in living tissue (Nagerl and Bonhoeffer, 2010). However, because STED will still rely on fluorescent reporters, it will still be challenging to image pre- and post-synaptic structures at the same time in order to assess the presence of a synaptic contact. In collaboration with Dr Graham Knott, at the École Polytechnique Fédérale de Lausanne, a total 11 *in vivo* imaged boutons were found back and reconstructed at the EM level (Figure 20). Serial Section Electron Microscopy (SSEM) was carried out on 9 boutons that were reconstructed from Young Adult somatosensory cortex (Figure 20 a – c) as in (De Paola et al., 2006). The remaining 2 boutons were obtained from Aged animals (Figure 20 d – f) using Focused Ion Beam / Scanning Electron Microscopy [FIB/SEM (Knott et al., 2008)]. This technique has the advantage that the acquired EM images do not need post hoc manual alignment. For all 11 cases the EM reconstructions confirmed that *in vivo* imaged varicosities contacted a postsynaptic spine forming synapses and contained synaptic vesicles (Figure 20 b and e). The axon portions and boutons of interest were reconstructed in 3D using the open source software Fiji (Figure 20 c and f), and the volume of each bouton was calculated in μm^3.

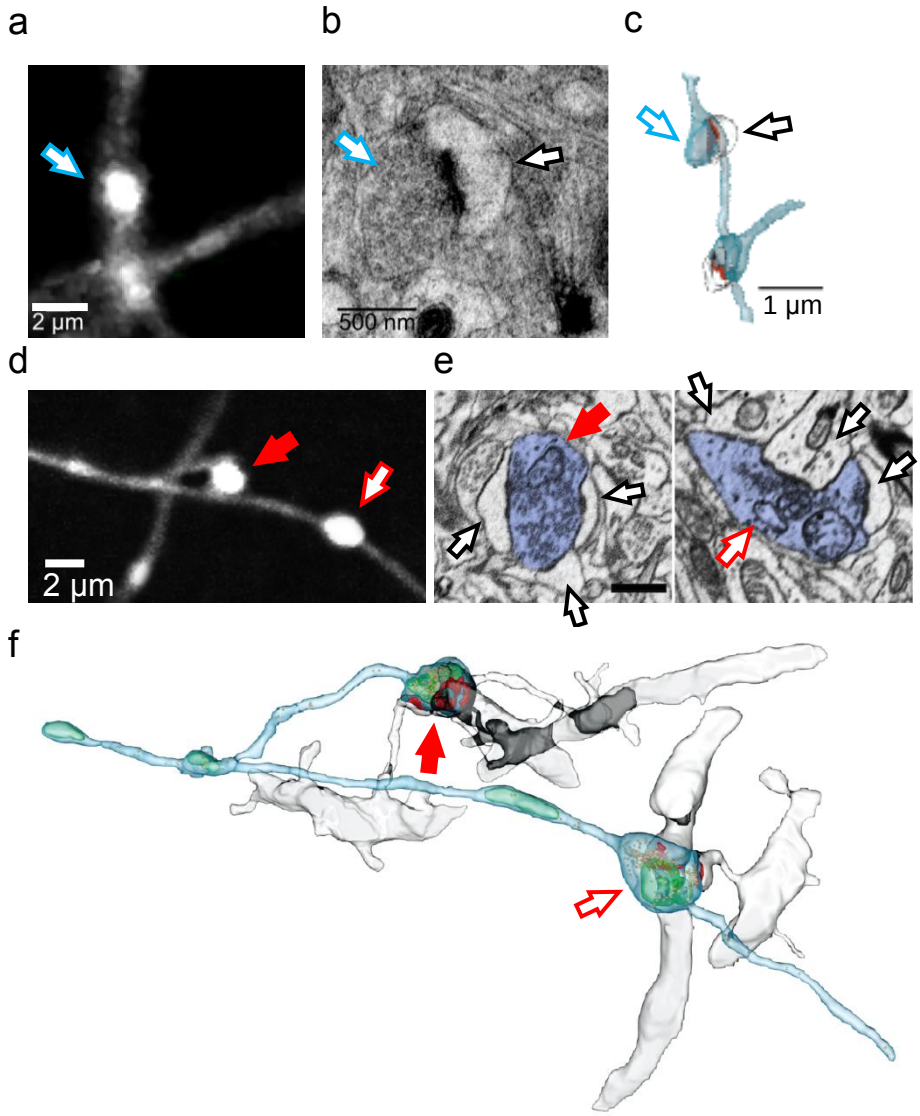

Figure 20 EM reconstruction of *in vivo* imaged presynaptic boutons. (a) two-photon imaged EPB (blue arrow) in the intact Young Adult cortex. (b) The same EPB (blue arrow) in (a) was imaged at the EM level uncovering its ultrastructure. The EPB contained synaptic vesicles, had an electron dense active zone and crucially contacted a postsynaptic spine (black arrow) with corresponding post-synaptic density. (c) 3D model of the EPB (blue arrow) in (a and b) obtained from SSEM images. The contacting spine is indicated by the black arrow. The axonal cytoplasm is shown in blue and the synaptic contact in red. (d) Two large boutons (red arrows) imaged in the intact Aged cortex. (e) EM sections of the two boutons of interest in (d), indicated by a solid red and an open red arrow. Both contain synaptic vesicles, mitochondria and contact multiple dendritic spines (open black arrows). Scale bar 500 nm. (f) 3D reconstruction obtained from the FIBSEM imaging. The axonal cytoplasm is rendered in blue, synaptic vesicles in yellow, mitochondria in green and synaptic contacts in red. The dendrites are in grey.

When present, mitochondria were also taken into consideration because they would effectively displace GFP molecules. As expected the size of the EPBs at the EM level were highly correlated with the estimated size at the two-photon microscopy level, which is detected through GFP intensity signal. The following results summarize the 9 boutons in the Young Adult group. The largest of these boutons had a volume of 1.31 μm^3 and a two-photon relative intensity value of 7.42 backbone units. The smallest bouton that was imaged both *in vivo* and at the EM level had a relative intensity of 1.92 times the axonal backbone intensity and a volume of 0.236 μm^3. Without considering the mitochondrial contribution to the final volume, a strong correlation was found between EM volume and two-photon relative intensity (Pearson's linear correlation: R = 0.86; *P* = 0.003; Figure 21 a). When subtracting mitochondrial volume from the final bouton size calculation the correlation of EM measured bouton volume with two-photon relative intensity is even stronger (R = 0.88; *P* = 0.002; Figure 20 21). The correlation is confirmed when including the two large Aged group boutons (Figure 20 d, e and f). These boutons were 1.78 μm^3 and 1.61 μm^3 in size while their two-photon detected intensity was 13.4 and 20.3 backbone units respectively (Figure 21). The overall correlation of EM measured bouton volumes with two-photon relative intensity was highly significant both when mitochondrial volume was not subtracted (R = 0.85; *P* = 0.001; Figure 21 a) and when mitochondrial volume was subtracted (R = 0.86; *P* = 0.0008; Figure 21 b). Interestingly the two boutons from the aged group have multiple synaptic connections both contacting at least three postsynaptic spines each (Figure 20 e).

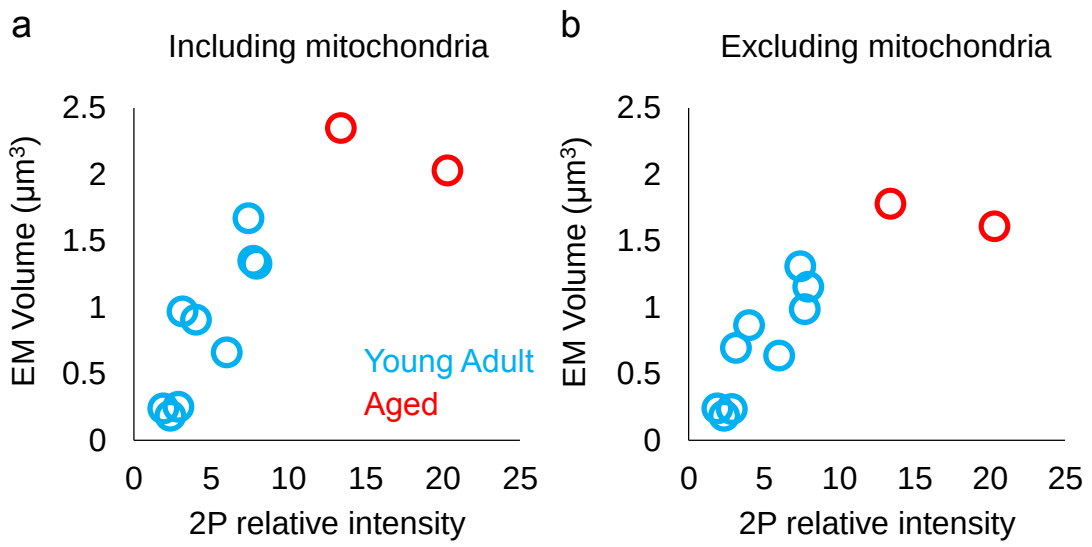

Figure 21 Two-Photon vs. EM correlation. The 2P relative intensity is plotted against the EM extracted volume. (a) Correlation graph, each circle represents a bouton imaged *in vivo* and at the EM level post mortem. Blue circles are Young Adult boutons and red circles are Aged boutons. The plotted EM measured size here is the total volume. (b) Same boutons as in (a) but with the mitochondrial volume (if present) subtracted.

Bouton	2P relative intensity	EM total volume	EM volume - mitochondria
YA 1	1.92	0.24	0.24
YA 2	2.36	0.18	0.18
YA 3	2.88	0.25	0.23
YA 4	3.15	0.97	0.69
YA 5	4.03	0.90	0.86
YA 6	6.02	0.66	0.63
YA 7	7.43	1.67	1.31
YA 8	7.73	1.35	0.98
YA 9	7.96	1.33	1.15
Ag 1	13.40	2.35	1.78
Ag 2	20.30	2.03	1.61

Table 2. Summary of 2P relative intensities and EM size measurements for each bouton. Young Adult boutons (YA) 1 to 9 in light blue rows, Aged (Ag) 1 and 2 in pink rows.

4.3.2 Estimating the noise in the intensity based volume measurement

To investigate the degree of error of the EPBscore software, a noise estimation experiment was carried out. To assess noise level in bouton intensity measurements repeated imaging (four days apart) was performed on fixed tissue, a condition in which bouton volume and hence intensity should remain constant. Also, short-term repetitions *in vivo* were performed with time intervals of 10 minutes and 30 seconds. The acquired images were compared and the absolute intensity ratio (IR) for individual boutons was calculated to highlight apparent volume change; $IR = \exp(|\log_{intensity\ A} - \log_{intensity\ B}|)$ where exp is the exponential of the absolute difference of the natural logarithms (log) of the intensities (A and B) of individual boutons in consecutive sessions (see methods). The IR nothing else is than the highest relative intensity value divided by the lowest regardless of the temporal sequence of acquisition for a specific bouton. Thus IR returns a measure of bouton size change between imaging sessions, if intensity A is equal to intensity B then IR is equal to 1. If, for example, A/B = 1.15 then a 15% change in size has occurred between session A and session B for that particular bouton. The IR describes how much the intensity, hence the size, has changed but it does not provide information on the direction of the variation. Ideally in a fixed brain the resulting IR value calculated between two sessions should be very close to 1 because no biological change can occur. The same should be true for short term image acquisition repetitions *in vivo*. The results are summarized in the graph below (Figure 22 a). The grey bar indicates the average IR for boutons imaged in a whole mount paraformaldehyde (PFA) fixed brain with a four-day imaging interval. The blue bars indicate average IR measured *in vivo* over different time scales, the lightest blue shows the value for repeated imaging that took place over the space of 30 seconds, the next darker blue represents what found increasing the interval to 10 minutes and the darkest blue bar on the far right represents *in vivo* data from Young Adult animals with repeated imaging spaced by the canonical four days. For the four-day fixed brain imaging a total of four animals and 341 boutons were imaged. The average IR was quantified at 1.13 ± 0.008. The *in vivo* 30

seconds interval group consisted of 3 animals and 122 EPBs for which the calculated average IR was 1.09 ± 0.007. 3 animals and 114 EPBs make up the *in vivo* 10 minutes interval group, in this case the average IR was 1.11 ± 0.009. The *in vivo* over four-day imaging returned a much larger average IR: 1.36 ± 0.01, calculated from 15 animals and 982 EPBs. The large difference indicates that the biological changes that occur over this time scale are within the detection range of the two-photon intensity analysis technique. The difference between the four-day fixed brain IR and the four-day *in vivo* imaging IR was extremely significant ($P = 1.09e^{-037}$). Along with the IR noise, also Turnover Rate (TOR) noise was tested in the same control dataset. In this case the slight changes in size detection described above might cause a small bouton to oscillate around the relative intensity threshold of 2, which determined whether a bouton was scored or not. The average four-day fixed brain bouton TOR was 0.008 ± 0.003. For the *in vivo* imaging with 30 seconds intervals bouton TOR was 0.015 ± 0.02. For the *in vivo* imaging with 10 minute interval TOR was 0.03 ± 0.03. For the experimental group, four-day intervals *in vivo*, the TOR was 0.08 ± 0.009. The four-day *in vivo* TOR was significantly higher than what observed in the four-day fixed brain imaging ($P = 0.007$; Figure 22 b). These results show that TOR results were minimally influenced by experimental and analytical noise.

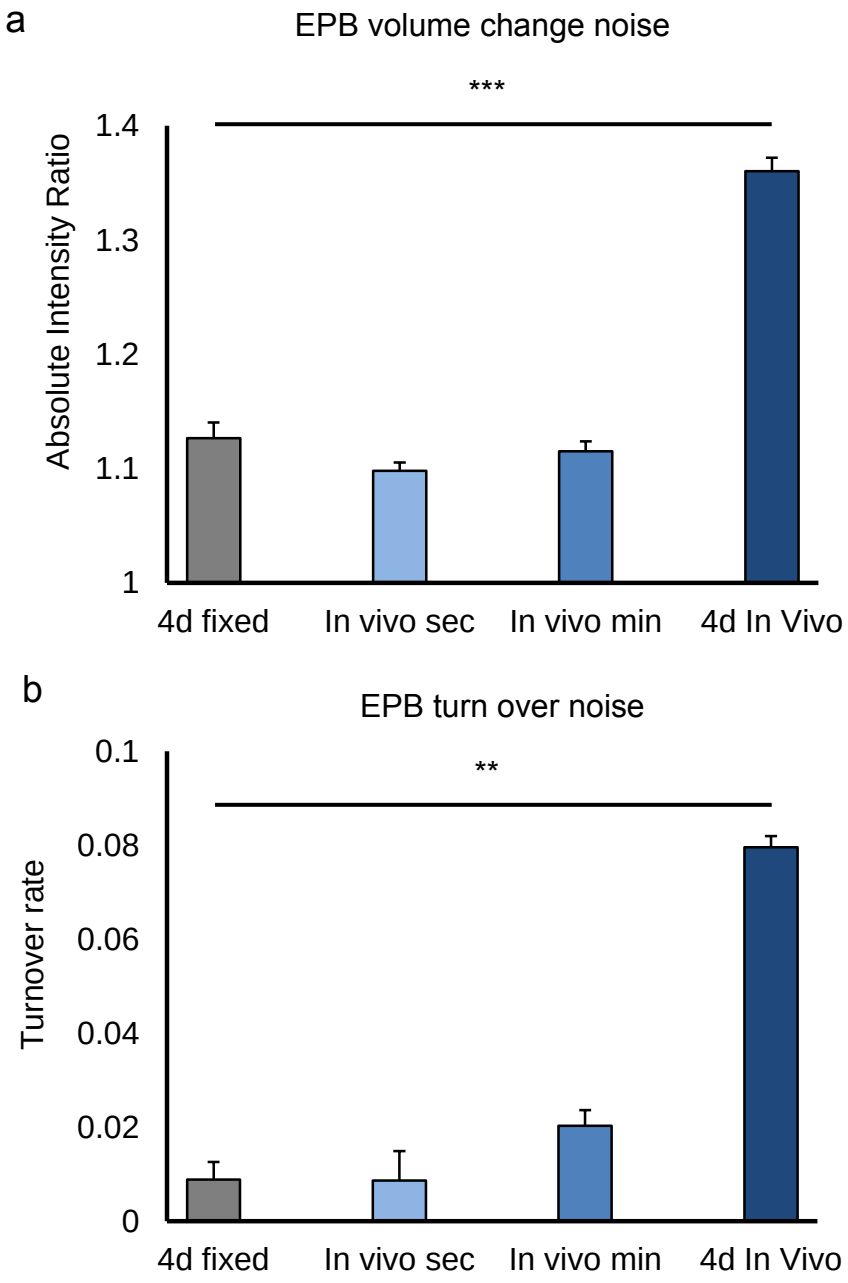

Figure 22 EPBscore noise estimation. (a) Noise estimation of intensity measurements. Grey bar is IR in EPBs imaged in the fixed brain four days apart. Blue bars are IR for *in vivo* imaged EPBs with growing intervals. Error bars are S.E.M. (b) Noise estimation of the four-day TOR. Grey bar is IR in EPBs imaged in the fixed brain four days apart. Blue bars are IR for *in vivo* imaged EPBs with growing intervals. Error bars are S.E.M. (** $P < 0.01$, *** $P < 0.001$)

4.4 EPB size estimation conclusions

Reproducible and robust analysis of synaptic structures in two-photon acquired images is an important goal for the *in vivo* imaging field (Holtmaat et al., 2009). Current analysis methods are still highly user dependent and this degree of subjectivity can produce differences in the results of up to twofold between different labs given the same set of images (Holtmaat et al., 2009). EPBscore represents an improvement in this direction making the detection, size estimation and the tracking of *en passant boutons* highly reproducible and reasonably accurate. Bouton detection is based on the axon relative intensity given by the number of GFP molecules present which in turn depends on the size of the compartment (varicosity or bouton). To test the fidelity of this relationship, 11 boutons were imaged both *in vivo* and at the EM level (Figure 19). The data collected show that a strong linear correlation exists between the intensity signal of the fluorophore and the actual volume measured reconstructing the boutons at the EM level (Figure 20). Such correlation was made even stronger when taking into account the fact that subcellular organelles, such as mitochondria, could displace the cytosolic GFP molecules hence diminish the strength of the intensity signal (Figure 20 b). These results suggest that the brighter a bouton, the larger the volume. Importantly, larger boutons may mean stronger synapses (Cheetham et al., 2012; Knott et al., 2006). It is worth reminding that the volume measured at the EM level, although being the best approach available, could carry errors introduced by the fixation procedure which may produce non-homogenous scaling. Further confirmation of the intensity to volume relation could come from technological advances such as super resolution optical microscopy which can be carried in living samples *ex vivo* or even *in vivo* (Berning et al., 2012). EPBscore works on the assumption that the size of EPBs is usually below the resolution of the microscope. In this work the point spread function, the minimum distance that allows two points to be separately resolved, of the microscope was measured at ~ 0.4 μm in the XY direction and at ~1 μm in the Z direction. These dimensional limits are above the size of the great majority of boutons especially in Z. Although some very large boutons

can exceed these boundaries so that their relative intensity might diverge from the linear relation with their real volume, such cases represent a minority when considering the distribution of bouton sizes (see below). EPBscore is a precise tool that coupled with chronic *in vivo* two-photon microscopy is sensitive enough to detect biologically significant variations of bouton size that happen over days. This conclusion is supported by the data presented, where it is shown that the variations in intensity, for individual boutons, are much larger in experimental conditions (*in vivo* over four days) compared to imaging experiments in fixed tissue (Figure 22). The intensity ratio parameter highlights the amount of change in intensity (hence size) between imaging sessions regardless of the direction of each individual bouton variation (i.e., shrinkage/enlargement, Figure 22 a). The IR measured in the fixed brain should theoretically be equal to 1 because boutons in PFA fixed tissue should not change in size. The small measurement differences over different sessions are due to sensitivity and precision issues inherent to the system (laser, microscope, detectors, analysis software), but are in part shared with the *in vivo* situation. Issues which contribute to the noise inherent to the fixed brain preparation include: 1) the positioning of the fixed brain, which is more difficult to control than for the *in vivo* preparation where a head bar helps keeping track of the brain position down to 1^{o}; 2) Photobleaching, as GFP in fixed tissue is not replenished; 3) GFP leakage, due to microscopic membrane ruptures contributing to increased background signal. For these reasons the noise level of bouton intensity measurements could be overestimated. Further controls performed *in vivo* but over very short imaging intervals confirmed that the noise of the system is relatively low. It is unlikely that changes in bouton size occur in the space of 30 seconds, such fast repeated imaging displays a similar IR to the fixed brain experiment. If the gap is extended to 10 minutes the IR is slightly higher, though not significant (Figure 22 a). In this case small size changes might be possible. Noisy variations in intensity may introduce artificial turnover values because of the necessity of having strict scoring criteria (i.e. twofold backbone brightness), a small drop or increase in the relative intensity can determine whether a bouton disappears or is gained. Again the control experiments show that the contribution of the noise in the final turnover results *in vivo*

over four days was minimal (Figure 22 b). Turnover events in the fixed brain were, as expected, relatively rare. *In vivo,* over 30 second intervals, experiments also showed low turnover rates, comparable to the fixed brain. When the interval between acquisitions was extended to 10 minutes the turnover also increased slightly, reflecting the increase in IR, although still far from what measured over four days. Overall EPBscore is a valid tool that improves reproducibility in the crucial step of image analysis and minimises user dependency. When coupled with EM it provided an accurate estimation of bouton volume which is an important morphological feature as larger boutons contain more synaptic vesicles and potentially contact multiple or larger spines. EPBscore also provides an easy way to track individual boutons over multiple imaging sessions so that the evolution of many specific synaptic sites can be followed. Therefore besides the stability, disappearance and appearance of boutons, also EPB volume fluctuations can now be reliably traced and studied over time.

4.5 *En passant bouton* density does not decrease during ageing

Ageing can have a significant impact on cognitive function even in the absence of pathological processes (Burke and Barnes, 2006; Morrison and Baxter, 2012; Yeoman et al., 2012). The loss of synaptic elements, rather than neuronal death, on specific cell types has been related to cognitive decline in aged animals (Bloss et al., 2011; Dumitriu et al., 2010; Peters et al., 2008; Smith et al., 2000). As previously stated, EPB rich GFP positive axons were imaged in the superficial layers of the somatosensory cortex of Thy1-GFP-M mice (Feng et al., 2000). These axons represent a heterogeneous subset of excitatory axons originating from neurons localized in cortical *laminae* II/III and V but also in thalamic nuclei (De Paola et al., 2006). Overall the EPB rich axon dataset consisted of 14 animals, 27 axons spanning 17.8 mm and 1759 distinct boutons (1082 boutons present at day 4, second

imaging session) for the Young Adult group; the Aged mice group comprised 16 animals, 54 axons with 33.9 mm of length and 3504 distinct boutons (1900 boutons present at day 4). Against the initial expectation, bouton density was found to be comparable between Aged and Young Adult mice (Figure 23). The following data were collected on the second imaging session, day 4 on the imaging time line: (average bouton density Young Adult = 0.061 ± 0.0047 EPB/µm, Aged = 0.056 ± 0.0032 EPB/µm; *P* = 0.58; Figure 23 a). Importantly, the bouton density is not affected by repeated imaging and remained constant over the twenty-four-day imaging period (Figure 23 b). The total number of imaged animals in this case was reduced as only a subset completed the imaging protocol. In particular, 9 mice and 15 axons for the Young Adult group were imaged over the whole twenty-four-day period, while 9 mice and 22 axons were imaged in the Aged animal group. The average bouton density considering all time points (0 to 24 days) was comparable in the two age cohorts (Young Adult = 0.061 ± 0.005 EPB/µm, Aged = 0.059 ± 0.004 EPB/µm; *P* = 0.22). The average bouton density was constant over time in both age groups (Young Adult = 0.058 ± 0.005 EPB/µm on day 0, 0.062 ± 0.006 on day 4, 0.062 ± 0.005 on day 8, 0.061 ± 0.005 on day 12, 0.061 ± 0.005 on day 16, 0.062 ± 0.006 on day 20, 0.062 ± 0.006 on day 24; one way ANOVA: *P* = 0.99; Aged = 0.052 ± 0.004 EPB/µm on day 0, 0.059 ± 0.004 on day 4, 0.061 ± 0.004 on day 8, 0.063 ± 0.005 on day 12, 0.061 ± 0.004 on day 16, 0.061 ± 0.005 on day 20, 0.057 ± 0.004 on day 24; one way ANOVA: *P* = 0.92).

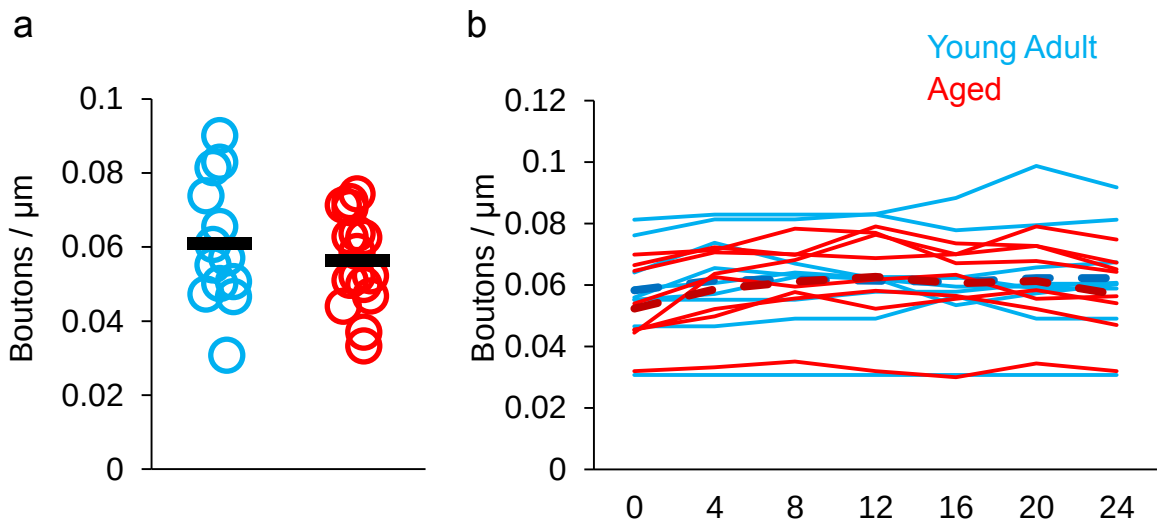

Figure 23 EPB density is similar and constant over time in the Aged and in the Young Adult cortex. (a) The average density per animal is comparable between Young Adult (n = 14) and Aged (n = 16). Blue markers (left) YA, red markers (right) Ag, Black markers are mean values for the corresponding group. (b) The average EPB density is constant over time (24 days, 7 imaging sessions) for both age cohorts. Aged animals (n = 9) red lines, Young Adult (n = 9) animals blue lines, dashed lines are mean values for each group.

4.6 Bouton dynamics are increased on Aged EPB rich axons

Functional synaptic plasticity has been extensively investigated in the ageing context (Barnes, 1979; Dieguez and Barea-Rodriguez, 2004; Landfield, 1988; Norris et al., 1996; Sierra-Mercado et al., 2008). In these studies, Long Term Potentiation (LTP) induction and maintenance were found to be less effective in aged neurons while Long Term Depression (LTD) was facilitated. These alterations correlate to memory deficits that aged animals display. Less is known on the role of structural plasticity during ageing, mainly because it was not possible to observe this phenomenon in real time in the intact brain before. Indirect evidence points to a reduction in synaptic structural plasticity with age (Bloss et al., 2011; Dumitriu et al., 2010), although a recent study challenges this view showing that spine density and dynamics increase in older animals (Mostany et al., 2013). This study followed dendritic spines and axonal boutons *in vivo* with the cranial window technique in Thy1-GFP-

M mice. Being able to look into the intact brain and track synaptic elements in real time represents a key advancement to directly study synaptic dynamics in the ageing cortex. So far, the results presented have shown that bouton density was not affected by the ageing process on neither TB rich nor EPB rich axons. Next the dynamic behaviour of EPBs was analysed.

4.6.1 EPB survival is lower in the Aged brain

First the survival of EPBs was studied in the two age groups. The two survival fraction curves calculated for the Young Adult and Aged mice groups were very different (Figure 24). Boutons on EPB rich axons imaged in the Aged brain are lost at a higher rate than the ones imaged in the Young Adult cortex. The survival fraction (SF) only considers boutons that are imaged and scored on the first day of imaging (day 0) also defined here as initial boutons. SF(t) = N(t)/No, where No is the number of boutons at t = 0, and N(t) is the number of boutons of the initial group surviving after time t. SF(t) is therefore a monotonically decreasing function of time, and SF(0) = 1. SFs for spines and boutons can be fit with an exponential function and a constant term. The time constant, τ, of the exponential is a measure of the rate of bouton/spine turnover reflecting an unstable population of spines or boutons that appear and disappear at high rates and that are thought to be critical for the process of learning (Holtmaat and Svoboda, 2009; Xu et al., 2009; Yang et al., 2009). The constant term reflects the persistent fraction, a highly stable population of synapses thought to encode lifelong memories. As previously stated, 9 animals and 15 axons for the Young Adult group were imaged for the whole twenty-four-day imaging period while 9 mice and 21 axons for the Aged group completed the seven time point imaging protocol under baseline conditions. The initial boutons count on day 0 for the Young was 371, of these less than 30% were lost by day 24 (Young Adult total number of EPBs surviving: day 4 = 348 EPBs, day 8 = 328, day 12 = 313, day 16 = 296, day 20 = 281, day 24 = 273). In the Aged cortical axons

852 initial EPBs were counted on day 0, of these nearly 40% were lost by the end of the imaging schedule (Aged total number of EPBs surviving: day 4 = 760 EPBs, day 8 = 685, day 12 = 631, day 16 = 586, day 20 = 562, day 24 = 523). Specifically in the Young Adult group 73.6% of initial EPBs survived until the last time point twenty-four days after the imaging started. On EPB rich axons imaged in the Aged brain this percentage dropped to 61.4% (Figure 24). These results are presented treating each bouton as an independent element. When analysing the data grouped by axons the results are similar. In this case the survival fraction was computed for each axon in both age groups, the survival curves are then shown as the mean for each age group (Young Adult EPB survival fraction: day 0 = 1, day 4 = 0.93 ± 0.02, day 8 = 0.89 ± 0.03, day 12 = 0.85 ± 0.04, day 16 = 0.82 ± 0.04, day 20 = 0.79 ± 0.05, day 24 = 0.77 ± 0.05; Aged EPB survival fraction: day 0 = 1, day 4 = 0.89 ± 0.02, day 8 = 0.79 ± 0.02, day 12 = 0.71 ± 0.03, day 16 = 0.64 ± 0.03, day 20 = 0.60 ± 0.03, day 24 = 0.57 ± 0.04; log rank: P = 0.00003). This clear result shows that the ageing process affected the EPB rich axon population by increasing the rate at which EPBs are lost.

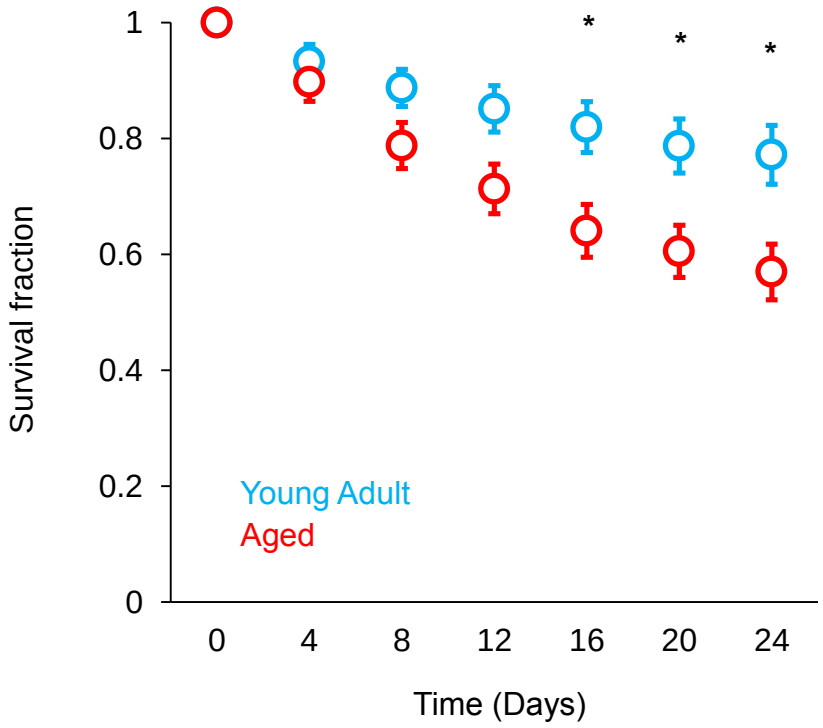

Figure 24 EPB survival curves for Young Adult (blue, n = 371 EPBs) and Aged (red, n = 852). The faster loss of initial EPBs for the Aged group reaches significance from day 16 onwards.

4.6.2 Bouton destabilization is more frequent on Aged EPB rich axons

The survival of EPBs imaged at the first time point was higher, as time goes by, in the Young Adults compared to the Aged animals. The ensemble of initial boutons included highly unstable boutons as well as more stable boutons that were more likely to have functional synaptic contacts. To distinguish these boutons from the more labile population a criterion of relative stability was adopted based on what known for dendritic spines and TBs (De Paola et al., 2006; Holtmaat et al., 2006; Knott et al., 2006; Trachtenberg et al., 2002). In these studies it has been shown that all spines (or TBs) present for over four days form synaptic contacts. Here all EPBs that were present in the first eight days of the imaging paradigm were considered as relatively stable synapses. The fraction of such EPBs that were lost before the end of the imaging protocol was computed. Thus a destabilized bouton was present on imaging day 0, day 4 and day 8 and subsequently lost before day 24. The

destabilization probability was then calculated as the number of destabilized EPBs divided by the total number of stable (from day 0 to day 8) boutons (Figure 25 a). Aged animals display a higher destabilization probability (Figure 25 a) for EPBs and a higher density of bouton destabilization events (Figure 25 b). The average destabilization probability per animal (destabilized EPBs / 8 day stable EPBs) was found to be significantly higher in the Aged (187 destabilized EPBs out of 658 EPBs considered) compared to the Young Adult (42 destabilized EPBs out of 327 EPBs considered) animals (Young Adult: destabilization probability = 0.14 ± 0.04, Aged: destabilization probability = 0.28 ± 0.01; *P* = 0.01; Figure 25 a). The density of destabilization events was calculated as the number of destabilized boutons per axonal length (destabilized EPBs / µm). Aged mice also in this case showed increased destabilization compared to the Young Adult group (Young Adult = 0.007 ± 0.002 destabilized EPBs / µm, Aged = 0.011 ± 0.001 destabilized EPBs / µm; *P* = 0.02; Figure 25 b). In view of these results, not only the survival of all boutons was affected but also the destabilization probability of relatively stable EPBs was altered in the Aged cortex.

Higher destabilization of synaptic boutons in the Aged brain was not accompanied by higher rates of stabilization (Figure 25 c and d). To study stabilization two slightly different parameters were used: 1) stabilization rate, 2) persistence rate. For the stabilization rate (Figure 25 c) all EPBs that were gained within the fifth imaging session (from day 4 to day 16) were considered, the ones that persisted to the end of the imaging (day 24) were divided by the total gained (stabilization rate = EPBs gained between day 4 – 16 and stable to day 24 / total EPBs gained between day 4 – 16; see methods). The initial window of four sessions (from the second to the fifth) was chosen to include enough boutons to make the calculation meaningful, if this window had been restricted to the second and third session the number of gained EPBs, especially for the Young Adult group, would not have been enough (61 EPBs in 9 animals). Stabilization rates were comparable between age groups [Young Adult stabilization rate = 0.32 ± 0.05 (33 stabilized EPBs out of 102 total gained in day 4 – 16), Aged = 0.29 ± 0.04 (152 stabilized EPBs out of 524 total gained in day 4 – 16); *P* =

0.71; Figure 25 c). For the persistence rate (Figure 25 d) the same population of boutons was considered as for the stabilization rate (i.e., EPBs gained between day 4 and day 16). Rather than being present at the end of the imaging protocol, EPBs that remained for at least three consecutive sessions (8 days: day of appearance, day +4 and day +8) were used to calculate the persistence rate (persistence rate = EPBs gained and present 8 days / total EPBs gained, see methods). The average persistence rate was similar in both age cohorts (Young Adult persistence rate = 0.68 ± 0.07 (73 EPBs out of 102 total gains), Aged = 0.69 ± 0.04 (353 EPBs out of 524 total gains); *P* = 0.84; Figure 25 d).

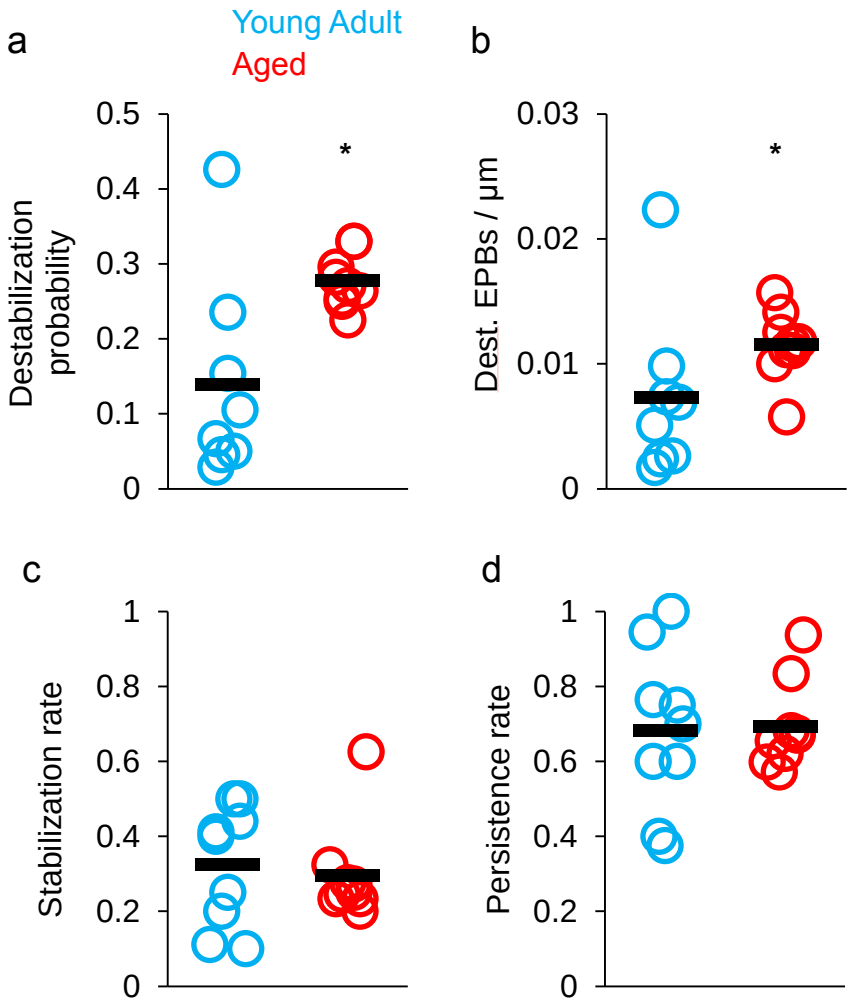

Figure 25 Destabilization vs. stabilization rates in Young Adult (blue, n = 9) and Aged (red, n = 9). (a) The EPB destabilization probability [(8 day stable EPBs that are lost) / (total 8 day stable EPBs) is higher for Aged mice. (b) Destabilization events per micron of imaged axon are more frequent in the Aged cortex. (c) The EPB stabilization rate [(EPBs gained days 4 to 16 and present to end) / (total EPBs gained 4 to 16)] is similar in both age cohorts. (d) EPB persistence rate [(gained EPBs that persist for 8 days) / (total gained EPBs)] is comparable in both age groups. (* $P < 0.05$).

4.6.3 Bouton turnover increases on Aged EPB rich axons

En passant boutons appeared to be less stable on Aged cortical axons compared to Young Adults. Both the survival fraction of initial EPBs and their destabilization probability increased in the Aged brain. As a consequence, more boutons were expected to be gained in order to maintain the stable bouton density throughout the imaging paradigm (see Figure 23 b). The

turnover rate (TOR) takes into account both gains and losses of boutons, it is a measure of bouton replacement over a specific period. The TOR is calculated as (*n* Gains + *n* Losses) / (2*n* total boutons, see methods) (De Paola et al., 2006; Holtmaat and Svoboda, 2009; Holtmaat et al., 2006; Trachtenberg et al., 2002). In order to keep the number of boutons constant, the TOR should be higher in Aged animals compared to Young Adults. This would represent a surprising result. Normally lower plasticity rates have been related to the ageing context (Bloss et al., 2011; Burke and Barnes, 2006, 2010; Dumitriu et al., 2010; Morrison and Baxter, 2012). Increased structural synaptic plasticity itself has been strongly linked to the contexts of development (Mostany et al., 2013; Portera-Cailliau et al., 2005), sensory alteration and peripheral lesion (Holtmaat et al., 2006; Keck et al., 2008; Keck et al., 2011; Trachtenberg et al., 2002) and importantly to the context of learning (Fu et al., 2012; Lai et al., 2012; Roberts et al., 2010; Xu et al., 2009; Yang et al., 2009). Because aged humans and aged animals (rats, mice and monkeys being the most studied) show a progressive decline of cognitive functions including the ability of learning specific tasks (Hara et al., 2012; Peters et al., 2008; Smith et al., 2000) the ageing brain is normally associated with decreased synaptic plasticity potential (Burke and Barnes, 2006, 2010; Grady, 2012; Morrison and Baxter, 2012; Park and Reuter-Lorenz, 2009). Although recently (Mostany et al., 2013) have shown that spine TOR increases in old mice, contradicting the consensus that spine dynamics, when altered, are lowered during the ageing process. EPB TOR over four days in the Young Adult imaged axons was comparable (~ 8% EPBs replaced every four days) to what previously described (De Paola et al., 2006). However, the Aged axons displayed a significantly higher TOR (~15% EPBs replaced every four days) compared to the younger mice (Young Adult TOR = 0.08 ± 0.009, Aged TOR = 0.15 ± 0.01; $P = 0.0001$; Figure 26 b). This result was further confirmed by calculating the density of turnover events (Figure 26 c). For each animal the sum of bouton gains and losses events was divided by the length of the imaged axons: (*n* gains + *n* losses) / unit length (μm). The average TOR density was significantly larger in the older age animal cohort (Young Adult = 0.009 ± 0.001

n gains + *n* losses / µm, Aged = 0.017 ± 0.002 *n* gains + *n* losses / µm; *P* = 0.001; Figure 26 c).

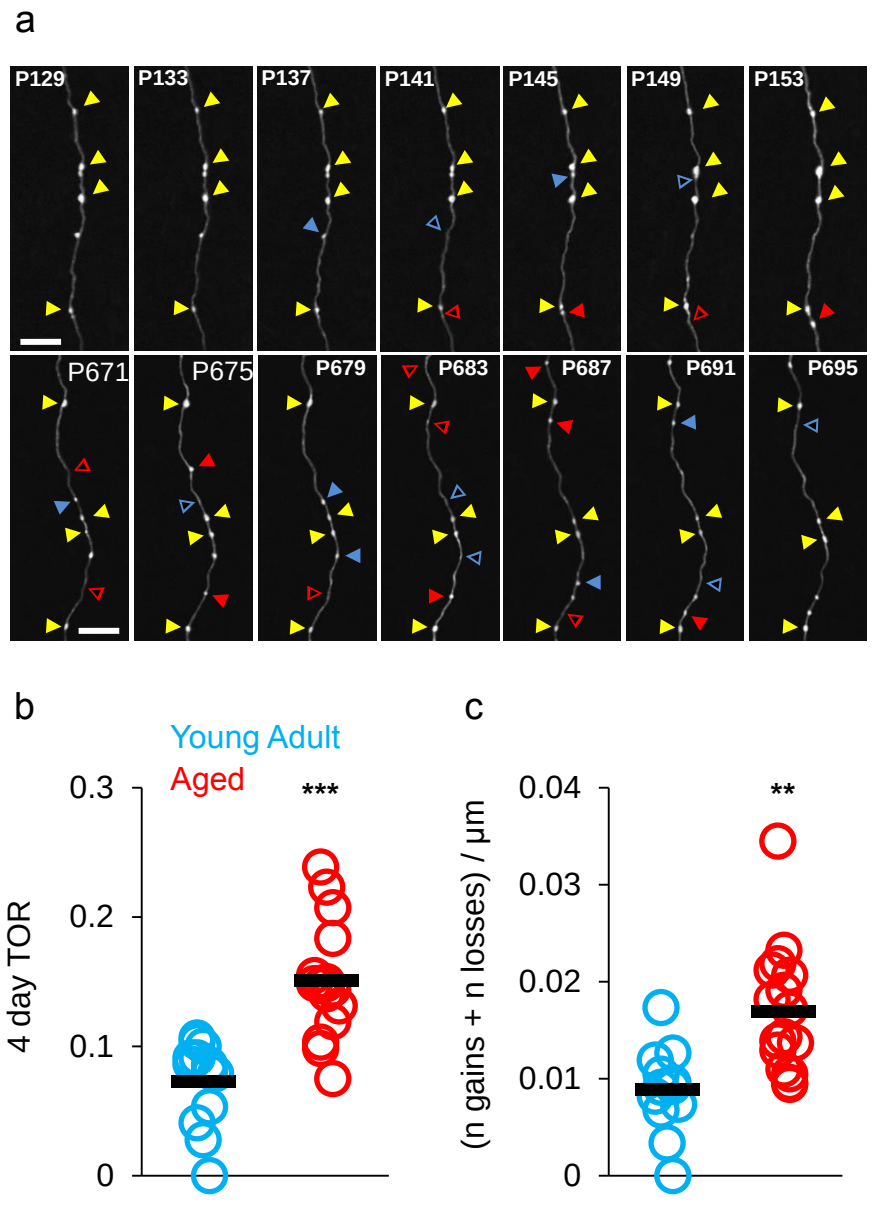

Figure 26 EPB four-day TOR is larger in Aged (red, n = 16) than in Young Adult (blue, n = 14) animals. (a) Time series (7 imaging sessions over 24 days) of two representative EPB rich axons in the Young Adult (upper row) and Aged (lower row) brain. In the top left corner of each panel the post natal (P) day of the mouse is indicated, scale bars are 10 µm. Yellow arrowheads point to persistent (always present) EPBs. Blue arrowheads highlight EPB losses, solid blue EPBs that will be lost in the following sessions and open blue the location of previously present EPBs. Red arrowheads point to EPB gains, open red the location of EPBs gained in the following time point, solid red EPBs gained. (b) EPBs are replaced more frequently in the Aged cortex as shown by the four-day EPB TOR. (c) the density of TOR events is higher in the Aged brain. (** *P* < 0.01, *** *P* < 0.001).

Importantly, EPB TOR on EPB rich axons was stable over time in both age cohorts (Figure 27). For both age groups no significant variation of TOR was found over time (Young Adult: TOR days 0 to 4 = 0.08 ± 0.01, days 4 to 8 = 0.07 ± 0.01, days 8 to 12 = 0.08 ± 0.01, days 12 to 16 = 0.07 ± 0.02, days 16 to 20 = 0.08 ± 0.01, days 20 to 24 = 0.06 ± 0.02; one way ANOVA: *P* = 0.88; Aged: TOR = days 0 to 4 = 0.16 ± 0.03, days 4 to 8 = 0.16 ± 0.02, days 8 to 12 = 0.14 ± 0.01, days 12 to 16 = 0.15 ± 0.02, days 16 to 20 = 0.15 ± 0.01, days 20 to 24 = 0.11 ± 0.01; one way ANOVA: *P* = 0.4; Figure 27).

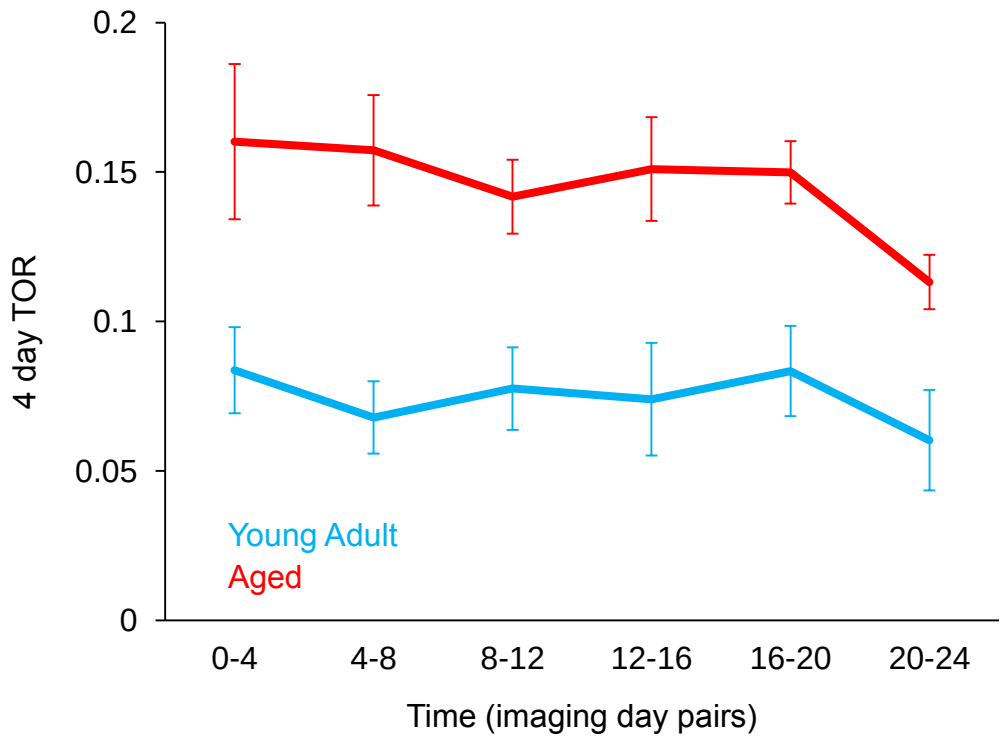

Figure 27 Four-day TOR is constant in both age groups. The Aged (red, n = 9) TOR remains higher than the Young Adult (blue, n = 9) TOR at all time point comparisons. Error bars are S.E.M.

4.6.4 TOR Increase due to increased EPB gains and losses on Aged axons

The unexpected higher TOR of EPBs on EPB rich axons in Aged animals was due to an increase in both bouton gains (gains fraction = *n* gains / *n* EPBs; gains density = *n* gains / µm) and losses (losses fraction = *n* losses / *n* EPBs; losses density = *n* losses / µm) (Figure 28). The average fraction of gained EPBs (Figure 28 a) was increased in Aged mice in comparison to Young Adult animals (Young Adult gains fraction = 0.046 ± 0.005, Aged gains fraction = 0.088 ± 0.006; *P* = 0.00002; Figure 28 a). The same trend was true for bouton losses (Figure 28 b), which were significantly more frequent in the Aged compared to what observed on Young Adult axons (Young Adult losses fraction = 0.032 ± 0.005, Aged losses fraction = 0.059 ± 0.005, *P* = 0.0007; Figure 28 b). Once again the results were further confirmed by the corresponding density parameters calculated on the basis of the total axonal length imaged for each animal (Figure 28 c and d). The number of gains per micron in the Young Adult group was lower than what found in the Aged cohort (Young Adult = 0.006 ± 0.0007 *n* gains / µm, Aged = 0.01 ± 0.0009 *n* gains / µm; *P* = 0.003; Figure 28 c). The density of EPB losses was also increased in the Aged group (Young Adult = 0.004 ± 0.0006 *n* losses / µm, Aged = 0.007 ± 0.0007 *n* losses / µm; *P* = 0.008; Figure 28 d).

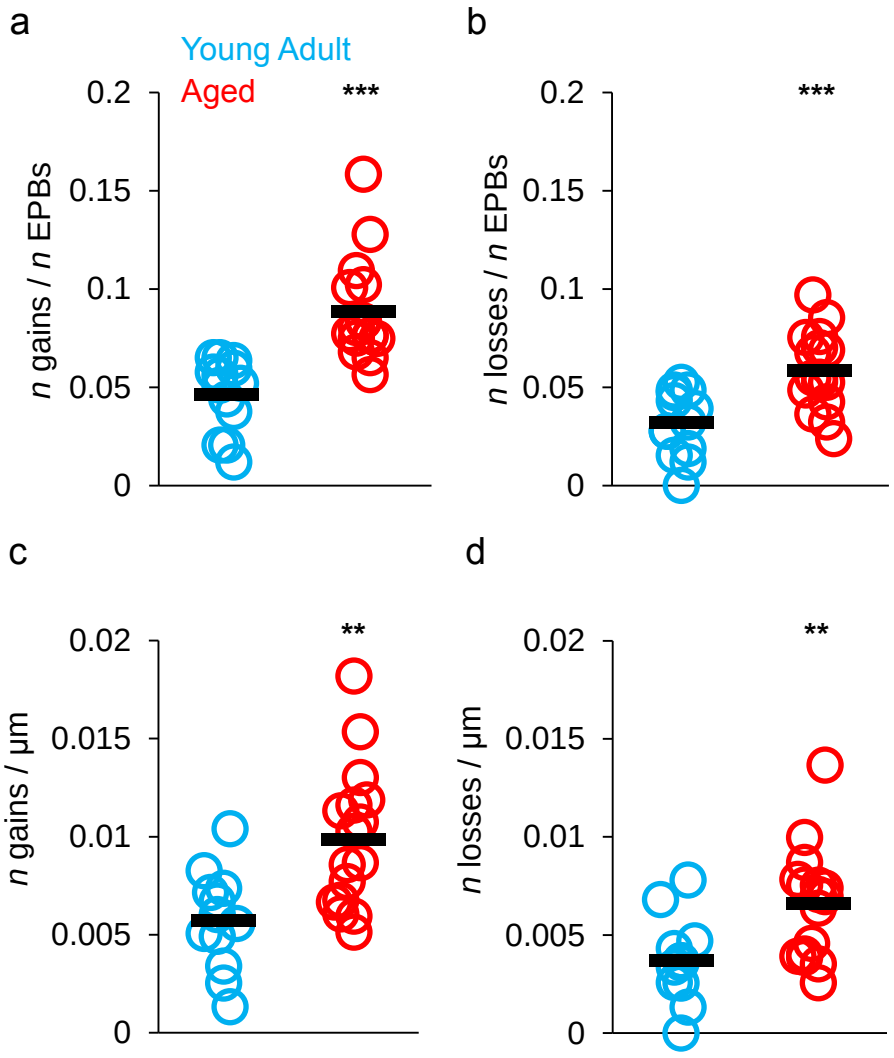

Figure 28 Both EPB gains and EPB losses contribute to the age related EPB TOR increase. (a) The fraction of EPB gains is higher in the Aged (red, n = 16) cortex compare to the Young Adult (blue, n = 14). (b) Fraction of EPB losses is higher in Aged animals. (c) The density of EPB gains is higher in Aged animals. (d) The density of EPB losses is higher in Aged mice. Black markers are mean values in corresponding groups. (** $P < 0.01$, *** $P < 0.001$).

Overall these data strongly suggest that *bona fide* synaptic boutons were added and eliminated more frequently in the Aged brain compared to the Young Adult brain, in a subset of excitatory neurons. Therefore the ageing process seems to target specific presynaptic elements, *en passant boutons* on intracortical and subcortical originating axons (De Paola et al., 2006; Feng et al., 2000). Contrary to what expected, the alteration of synaptic dynamics

was observed as an increase of structural plasticity in baseline conditions. EPBs were generally less stable and turned over more frequently in the Aged cortex, compared to the same axonal population imaged in Young Adult mice.

4.6.5 Similar EPB size in Aged and Young Adult animals

The development of the EPBscore software made possible to determine and follow over time the estimated size of individual EPBs. Bouton size is crucial to the synaptic function as larger boutons have more synaptic vesicles, more of which are docked (Knott et al., 2006), larger active zone areas, make contact with larger spines with wider postsynaptic densities and evoke larger post-synaptic potentials (Cheetham et al., 2012). Similar for what was observed for the overall EPB density, the average EPB intensity (Figure 29), hence size, was comparable between the Young Adult and Aged animals [Young Adult relative intensity = 5.46 backbone units ± 0.24 (n = 14 animals), Aged relative intensity = 5.16 backbone units ± 0.18 SEM (n = 16 animals); *P* = 0.35; Figure 29 a]. Intensity was stable over time for both age groups (Figure 29 b). Here a smaller number of animals was considered as not all animals completed the entire protocol lasting twenty-four days (Young Adult, n = 9; Aged, n = 9). In this case the average intensities seem further apart but are not significantly different and no significant difference is detected over time in either age group (Young Adult: relative intensity on day 0 = 5.66 ± 0.3, on day 4 = 5.52 ± 0.4, on day 8 = 5.76 ± 0.4, on day 12 = 5.61 ± 0.3, on day 16 = 5.64 ± 0.3, on day 20 = 5.47 ± 0.3, on day 24 = 5.45 ± 0.3; one way ANOVA: *P* = 0.99; Aged: relative intensity on day 0 = 5.29 ± 0.3, day 4 = 5.1 ± 0.2, on day 8 = 4.98 ± 0.2, on day 12 = 5.04 ± 0.3, on day 16 = 5.06 ± 0.3, on day 20 = 4.99 ± 0.2, on day 24 = 5.13 ± 0.3; one way ANOVA: P = 0.99; Figure 29 b).

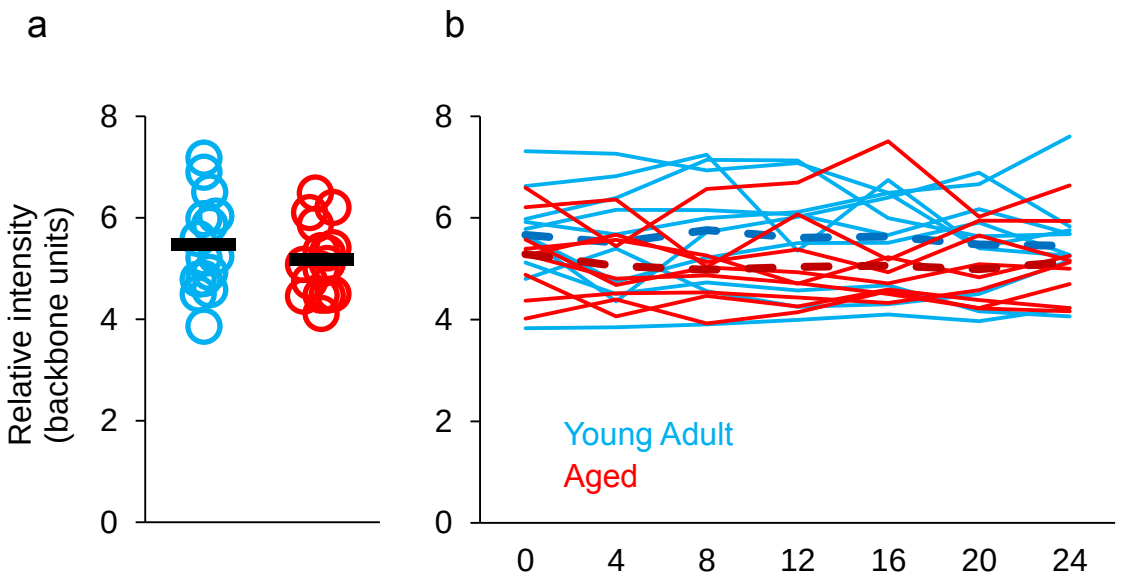

Figure 29 The average EPB intensity per animal is comparable between age groups. (a) Young Adult (blue, n = 14) and Aged (red, n = 16) animals have comparable EPB average size. Black markers are mean values for each group. (b) EPB size is constant over time for a subset of animals: 9 Young Adult, 9 Aged. Dashed lines are the mean values for each group over time.

Bouton intensity was further investigated by separating the stable EPB population from the unstable (persistent vs. non persistent boutons, Figure 30). Persistent EPBs were found at all imaging time points. These highly stable boutons may form crucial synapses that encode life long memories. No significant difference was found between the persistent EPBs of the Young Adult and Aged cohorts regarding their intensity, hence their volume [Young Adult (n = 14) persistent EPBs relative intensity = 5.99 backbone units ± 0.28, Aged (n = 16) persistent EPBs relative intensity = 6.4 backbone units ± 0.26; *P* = 0.28; Figure 30 a). As for the entire EPB population also persistent EPBs had a stable intensity on average over time [Young Adult (n = 9): persistent EPBs relative intensity on day 0 = 6.23 ± 0.3, on day 4 = 6.20 ± 0.4, on day 8 = 6.44 ± 0.4, on day 12 = 6.22 ± 0.4, on day 16 = 6.25 ± 0.3, on day 20 = 6.08 ± 0.3, on day 24 = 6.05 ± 0.3; one way ANOVA: *P* = 0.99; Aged: persistent EPBs relative intensity on day 0 = 6.18 ± 0.4, on day 4 = 6.45 ± 0.4, on day 8 = 6.46 ± 0.4, on day 12 = 6.7 ± 0.5, on day 16 = 6.48 ± 0.4, on day 20 = 6.44 ± 0.4, on day 24 = 6.27 ± 0.4; one

way ANOVA; *P* =0.98; Figure 30 b). When considering the non-persistent (Figure 30 c and d) population of EPBs, boutons that were absent at least once in any of the seven imaging sessions, the overall intensity was lower than what found for the persistent EPBs (i.e. non persistent EPBs are smaller than persistent EPBs, on average), but no difference was highlighted among age groups [Young Adult (n = 14) non-persistent EPBs relative intensity = 3.39 backbone units ± 0.07, Aged (n = 16) non-persistent EPBs relative intensity = 3.59 ± 0.1; *P* = 0.1; Figure 30 c). Finally, over time, the mean intensities of non-persistent EPBs (i.e. their average sizes) remained stable for both cohorts (Figure 30 d). No significant difference was observed over consecutive imaging sessions for either age group [Young Adult: (n = 9) non-persistent EPBs relative intensities on day 0 = 3.11 backbone units ± 0.2, on day 4 = 3.4 ± 0.2, on day 8= 3.64 ± 0.2, on day 12 = 3.73 ± 0.2, on day 16 = 3.62 ± 0.3, on day 20 = 3.37 ± 0.1, on day 24 = 3.43 ± 0.07; one way ANOVA: *P* = 0.44; Aged: (n = 9) non-persistent EPBs relative intensities on day 0 = 4.03 backbone units ± 0.2, day 4 = 3.53 ± 0.1, day 8 = 3.53 ± 0.1, day 12 = 3.41 ± 0.1, day 16 = 3.46 ± 0.1, day 20 = 3.56 ± 0.1, day 24 = 3.82 ± 0.1; one way ANOVA: *P* = 0.32; Figure 30 d).

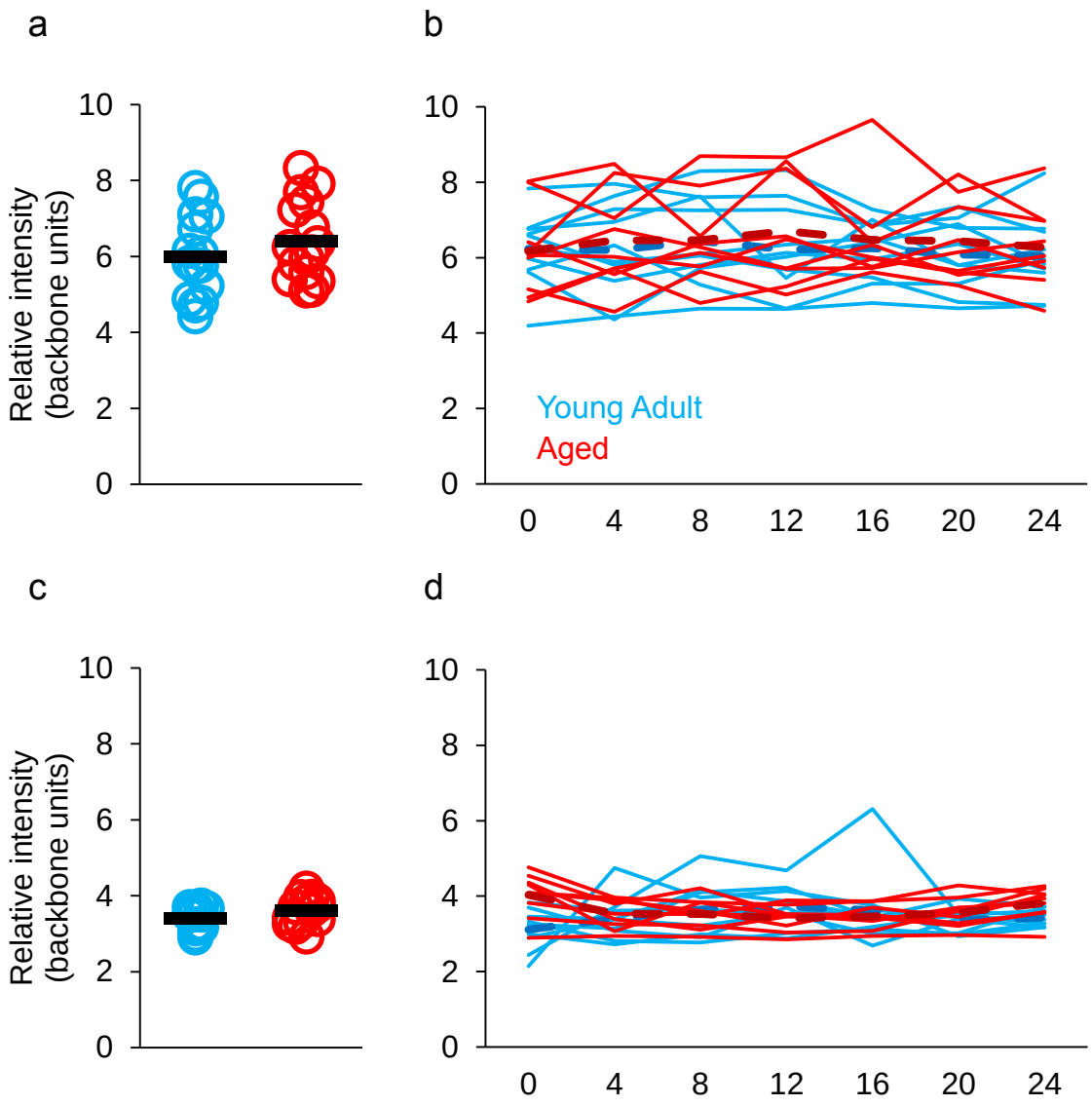

Figure 30 Persistent and non-persistent EPBs have comparable sizes in Young Adult and Aged animals. (a) Persistent (always present) EPBs size is similar in Young Adult (blue, n = 14) and Aged (red, n = 16) mice. Black markers are the mean value for each group. (b) Persistent EPBs have a constant average size for both age cohorts, Young Adult (n = 9), Aged (n = 9). Dashed lines are mean values. (c) Non-persistent (absent in one imaging session) EPBs average size is similar in Young Adult (blue, n = 14) and Aged (red, n = 16) mice. Black markers are the mean value for each group. (d) Non-persistent EPBs average size is constant over time in Young Adult (n = 9) and Aged (n = 9) mice. Dashed lines are mean values.

4.6.6 Large EPBs are greatly affected in the aged cortex

On average the intensity, hence the size, of EPBs was comparable between Aged and Young Adult animals. Furthermore, the average intensities were stable over the entire imaging period. This was true for both the persistent and non-persistent EPB populations in Aged and Young Adult animals. To gain further insights into potential synaptic bouton alterations the distribution of bouton intensities was taken into consideration. The two distribution curves were highly similar and overlapping (Figure 31), these were calculated on day 4 of imaging and take into account all EPBs for both age groups. The curves highlighted a log-normal behaviour of EPB intensity, with many EPBs on the small side and only few large boutons, similar for what previously known for dendritic spines (Loewenstein et al., 2011; Song et al., 2005).

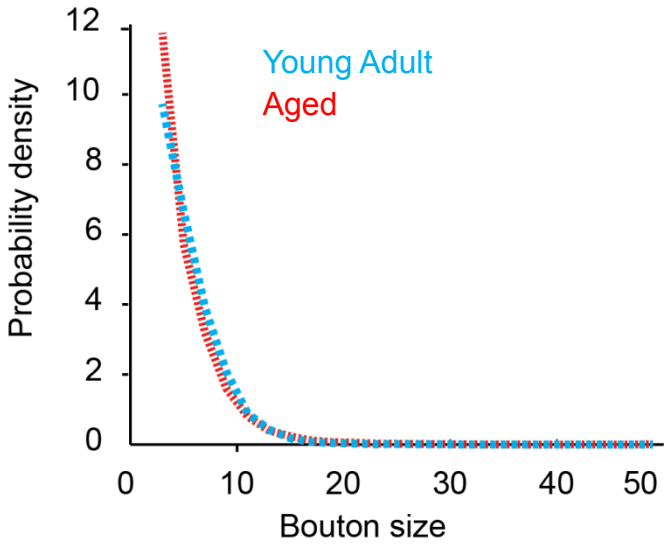

Figure 31 The distribution of EPB sizes in Young Adult (blue, n = 1082 EPBs) and Aged (red, n = 1900) animals is similar.

The next step was to check how bouton size influenced the synaptic dynamics (Figures 31 and 32). Bouton size is not only important in synaptic transmission (Cheetham et al., 2012), it should also determine the stability of a bouton, as larger boutons are more likely to persist. As previously seen, the persistent EPBs are considerably larger than the non-persistent EPBs (~2 fold difference, relative intensity ~6 vs. ~3 backbone units), similarly large spines are more stable than the more labile thin spines (Holtmaat and Svoboda, 2009). To study the behaviour of large as opposed to small EPBs a subset of EPBs were selected, both in Young Adults and Aged mice, corresponding to the top third of each distribution (large) and the bottom third of each distribution (small). As a consequence large EPBs were defined as boutons above 5.9 backbone intensity units in the Young Adult cohort and above 5.4 in the Aged. Small boutons were defined as between 2 and 3.6 backbone intensity units in the Young Adult group and between 2 and 3.2 in the Aged. While small EPBs displayed similar rates of destabilization [Young Adult (n = 9) small EPBs destabilization probability = 0.41 ± 0.07; Aged (n = 9) small EPBs destabilization probability = 0.52 ± 0.05; P = 0.26; Figure 32 a], their four-day TOR was higher in the Aged cortex compared to the Young Adult [Young Adult: (n = 14) small EPB 4 day TOR = 0.30 ± 0.03, Aged: (n = 16) small EPB 4 day TOR = 0.43 ± 0.04; P = 0.02; Figure 32 b]. Both turnover rates resulted higher than what previously shown for all boutons (Figure 26). As expected small EPBs (i.e. weak) were overall highly destabilized and replaced in both age groups.

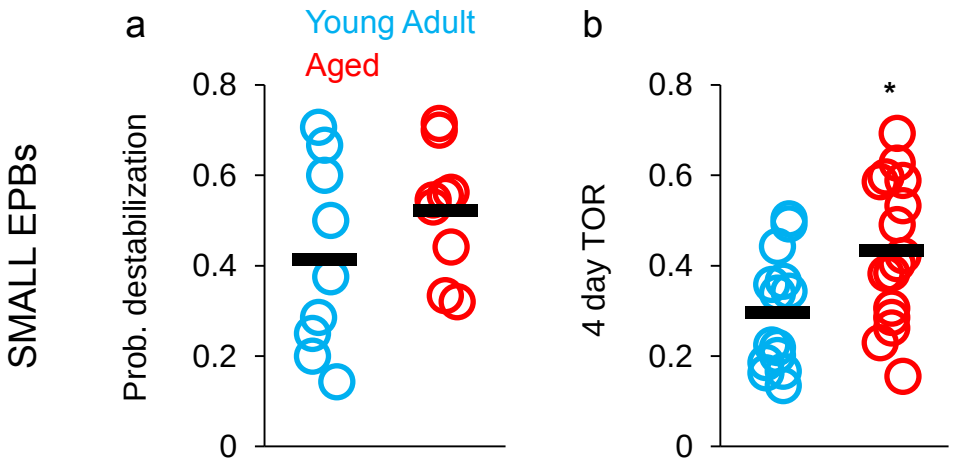

Figure 32 Small EPBs are highly unstable in both age groups. Small EPBs are defined as part of the lower third of EPB size distribution for each age group. (a) The destabilization probability of small EPBs is similar for Young Adult (blue, n = 9) and Aged (red, n = 9) mice. The four-day TOR for small EPBs is significantly higher for the Aged (n = 16) than for the Young Adult (n = 14) animals. Black markers are mean values for each group. (* $P < 0.05$).

On the contrary, large EPBs, although more stable than small EPBs and the overall bouton population (Figures 24 and 25), were found to have up to 6 times larger destabilization probability and 16 times larger four-day TOR in the Aged brain compared to the Young Adult cortex (Figure 33). Large EPBs were more likely to be destabilized in the Aged animals compared to the younger ones [Young Adult (n = 9 animals, 5 destabilized EPBs out of 151 stable EPBs) large EPBs destabilization probability = 0.03 ± 0.02, Aged (n = 9 animals, 41 destabilized EPBs out of 246 stable EPBs) large EPBs destabilization probability = 0.17 ± 0.04; $P = 0.004$; Figure 33 c). The four-day TOR was also markedly higher in Aged mice compared to the younger group [Young Adults (n = 14 animals, 3 TOR events out of 343 total EPBs) large EPB TOR = 0.001 ± 0.001; Aged (n = 16, 46 TOR events out of 599 total EPBs) large EPBs TOR = 0.02 ± 0.005 SEM; $P = 0.0001$; Figure 33 d). Thus, it appeared that the stability of large (i.e. strong) EPBs was critically affected during ageing. These EPBs are likely to form large multiple synapses (Figure 20) with strong synaptic transmission, possibly encoding for long lasting memory traces.

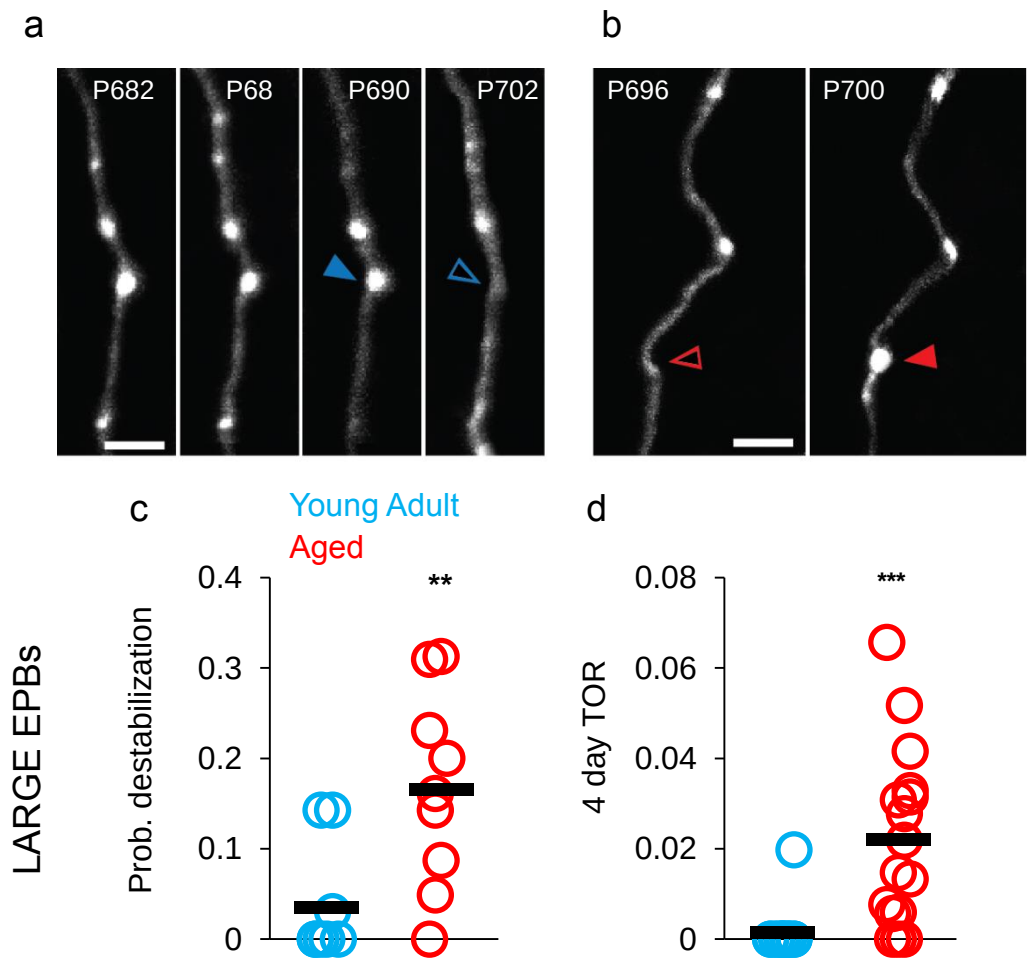

Figure 33 Large EPBs are greatly affected in the Aged brain. (a) Time series showing a large (bright) EPB (blue arrowhead) destabilized at postnatal (P) day 702 in the intact brain. (b) A large EPB (red arrowhead), which was not present four days earlier, is being added at P700 in the intact brain. (c) The average destabilization probability is very low for Young Adult (blue, n = 9) large EPBs, and it is significantly higher for the Aged (red, n = 9) population. Large EPB TOR is rare in Young Adult (n = 14) mice and considerably more frequent in Aged (n = 16) animals. Black markers are mean values for each group. (** $P < 0.01$, *** $P < 0.001$).

4.7 Volume changes of individual EPBs are larger on Aged axons

Overall EPB dynamics were increased in the Aged cortex. EPBs turned over more frequently, destabilized more frequently and large EPBs were greatly affected. Despite the heightened dynamic behaviour, EPB rich axons in Aged and Young Adult mice displayed

similar EPB density and similar EPB size. Besides the appearance and disappearance of synaptic boutons, their variation in size is an important parameter. The size of a bouton positively correlates with the number of vesicles it contains (Knott et al., 2006) and with the Post-Synaptic Density (PSD) surface it contacts (Cheetham et al., 2012; Knott et al., 2006). Bouton size and PSD area can be increased in an experience dependent manner leading to synaptic strengthening (Cheetham et al., 2012). Therefore changes in volume of existing EPBs and could play a major role in the ability of the circuit to encode and store new information. How well the two-photon in vivo imaging system, coupled with the EPBscore application, is able to pick biologically meaningful changes in EPB size (Figure 22) has been described in previous sections. To express size changes, the Intensity Ratio (IR) measure was adopted, $IR = \exp[\mathrm{abs}(\log_{\text{intensity A}} - \log_{\text{intensity B}})]$. The IR simply divides the higher intensity value by the lower, per each individual EPB, in consecutive sessions regardless of the temporal sequence of acquisition. IR is independent on bouton size whereas the absolute intensity difference is correlated to it (Figure 34). Similarly, as what happens for dendritic spines (Loewenstein et al., 2011) the amount of change that a bouton undergoes between imaging sessions is proportional to its size. The absolute intensity difference ($|\text{Intensity}_a - \text{Intensity}_b|$, see methods) for both Young Adults and Aged animals significantly correlated with the size of the boutons [Young Adult (n = 1082 EPBs) linear correlation coefficient R = 0.46, $P = 0.001$, Figure 34 a; Aged (n = 1588 EPBs) correlation coefficient R = 0.63, $P < 0.001$; Figure 34 b]. On the other hand, the absolute intensity ratio does not correlate with bouton size, as expected because of the normalization [Young Adult (n = 1082 EPBs) correlation coefficient R = -0.013, $P = 0.69$, Figure 34 c; Aged (n = 1900 EPBs) correlation coefficient R = 0.006, and $P = 0.75$, Figure 34 d]. Therefore, to avoid bias due to EPB size, the IR was adopted to measure EPB size changes *in vivo*.

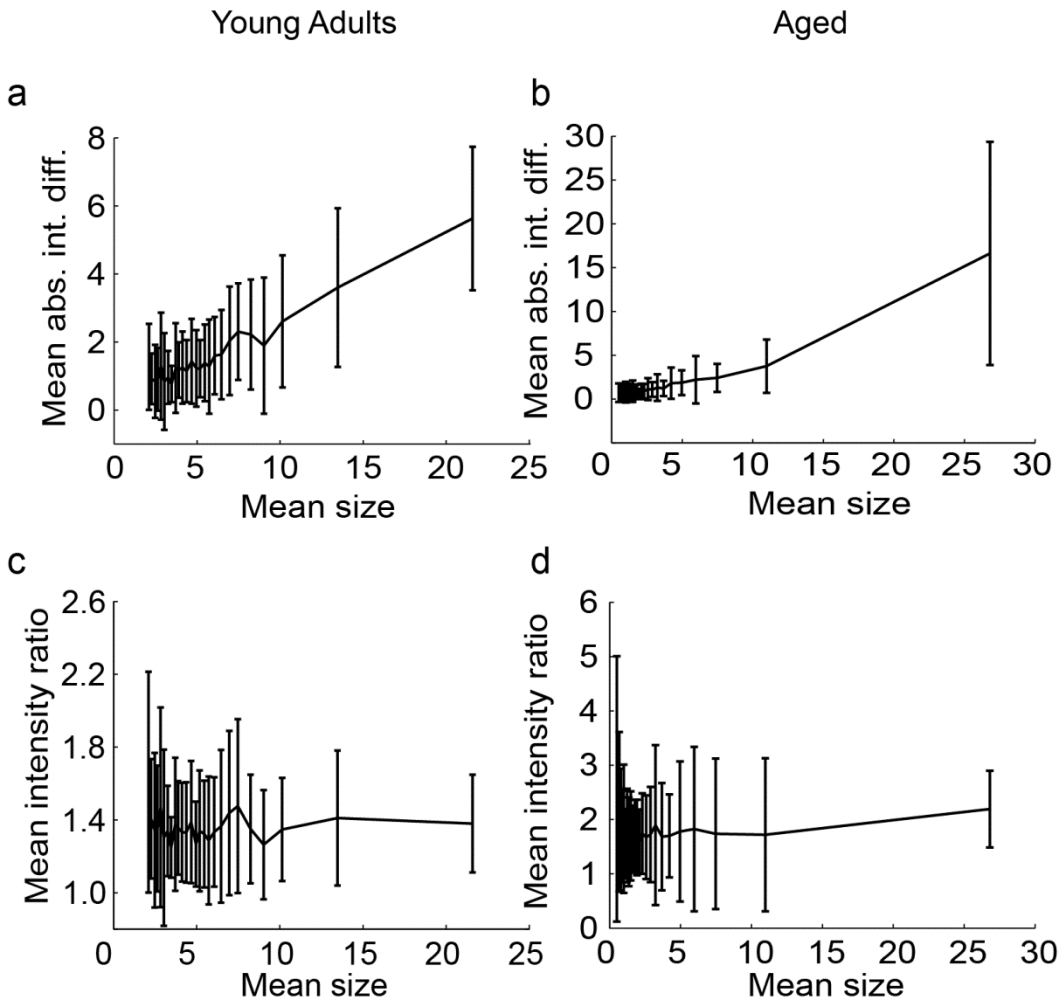

Figure 34 The mean EPB size is proportional to the mean absolute intensity difference between consecutive imaging sessions (in a and b) but not to the mean intensity ratio between sessions (in c and d). The size of an EPB positively correlates to the absolute intensity difference ($|intensity_A - intensity_B|$) in consecutive imaging sessions, both in Young Adult (a) and in Aged (b) mice. The mean IR of an EPB does not correlate with the mean EPB size neither in Young Adult (c) nor in Aged (d) animals. Error bars are standard deviation.

EPBs display a constant average size that is not affected by continuous imaging (Figures 29 b, 30 b and d). Such descriptions do not account for the possible shrinkage (i.e. weakening) and enlargement (i.e. strengthening) of individual boutons over time. The rate at which EPB volumes fluctuate between imaging sessions is greater in the Aged rather than in the Young Adult brain (Figures 35 and 36).

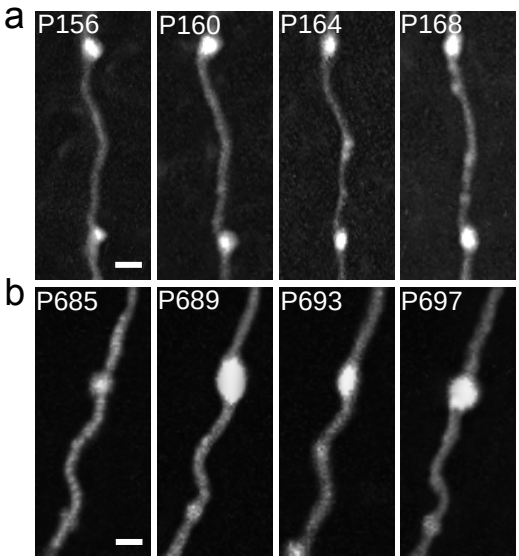

Figure 35 Volume fluctuations of EPBs over time are larger in Aged (lower row) than in Young Adult (upper row) mice. P (postnatal day), scale bars 2 µm.

Mean volume fluctuations, considering all individual EPBs, were larger on the Aged cortical axons compared to the Young Adult axons [Young Adult: (n = 980 EPBs) IR = 1.36 ± 0.01, Aged: (n = 1636 EPBs) IR = 1.43 ± 0.01; *P* = 0.006; Figure 36 a]. Young Adults display a ~ 36% EPB volume change while Aged mice ~ 43%. Interestingly, such increase in the rate of volume change of Aged EPBs compared to the Young Adult group was mainly due to the population of persistent EPBs, those present in all imaging sessions (stable for twenty-four days). The mean IR of persistent EPBs was significantly higher for the Aged group [Young Adult: (n = 707 EPBs) IR = 1.35 ± 0.01, Aged: (n = 1013 EPBs) IR = 1.44 ± 0.01; *P* = 0.002; Figure 36 b]. The non-persistent population of boutons (EPBs that were not present at every time point) did not show a significant difference between age groups in the rate of EPB size change over time [Young Adult: (n = 273 EPBs) IR = 1.38 ± 0.02, Aged: (n = 623 EPBs) IR = 1.41 ± 0.02; *P* = 0.54; Figure 36 c].

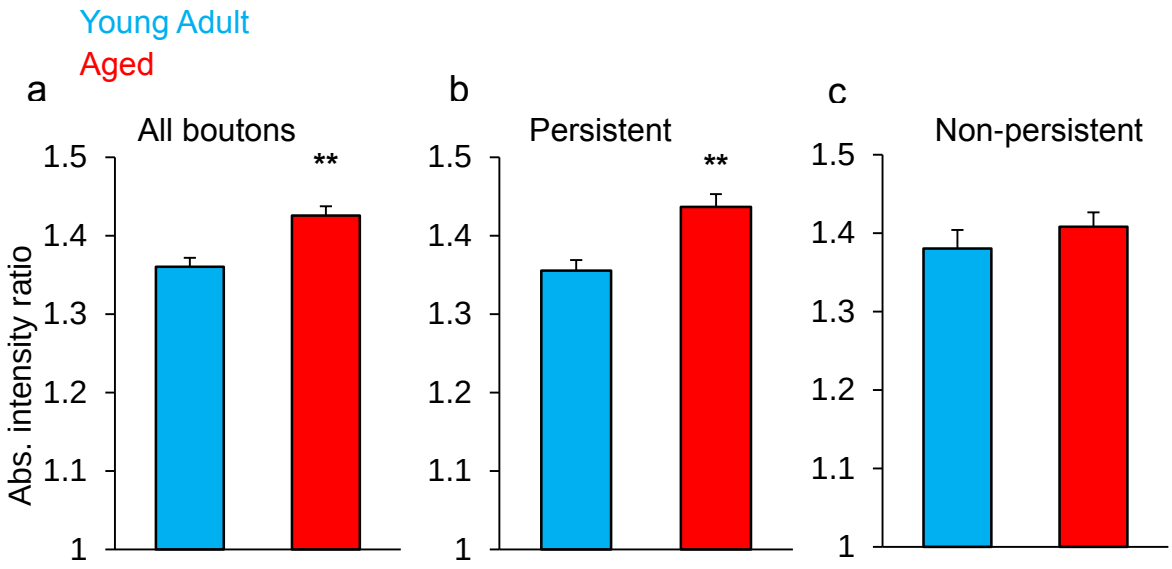

Figure 36 EPB size changes are more prominent on EPB rich axons imaged in the Aged (red) cortex compared to the Young Adult (blue) brain. (a) IR for all boutons on Young Adult (n = 980) and Aged (n = 1636) axons is larger in the Aged group. (b) The increase in IR for Aged (n = 1013) compared to Young Adult (n = 707) EPBs is mainly due to persistent (always present) EPBs. (c) No significant difference is seen between IR values of non-persistent (absent at least once) EPBs, Aged (n = 623) Young Adult (n = 273). Error bars are S.E.M. (** $P < 0.01$).

The IR of persistent EPBs was also constant over time in the animals that underwent the entire imaging paradigm (twenty-four days – seven sessions, Figure 37). The average IR in the Aged mice remained constantly above what measured in the Young Adult animals and in both age groups no significant variation was detected over time [Young Adults: (n = 9 animals, 273 EPBs) IR on days o to 4 = 1.37 ± 0.03, on days 4 to 8 = 1.39 ± 0.03, on days 8 to 12 = 1.34 ± 0.05, on day 12 to 16 = 1.34 ± 0.05, on days 16 to 20 = 1.33 ± 0.04, on days 20 to 24 = 1.34 ± 0.02; one way ANOVA: $P = 0.88$; Aged: (n = 9 animals, 471 EPBs) IR on days 0 to 4 = 1.44 ± 0.05, on days 4 to 8 = 1.44 ± 0.03, on days 8 to 12 = 1.40 ± 0.02, on day 12 to 16 = 1.38 ± 0.03, on days 16 to 20 = 1.39 ± 0.04, on days 20 to 24 = 1.41 ± 0.02; one way ANOVA: $P = 0.74$; Figure 37].

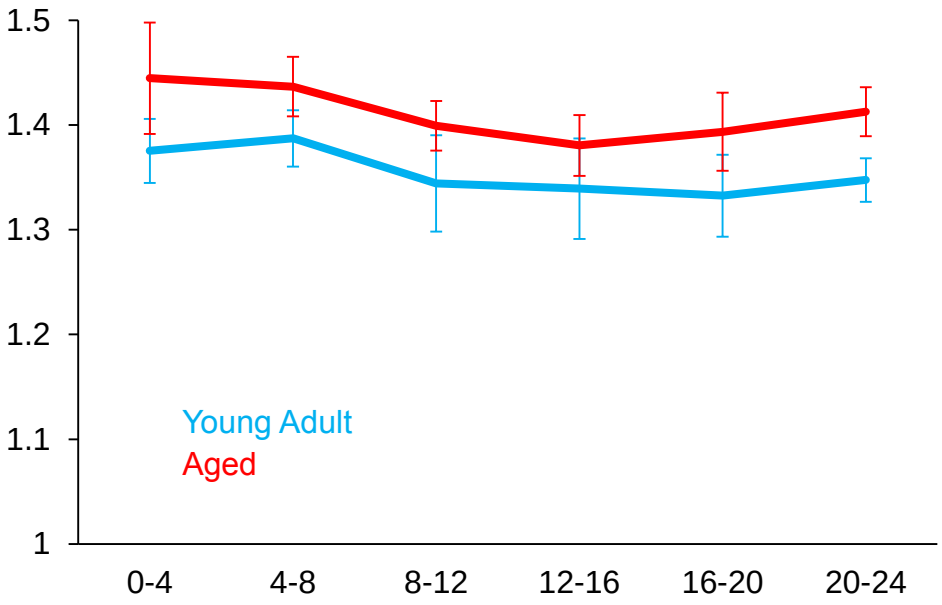

Figure 37 The average IR of EPBs is constant in both age groups. IR is maintained higher in the Aged (red, n = 9) than in the Young Adult (blue, n = 9) mice in all time point comparisons.

In summary, although the average size of EPBs was similar on EPB rich axons in the two age cohorts, the rate at which sizes were changing was different, unexpectedly larger in the Aged brain. Moreover, the main contribution to such difference was brought by highly stable EPBs (persistent population) which should represent the physical substrate of long lasting mnemonic traces.

4.8 Correlation analysis of TOR, destabilization and IR.

Compared to the Young Adult, the Aged brain has increased EPB turnover, increased EPB destabilization probability and increased EPB size variations. To check whether these parameters were somehow linked together a correlation analysis was carried out on data from single axons imaged in the Aged cortex (Figure 38). A correlation matrix was employed

to calculate the correlation coefficients of each of the three possible pairs, including all the axons that completed the entire imaging paradigm. This was limited by the destabilization probability parameter as it had to be computed necessarily over twenty-four days of imaging. This reduced dataset was extracted from 9 animals and 21 axons. The analysis revealed a strong correlation between the four-day TOR and the IR and a correlation trend between the four-day TOR and the destabilization probability, but no obvious correlation between the IR and destabilization probability (correlation matrix: IR vs. 4 day TOR R = 0.55, *P* = 0.009, Figure 38 a; destabilization probability vs. 4 day TOR R = 0.39, *P* = 0.08, Figure 38 b; IR vs. destabilization probability R = 0.28, *P* = 0.22, Figure 38 c). Many more axons were imaged over a shorter period for which it was possible to extract information regarding four-day TOR and IR (n = 16 animals, 54 axons). When considering all axons the correlation coefficient was lower but the significance stronger (linear correlation 4 day TOR vs. IR R = 0.39, *P* = 0.004, Figure 38 d).

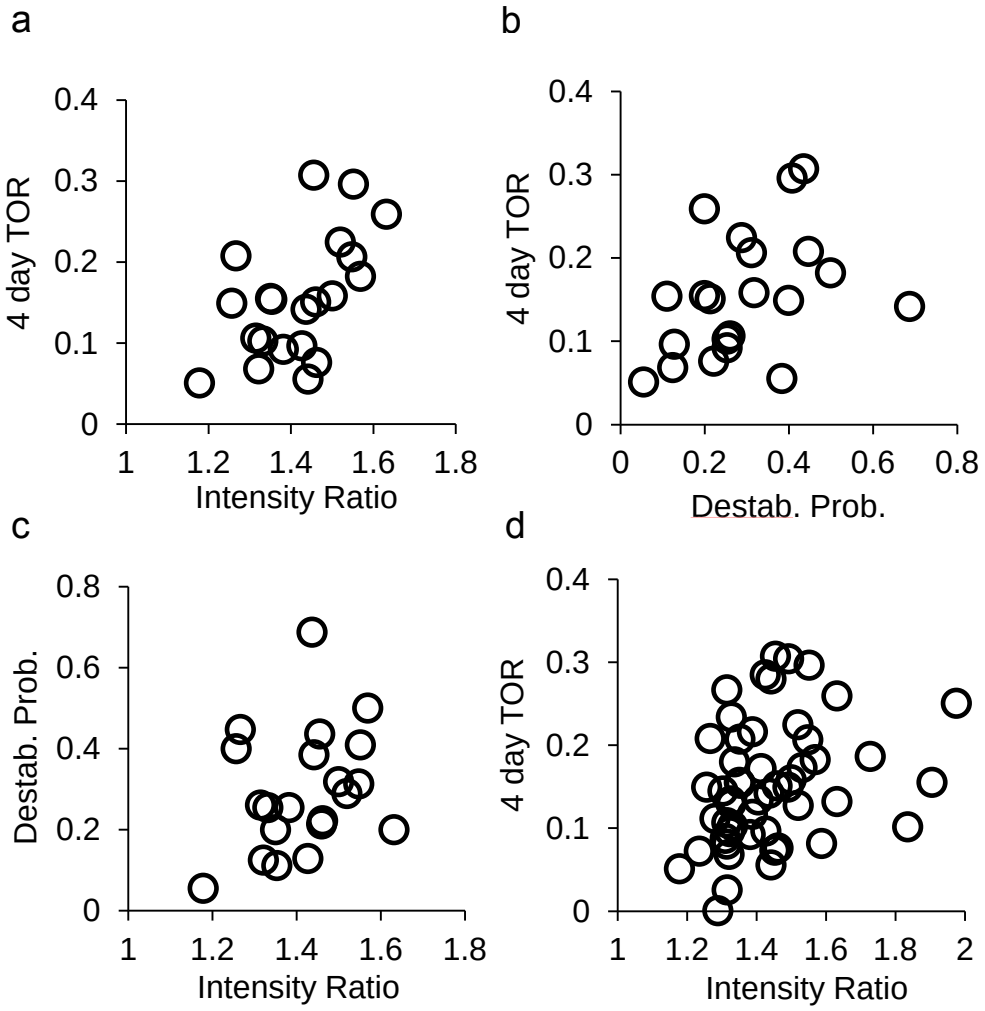

Figure 38 Correlation plots of EPB dynamic parameters in the Aged cortical axons. (a – c) a correlation matrix was employed to find correlation coefficients and significance levels for the axons that completed the imaging paradigm (n = 21 from 9 mice). Only the four day TOR and the IR show a significant positive correlation (a). (d) Correlation plot of four day TOR and IR including all available data (n = 54 from 16 animals) confirms strong correlation.

4.9 Conclusions

While neuronal loss has long been ruled out as a cause for physiological ageing (Peters et al., 1998a), synaptic impairments have often been described as the main age related mechanisms of cognitive decline (Burke and Barnes, 2006). It has been widely documented that the ageing process is accompanied by a loss of synaptic elements in different brain regions, mainly in the hippocampus and the prefrontal cortex (Morrison and Baxter, 2012).

Generally, synaptic plasticity is thought to decrease in the older stages of life. This view derives from the notion that ageing is accompanied by learning difficulties and learning, in turn, positively correlates with synaptic plasticity (Bliss and Collingridge, 1993; Caroni et al., 2012; Holtmaat and Svoboda, 2009; Hubener and Bonhoeffer, 2010).

In this chapter, a detailed description of the structure and dynamics of axonal boutons on EPB rich axons in the intact brain of Aged and Young Adult animals has been presented. EPBs, which form synapses mainly with dendritic spines (Anderson and Martin, 2001), had comparable densities in the Aged and Young Adult superficial layers of somatosensory cortex (Figure 23 a). Moreover, the density of EPBs was constant over the twenty-four-day imaging period (Figure 23 b). This result was not anticipated as it is generally accepted that ageing correlates with decreased synaptic density, although such decrease might be region and circuit specific and recent evidence challenges this view (Benice et al., 2006; Mostany et al., 2013). Contrary to what found by Mostany and colleagues, the size of EPBs was not larger in Aged mice compared to the Young Adult animals (Figures 29, 30 and 31). Furthermore, what was profoundly different to all of these mentioned studies was the increase of synaptic structural plasticity found in the Aged cortex compared to the Young Adult brain. In particular EPBs were found to be less stable in the Aged brain. The SF of boutons imaged on the first imaging session was lowered significantly, ~ 20% less EPBs (over twenty-four days) survived on Aged axons compared to Young Adult processes Figure 24). EPBs that were initially stable were lost more frequently in the Aged cohort (Figure 25 a and b). Both the destabilization probability and density were higher for Aged EPBs, compared to Young Adult EPBs. Relatively stable EPBs (present for the first eight days) were twice as much more likely to be lost in the Aged compared to the Young Adult mice. In contrast, measurements of stabilization were not increased and were similar in both age groups (Figure 25 c and d). To maintain constant EPB density Aged axons displayed augmented EPB turnover (Figure 26). Both the fraction and density of four-day TOR events were higher, by twofold, in Aged animals. Over an extended time course (twenty-four days)

the four-day TOR remained constant in the two age groups (Figure 27). Such increased four-day TOR was generated equally by increased rates in EPB gains and EPB losses (Figure 28). A remarkable difference was found in the destabilization probability and the amount of four-day TOR of large EPBs (Figure 33). Large EPBs, that form stronger synapses (Cheetham et al., 2012; Harris and Stevens, 1989; Knott et al., 2006), were 6 times more likely to destabilize in the Aged compared to the Young Adult cortex (Figure 33 c). The four-day TOR for large EPBs was up to 20 times higher, than what observed in Young Adults, in the Aged animals (Figure 33 d). On the other hand, small EPB dynamics were more comparable. The destabilization probability, high in both groups, was not significantly different between Aged and Young Adult animals (Figure 32 a). Small EPBs were turned over frequently in both age cohorts; the four-day TOR was significantly larger for the Aged group (Figure 32 b). The difference in TOR, however, was not as striking as for what seen in the large EPB population, which were hardly ever turned over on axons belonging to Young Adult mice.

Besides the appearance and disappearance of EPBs from the axonal process, size changes of persistent and non-persistent EPBs were studied (Figures 35 and 36). Thanks to the EPBscore tool it was possible to accurately track the volume changes of individual boutons over time. The best way to express bouton size change was found to be the Intensity Ratio parameter, which was independent of EPB size unlike the absolute intensity difference (Figure 34). The IR revealed that EPBs in the Aged brain undergo larger volume fluctuations compared to what happens in the Young Adult brain. In particular, it was the population of persistent EPBs that contributed the most to such increased rate of size change, whilst the non-persistent EPBs did not display a significant difference on Aged as opposed to Young Adult axons (Figure 36). The fact that non-persistent EPBs are not affected in terms of size changes during ageing suggests that volume fluctuations and turnover are not coupled at the bouton level. At the level of single axons, though, IR and four-day TOR were positively

correlated in the Aged brain, so that for axons on which EPBs turned over more, the IR was also higher (Figure 38).

In summary, the heightened EPB dynamics found in Aged mice was an unexpected but robust finding. The increased destabilization and turnover of EPBs seen in Aged individuals could underlie a decreased synaptic tenacity, which in turn might impede efficient functionality of neural circuits.

5. Recognition memory deficit in aged mice

5.1 Introduction

Increased synaptic plasticity is generally linked to heightened cognitive performance. Ageing, in turn, is generally linked to cognitive decline. For this reason it was important to assess the cognitive performance of the animals used in this study, to exclude the possibility that Aged mice have improved cognitive abilities. Rodents have the natural tendency to explore for longer a novel object rather than a previously encountered object (Bevins and Besheer, 2006). This behaviour can be exploited to test whether the animals correctly remember the familiar item hence forming a durable memory. The classical test is termed Novel Object Recognition test and was first described by (Ennaceur and Delacour, 1988). The test is normally based on visual exploration and recognition. Typically, it consists of a familiarization period with the testing environment, a sample trial with the familiar object presented, a retention period that normally lasts 1 hour for short-term or 1 day for long-term memory tests and a test trial where the novel object is presented along with the familiar one (Bevins and Besheer, 2006). In this study the test was adapted to be more relevant to the cortical area under consideration, somatosensory cortex S1. The experiments were performed in the dark to impede visual exploration and recognition of the objects. The mice were therefore forced to explore and eventually recognize the objects by physical contact mainly using their *vibrissae*. The objects were designed to be distinguishable by tactile discrimination only. The two object classes had either a rough or smooth surface texture but shared same size and shape. The objects were custom made using 60 ml sample cylinders, sand paper was applied to obtain either a rough or smooth surface. The two different textures were given by sand paper with coarse grit size (P80 – average particle diameter 201 μm) for the rough objects and with superfine grit size (P1000 – average particle

diameter 18.3 μm) for smooth objects. Tactile discrimination of rough and smooth objects has previously been demonstrated in rodents (Maricich et al., 2012; von Heimendahl et al., 2007; Wu et al., 2013). Using these tools the ability to form long-term memories was tested in Young Adults and Aged mice.

5.2 Aged mice fail to form long term recognition memory

The animals underwent a 5-minute familiarization trial with no objects in the open field. Then they were exposed to the familiar objects in three successive 6-minute sample trials. Between each trial a 3-minute inter-trial period was observed. The test trial was performed 24 hours later. In the test trial animals were presented with the familiar object (identical to the objects previously explored) and a novel object that could be rough or smooth depending on what was used as the familiar. Aged mice failed to recognize the familiar object in the test trial and did not spend a significantly larger amount of time exploring the novel object while Young Adult mice were able to remember the familiar object (Figure 39). In total 13 Aged animals and 13 Young Adult mice were tested. The two graphs shown below (Figure 39 a and b) summarize the average exploration time expressed in seconds that the animals spent on both objects during each trial, each graph belonging to one age group. Young Adult mice explored the two objects during all 3 sample trials for a total of 25.2 seconds ± 6.01. Through the sessions a habituation process was evident as exploration time decreased considerably, in sample 1 the mice spent on average 13.3 ± 3.7 seconds exploring the objects (6.2 ± 1.6 s object A and 7.1 ± 2.1 s object B), in sample 2 a total 7.4 ± 2.1 seconds (3.5 ± 1.1 s and 3.9 ± 3.1 s) and in sample 3 4.4 ± 1.4 seconds (2 ± 0.7 s and 2.4 ± 0.8 s). In the test trial, 24 hours later, Young Adult mice explored on average the objects for a total 8.6 ± 1.5 seconds, they spent 5.4 ± 0.99 s on the novel object (always in position A) and 3.2 ± 0.62s on the familiar object (in position B). To assess if the increase for the novel object exploration time was a sign of memory formation a Two-Way ANOVA test was performed (P = 0.043, Figure

39 a). This indicated that Young Adult mice between 4 and 5 months of age were able to remember and recognize a familiar object after a retention period of a day. On the other hand, Aged mice have difficulty retaining such memory for 24 hours, although they show a similar habituation to the familiar objects during the 3 sample periods, spaced only 3 minutes apart. Overall, Aged mice spent 25.6 ± 5.2 seconds actively exploring the objects in the 3 sample trials. In sample trial 1 Aged animals explore on average the two objects for a total 13.3 ± 3.05 seconds (6.7 ± 1.5s object A and 6.6 ± 1.6s object B), in sample 2 the average total exploration time was 7.4 ± 1.7 seconds (3.1 ± 0.7s and 4.3 ± 1.2s) and in sample 3 it was 4.9 ± 1.4 seconds (2.5 ± 0.7s and 2.4 ± 0.7s). The next day during the test Aged animals spent a similar amount of time exploring the novel and the familiar object (which was always placed in position B as for Young Adult mice), respectively 3.44 ± 0.72 s and 3.29 ± 0.67 s for a total 6.73 ± 1.33 seconds. Two-Way ANOVA analysis confirmed that Aged mice did not recognize the familiar object (P = 0.93, Figure 39 b). A difference between the two age groups also arose when calculating the discrimination index (DI), a common way of expressing novel object recognition test results (Bevins and Besheer, 2006). The DI takes into consideration the difference between novel and familiar object exploration times and normalizes it to the total exploration time in the test trial, DI = [(novel exploration time / total exploration time) – (familiar exploration time / total exploration time) x 100]. The average DI values were significantly higher for the Young Adult compared to the Aged mice (Young Adult DI = 29.78 ± 5.5, Aged DI = 3.99 ± 6.65; unpaired t-test, P = 0.005; Figure 39 c).

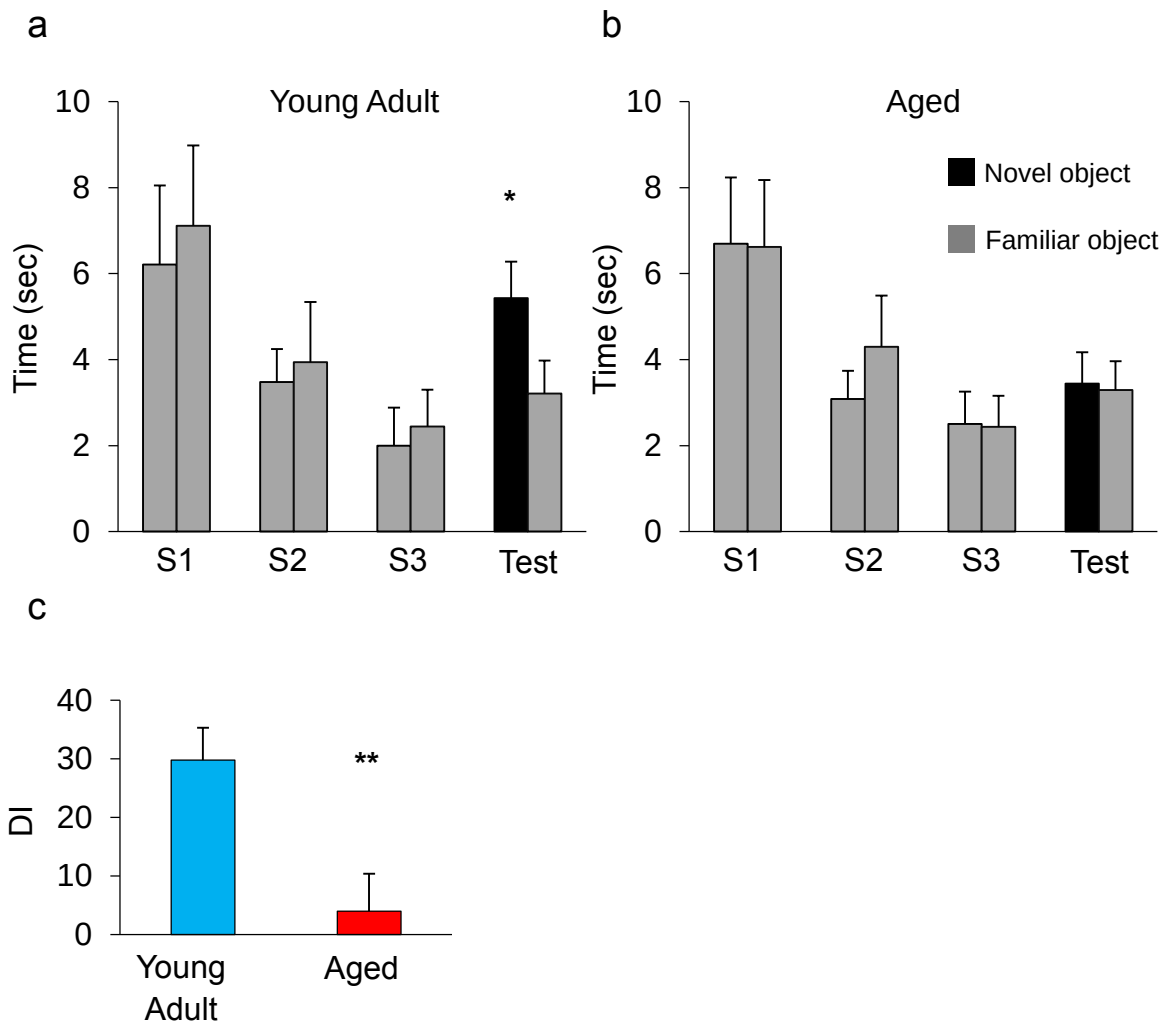

Figure 39 Aged mice fail to form long term memory recognition. (a – b) In the sample period (S1, S2 and S3) the exploration time decreases for successive trials. (a) Young Adult (n = 13) mice spend more time exploring the novel object (black bar) in the test session than the familiar object (grey bars). (b) Time spent exploring novel and familiar objects by the Aged (n = 13) mice is comparable in the test trial. (c) The Discrimination Index is significantly lower for Aged (red bar) mice compared to the Young Adult (blue bar) cohort. (* $P < 0.05$, ** $P < 0.01$).

5.3 Whiskers are essential for recognition memory formation

Intact whiskers were essential for texture discrimination in rodents (Maricich et al., 2012; Wu et al., 2013). To further strengthen the link between the chosen behavioural essay and the *in vivo* imaged area (Somatosensory / Barrel cortex) 13 Young Adult animals had their

whiskers trimmed the day before the object recognition task started. Whisker-trimmed mice failed to recognize the familiar object [Whisker Trimmed mice exploration times: Sample 1 = total 11.3 seconds ± 1.5 (5.3 ± 0.8 seconds object A, 5.9 ± 0.7 seconds object B), Sample 2 = total 5.3 ± 1.4 seconds (2.4 ± 0.7 seconds object A, 2.9 ± 0.8 seconds object B), Sample 3 = total 4.1 ± 1.4 seconds (2.1 ± 0.9 seconds object A, 1.9 ± 0.6 seconds object B), Test = total 6.8 ± 1.4 seconds (3.1 ± 0.6 seconds the novel object, 3.7 ± 0.8 seconds the familiar object), two way ANOVA: *P* = 0.58; Figure 40 a]. The calculated discrimination index for whisker-trimmed animals was significantly lower compared to the age matched untreated Young Adults (Young Adult DI = 29.78 ± 5.5, whisker-trimmed DI = -8.7 ± 6.3; *P* = 0.0001; Figure 40 b).

Figure 40 Whisker deprived Young Adults (n = 13) fail to recognize the familiar object. (a) In the sample period (S1, S2 and S3) the exploration time decreases for successive trials. In the test trial no difference is found in the exploration times of the novel versus the familiar objects. (b) The Discrimination Index of the Whisker-trimmed (black bar) group is significantly lower than what previously described for the Young Adult (blue bar) cohort. (*** *P* < 0.001).

5.4 Aged mice form short term recognition memory

Importantly, Aged mice were able to recognize the familiar and spent more time exploring the novel object when the latency between the sample period and the test was reduced to 1 hour (Figure 41). This finding rules out the possibility that Aged mice were unable to discriminate different textures due to age related sensory impairments. Aged (n = 11) mice, in the 1 hour latency test, spent more time in contact with the novel object [Aged 1h exploration: Sample 1 = total 23.4 seconds ± 3.7 (11.4 ± 1.8 seconds object A, 11.9 ± 1.9 seconds object B), Sample 2 = total 12.8 ± 2.8 seconds (5.8 ± 1.3 seconds object A, 7.0 ± 1.5 seconds object B), Sample 3 = total 9.1 ± 1.4 seconds (4.4 ± 0.7 seconds object A, 4.6 ± 0.7 seconds object B), Test = total 11.3 ± 2.6 seconds (8.1 ± 2.1 seconds the novel object, 3.2 ± 0.7 seconds the familiar object), two way ANOVA: $P = 0.049$; Figure 41 a]. The DI in Aged mice was significantly higher when the delay between sample period and test trial was reduced to 1 hour compared to the DI previously reported for the 24 hour latency test (Aged 1 hour: DI = 37.4 ± 8.5, Aged 24 hours: 3.99 ± 6.65; $P = 0.005$; Figure 41 b).

Figure 41 Aged (n = 11) mice were able to form short-term recognition memory. (a) In the sample period (S1, S2 and S3) the exploration time decreases for successive trials. The test trials took place 1 hour after the sample period ended. In this case Aged animals spent more time exploring the novel object. (b) The Discrimination Index of the Aged 1 hour cohort (black bar) is significantly higher than what previously described for the Aged 24 hour (red bar) group. (* $P < 0.05$, ** $P < 0.01$).

5.5 Conclusions

Ageing has been shown to affect the cognitive performance of humans as of animals (Morrison and Baxter, 2012). In mice, in particular, spatial memory impairments (Bach et al., 1999; Barreto et al., 2010) and deficits in implicit learning like fear memory renewal, (Sanders, 2011) have been reported. In the previous chapter it has been shown how the Aged cortex is characterized by increased synaptic dynamics when compared to the Young Adult brain. Generally a change in synaptic plasticity has been linked to learning through new experiences.

Here, impairment in a form of explicit learning, object recognition, has been shown to affect Aged mice. In particular Aged mice were unable to discriminate novel textures 24 hours after being exposed to the familiar texture (Figure 39 b and c). On the other hand, Young Adult animals were able to remember the familiar object and spent more time exploring the novel

object in the test phase (Figure 39 a). This difference suggests that Aged mice have a difficulty to consolidate new long-term tactile memories over the space of a day. Overall these results show that heightened synaptic dynamics in the Aged, compared to the Young Adult cortex, are associated with a specific cognitive deficit in an explicit memory task.

To better associate the task with the two-photon *in vivo* imaged area (Barrel field and primary somatosensory cortex) a group of Young Adult animals was tested after their *vibrissae* had been trimmed bilaterally. This group of animals did not display a preference for the novel object in the test trial (Figure 40), indicating that intact whiskers (which provide the sensory input to the barrels) are essential in tactile object recognition and texture discrimination as previously thought (Diamond et al., 2008; Maricich et al., 2012; von Heimendahl et al., 2007; Wu et al., 2013). The fact that Aged animals could successfully explore for longer the novel object, when the test phase was temporally closer to the sample period, suggests that ageing primarily affects memory retention rather than sensation (Figure 41). Furthermore it shows that Aged mice retain the recognition memory over a short period (1 hour) but cannot consolidate it for longer (24 hours).

6. Immunohistochemical analysis of astrocytes under the cranial window

6.1 Introduction

The increased synaptic dynamics in the Aged brain, which have been extensively described above, could be an indirect cause of the craniotomy on Aged mice. It is possible that a stronger reaction takes place in aged tissues rather than in younger ones. However, by the simple observation of the data presented, this does not seem to be the case. For instance in both the Aged and Young Adult all the parameters presented are not affected over time: there is no significant increase or decrease in bouton number (Figures 14 b, 23 b), bouton size (Figures 29 b, 30 b), bouton turnover (Figures 17, 26). Furthermore the rates of bouton gains and losses do not display a net variation as the imaging progresses, nor do the intensity ratio levels (Figure 37). This relative stability within the two groups points out that the preparation is not affected by post-surgery side effects, or that, at the very least, it has reached a stable phase for both age groups (15 to 40 days post-surgery). The craniotomy, shortly after the procedure is carried out, does in fact cause a typically transient astrocytic reaction and proliferation (Holtmaat et al., 2009) which is correlated to boosted structural spine rearrangements (Xu et al., 2007). The heightened synaptic dynamics seen here though are specifically confined to one presynaptic element, the EPBs, and do not occur on a different circuit and presynaptic class, the TBs. If the craniotomy had a role it would be expected that both morphological classes would suffer the same fate.

6.2 Immunohistochemical analysis of astrocytes under the cranial window

To exclude any astrocytic contribution, to the aforementioned increase in EPB dynamics, antibody stainings were performed on cortical sections containing the superficial layers immediately below the cranial window. Coronal sections of the region of interest were employed in order to have direct comparison with the contralateral corresponding region, which should not be affected by the window implantation. The sections were stained (Figure 42 a) with anti-GFAP (Glial Fibrillary Acidic Protein – an astrocytic marker) antibody and DAPI (4',6-diamidino-2-phenylindole – a nuclear marker for all cells). GFAP positive cells that colocalized with a DAPI stained nucleus were counted. Astrocytes were not found to be upregulated in the Aged cortex compared to the Young Adult cortex [Young Adult: (n = 3 animals, 24 regions of interest) average GFAP positive cell count = (ipsilateral = 276.8 ± 63.1 *n* cells / mm^2, contralateral = 200.2 ± 53.9 *n* cells / mm^2; *P* = 0.41; Figure 35 b); Aged (n = 4 animals, 28 regions of interest) average GFAP positive cell count = (ipsilateral = 253.7 ± 83.9 *n* cells / mm^2, contralateral = 180 ± 47 *n* cells / mm^2; *P* = 0.47, Figure 42 b)]. No significant difference was found between age groups either (ipsilateral, Aged vs. Young Adult, *P* = 0.84; contralateral, Aged vs. Young Adult, *P* = 0.79; Figure 42 b).

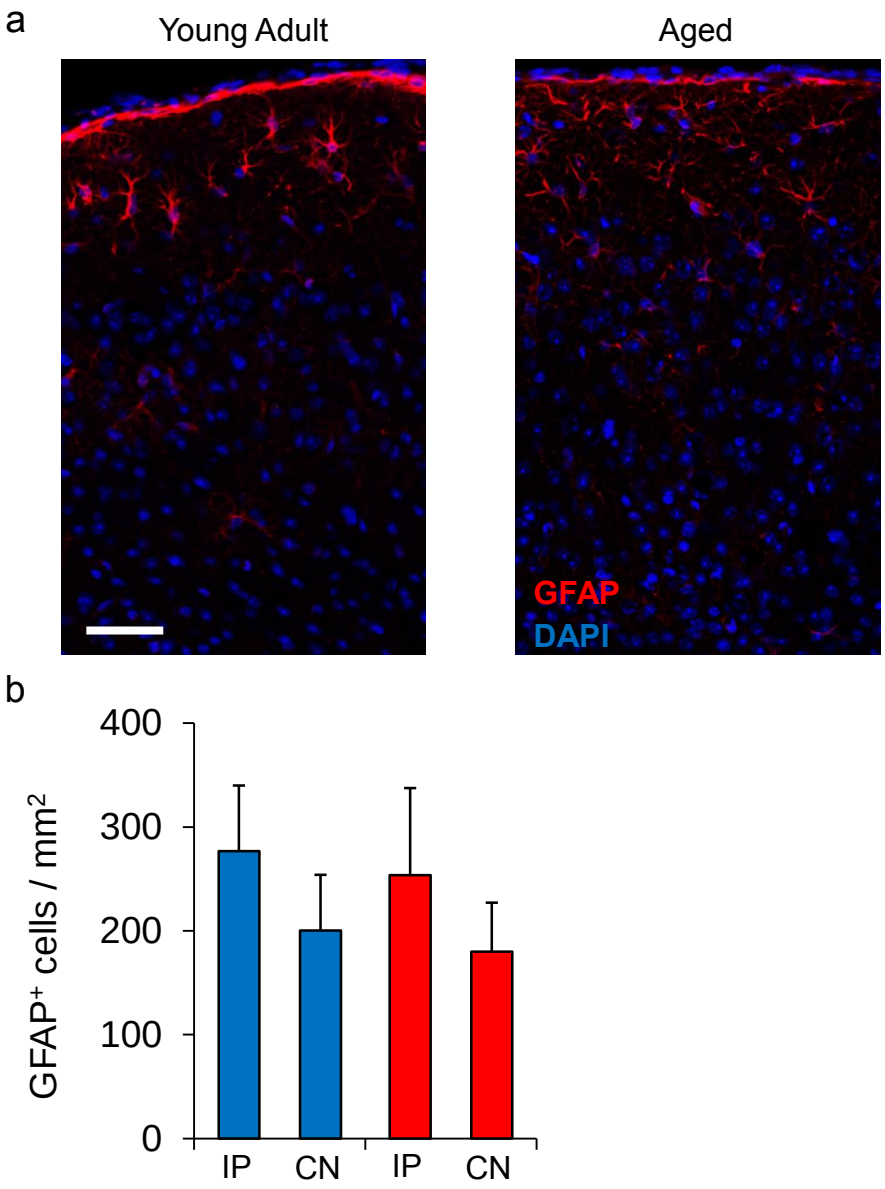

Figure 42 Astrocytic cell counts are comparable in Young Adult (n = 3) and Aged mice (n = 4) during the imaging time window (25 – 35 days post-surgery). (a) Representative ipsilateral regions of interest under the viewing windows of a Young Adult (left) and an Aged (right) mouse. Astrocytes are stained in red (anti-GFAP) and all cells nuclear staining in blue (DAPI). Scale bar is 50 μm. (b) GFAP positive cell counts per surface area (mm^2) are comparable between age groups. Though reduced, the average GFAP cell count is not significantly different in areas ipsilateral (IP) and contralateral (CN) to the window.

6.3 Conclusions

Immunohistochemical stainings were able to confirm that the upregulation of synaptic dynamics, seen in Aged mice, was not associated with an upregulation of astrocytes caused by the craniotomy procedure. In both age cohorts more astrocytes (GFAP positive cells) were found on the ipsilateral (to the viewing window) side of the cortex although this increase was far from being significant. More importantly, no significant difference was found across age groups when comparing the corresponding cortical sides, suggesting that the amount of cortical reaction to the surgery is comparable and does not play a role in the differences in synaptic remodelling that the Aged mice display. Furthermore the result is in line with the indications extracted from the data in paragraph 6.2.

7. Middle Age mice: EPB dynamics and cognition

7.1 Middle Age mouse group

The increase in bouton dynamics and destabilization between Aged and Young Adult cohorts was striking. These two age groups represent the final stage of a mouse life and the fully mature stage of adulthood respectively. Ageing, in these animals, affects cognition (long-term memory impairment) and the dynamic behaviour of *en passant boutons*. A key question is at what stage of life these increased synaptic dynamics manifest themselves in the intact rodent brain. A preliminary set of data was collected to try to address this point. Three Middle Age (12 to 14 months old) mice were studied (n = 11 EPB rich axons, 7.4 mm, 401 initial EPBs and 701 unique EPBs). Though a reduced animal cohort, the Middle Age mice data were used to check parameters of EPB dynamics at an earlier stage of life compared to the Aged group. Results from such a small group of animals cannot be taken as conclusive; however they offer an indication of when the EPB defects described above might start taking place.

7.2 EPB dynamics in the Middle Age resemble the Aged group results

Here the main parameters that have been presented in the previous sections are proposed with the inclusion of the three Middle Age animals. Interestingly, this small group of individuals behaved, in terms of EPB dynamics, similarly to the Aged cohort. Overall, EPB rich axon plasticity rates seemed heightened compared to the Young Adult group, suggesting a relatively early onset for age related synaptic plasticity alterations.

7.2.1 EPB survival and destabilization

The survival fraction of EPBs observed at the start of the imaging period was considerably lower in the Aged cortex compared to the Young Adult brain (Figure 24). In the Middle Age group the survival fraction was significantly lower than what seen in the Young Adult brain (Figure 43 a). The SF curves, the average EPB survival on each imaged axon, were comparable between Aged and Middle Aged groups. Of the initial Middle Age EPBs (present on day 0) nearly half were lost by the end of the imaging (Middle Age total EPBs: day 0 = 401, day 4 = 347, day 8 = 284, day 12 = 253, day 16 = 233, day 20 = 217, day 24 = 204; Middle Age average EPB survival fraction by axon: day 0 = 1, day 4 = 0.88 ± 0.02, day 8 = 0.75 ± 0.04, day 12 = 0.67 ± 0.05, day 16 = 0.63 ± 0.06, day 20 = 0.6 ± 0.06, day 24 = 0.57 ± 0.06; Figure 43 a). Compared to the Young Adult survival fraction, the Middle Age one was significantly lower [considering individual EPBs independently (Young Adult, n = 371; Middle Age, n = 401; log rank test: P = 0.0000004); comparing average survival by axon (Young Adult, n = 15; Middle Age, n = 11; Wilcoxon rank sum: P = 0.038); Figure 43 a].

EPBs were lost at similar rates in Aged and Middle Age mice; the destabilization probability followed a similar pattern. Though higher than the Young Adult, the Middle Age destabilization probability did not reach significance possibly due to the small sample size (3 animals, Figure 43 b). 284 EPBs were present in each of the first three imaging sessions (from day 0 to day 8) in the Middle Age group. From this stable pool of EPBs 80 boutons were lost by the end of the imaging (Middle Age destabilization probability = 0.29 ± 0.07; Young Adult = 0.14 ± 0.05; P = 0.08; Figure 43 b). The result was not significantly different to the Young Adults, though a trend towards significance was present.

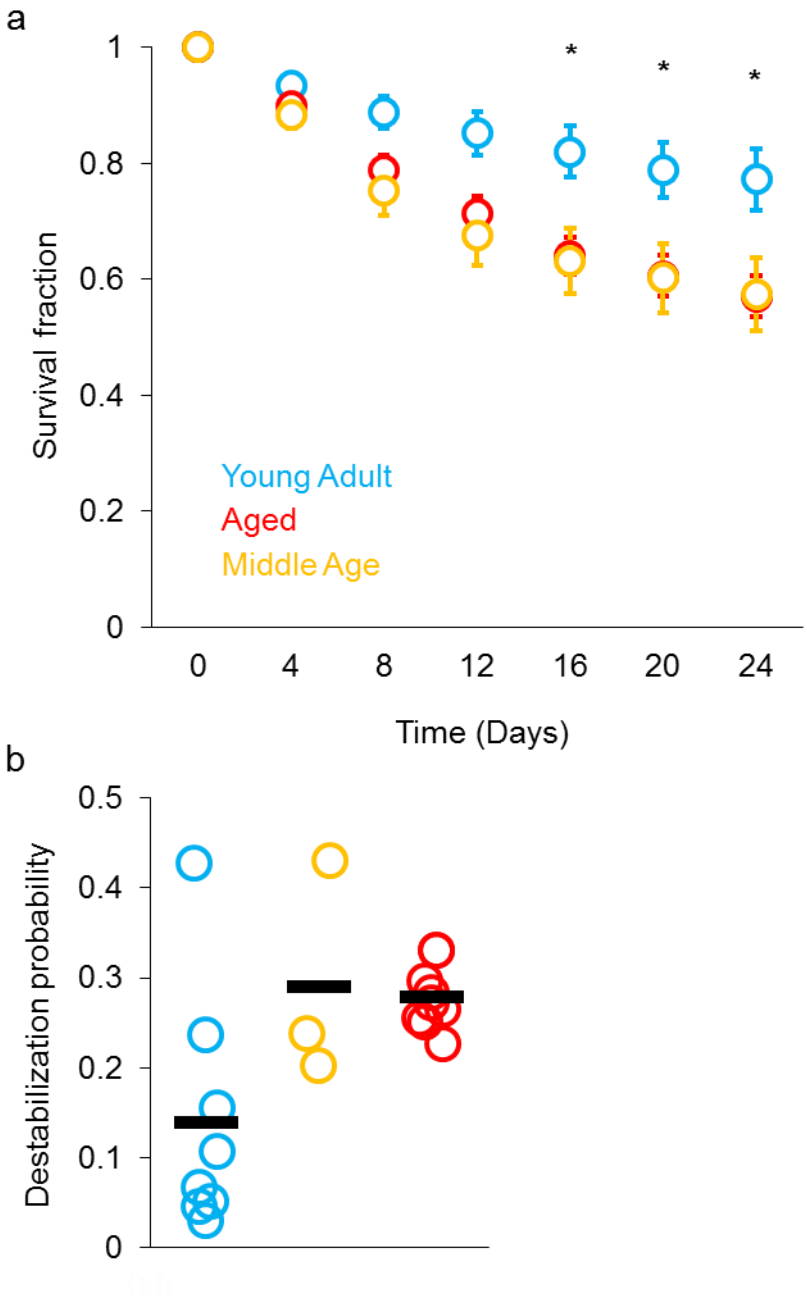

Figure 43 Middle Age EPBs survival and destabilization. (a) EPB survival curves for Young Adult (blue, n = 371 EPBs), Aged (red, n = 852) and Middle Age (yellow, n = 401). By day 24 (final imaging time point) the average Middle Age survival fraction was 0.57 ± 0.06, Aged was 0.57 ± 0.04, Young Adult was 0.77 ± 0.05. (b) The destabilization probability of the Middle Age group (0.29 ± 0.07) seemed comparable to the Aged group (0.28 ± 0.01) average, though not significantly larger than the Young Adult average (0.14 ± 0.05, $P = 0.08$).

7.2.2 EPB turnover increase in Middle Age animals

The preliminary analysis of EPB TOR, gains and losses essentially confirmed that the Middle Age group of animals was more similar to the Aged group than the Young Adult cohort (Figure 44). The mean four-day TOR per animal was significantly larger in the Middle Age mice compared to the Young Adult (Middle Age 4 day TOR = 0.2 ± 0.03, Young Adult = 0.07 ± 0.03; P = 0.004; Figure 44 a). EPB replacement was then higher in the Middle Age group, resembling the result of the Aged cohort. Furthermore, both the fraction of gains and the fraction of losses were increased in the Middle Age cortical axons (Middle Age gains fraction = 0.1 ± 0.007, Young Adult = 0.04 ± 0.02; P = 0.004; Figure 44 b; Middle Age losses fraction = 0.1 ± 0.03, Young Adult = 0.03 ± 0.02; P = 0.004; Figure 44 c). Overall, the increased rates of bouton addition and elimination were detectable in the Middle Age group at similar values to what observed in the Aged brain.

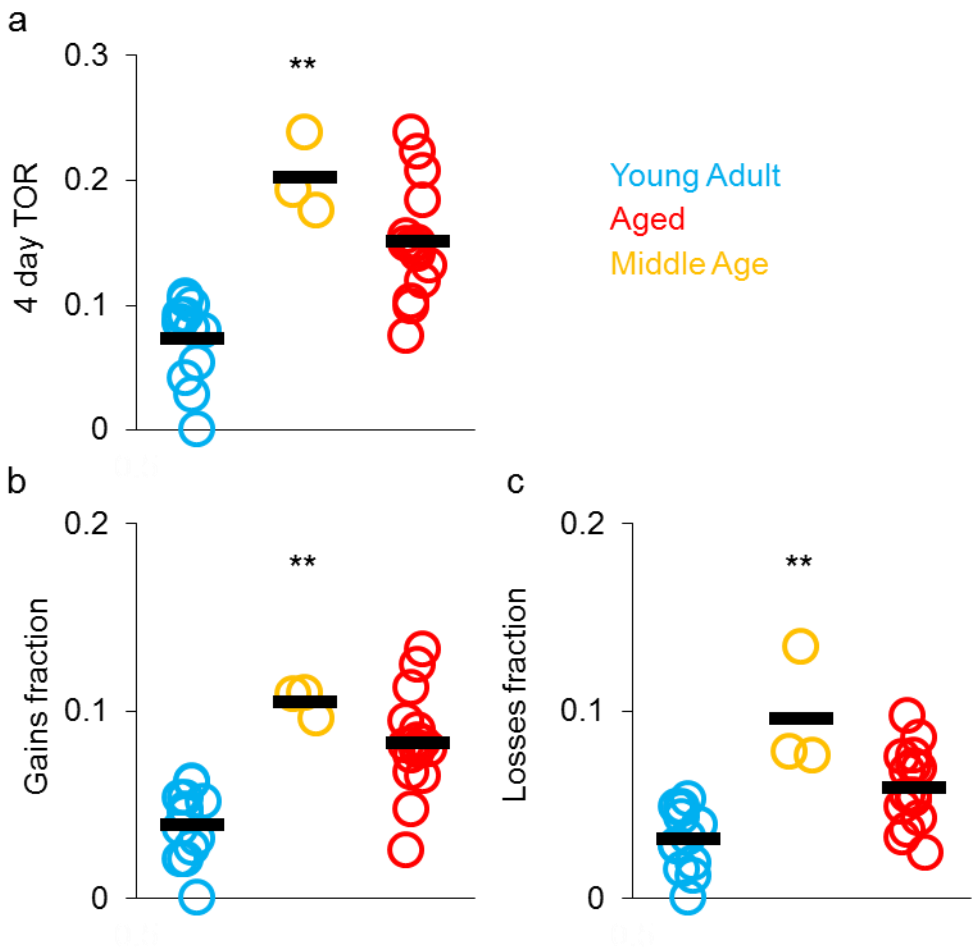

Figure 44 EPB replacement rates are larger than Young Adult (YA) mice in the Middle Age (MA) group. (a) Age related increased four-day TOR is already detectable in Middle Age group. (b) The fraction of gains and (c) the fraction of losses are higher in the Middle Age group compared to the Young Adult. Aged EPB dynamics are comparable to the observed Middle Age EPB dynamics. (Young Adult, n = 14, blue; Middle Age, n = 3, yellow; Aged n = 16, red). (** $P < 0.01$ – comparison YA vs. MA).

7.2.3 Large and small EPB dynamics on Middle Age cortical axons

One of the major findings presented in the previous sections was that large EPBs, thought to represent a stable memory encoding population of synapses, were greatly affected by the destabilizing effect of ageing. On axons imaged in the Young Adult cortex large EPBs were highly stable and destabilization events were rare (Figure 33). Conversely, large EPBs were found to be destabilized considerably more frequently in the Aged cortex. The TOR of large

EPBs was also higher in the Aged brain in comparison to the Young Adult one. In the small group of Middle Age mice a similar behaviour was observed (Figure 45). Large EPBs had a destabilization probability similar to what described for the Aged group [Middle Age (n = 3 animals, 81 large stable EPBs, 15 destabilized EPBs) destabilization probability = 0.18 ± 0.03; compared to Young Adult: P = 0.009; Figure 45 a]. Moreover, the four-day TOR of large EPBs in Middle Age imaged mice resembled the previous observation in Aged animals (Middle Age 4 day large EPB TOR = 0.036 ± 0.03; compared to Young Adult: P = 0.01; Figure 45 b). It seemed that large EPBs in the Middle Age brain were affected at a similar level to what was detected in the Aged brain. On the other hand, small EPBs showed high degrees of destabilization (Figure 45 c) and TOR (Figure 45 d) in all three age groups. Such parameters for small EPBs in the Middle Age group were comparable to the Aged and Young Adult cohorts and not statistically different [Middle Age (n = 3 animals, 66 small stable EPBs, 38 destabilized EPBs) destabilization probability = 0.57 ± 0.15; ; P = 0.36; Figure 45 c; small EPB 4 day TOR = 0.35 ± 0.01; P = 0.36; Figure 45 d]. Considering EPB size, which is directly related to synaptic strength, it emerged that large EPBs may be affected by the Ageing process as early as the Middle Age stage in mice, while smaller boutons might be unaffected.

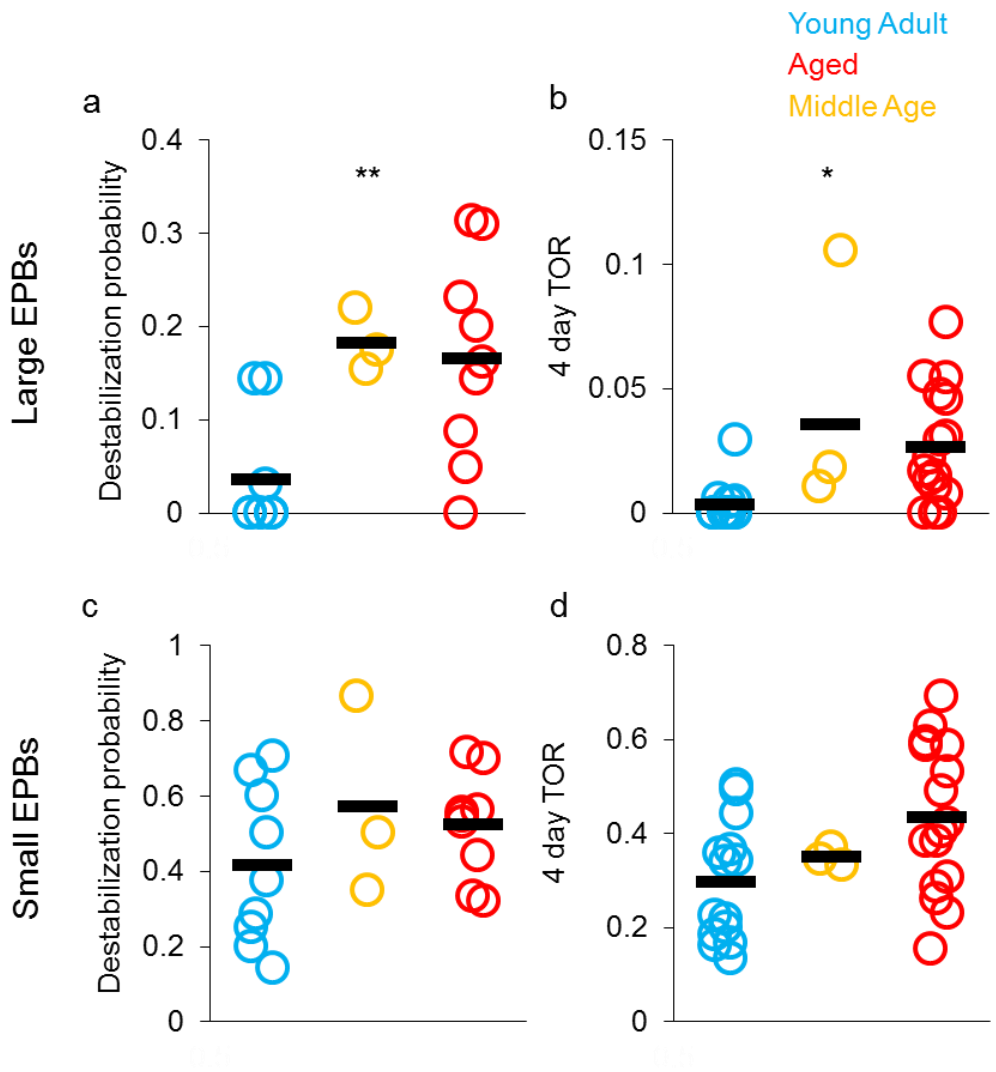

Figure 45 Large EPBs in the Middle Age group had similar dynamics as in the Aged cohort. (a) Large EPBs in the Middle Age (n = 3, yellow) and Aged (n = 9, red) groups were destabilized more frequently than in the Young Adult (n = 9, blue) group; black markers are mean values for respective groups. (b) The four-day TOR for large EPBs was low for the Young Adult group but considerably higher for Middle Age and Aged animals. (c, d) Small EPBs had high rates of destabilization (c) and TOR (d) in all age cohorts. (* $P < 0.05$, ** $P < 0.01$ – comparison YA vs. MA).

7.2.4 Volume fluctuations of EPBs in the Middle Age brain

Though the size of EPBs, measured with their relative intensity, was comparable between Aged and Young Adult mice, the rate at which EPB volumes changed between imaging sessions, measured with the intensity ratio (IR), was different. On axons imaged in the Aged

group, individual persistent EPBs changed their size to a greater extent compared to the Young Adult volume fluctuations (~ 44% vs. ~ 36%). Interestingly, Middle Age volume fluctuations had similar values to the Aged fluctuations (Figure 46). Probably due to the reduced sample size, the difference between Young Adult IR and Middle Age IR was not significant. Considering all boutons (Middle Age, n = 284, IR = 1.42 ± 0.03; compared to Young Adult: P = 0.3; Figure 46 a). Considering persistent EPBs (Middle Age, n = 204, IR = 1.43 ± 0.04; compared to Young Adult: P = 0.2; Figure 46 b). Considering non-persistent EPBs only (Middle Age, n = 80, IR = 1.40 ± 0.05; compared to Young Adult: P = 0.9; Figure 46 c). The relatively smaller number of EPBs collected (n = Young adult 980, Aged 1636, Middle Age 284) probably prevents the result being significantly different from the Young Adult, however the values closely resemble what found in the Aged brain. Such similarity further suggests that the age related bouton dynamics alterations are initiated as early as 12 – 14 months of age in mice.

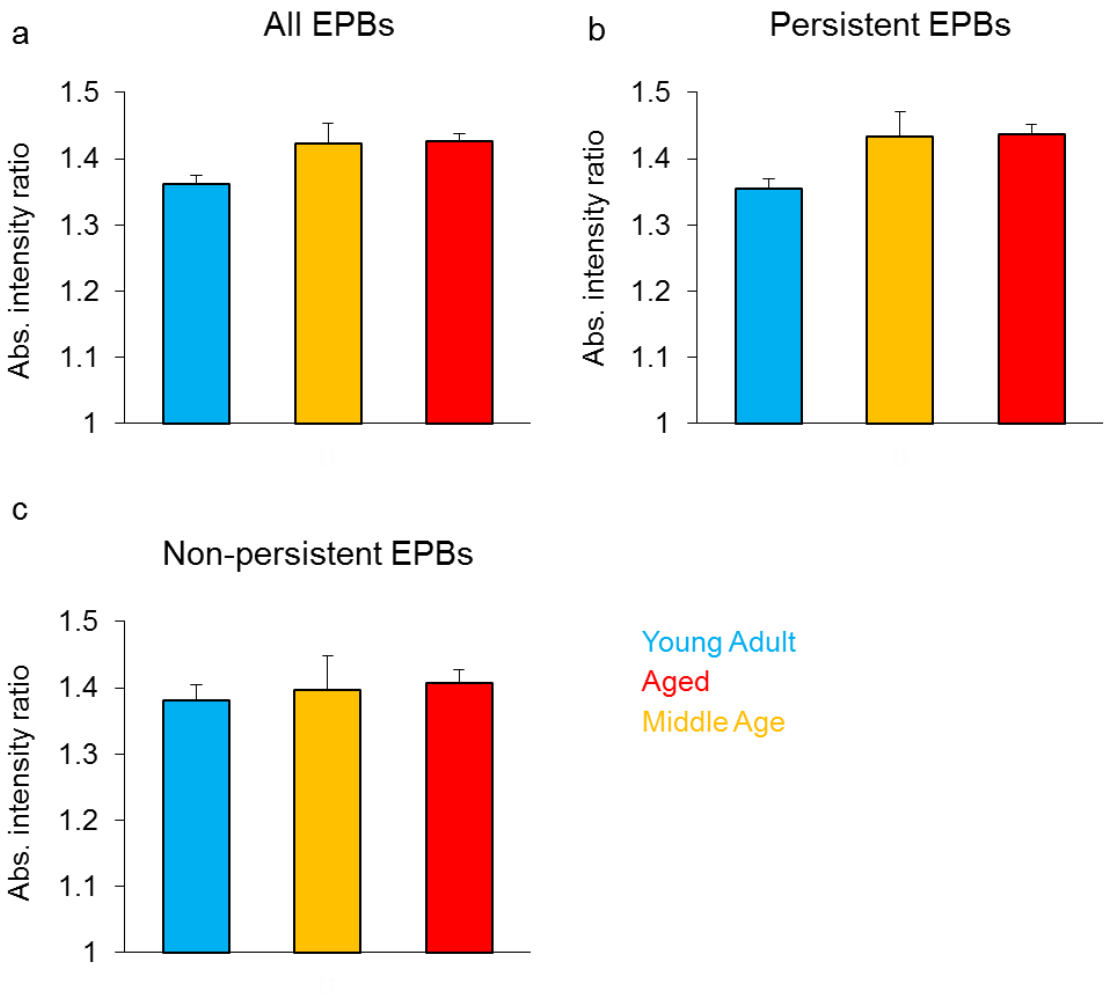

Figure 46 IR in Middle Age mice had similar mean values to Aged group but not significantly higher than Young Adult mice. (a) All boutons considered, (Young Adult, n = 980, four-day mean variation ~ 36%, blue bar; Middle Age, n = 284, mean variation ~ 42% yellow bar; Aged n = 1636, mean variation ~ 42% red bar). (b) Persistent boutons considered, (Young Adult, n = 707, mean variation ~ 35%, blue bar; Middle Age, n = 204, mean variation ~ 43% yellow bar; Aged n = 1013, mean variation ~ 44% red bar). (c) Non-persistent boutons considered, (Young Adult, n = 273, mean variation ~ 38%, blue bar; Middle Age, n = 80, mean variation ~ 40% yellow bar; Aged n = 623, mean variation ~ 41% red bar).

7.3 Long-term memory impairment in Middle Age mice

The ability to form a long-term memory in a tactile recognition task was impaired in Aged mice compared to Young Adults (Figure 39). The same task was employed to test Middle Age mice. A total of 10 mice were used in this behavioural assay (Aged and Young Adult, n

= 13). In the test phase, Middle Age mice spent on average more time exploring the novel object, though the difference in exploration time was not significant [Middle Age exploration times: sample 1 (object A = 10.02 seconds ± 1.43, object B = 11.42 seconds ± 1.79), sample 2 (object A = 5.1 seconds ± 0.9, object B = 4.67 seconds ± 0.78), sample 3 (object A = 3.4 seconds ± 0.66, object B = 3.6 seconds ± 0.75), test (novel object = 4.25 seconds ± 0.4, object B = 2.95 seconds ± 0.29); two way ANOVA: *P* = 0.22; Figure 47 a]. Though the performance of Middle Age mice was not strong enough to indicate successful object recognition, the computed discrimination index had an average value in between those of the Young Adult and Aged groups (Middle Age discrimination index = 17.7 ± 3.5, Young Adult = 29.8 ± 5.5, Aged = 3.99 ± 6.4; one way ANOVA: *P* = 0.007; Figure 47 b). The overall performance in the test is affected by advancing age, though the Middle Age group performance is not significantly different from both the Young Adult and the Aged discrimination indexes.

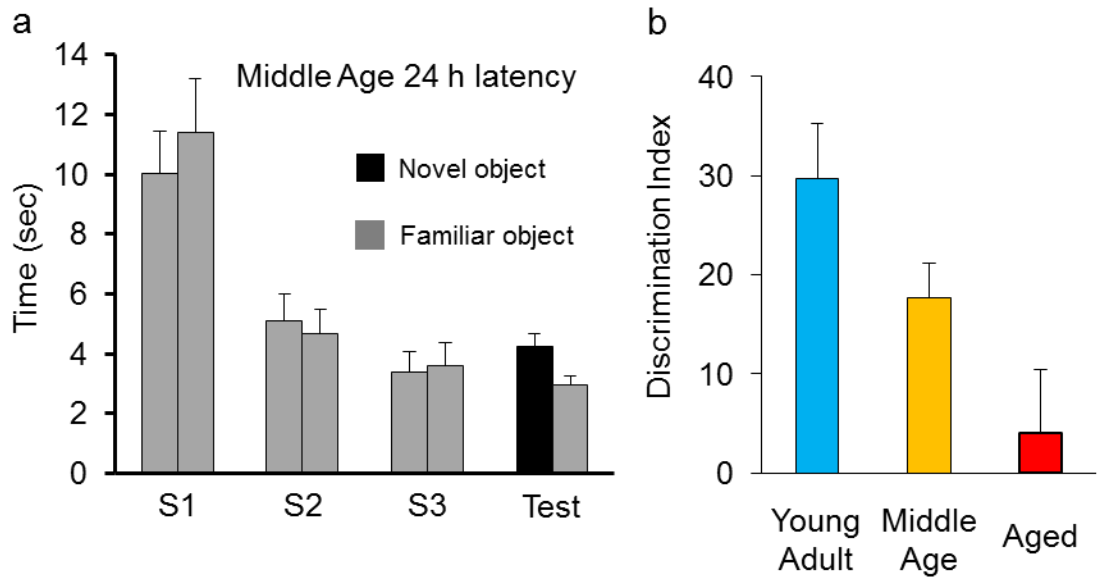

Figure 47 The average performance of Middle Age mice was half way that of Young Adults and Aged animals. (a) Exploration times of the objects in sample trials (S1, S2, S3) and during the test phase. (b) Middle Age discrimination index was not significantly different from the Young Adult or Aged ones, however an age related decrease was detected.

7.4 Conclusions

To study the development of age related changes in the brain an initial set of experiments on Middle Age mice were started. Previous work has shown that intermediate stages of ageing display an intermediate degree of age associated defects. Behavioural defects have been observed in middle age rats (Weiss and Thompson, 1991). Structural spine plasticity defects have been found in middle age rats, the degree of the deficit further progressed in fully aged rats (Bloss et al., 2011). In the *dl*PFC of the monkey brain, middle age neurons had a degraded firing pattern that worsened in fully aged monkeys (Wang et al., 2011). Recently, a two-photon imaging study has looked at spine and bouton dynamics in Thy1-GFPM mice at different stages of life (Mostany et al., 2013). In this study a broad middle age group (8 to 15 months old) generally had average spine density and dynamics more similar to the aged group than the younger adult group. Furthermore, bouton density, size and dynamics were comparable between the older and middle age groups. However differences were found in the size of dendritic spines (larger spines in the middle age cohort) and in the stabilization rates of boutons (lower rate of stabilization in the middle age group). From this evidence it appears that the process of ageing is gradual and starts affecting the brain in the middle stages of life.

In this chapter preliminary data has been presented from an intermediate age stage, 12 to 14 months. Attention was given to the parameters that were found to be highly affected on the Aged cortical axons, i.e., the increased dynamic behaviour of synaptic boutons on EPB rich axons. It emerged that the EPB rich axon population imaged in the Middle age mouse group had similar features to the Aged population. The survival fraction curve of EPBs in the Aged and Middle Age groups were comparable (Figure 43 a), Middle Age EPB survival was significantly lower than the Young Adult EPB survival. As more boutons were lost, more EPBs were destabilized in the Middle Age group compared to the Young Adult. The average destabilization probability was similar to what previously observed for the Aged animals (Figure 43 b). In this case it seemed that the contribution to the increased destabilization rate

was mainly given by one of the three Middle Age mice. It is possible that with a larger set of animals the spread of mean values per animal would have been larger in the Middle Age group than in the Aged, as a greater variability might be expected in the former group compared to the latter. Furthermore, the turnover rates of EPBs in the Middle Age group were considered. Again, the EPB TOR for the Middle Age was similar to the Aged group and significantly increased compared to the Young Adult (Figure 44 a). Both the gains and losses fraction, in the Middle Age cohort, were higher than those in the Young Adults and similar to gain and loss rates observed in the Aged group (Figure 44 b and c). A major finding in the Aged brain was that large EPBs were greatly destabilized and turned over more often than in a younger adult brain (Figure 33). Large EPBs in the Middle Age cortex tended to behave similarly. The destabilization probability and the TOR were significantly higher for these boutons in the Middle Age group compared to the Young Adult cohort (Figure 45 a and b), while the small portion of EPBs were greatly destabilized and replaced in all three groups at comparable rates (Figure 45 c and d). Large EPBs were affected in the Middle Age brain, though the small number of animals presented does not rule out the possibility that the variability of the Middle Age group is greater than what seen in the Aged cohort. Large EPBs arguably form strong synapses, therefore alterations in the stability of such structures might have a big impact on neural processing. The results suggest that such altered behaviour of large EPBs arises as early as a middle life stage in mice.

In previous sections it has been shown how the IR of Aged animals was significantly higher than what observed in the Young Adult (Figure 36). Such difference was mainly contributed by the persistent population of boutons (~ 44% vs. ~ 36%, average four- day size change in Aged and Young Adult respectively). The stability of these boutons (present for twenty-four days) implies their importance in the circuit; hence variations of the basal level of size change might be affecting a critical population of synaptic connections. The mean IR for the Middle Age group was just below the mean of the Aged group (Figure 46). Though at a similar level as the Aged IR, the Middle Age mean IR was not significantly higher than what

measured in the Young Adult EPB population. Probably, the smaller sample size prevented a significant result to emerge. It could be possible that the Middle Age group had an intermediate mean IR value, which would be even more difficult to detect. Whatever the case, more experiments would be needed to clear the effective age related progression of EPB dynamics.

Progressive increase in EPB dynamics appeared to be associated with progressive deterioration of long-term recognition memory in each mouse group. A defect, specifically in long-term (24 hours) maintenance of a recognition memory, was earlier found in the Aged group compared to the Young Adult cohort (Figure 39). Middle Age animals were tested in the same task. Though a net preference for the novel object over the familiar one was not statistically verifiable, the average Middle Age animals performance was in between those of the older and younger mice (Figure 47 a). Overall, an age related effect on performance was found but the Middle Age performance was not significantly worse than the Young Adult and not significantly better than the Aged animals' performances (Figure 47 b).

The results presented here point to a fast progression of the ageing process, which affected mice relatively early at a middle life stage (12 to 14 months old). It would be interesting to understand if the Aged phenotype is manifesting as early as the Middle Age stage or if Middle Age mice would display a greater variability, with some individuals close to the Young Adult EPB properties. With only three mice in the imaging data it is hard to make strong conclusions and more animals should be added in order to clarify this issue.

8. Discussion

The ageing brain has been a matter of study for the past 50 years. One of the early challenges of the field was to discriminate healthy ageing and pathological conditions related to ageing. At first, when such discrimination was not considered, the general assumption was that brain ageing was accompanied by neuronal cell death. This view provided a simple explanation for the progressive decline of cognitive function experienced by ageing humans and animals. However, the advent of more rigorous investigative methodologies [e.g., the dissector method (West, 1993)] turned this view around. As refined anatomical analysis techniques were employed to yield more reliable data, a clearer distinction between physiological and pathological ageing started to emerge. Thanks to these innovations, and possibly to the growing interest in ageing research, the prevailing view gradually shifted from broad neuronal loss, causing age related cognitive decline, to more subtle changes mainly involving the synapse (Burke and Barnes, 2006; Morrison and Baxter, 2012). Moreover, the age related structural changes in the brain were found to affect different regions and sub-regions to different degrees, in some cases with opposite effects. With the discovery of forms of activity-induced synaptic plasticity, such as long-term potentiation [LTP (Bliss and Lomo, 1973)] and their involvement in memory formation (Bliss and Collingridge, 1993), the role of synaptic plasticity has been since widely studied in the ageing context. Induction and maintenance impairments in LTP and long-term depression (LTD) and the unbalance between them, pointed to the general view of reduced plasticity in the ageing brain (Burke and Barnes, 2010). Given the connection between plasticity and memory formation and the memory impairments observed in aged subjects, it was not surprising that the ageing brain was found to have reduced synaptic plasticity. Besides functional plasticity (synaptic strengthening or weakening) the active growth and remodelling of mature neural structures is involved in memory encoding and storage (Caroni et al., 2012), two cognitive domains

deeply affected during ageing. Recently, reduced structural plasticity has been involved in ageing and cognitive decline (Bloss et al., 2011; Dumitriu et al., 2010). Such studies though, which analyse neuronal changes post mortem, lack the possibility of observing structural plasticity events in the intact brain. Observing structural plasticity as it happens, in living animals, has been made possible thanks to chronic two-photon imaging (Fu and Zuo, 2011; Holtmaat and Svoboda, 2009). *In vivo* imaging has shown how neuronal processes and their synaptic terminals are relatively stable in the mature brain, whereas a larger degree of remodelling characterizes the developing brain (Holtmaat and Svoboda, 2009). This would suggest a further decrease of synaptic remodelling during ageing. Recently, structural plasticity of postsynaptic spines has been linked to learning, where the selective stabilization (Fu et al., 2012; Roberts et al., 2010; Xu et al., 2009; Yang et al., 2009) and the selective elimination of dendritic spines (Lai et al., 2012) have been correlated to learning a specific behavioural paradigm. Applying *in vivo* imaging of synaptic structures to the context of ageing has been the main aim of this thesis. The focus of the study was to identify dynamic properties of axons and their synaptic boutons influenced by ageing. Presynaptic boutons have received comparably less attention than dendritic spines during adulthood. The study of two populations of axons was possible with the aid of distinct morphological features, the accurate analysis of *en passant bouton* rich axons required the development of a new analytical tool that will prove useful also in future studies.

8.1 Axonal branches: preserved density and dynamics during ageing

Terminaux bouton rich axons are characterized by the presence of a large number of protrusions. The majority of such protrusions are short synaptic terminals, named TBs. Protrusions over 5 µm in length were considered as axon branches, following a previously published empirical classification based on stability [see methods (De Paola et al., 2006)].

Axon side branches have been shown to be relatively stable (extension/retraction events over tens of microns over few days) in the mature brain of mice (De Paola et al., 2006) and macaque monkeys (Stettler et al., 2006), whereas branches undergo a higher degree of remodelling in the developing brain [extension/retraction events over hundreds of microns over few days (Portera-Cailliau et al., 2005)]. It might be expected that the passage from a mature adult environment to an ageing state is accompanied by further reduction of branch remodelling. Large scale growth and pruning of axons is needed for the correct development of the neocortex. In addition, long range remodelling might also confer large memory capacity to the brain, through higher variability (e.g., recruitment of neurons from a wider pool) of synapse formation allowing rewiring circuits greater flexibility (Chklovskii et al., 2004). In the adult brain, a boost to axonal branch remodelling is given by some protocols of sensory deprivation [(Florence et al., 1998; Marik et al., 2010; Oberlaender et al., 2012; Yamahachi et al., 2009) but not in others (Keck et al., 2011) see main introduction]. Ischemic events are also able to elicit axonal sprouting from adjacent regions (Dancause et al., 2005). Therefore, axonal sprouting in the mature brain might be a repair mechanism, aimed at recovery of function.

In this study axonal branches were imaged and analysed in Young Adult (4 to 5 months old) and Aged (22 to 24 months old) mice (Figures 10, 11, 12 and 13). Interestingly, axonal branches were not affected by ageing. The number of side branches per unit length found on imaged axons was not altered in the Aged brain compared to the Young Adult animals. Furthermore, the average length of such branches was comparable at both ages (Figure 11). Chronic *in vivo* imaging allowed assessing the dynamic behaviour of the side protrusions. Unexpectedly, the proportion of branches actively elongating or retracting, over 20 days of imaging, was comparable between age groups. Furthermore, the dynamic branches from both groups had comparable length variations over a four-day period (Figure 12). The amount of growth and retraction was balanced in both cohorts as the overall length remained stable over time (Figure 13). Overall, no detectable difference was highlighted in the amount

and behaviour of axonal side branches between Young Adults and Aged mice. The results were unexpected in light of the changes known to happen in the ageing brain which might suggest different outcomes. Firstly, axonal tracts are affected in the central nervous system during ageing (Peters, 2007). The age related changes described mainly affect myelinated fibres, especially long projecting axons. It might be expected to see changes (i.e. retractions) in the imaged area as a consequence of the reduction of white matter and the age related damage to myelin. In this case the axonal arbors considered originate from *lamina* VI neurons, supposedly originating within the ipsilateral somatosensory cortex (De Paola et al., 2006). It could be argued that no changes were observed because the affected axons simply were not present as a consequence of degeneration. The imaging, though, spanned a twenty-day period, a significant period of time compared to the total lifespan of a mouse. In such time no major axonal length retraction was observed in Aged animals, an event that would be expected if the same axons were degenerating. Age related structural changes of neuronal architecture might be interpreted as a form of tissue damage. According to this view, similar for what happens in the case of a confined stroke, it might be expected that the remaining axons would sprout in an attempt to compensate deficit. Compensation is observed at the functional level during ageing: aged subjects activate larger portions of the brain to perform a specific task, compared to younger subjects which activate smaller regions for the same purpose (Grady, 2012). At the structural level, the chronic nature of the gradual and global ageing process, might not result in a dramatic axonal response, whereas an acute injury, which is confined, might induce neighbouring axons to sprout. Although controversial (see above), there is evidence indicating that altered sensory information input can induce sprouting. To some degree peripheral sensory systems are degraded in aged humans (Glisky, 2007) and mice (Wang and Albers, 2009). The primary cortices of aged animals, in this case the somatosensory cortex, would then be receiving a reduced peripheral input compared to younger adults. Such reduced input could possibly lead to a progressive retraction or elongation of the imaged axonal processes in response to a partial functional loss. Compared to the confined sensory depletions (retinal lesions, selective

ablation of facial *vibrissae*) studied in the context of structural plasticity, ageing might represent a global reduction of cortical activity derived from a generalized reduction in sensory input. In other words there would not be spared versus deprived areas which are typical features of experience dependent manipulative experiments, rather a global deprivation that might not be able to drive any significant alteration to the circuit. Finally, it is widely accepted that neuronal plasticity is reduced in aged individuals (Burke and Barnes, 2010) and recent evidence suggests that structural plasticity is reduced on the postsynaptic site (Bloss et al., 2011; Dumitriu et al., 2010). Although imaged in a baseline condition, the TB rich axons in this study did not show any significant reduction in structural changes concerning their side branches.

8.2 Preserved bouton density during ageing

Synaptic loss is one of the major hallmarks of ageing in the central nervous system (Burke and Barnes, 2006; Morrison and Baxter, 2012) and a possible cause for age related cognitive decline. Region specific decreases in synaptic density have been described in human samples (Anderson and Rutledge, 1996; Jacobs et al., 1997; Nakamura et al., 1985; Scheff et al., 2007; Scheff et al., 2001). In animal models the reduction in synaptic density has been correlated to cognitive performance (Dumitriu et al., 2010; Peters et al., 2008; Peters et al., 1998b; Wallace et al., 2007). In this thesis a subset of axons were studied as a consequence of the sparse labelling induced by the Thy1 promoter. The imaged axons were located in the primary somatosensory cortex, including part of the barrel cortex. The subset of imaged axons included TB rich axons, originating from *lamina* VI neurons, and EPB rich axons, originating in *laminae* II/III, V and in the thalamus (De Paola et al., 2006). In both classes, the density of presynaptic boutons was comparable between the Young Adult and Aged animal groups (Figures 14 and 23). Generally, in *lamina* I, the presence of a bouton

corresponds to a structurally complete synapse (De Paola et al., 2006; Knott et al., 2006), an assumption which is strengthened by the stringent criteria adopted for bouton scoring in two-photon images (see methods). A comparable bouton density should then reflect a comparable synapse density, on the imaged axons, in both age cohorts. Such conclusion, strengthened by the fact that it originated from the analysis of two different axonal populations, is in disagreement with the view that synapse number is lowered in the aged brain. Preservation of synapses might, though, be specific to cortical *lamina* I. Moreover, preserved density does not directly mean that the total number of synapses is conserved; it is possible that axonal total length is lost during ageing. As previously stated a progressive loss of axonal arbor length should be evident over a relatively long imaging period (up to twenty-four days) in the Aged brain. Instead, axonal retraction was not observed, indicating that bouton density should reflect bouton number. However it cannot be ruled out that not all boutons are forming synapses, or that the proportion of non-synaptic boutons is greater in the Aged group. A recent study, found an increase in bouton density and an increase in dendritic spine density (Mostany et al., 2013). This work was carried out on the same animals (Thy1-GFP M line) and in the same cortical area (S1) as the present. An increase in spine density, in the same region, during ageing provides the postsynaptic partners for a preserved population of boutons, suggesting that synapses are formed. Furthermore it raises the possibility of increased multiple synapse boutons in older animals. Considering the present work and the work of Mostany and colleagues, a total of three two-photon imaged EPBs were reconstructed at the EM level in the ageing mouse brain, all of which were forming synapses (Figure 20). Furthermore a total of six imaged spines where reconstructed and confirmed to form synapses at the EM level (Mostany et al., 2013). These data suggest that synapses are preserved during ageing on the studied axonal population, nevertheless the mean values of bouton density are slightly lower in both TB rich (Figure 14) and EPB rich (Figure 23) axons in the Aged compared to the Young Adult group. It is possible that such small density decrease would need larger numbers to reach statistical significance. Undoubtedly the variability within groups is contributing to such difficulty. However, the mean

bouton density values are closer than what could have been anticipated, given the region specific but widespread nature of age related synaptic loss.

8.3 Increased bouton dynamics in the aged brain

The mature adult brain is capable of structural remodelling that allows neural circuits to adapt in response to experience (Grutzendler et al., 2002; Lendvai et al., 2000; Trachtenberg et al., 2002). Changes in experience cause the emergence of new synapses (Jung and Herms, 2012) that are more likely to stabilize (Holtmaat et al., 2006). Importantly, during learning synapse formation is increased on cortical neurons, the newly formed synapses are then selectively stabilized by training (Fu et al., 2012; Roberts et al., 2010; Xu et al., 2009; Yang et al., 2009). In at least one particular case, deleting an acquired memory results in the elimination of synapses associated with that memory (Lai et al., 2012). It is possible that factors such as learning, experience and age, influence the rate of formation of new synapses. In this view memory consolidation selectively stabilizes the most relevant of those dynamic synapses, hence an increase in the basal levels of plasticity (more dynamic synapses) should benefit the learning process [i.e., greater choice of synapses to stabilize (Caroni et al., 2012)]. Because ageing is associated with cognitive decline and difficulties forming novel long lasting memories, the general assumption has been that advancing age should correspond to a decrease in synaptic structural plasticity. In accordance with such view, reports have highlighted a reduction in thin spines and filopodia, thought to be highly plastic elements crucial for learning (Kasai et al., 2003), in the ageing brain (Bloss et al., 2011; Dumitriu et al., 2010). Over the past decade the development of two-photon *in vivo* imaging has given the opportunity of observing structural plasticity *in situ*. No studies had looked at structural changes in the intact aged brain before. The work here presented, together with the work of Mostany and colleagues, are the first two descriptions of the

dynamics of synaptic elements during ageing. Surprisingly, rather than generalized decreased bouton dynamics, the present study highlighted a net increase in the basal number of dynamic boutons in the Aged cortex compared to the Young Adult brain, specifically on EPB rich axons. Moreover, initially stable boutons are more likely to be replaced in the Aged brain, while the boutons that survive undergo larger size fluctuations which should affect their efficacy.

8.3.1 Heightened bouton turnover rates during ageing

Against initial expectations, EPB rich axons displayed a greater rate of bouton turnover (TOR) in the Aged compared to the Young Adult group (Figure 26). The mean TOR of EPBs every four days increased twofold on axons imaged in the Aged brain compared to the Young Adult. As previously stated, the density of boutons on axons in both groups was comparable and constant over time. There was in fact an overall balance of gains and losses of boutons for both age cohorts, with the gains and losses in the Aged higher than those in the Young Adult brain (Figure 28). When followed over time the four-day TOR was constant in both groups, with the mean of the Aged group always higher than that of Young Adults (Figure 27). Because Ageing is associated with cognitive decline (Burke and Barnes, 2006; Morrison and Baxter, 2012) it is possible that an increase in the dynamic bouton number is detrimental to cognitive processes when such increase is over a certain threshold. It might also be possible that such increase is not regulated, as it should be. Though, the principle of random emergence and selective stabilization of synapses underlying structural plasticity [see above (Caroni et al., 2012)] would go against a theoretical regulation of the dynamic population of synapses. Alternatively, heightened TOR might be affecting the wrong synapses (i.e., the stable population), eliminating those boutons that should not be, and failing to improve the circuit properties by adding new synapses. Interestingly, in a small set of experiments done on an intermediate age group the increased TOR appears to start

earlier than a late life stage (Figure 44). The Middle Age animals had higher four-day TOR, higher gain fraction and higher losses fraction than their Young Adult counterpart. Although only three animals were imaged, all three had mean values larger than any Young Adult mouse shown for all parameters. Individual Middle Age mice had mean values of TOR, gains and losses in the range of the highest means for individual Aged animals. Because Middle Age mice had an intermediate performance outcome in the long-term memory test, they explored the novel object less than the Young Adults but more than the Aged mice (Figure 47), perhaps the associated TOR increase is a compensatory mechanism. Increased TOR might be a reaction to the degradation of other circuits. On the other hand, it might be that the Thy1 labelled EPB rich axons are among the first classes of axons to be affected by the ageing process, while worsening of the behavioural phenotype is a consequence of further degradation of more elements. Contrary to most of the literature that promotes age related decrease in synaptic plasticity (Bloss et al., 2011; Burke and Barnes, 2010; Dumitriu et al., 2010) there are indications here of an increase in plasticity in a subset of neurons. Recently, an increase in spine dynamics has been shown in old and an intermediate age of Thy1-GFPM mice (Mostany et al., 2013) by an independent team, further strengthening the finding. In the same study, EPBs were imaged but an increase in TOR failed to reach significance, though a trend pointing to an age related increase in four-day TOR was visible. Overall, these results show for the first time an increase in the rate of structural plasticity in the Aged brain. It might be argued that the observations here presented were obtained in basal conditions, in the absence of a well defined stimulus inducing plasticity. In numerous studies, after an initial baseline, *in vivo* imaging is performed under a sensory deprivation paradigm (e.g., whisker trimming or retinal lesions), an environmental enrichment condition or behavioural learning. Such manipulations normally alter the levels of synaptic structural plasticity. The so-called baseline condition though, on which such manipulations are added, implies intensified animal handling, stress and repeated anaesthesia (IP injection). Such factors, necessary for the experiment itself, constitute elements of novel experience and cannot be discriminated from a true basal condition. These factors might be driving synaptic

changes that would not normally happen under standard housing conditions. A small indication can be found in Figure 27. Although no variation over time in terms of statistical significance was detected, in both cohorts the mean four-day TOR decreases at the final time point comparison (20 – 24 days). It might be that such effect is caused by a habituation to the imaging routine, which might lower the plasticity response.

8.3.2 Bouton instability during ageing

A larger EPB TOR is associated with ageing in somatosensory cortex, resulting in a larger number of dynamic EPBs compared to stable ones. The disproportion is evident by observing the bouton survival curves. In the Aged the survival fraction of EPBs was lower than in the Young Adult brain (Figure 24). Because EPB density is not altered, overall the number of persistent boutons (i.e. always present) is lowered in the Aged brain. This opens the question of whether, during ageing, the increased TORs affects relatively stable EPBs, that should in principle not be replaced. Supporting this view is the fact that the destabilization probability was higher on Aged cortical axons compared to Young Adult ones (Figure 25). Synaptic elements that are present for four days or more are likely to be forming meaningful synaptic contacts (De Paola et al., 2006; Holtmaat et al., 2006; Knott et al., 2006). EPBs that were present from the start of the imaging and for at least three time points (eight days in total) were more likely to be removed in the older animal group, by a factor of two. It is possible that such EPBs were wrongly selected in the Aged brain, suggesting that in this case augmented structural plasticity might be detrimental rather than beneficial. Conversely, newly formed EPBs (present for four days or more) had comparable rates of stabilization (scored by looking at the end of the imaging protocol) indicating that ageing is not acting on the dynamic fraction of EPBs (Figure 25). It is however possible that EPB stabilization would be altered during ageing, compared to younger animals, under a training regime known to induce spine stabilization (Xu et al., 2009; Yang et al., 2009). The Middle

Age cohort, behaved similarly to the Aged group. The survival fraction was lowered, compared to the Young Adult mice, and virtually overlapped with the Aged curve (Figure 43). The reduced survival of EPBs reflects the heightened dynamic fraction of EPBs, highlighted by the increased TOR in Middle Age mice (Figure 44). The average destabilization probability (Figure 43) had a similar value to the Aged but not significantly higher than the Young Adult destabilization probability. As opposed to the strong effect on TOR (see previous section), the three animals had a more variable destabilization probability with one main outlier. It is possible that adding more animals to the experimental group might lead to an intermediate value of EPB destabilization, in between the two age extremes. Curiously, EPBs in old age have been described to have a greater chance of being stabilized (by a factor of ~ 4) compared to an intermediate age stage (Mostany et al., 2013). Such conflicting results might be caused by differences in the age of the mouse cohorts, data analysis and imaging regime. 1) Here Aged and Middle Age were: (22 – 24 months and 12 – 14 months old respectively), compared to: (> 20 months and 8 – 15 months old) for Mostany et al. 2) Image analysis in the present study was carried out with a novel semi-automated tool that was proven to be accurate [Figures 20 and 21; (Grillo et al., 2013)], whereas Mostany et al. used an image J based manual approach. 3) The imaging protocol differs in the two studies. Here seven repeated time points four days apart (twenty-four days total, Figure 3) were used. Instead, Mostany and colleagues checked for EPB stabilization 30 days after an initial set of imaging without intermediate sessions. It is possible that EPBs considered stable had appeared and disappeared several times during the 30-day imaging gap. All together, the data in the present work indicate that the larger proportion of dynamic EPBs observed in the Aged brain are leading to the destabilization of potentially important synapses.

8.3.3 Increased instability of large boutons

The strength of a synapse is correlated to its size (Pierce and Lewin, 1994). Larger bouton compartments contain more synaptic vesicles and the neurotransmitter release probability is related to the number of docked vesicles. More docked vesicles are present when the active zone area (related to bouton size) is wider and larger active zones are apposed to larger postsynaptic densities (Murthy et al., 2001). In somatosensory cortex, bouton volume directly co-varies with PSD size, indicating stronger signal transmission (Knott et al., 2006). Larger boutons share larger contact zones with the opposing postsynaptic element, in turn larger contact zones correspond to greater evoked synaptic responses (Cheetham et al., 2012). Activity dependent structural plasticity is thought to play a major role in cognitive processes. For example, highly dynamic thin spines are readily enlarged and stabilized in response to activity (Kasai et al., 2010a). Thin spines represent a plastic population that can be recruited to form larger and stronger synapses encoding long lasting memories. It is not surprising then that, in some cases, the average spine size has been reported to be greater in aged rather than in younger animals (Bloss et al., 2011; Dumitriu et al., 2010), as if the brain ran out of thin spines. Synaptic boutons have been reported to have preserved average volumes at different ages (Hara et al., 2011), but age related size increase has also been reported (Mostany et al., 2013) in Thy1 labelled axons. In contrast, in this work no significant difference was found in the average size of EPBs comparing age groups (Figure 29 and 29). Persistent boutons were larger than non-persistent boutons within the same age group. However, comparing Aged and Young Adult EPBs, no significant size change was detected in persistent and non-persistent boutons. Furthermore, the distribution of EPB sizes was similar among the two cohorts (Figure 31). Importantly, a size dependent effect on bouton dynamics was detected among age groups (Figures 32 and 33). Small EPBs were highly unstable both in Aged and Young Adult animals and their TOR and destabilization probability were similar (Figure 32). Conversely, large EPBs were highly stable on axons in the Young Adult brain, with their TOR and destabilization probability close to zero. In contrast, many

Aged animals showed a relatively frequent destabilization and turnover of their large EPBs (Figure 33). The highly significant increase in large EPB instability might underlie a serious defect in the Aged cortex. Assuming that these large boutons are forming synapses, an idea supported by the EM reconstruction of two large EPBs in the Aged brain (Figure 20), it appears that strong synaptic contacts undergo an age related decrease in synaptic tenacity. Reduced tenacity may result in the erasure of potentially important synapses, meant to persist for long periods. Large EPBs were also analysed in the Middle Age set of experiments (Figure 45). Once again the data cannot be taken as conclusive, as the number of animals imaged is not comparable to the two main age groups. Middle Age mice seem to have large EPB dynamics closer to the Aged than to the Young Adult cohort. Middle Age mice show a significant increase in large EPB dynamics compared to the Young Adult group. Though, due to the small sample size, it is not possible to appreciate the variability within the Middle Age cohort. Especially for the four-day TOR, the result is greatly driven by one outlier; it would be interesting to know if a generalized variability is present or if the distribution is bimodal, with some animals with an ageing-like phenotype and some with a young adult-like one.

Overall, while average EPB size is preserved during ageing, the larger EPBs are more likely to be replaced in the Aged brain. The instability of large EPBs, which would have been missed in a fixed tissue study, represents an important result likely to have a significant impact on circuit function. Large excitatory synapses, in fact, have predominantly AMPA receptors on the postsynaptic spine as opposed to the NMDA receptor predominance on smaller spines (Kasai et al., 2010a). Such large synapses are thought to represent the physical substrate of long-term memory traces (Holtmaat and Svoboda, 2009; Kasai et al., 2003).

8.3.4 Greater volume fluctuations of boutons during ageing

Aged and Young Adult mice had comparable mean densities and sizes of EPBs on their EPB rich axons. The advantage of being able to image these axons repeatedly and to detect individual EPB intensity accurately was that the variation in volume of single boutons was accessible. Besides appearing and disappearing individual boutons (and dendritic spines) also undergo remodelling over time, leading to bouton growth or shrinkage. For dendritic spines, these spontaneous changes in size happen over four-day intervals and depend on the initial spine size. Such size dependency of spine head volume variation produces the log normal distribution of spine sizes (Loewenstein et al., 2011). Large spines are more likely to change more, so they can easily become small. Smaller spines are unlikely to change much, meaning that they'll tend to stay small. This effect creates a large proportion of spines to be small and relatively few spines to be large, a situation that resembles the size distribution of EPBs described here (Figure 31). Accordingly, EPBs were found to grow or shrink to a degree dependent on their initial size (Figure 34), an observation which led to the adoption of the intensity ratio (IR) rather than the absolute intensity difference to measure bouton size changes *in vivo*. The rates of growth or shrinkage of boutons are not only important to explain the distribution of sizes but, importantly, might reflect changes in synaptic strength. The size of a bouton is positively linked to the size of the whole synapse it makes (Knott et al., 2006; Murthy et al., 2001) and to the synaptic efficacy (Cheetham et al., 2012). Structurally, a larger bouton has a greater active zone, apposed to a wider PSD, with more docked vesicles ready to release more neurotransmitter that will bind to more postsynaptic receptors. The result is a larger evoked postsynaptic potential. Large boutons also contain large vesicle pools (Knott et al., 2006) that are not docked. These resting pools have been involved in spontaneous activity (Fredj and Burrone, 2009) at the synapse. Changes in the volume of a bouton, hence the number of total vesicles, might have an impact on spontaneous activity too. Beside volume fluctuations that happen spontaneously, spine head growth and synaptic strengthening has been associated with learning (Roberts et al., 2010)

and past experience recall (Hofer et al., 2009), whilst sensory deprivation caused spine shrinkage (Tschida and Mooney, 2012). Here, the average IR of EPBs imaged in Aged animals was found to be significantly larger compared to the IR of Young Adult EPBs (Figure 36). The contribution to such increased rate of volume variation was accountable to persistent EPBs and not to EPBs that were turned over (i.e., non-persistent), suggesting that the two processes are uncoupled at the bouton level. The mean volume variation of individual EPBs on axons imaged in the Middle Age mouse brain was in between the Aged and Young Adult means, though considerably closer to the Aged group (Figure 46). However, the increased IR in Middle Age did not reach significance compared to the Young Adult baseline. As for other parameters presented, more experiments would be needed to clarify the emergence of increased morphological changes in the Middle Age group. Overall, the age related increase in IR reflects greater size changes over the four-day period at the individual EPB level. Ageing is associated with LTP deficits. Generally LTP is harder to elicit in aged neurons (Barnes et al., 2000). When LTP is induced in aged preparations it displays lower levels of maintenance (Dieguez and Barea-Rodriguez, 2004). LTD, on the other hand, is facilitated in aged neurons generating a shift between LTP and LTD induction towards depression (Norris et al., 1996). Spine enlargement is known to follow Ca^{2+} dependent LTP induction (Matsuzaki et al., 2004). Therefore, it is possible that changes in EPB size reflect basal LTP – LTD like phenomena happening *in vivo*. A consequence of larger fluctuations might then be a decrease in the signal to noise ratio in EPB volume changes, salient changes would be more likely to be masked by a noisier background. Furthermore, the increased size variations took place on the persistent population of EPBs, therefore not directly related at the bouton level to turnover rates and destabilization. Because spine emergence has been linked to synapse formation on existing boutons (Knott et al., 2006), persistent EPBs are relatively likely to form multiple synapse boutons. More frequent volume changes in the aged brain might reflect more frequent addition or loss of synapses with dynamic spines without the formation or elimination of a new bouton. Increased spine TOR has been in fact described during ageing (Mostany et al., 2013). Increased size fluctuations

might then be associated to cognitive impairments by increasing the noise of presynaptic structural changes and by reflecting a decreased synaptic tenacity that involves postsynaptic elements which turned over more frequently.

8.3.5 Specificity of bouton dynamics increase

The process of ageing in the central nervous system is characterised by differential region specific effects. For example, structural and functional defects have been found in the PFC and hippocampus of aged animals and humans but not in other brain regions (Burke and Barnes, 2006, 2010; Morrison and Baxter, 2012; Yeoman et al., 2012). Moreover, age related effects can be confined to sub-regions and cell types (see introduction). Importantly, in this thesis the age related changes observed applied to one morphological class of axons, EPB rich axons. The specific TB rich axon type, arising from *lamina* VI neurons in Thy1 labelled mice, had comparable bouton dynamics in Aged and Young Adult animals (Figure 15, 16 and 17). TB rich axons have been described to be more plastic than EPB rich axons in the adult somatosensory cortex (De Paola et al., 2006). There appears to be no further increase in the plasticity rates during ageing. The role of these axons and their boutons is still not clear, though evidence exists that they make more synapses directly on the dendritic shaft than EPBs on EPB rich axons do (McGuire et al., 1984). The synapses they form have been shown to produce weak postsynaptic responses with a degree of synaptic facilitation (Lee and Sherman, 2009), leading to the theory that TBs on TB rich axons mediate a modulatory effect on the postsynaptic compartment. It is therefore possible that age related defects on EPBs, forming strong driving synapses, are more likely to be associated with cognitive decline. Similar age related alterations, which were not observed, of TB structure and function might have a smaller impact on the older brain. The fact that TBs were not affected by ageing is important because it supports the view that effects of ageing are not homogeneous in the brain. It would be interesting, in the future, to study genetically defined

circuits and brain areas to gather a comprehensive picture of age related structural plasticity changes in the brain.

8.4 Mechanisms of age related bouton dynamics increase

Extensive evidence has been presented showing that EPB dynamics are increased in the Aged brain. EPBs are subject to an age related increase in instability, turnover and size change rates (Figure 48). Compared to the Young Adult group (Figure 48 c) EPBs in the Aged brain are more frequently replaced (Figure 48 d), including large EPBs, which are rarely turned over on Young Adult axons. The EPBs that persist on Aged axons undergo size fluctuations that are significantly larger than those seen in the Young Adult cortex. Though boutons turning over are not the same that have increased size changes (Figure 36), at the level of axons increased TOR correlates to increased IR (Figure 38). Moreover, increased TOR corresponds to an increased destabilization probability. Therefore, the ageing process seems to affect different dynamic parameters on the same axons (Figure 38), a further indication of the specificity of its effects.

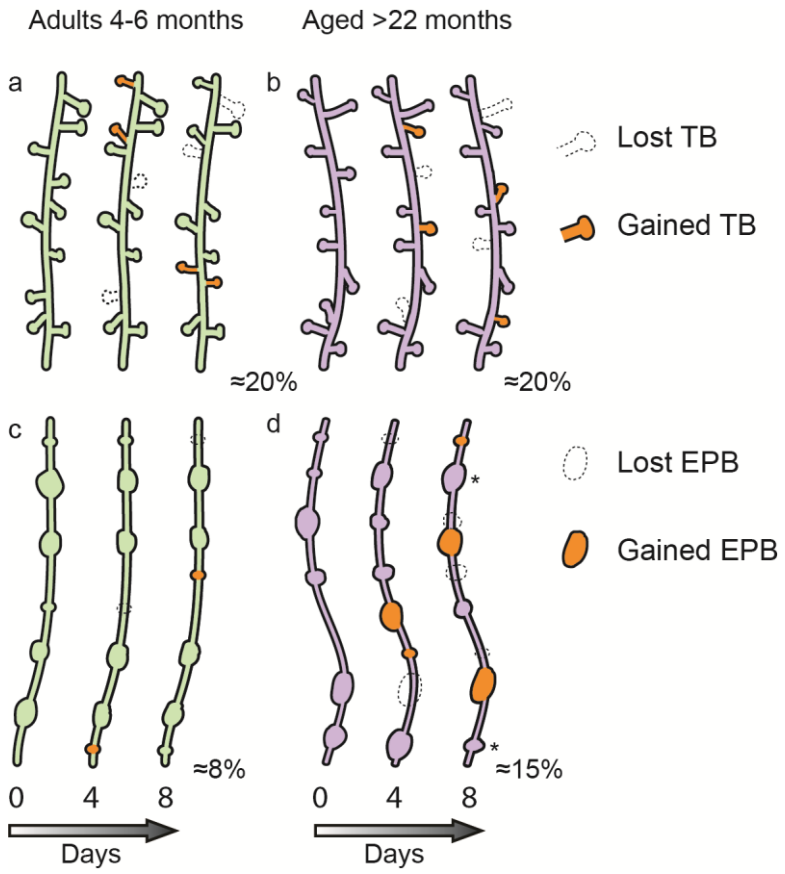

Figure 48 Schematic representation of the circuit specific effect of ageing on cortical synaptic bouton dynamics. (a – b) Synaptic turnover is comparable on *terminaux bouton* rich axons in Young Adult (green) and Aged (purple) mice. TBs are gained and lost at similar rates in both age groups every four days. (c – d) *En passant bouton* rich axons have larger rates of synaptic change in the Aged compared to the Young Adult cortex. EPBs are gained and lost more frequently on Aged axons. The size of EPBs on Aged axons is subject to larger changes between sessions (*). Large EPBs are very stable on Young Adult axons while they are turned over more frequently in the Aged brain. Percentages in each panel represent an approximation of bouton turnover every four days for each condition.

The ageing process implies various changes in the structure and function of the mammalian brain. At the synaptic level, ageing is known to produce an unbalance in Ca^{2+} concentration (Landfield and Pitler, 1984; Thibault and Landfield, 1996; Toescu and Verkhratsky, 2003). Ca^{2+} concentration increases during ageing are caused by the higher density of voltage sensitive Ca^{2+} channels (Veng et al., 2003) and by an increased release of Ca^{2+} from internal stores (Kumar and Foster, 2005). Furthermore, mitochondria are affected during ageing, showing a diminished ability of buffering Ca^{2+} transients at the presynaptic level. The

resulting increased Ca^{2+} concentration affects synaptic function (Tonkikh and Carlen, 2009). Ca^{2+} signalling plays a key role in structural plasticity (Matsuzaki et al., 2004). Ca^{2+} dependent mechanisms have been linked to LTP maintenance and learning behavioural tasks (Lisman et al., 2012; Sacktor, 2011) but also to spine enlargement (Yamagata et al., 2009) and synaptic stability (Bednarek and Caroni, 2011). Because of the central role of Ca^{2+} in synaptic plasticity, disruptions in the fine regulation of Ca^{2+} concentrations might produce the increased synaptic dynamics observed in the aged brain. Inefficient Ca^{2+} buffering might be particularly detrimental to strong active synapses (Tonkikh and Carlen, 2009). Continuous Ca^{2+} accumulation might have excitotoxic effects on large EPBs in the Aged group favouring bouton removal. In this respect large EPBs often accommodate mitochondria (Figure 19 e and f), a possible source of Ca^{2+} buffering deficiencies. In contrast TBs, which are generally small on TB rich axons, might not be affected by Ca^{2+} alterations. The TB shape itself leads to Ca^{2+} compartmentalization which is responsible for the higher facilitation typical of these boutons (Lee and Sherman, 2009) in young adults. This phenomenon might explain the heightened dynamic properties of TBs compared to EPBs in the young adult cortex. Such dynamics might not be affected by a further increase in Ca^{2+} concentrations during ageing; in addition the weaker synaptic signalling of TBs might not be enough to generate significant increases in Ca^{2+} concentration. Alternatively, the lack of an age related effect on aged TBs might be due to the properties of their postsynaptic targets.

Besides changes in Ca^{2+} homeostasis that might directly affect the imaged aged neurons, a shift in the excitatory/inhibitory transmission system balance might further concur to altered structural plasticity during ageing. Inhibitory circuits have been shown to be affected in the aged brain (Stanley and Shetty, 2004; Vela et al., 2003), though the function of inhibitory systems has not yet been thoroughly investigated. Decreased GABAergic transmission, which may lead to decreased synchronization and increased neural noise, has been shown in the auditory cortex of aged rats (Caspary et al., 2008). In the case of peripheral lesions, altered synaptic dynamics on inhibitory neurons have been shown to precede the induced

changes on excitatory neurons, thus raising the possibility that inhibitory input greatly modulates structural plasticity on excitatory neurons (Keck et al., 2011). It is possible that changes in the functional and structural properties of inhibitory neurons during ageing are further affecting the enhanced structural plasticity of Thy1 labelled axons.

8.5 Long term memory impairment in Aged animals

One of the landmarks of ageing is a variable degree of cognitive decline in higher order organisms (Yeoman et al., 2012). Age related cognitive impairments have been thoroughly described in previous sections (see introduction). Importantly, the Aged animals imaged in this study had a long-term memory defect compared to Young Adult mice (Figure 39). Though the behavioural impairment is associated with increased EPB dynamics, a direct correlation of the performance with synaptic structural parameters was not possible. The main reason lies in the fact that few Aged animals that underwent the complete imaging protocol were also able to undergo the behavioural test. The object recognition test itself has a highly variable output which does not rely on a strong reinforcement stimulus. Furthermore, of the animals that did complete imaging and behaviour, the majority had negative discrimination indexes indicating the inability to memorize the object with no further indication on the degree of the impairment. Nevertheless, Aged animals showed a selective impairment in the object recognition memory in the long-term version but not on shorter version of the task (Figure 41), suggesting that perceptive defects are absent or negligible. The link between increased EPB dynamics and decreased performance would have been strengthened by a direct correlation in the same animals. However, further indications might come from the completion of the Middle Age imaging dataset. If EPB parameters were to be, on average, at an intermediate level between Aged and Young Adult animals, this would point to a gradual concurrent increase in EPB dynamics and decrease in performance

(Figure 47). Importantly, though, the behavioural data so far suggest that EPB heightened dynamics are not boosting an eventual increase in performance. In other words, in this case what is generally thought to be linked to better learning (heightened synaptic dynamics) is not associated with successful memory formation.

8.6 EPBscore reliability and accuracy

Image analysis represents a major bottleneck in two-photon imaging studies (Canty and De Paola, 2011). In addition, analytical tools to identify synaptic sites have relied so far on manual routines that arguably introduce a user dependent bias (Holtmaat et al., 2009). EPBscore represents an improvement, as it assists neurite tracing. More importantly, it detects EPBs automatically without an input from the user, given an initial set of scoring criteria which are kept constant. EPBscore provides an accurate estimation of bouton size (Figure 21), and the relative intensity value of each bouton detected is reproducible. Here, EPBscore opened the possibility of reliably detecting significant size changes observed *in vivo* (Figure 22 a) and made TOR measurements more consistent (Figure 22 b). Limits of the pipeline reside in the difficulties it encounters during automatic axonal tracing and the alignment of images over time. Although automatic neuronal tracing is not always perfect (especially were axons are densely labelled) and often requires manual editing, it does not impact on the final output of normalized intensity values for the scored EPB. Full automation would though benefit the throughput of the procedure, possibly increasing the speed of the analysis step. The alignment issues mainly appear in the case of densely packed boutons on an axonal stretch. Because imaged axons undergo, to some degree, distortion and curvature they are not identical at different time points. Although the alignment processing step accounts for distortion, errors may be introduced as a result of the vicinity of intensity peaks (i.e. EPBs) or because the fiducial points on which the alignment is based are added

manually. The user must then learn to carefully check that the correlation of EPBs over time is correct, editing the results when necessary to ensure that the correct values correspond to the correct boutons. Improvement in such a critical step would surely cut considerably the amount of time needed to perform a high quality image analysis. Overall, EPBscore is a valuable tool that will be employed in future studies in different contexts. The principles on which it is founded (backbone estimation and maximal intensity profile analysis) may be used to analyse also other synaptic structures, such as dendritic spines and axonal TBs.

8.7 Closing remarks

In this thesis a novel, surprising, feature of the ageing brain has been uncovered. Rather than the expected decrease in synaptic structural plasticity, synaptic elements were found to be more dynamic in the ageing brain. An increase in synaptic elimination was counteracted by increased synaptic formation, indicating that the aged brain suffers from synaptic destabilization in specific circuits. For the first time bouton volumes were followed *in vivo* with size changes more prominent in the Aged compared to the Young Adult cortex. Future work should aim at establishing the causes for the altered synaptic dynamics and also if these synaptic alterations occur in other brain areas other than the somatosensory cortex. If further specific biochemical pathways controlling synaptic destabilization were to be identified they could represent targets to modulate the age related effects aiming at promoting synaptic stability. Such modulation may represent a treatment strategy of age related cognitive decline and it might also help ameliorate symptoms of pathological states of senile dementia.

9. Bibliography

Anderson, B., and Rutledge, V. (1996). Age and hemisphere effects on dendritic structure. Brain *119 (Pt 6)*, 1983-1990.

Anderson, J.C., and Martin, K.A. (2001). Does bouton morphology optimize axon length? Nature neuroscience *4*, 1166-1167.

Arellano, J.I., Espinosa, A., Fairen, A., Yuste, R., and DeFelipe, J. (2007). Non-synaptic dendritic spines in neocortex. Neuroscience *145*, 464-469.

Bach, M.E., Barad, M., Son, H., Zhuo, M., Lu, Y.F., Shih, R., Mansuy, I., Hawkins, R.D., and Kandel, E.R. (1999). Age-related defects in spatial memory are correlated with defects in the late phase of hippocampal long-term potentiation in vitro and are attenuated by drugs that enhance the cAMP signaling pathway. Proceedings of the National Academy of Sciences of the United States of America *96*, 5280-5285.

Baker, D.J., Wijshake, T., Tchkonia, T., LeBrasseur, N.K., Childs, B.G., van de Sluis, B., Kirkland, J.L., and van Deursen, J.M. (2011). Clearance of p16Ink4a-positive senescent cells delays ageing-associated disorders. Nature *479*, 232-236.

Barense, M.D., Fox, M.T., and Baxter, M.G. (2002). Aged rats are impaired on an attentional set-shifting task sensitive to medial frontal cortex damage in young rats. Learn Mem *9*, 191-201.

Barnes, C.A. (1979). Memory deficits associated with senescence: a neurophysiological and behavioral study in the rat. J Comp Physiol Psychol *93*, 74-104.

Barnes, C.A. (2011). Secrets of aging: What does a normally aging brain look like? F1000 Biol Rep *3*, 22.

Barnes, C.A., and McNaughton, B.L. (1980). Physiological compensation for loss of afferent synapses in rat hippocampal granule cells during senescence. The Journal of physiology *309*, 473-485.

Barnes, C.A., Rao, G., Foster, T.C., and McNaughton, B.L. (1992). Region-specific age effects on AMPA sensitivity: electrophysiological evidence for loss of synaptic contacts in hippocampal field CA1. Hippocampus *2*, 457-468.

Barnes, C.A., Rao, G., and Houston, F.P. (2000). LTP induction threshold change in old rats at the perforant path--granule cell synapse. Neurobiol Aging *21*, 613-620.

Barnes, C.A., Rao, G., and Shen, J. (1997). Age-related decrease in the N-methyl-D-aspartateR-mediated excitatory postsynaptic potential in hippocampal region CA1. Neurobiol Aging *18*, 445-452.

Barreto, G., Huang, T.T., and Giffard, R.G. (2010). Age-related defects in sensorimotor activity, spatial learning, and memory in C57BL/6 mice. J Neurosurg Anesthesiol *22*, 214-219.

Bartley, A.J., Jones, D.W., and Weinberger, D.R. (1997). Genetic variability of human brain size and cortical gyral patterns. Brain *120 (Pt 2)*, 257-269.

Becker, N., Wierenga, C.J., Fonseca, R., Bonhoeffer, T., and Nagerl, U.V. (2008). LTD induction causes morphological changes of presynaptic boutons and reduces their contacts with spines. Neuron *60*, 590-597.

Bednarek, E., and Caroni, P. (2011). beta-Adducin is required for stable assembly of new synapses and improved memory upon environmental enrichment. Neuron *69*, 1132-1146.

Benice, T.S., Rizk, A., Kohama, S., Pfankuch, T., and Raber, J. (2006). Sex-differences in age-related cognitive decline in C57BL/6J mice associated with increased brain microtubule-associated protein 2 and synaptophysin immunoreactivity. Neuroscience *137*, 413-423.

Berning, S., Willig, K.I., Steffens, H., Dibaj, P., and Hell, S.W. (2012). Nanoscopy in a living mouse brain. Science *335*, 551.

Bevins, R.A., and Besheer, J. (2006). Object recognition in rats and mice: a one-trial non-matching-to-sample learning task to study 'recognition memory'. Nat Protoc *1*, 1306-1311.

Bishop, D., Nikic, I., Brinkoetter, M., Knecht, S., Potz, S., Kerschensteiner, M., and Misgeld, T. (2011). Near-infrared branding efficiently correlates light and electron microscopy. Nat Methods *8*, 568-570.

Blank, T., Nijholt, I., Kye, M.J., Radulovic, J., and Spiess, J. (2003). Small-conductance, Ca2+-activated K+ channel SK3 generates age-related memory and LTP deficits. Nature neuroscience *6*, 911-912.

Bliss, T.V., and Collingridge, G.L. (1993). A synaptic model of memory: long-term potentiation in the hippocampus. Nature *361*, 31-39.

Bliss, T.V., and Lomo, T. (1973). Long-lasting potentiation of synaptic transmission in the dentate area of the anaesthetized rabbit following stimulation of the perforant path. J Physiol *232*, 331-356.

Bloss, E.B., Janssen, W.G., Ohm, D.T., Yuk, F.J., Wadsworth, S., Saardi, K.M., McEwen, B.S., and Morrison, J.H. (2011). Evidence for reduced experience-dependent dendritic spine plasticity in the aging prefrontal cortex. J Neurosci *31*, 7831-7839.

Bluher, M., Kahn, B.B., and Kahn, C.R. (2003). Extended longevity in mice lacking the insulin receptor in adipose tissue. Science *299*, 572-574.

Bodhinathan, K., Kumar, A., and Foster, T.C. (2010). Intracellular redox state alters NMDA receptor response during aging through Ca2+/calmodulin-dependent protein kinase II. J Neurosci *30*, 1914-1924.

Bondareff, W., and Geinisman, Y. (1976). Loss of synapses in the dentate gyrus of the senescent rat. Am J Anat *145*, 129-136.

Brizzee, K.R., Ordy, J.M., and Bartus, R.T. (1980). Localization of cellular changes within multimodal sensory regions in aged monkey brain: possible implications for age-related cognitive loss. Neurobiol Aging *1*, 45-52.

Brody, H. (1955). Organization of the cerebral cortex. III. A study of aging in the human cerebral cortex. J Comp Neurol *102*, 511-516.

Buell, S.J., and Coleman, P.D. (1979). Dendritic growth in the aged human brain and failure of growth in senile dementia. Science *206*, 854-856.

Buell, S.J., and Coleman, P.D. (1981). Quantitative evidence for selective dendritic growth in normal human aging but not in senile dementia. Brain Res *214*, 23-41.

Burke, S.N., and Barnes, C.A. (2006). Neural plasticity in the ageing brain. Nat Rev Neurosci *7*, 30-40.

Burke, S.N., and Barnes, C.A. (2010). Senescent synapses and hippocampal circuit dynamics. Trends Neurosci *33*, 153-161.

Canty, A.J., and De Paola, V. (2011). Axonal reconstructions going live. Neuroinformatics *9*, 129-131.

Caroni, P., Donato, F., and Muller, D. (2012). Structural plasticity upon learning: regulation and functions. Nat Rev Neurosci *13*, 478-490.

Caspary, D.M., Ling, L., Turner, J.G., and Hughes, L.F. (2008). Inhibitory neurotransmission, plasticity and aging in the mammalian central auditory system. J Exp Biol *211*, 1781-1791.

Chang, Y.M., Rosene, D.L., Killiany, R.J., Mangiamele, L.A., and Luebke, J.I. (2005). Increased action potential firing rates of layer 2/3 pyramidal cells in the prefrontal cortex are significantly related to cognitive performance in aged monkeys. Cereb Cortex *15*, 409-418.

Cheetham, C.E., Barnes, S.J., Albieri, G., Knott, G.W., and Finnerty, G.T. (2012). Pansynaptic Enlargement at Adult Cortical Connections Strengthened by Experience. Cereb Cortex.

Chen, S., and Hillman, D.E. (1999). Dying-back of Purkinje cell dendrites with synapse loss in aging rats. J Neurocytol *28*, 187-196.

Chklovskii, D.B., Mel, B.W., and Svoboda, K. (2004). Cortical rewiring and information storage. Nature *431*, 782-788.

Clancy, D.J., Gems, D., Harshman, L.G., Oldham, S., Stocker, H., Hafen, E., Leevers, S.J., and Partridge, L. (2001). Extension of life-span by loss of CHICO, a Drosophila insulin receptor substrate protein. Science *292*, 104-106.

Coleman, P.D., and Flood, D.G. (1987). Neuron numbers and dendritic extent in normal aging and Alzheimer's disease. Neurobiol Aging *8*, 521-545.

Craik, F.I., and Byrd, M. (1982). Aging and cognitive deficits. In Aging and cognitive processes (Springer), pp. 191-211.

Curcio, C.A., and Hinds, J.W. (1983). Stability of synaptic density and spine volume in dentate gyrus of aged rats. Neurobiol Aging *4*, 77-87.

Dancause, N., Barbay, S., Frost, S.B., Plautz, E.J., Chen, D., Zoubina, E.V., Stowe, A.M., and Nudo, R.J. (2005). Extensive cortical rewiring after brain injury. J Neurosci *25*, 10167-10179.

de Brabander, J.M., Kramers, R.J., and Uylings, H.B. (1998). Layer-specific dendritic regression of pyramidal cells with ageing in the human prefrontal cortex. Eur J Neurosci *10*, 1261-1269.

De Felipe, J., Marco, P., Fairen, A., and Jones, E.G. (1997). Inhibitory synaptogenesis in mouse somatosensory cortex. Cereb Cortex *7*, 619-634.

de Groot, J.C., de Leeuw, F.E., Oudkerk, M., van Gijn, J., Hofman, A., Jolles, J., and Breteler, M.M. (2000). Cerebral white matter lesions and cognitive function: the Rotterdam Scan Study. Annals of neurology *47*, 145-151.

De Paola, V., Arber, S., and Caroni, P. (2003). AMPA receptors regulate dynamic equilibrium of presynaptic terminals in mature hippocampal networks. Nat Neurosci *6*, 491-500.

De Paola, V., Holtmaat, A., Knott, G., Song, S., Wilbrecht, L., Caroni, P., and Svoboda, K. (2006). Cell type-specific structural plasticity of axonal branches and boutons in the adult neocortex. Neuron *49*, 861-875.

Dellu, F., Mayo, W., Cherkaoui, J., Le Moal, M., and Simon, H. (1992). A two-trial memory task with automated recording: study in young and aged rats. Brain research *588*, 132-139.

Deupree, D.L., Turner, D.A., and Watters, C.L. (1991). Spatial performance correlates with in vitro potentiation in young and aged Fischer 344 rats. Brain research *554*, 1-9.

Diamond, M.E., von Heimendahl, M., Knutsen, P.M., Kleinfeld, D., and Ahissar, E. (2008). 'Where' and 'what' in the whisker sensorimotor system. Nat Rev Neurosci *9*, 601-612.

Diana, G., Domenici, M.R., Loizzo, A., Scotti de Carolis, A., and Sagratella, S. (1994a). Age and strain differences in rat place learning and hippocampal dentate gyrus frequency-potentiation. Neurosci Lett *171*, 113-116.

Diana, G., Scotti de Carolis, A., Frank, C., Domenici, M.R., and Sagratella, S. (1994b). Selective reduction of hippocampal dentate frequency potentiation in aged rats with impaired place learning. Brain Res Bull *35*, 107-111.

Dickson, D.W., Crystal, H.A., Mattiace, L.A., Masur, D.M., Blau, A.D., Davies, P., Yen, S.H., and Aronson, M.K. (1992). Identification of normal and pathological aging in prospectively studied nondemented elderly humans. Neurobiol Aging *13*, 179-189.

Dickstein, D.L., Kabaso, D., Rocher, A.B., Luebke, J.I., Wearne, S.L., and Hof, P.R. (2007). Changes in the structural complexity of the aged brain. Aging Cell *6*, 275-284.

Dieguez, D., Jr., and Barea-Rodriguez, E.J. (2004). Aging impairs the late phase of long-term potentiation at the medial perforant path-CA3 synapse in awake rats. Synapse *52*, 53-61.

Drew, P.J., Shih, A.Y., Driscoll, J.D., Knutsen, P.M., Blinder, P., Davalos, D., Akassoglou, K., Tsai, P.S., and Kleinfeld, D. (2010). Chronic optical access through a polished and reinforced thinned skull. Nat Methods *7*, 981-984.

Duan, H., Wearne, S.L., Rocher, A.B., Macedo, A., Morrison, J.H., and Hof, P.R. (2003). Age-related dendritic and spine changes in corticocortically projecting neurons in macaque monkeys. Cereb Cortex *13*, 950-961.

Dumitriu, D., Hao, J., Hara, Y., Kaufmann, J., Janssen, W.G., Lou, W., Rapp, P.R., and Morrison, J.H. (2010). Selective changes in thin spine density and morphology in monkey prefrontal cortex correlate with aging-related cognitive impairment. J Neurosci *30*, 7507-7515.

Dunnett, S.B., Evenden, J.L., and Iversen, S.D. (1988). Delay-dependent short-term memory deficits in aged rats. Psychopharmacology (Berl) *96*, 174-180.

Ennaceur, A., and Delacour, J. (1988). A new one-trial test for neurobiological studies of memory in rats. 1: Behavioral data. Behav Brain Res *31*, 47-59.

Feldman, M.L., and Dowd, C. (1975). Loss of dendritic spines in aging cerebral cortex. Anat Embryol (Berl) *148*, 279-301.

Feng, G., Mellor, R.H., Bernstein, M., Keller-Peck, C., Nguyen, Q.T., Wallace, M., Nerbonne, J.M., Lichtman, J.W., and Sanes, J.R. (2000). Imaging neuronal subsets in transgenic mice expressing multiple spectral variants of GFP. Neuron *28*, 41-51.

Flood, D.G. (1991). Region-specific stability of dendritic extent in normal human aging and regression in Alzheimer's disease. II. Subiculum. Brain Res *540*, 83-95.

Flood, D.G., Buell, S.J., Horwitz, G.J., and Coleman, P.D. (1987a). Dendritic extent in human dentate gyrus granule cells in normal aging and senile dementia. Brain Res *402*, 205-216.

Flood, D.G., Guarnaccia, M., and Coleman, P.D. (1987b). Dendritic extent in human CA2-3 hippocampal pyramidal neurons in normal aging and senile dementia. Brain Res *409*, 88-96.

Florence, S.L., Taub, H.B., and Kaas, J.H. (1998). Large-scale sprouting of cortical connections after peripheral injury in adult macaque monkeys. Science *282*, 1117-1121.

Fontana, L., Partridge, L., and Longo, V.D. (2010). Extending healthy life span--from yeast to humans. Science *328*, 321-326.

Foster, T.C. (2007). Calcium homeostasis and modulation of synaptic plasticity in the aged brain. Aging Cell *6*, 319-325.

Foster, T.C., Barnes, C.A., Rao, G., and McNaughton, B.L. (1991). Increase in perforant path quantal size in aged F-344 rats. Neurobiol Aging *12*, 441-448.

Foster, T.C., and Norris, C.M. (1997). Age-associated changes in Ca(2+)-dependent processes: relation to hippocampal synaptic plasticity. Hippocampus *7*, 602-612.

Fredj, N.B., and Burrone, J. (2009). A resting pool of vesicles is responsible for spontaneous vesicle fusion at the synapse. Nature neuroscience *12*, 751-758.

Frick, K.M., Baxter, M.G., Markowska, A.L., Olton, D.S., and Price, D.L. (1995). Age-related spatial reference and working memory deficits assessed in the water maze. Neurobiol Aging *16*, 149-160.

Frick, K.M., Burlingame, L.A., Arters, J.A., and Berger-Sweeney, J. (2000). Reference memory, anxiety and estrous cyclicity in C57BL/6NIA mice are affected by age and sex. Neuroscience *95*, 293-307.

Fu, M., Yu, X., Lu, J., and Zuo, Y. (2012). Repetitive motor learning induces coordinated formation of clustered dendritic spines in vivo. Nature *483*, 92-95.

Fu, M., and Zuo, Y. (2011). Experience-dependent structural plasticity in the cortex. Trends in neurosciences *34*, 177-187.

Gage, F.H., Dunnett, S.B., and Bjorklund, A. (1984). Spatial learning and motor deficits in aged rats. Neurobiol Aging *5*, 43-48.

Galimberti, I., Gogolla, N., Alberi, S., Santos, A.F., Muller, D., and Caroni, P. (2006). Long-term rearrangements of hippocampal mossy fiber terminal connectivity in the adult regulated by experience. Neuron *50*, 749-763.

Gazzaley, A.H., Thakker, M.M., Hof, P.R., and Morrison, J.H. (1997). Preserved number of entorhinal cortex layer II neurons in aged macaque monkeys. Neurobiol Aging *18*, 549-553.

Geinisman, Y., Bondareff, W., and Dodge, J.T. (1977). Partial deafferentation of neurons in the dentate gyrus of the senescent rat. Brain Res *134*, 541-545.

Geinisman, Y., de Toledo-Morrell, L., and Morrell, F. (1986). Loss of perforated synapses in the dentate gyrus: morphological substrate of memory deficit in aged rats. Proc Natl Acad Sci U S A *83*, 3027-3031.

Geinisman, Y., Detoledo-Morrell, L., Morrell, F., and Heller, R.E. (1995). Hippocampal markers of age-related memory dysfunction: behavioral, electrophysiological and morphological perspectives. Progress in neurobiology *45*, 223-252.

Geinisman, Y., deToledo-Morrell, L., Morrell, F., Persina, I.S., and Rossi, M. (1992). Age-related loss of axospinous synapses formed by two afferent systems in the rat dentate gyrus as revealed by the unbiased stereological dissector technique. Hippocampus *2*, 437-444.

Geinisman, Y., Ganeshina, O., Yoshida, R., Berry, R.W., Disterhoft, J.F., and Gallagher, M. (2004). Aging, spatial learning, and total synapse number in the rat CA1 stratum radiatum. Neurobiol Aging *25*, 407-416.

Glazewski, S., and Fox, K. (1996). Time course of experience-dependent synaptic potentiation and depression in barrel cortex of adolescent rats. J Neurophysiol *75*, 1714-1729.

Glisky, E.L. (2007). Changes in Cognitive Function in Human Aging. In Brain Aging: Models, Methods, and Mechanisms, D.R. Riddle, ed. (Boca Raton (FL)).

Glisky, E.L., Rubin, S.R., and Davidson, P.S. (2001). Source memory in older adults: an encoding or retrieval problem? J Exp Psychol Learn Mem Cogn *27*, 1131-1146.

Grady, C. (2012). The cognitive neuroscience of ageing. Nat Rev Neurosci *13*, 491-505.

Grill, J.D., and Riddle, D.R. (2002). Age-related and laminar-specific dendritic changes in the medial frontal cortex of the rat. Brain Res *937*, 8-21.

Grillo, F.W., Song, S., Teles-Grilo Ruivo, L.M., Huang, L., Gao, G., Knott, G.W., Maco, B., Ferretti, V., Thompson, D., Little, G.E.*, et al.* (2013). Increased axonal bouton dynamics in the aging mouse cortex. Proc Natl Acad Sci U S A.

Grottick, A.J., and Higgins, G.A. (2002). Assessing a vigilance decrement in aged rats: effects of pre-feeding, task manipulation, and psychostimulants. Psychopharmacology (Berl) *164*, 33-41.

Grutzendler, J., Kasthuri, N., and Gan, W.B. (2002). Long-term dendritic spine stability in the adult cortex. Nature *420*, 812-816.

Hanks, S.D., and Flood, D.G. (1991). Region-specific stability of dendritic extent in normal human aging and regression in Alzheimer's disease. I. CA1 of hippocampus. Brain Res *540*, 63-82.

Hao, J., Rapp, P.R., Janssen, W.G., Lou, W., Lasley, B.L., Hof, P.R., and Morrison, J.H. (2007). Interactive effects of age and estrogen on cognition and pyramidal neurons in monkey prefrontal cortex. Proc Natl Acad Sci U S A *104*, 11465-11470.

Hara, Y., Park, C.S., Janssen, W.G., Punsoni, M., Rapp, P.R., and Morrison, J.H. (2011). Synaptic characteristics of dentate gyrus axonal boutons and their relationships with aging, menopause, and memory in female rhesus monkeys. J Neurosci *31*, 7737-7744.

Hara, Y., Park, C.S., Janssen, W.G., Roberts, M.T., Morrison, J.H., and Rapp, P.R. (2012). Synaptic correlates of memory and menopause in the hippocampal dentate gyrus in rhesus monkeys. Neurobiol Aging *33*, 421 e417-428.

Harman, D. (1991). The aging process: major risk factor for disease and death. Proc Natl Acad Sci U S A *88*, 5360-5363.

Harris, K.M., Jensen, F.E., and Tsao, B. (1992). Three-dimensional structure of dendritic spines and synapses in rat hippocampus (CA1) at postnatal day 15 and adult ages: implications for the maturation of synaptic physiology and long-term potentiation. J Neurosci *12*, 2685-2705.

Harris, K.M., and Stevens, J.K. (1989). Dendritic spines of CA 1 pyramidal cells in the rat hippocampus: serial electron microscopy with reference to their biophysical characteristics. J Neurosci *9*, 2982-2997.

Hedden, T., and Gabrieli, J.D. (2004). Insights into the ageing mind: a view from cognitive neuroscience. Nat Rev Neurosci *5*, 87-96.

Helmchen, F., and Denk, W. (2005). Deep tissue two-photon microscopy. Nat Methods *2*, 932-940.

Herndon, J.G., Moss, M.B., Rosene, D.L., and Killiany, R.J. (1997). Patterns of cognitive decline in aged rhesus monkeys. Behav Brain Res *87*, 25-34.

Hof, P.R., and Morrison, J.H. (2004). The aging brain: morphomolecular senescence of cortical circuits. Trends Neurosci *27*, 607-613.

Hofer, S.B., Mrsic-Flogel, T.D., Bonhoeffer, T., and Hubener, M. (2006). Prior experience enhances plasticity in adult visual cortex. Nature neuroscience *9*, 127-132.

Hofer, S.B., Mrsic-Flogel, T.D., Bonhoeffer, T., and Hubener, M. (2009). Experience leaves a lasting structural trace in cortical circuits. Nature *457*, 313-317.

Holahan, M.R., Rekart, J.L., Sandoval, J., and Routtenberg, A. (2006). Spatial learning induces presynaptic structural remodeling in the hippocampal mossy fiber system of two rat strains. Hippocampus *16*, 560-570.

Holliday, R. (2006). Aging is no longer an unsolved problem in biology. Ann N Y Acad Sci *1067*, 1-9.

Holtmaat, A., Bonhoeffer, T., Chow, D.K., Chuckowree, J., De Paola, V., Hofer, S.B., Hubener, M., Keck, T., Knott, G., Lee, W.C., *et al.* (2009). Long-term, high-resolution imaging in the mouse neocortex through a chronic cranial window. Nat Protoc *4*, 1128-1144.

Holtmaat, A., and Svoboda, K. (2009). Experience-dependent structural synaptic plasticity in the mammalian brain. Nat Rev Neurosci *10*, 647-658.

Holtmaat, A., Wilbrecht, L., Knott, G.W., Welker, E., and Svoboda, K. (2006). Experience-dependent and cell-type-specific spine growth in the neocortex. Nature *441*, 979-983.

Holtmaat, A.J., Trachtenberg, J.T., Wilbrecht, L., Shepherd, G.M., Zhang, X., Knott, G.W., and Svoboda, K. (2005). Transient and persistent dendritic spines in the neocortex in vivo. Neuron *45*, 279-291.

Holzenberger, M., Dupont, J., Ducos, B., Leneuve, P., Geloen, A., Even, P.C., Cervera, P., and Le Bouc, Y. (2003). IGF-1 receptor regulates lifespan and resistance to oxidative stress in mice. Nature *421*, 182-187.

Hu, D., Serrano, F., Oury, T.D., and Klann, E. (2006). Aging-dependent alterations in synaptic plasticity and memory in mice that overexpress extracellular superoxide dismutase. J Neurosci *26*, 3933-3941.

Hubener, M., and Bonhoeffer, T. (2010). Searching for engrams. Neuron *67*, 363-371.

Iqbal, A., Piper, M., Faragher, R.G., Naughton, D.P., Partridge, L., and Ostler, E.L. (2009). Chemical changes in aging Drosophila melanogaster. Age (Dordr) *31*, 343-351.

Jacobs, B., Driscoll, L., and Schall, M. (1997). Life-span dendritic and spine changes in areas 10 and 18 of human cortex: a quantitative Golgi study. J Comp Neurol *386*, 661-680.

Jacobs, B., and Scheibel, A.B. (1993). A quantitative dendritic analysis of Wernicke's area in humans. I. Lifespan changes. J Comp Neurol *327*, 83-96.

Jagust, W. (2013). Vulnerable neural systems and the borderland of brain aging and neurodegeneration. Neuron *77*, 219-234.

Jennings, J.M., and Jacoby, L.L. (1997). An opposition procedure for detecting age-related deficits in recollection: telling effects of repetition. Psychol Aging *12*, 352-361.

Jung, C.K., and Herms, J. (2012). Structural Dynamics of Dendritic Spines are Influenced by an Environmental Enrichment: An In Vivo Imaging Study. Cereb Cortex.

Kamsler, A., and Segal, M. (2004). Hydrogen peroxide as a diffusible signal molecule in synaptic plasticity. Mol Neurobiol *29*, 167-178.

Kasai, H., Fukuda, M., Watanabe, S., Hayashi-Takagi, A., and Noguchi, J. (2010a). Structural dynamics of dendritic spines in memory and cognition. Trends in neurosciences *33*, 121-129.

Kasai, H., Hayama, T., Ishikawa, M., Watanabe, S., Yagishita, S., and Noguchi, J. (2010b). Learning rules and persistence of dendritic spines. Eur J Neurosci *32*, 241-249.

Kasai, H., Matsuzaki, M., Noguchi, J., Yasumatsu, N., and Nakahara, H. (2003). Structure-stability-function relationships of dendritic spines. Trends in neurosciences *26*, 360-368.

Keck, T., Mrsic-Flogel, T.D., Vaz Afonso, M., Eysel, U.T., Bonhoeffer, T., and Hubener, M. (2008). Massive restructuring of neuronal circuits during functional reorganization of adult visual cortex. Nature neuroscience *11*, 1162-1167.

Keck, T., Scheuss, V., Jacobsen, R.I., Wierenga, C.J., Eysel, U.T., Bonhoeffer, T., and Hubener, M. (2011). Loss of sensory input causes rapid structural changes of inhibitory neurons in adult mouse visual cortex. Neuron *71*, 869-882.

Kelly, L., Grehan, B., Chiesa, A.D., O'Mara, S.M., Downer, E., Sahyoun, G., Massey, K.A., Nicolaou, A., and Lynch, M.A. (2011). The polyunsaturated fatty acids, EPA and DPA exert a protective effect in the hippocampus of the aged rat. Neurobiol Aging *32*, 2318 e2311-2315.

Kenessary, A., Zhumadilov, Z., Nurgozhin, T., Kipling, D., Yeoman, M., Cox, L., Ostler, E., and Faragher, R. (2012). Biomarkers, interventions and healthy ageing. N Biotechnol.

Kenyon, C. (2005). The plasticity of aging: insights from long-lived mutants. Cell *120*, 449-460.

Kenyon, C., Chang, J., Gensch, E., Rudner, A., and Tabtiang, R. (1993). A C. elegans mutant that lives twice as long as wild type. Nature *366*, 461-464.

Kenyon, C.J. (2010). The genetics of ageing. Nature *464*, 504-512.

Keuker, J.I., Luiten, P.G., and Fuchs, E. (2003). Preservation of hippocampal neuron numbers in aged rhesus monkeys. Neurobiol Aging *24*, 157-165.

Knott, G., Marchman, H., Wall, D., and Lich, B. (2008). Serial section scanning electron microscopy of adult brain tissue using focused ion beam milling. J Neurosci *28*, 2959-2964.

Knott, G., Rosset, S., and Cantoni, M. (2011). Focussed ion beam milling and scanning electron microscopy of brain tissue. Journal of visualized experiments : JoVE, e2588.

Knott, G.W., Holtmaat, A., Wilbrecht, L., Welker, E., and Svoboda, K. (2006). Spine growth precedes synapse formation in the adult neocortex in vivo. Nat Neurosci *9*, 1117-1124.

Knott, G.W., Quairiaux, C., Genoud, C., and Welker, E. (2002). Formation of dendritic spines with GABAergic synapses induced by whisker stimulation in adult mice. Neuron *34*, 265-273.

Koivisto, K., Reinikainen, K.J., Hanninen, T., Vanhanen, M., Helkala, E.L., Mykkanen, L., Laakso, M., Pyorala, K., and Riekkinen, P.J., Sr. (1995). Prevalence of age-associated memory impairment in a randomly selected population from eastern Finland. Neurology *45*, 741-747.

Kossut, M., and Juliano, S.L. (1999). Anatomical correlates of representational map reorganization induced by partial vibrissectomy in the barrel cortex of adult mice. Neuroscience *92*, 807-817.

Kumar, A. (2011). Long-Term Potentiation at CA3-CA1 Hippocampal Synapses with Special Emphasis on Aging, Disease, and Stress. Front Aging Neurosci *3*, 7.

Kumar, A., and Foster, T.C. (2004). Enhanced long-term potentiation during aging is masked by processes involving intracellular calcium stores. Journal of neurophysiology *91*, 2437-2444.

Kumar, A., and Foster, T.C. (2005). Intracellular calcium stores contribute to increased susceptibility to LTD induction during aging. Brain research *1031*, 125-128.

Kumar, A., and Foster, T.C. (2007). Neurophysiology of Old Neurons and Synapses. In Brain Aging: Models, Methods, and Mechanisms, D.R. Riddle, ed. (Boca Raton (FL)).

Lai, C.S., Franke, T.F., and Gan, W.B. (2012). Opposite effects of fear conditioning and extinction on dendritic spine remodelling. Nature *483*, 87-91.

Landfield, P.W. (1988). Hippocampal neurobiological mechanisms of age-related memory dysfunction. Neurobiol Aging *9*, 571-579.

Landfield, P.W., McGaugh, J.L., and Lynch, G. (1978). Impaired synaptic potentiation processes in the hippocampus of aged, memory-deficient rats. Brain research *150*, 85-101.

Landfield, P.W., and Pitler, T.A. (1984). Prolonged Ca2+-dependent afterhyperpolarizations in hippocampal neurons of aged rats. Science *226*, 1089-1092.

Lee, C.C., and Sherman, S.M. (2009). Modulator property of the intrinsic cortical projection from layer 6 to layer 4. Front Syst Neurosci *3*, 3.

Lendvai, B., Stern, E.A., Chen, B., and Svoboda, K. (2000). Experience-dependent plasticity of dendritic spines in the developing rat barrel cortex in vivo. Nature *404*, 876-881.

Leuba, G. (1983). Aging of dendrites in the cerebral cortex of the mouse. Neuropathol Appl Neurobiol *9*, 467-475.

Lintl, P., and Braak, H. (1983). Loss of intracortical myelinated fibers: a distinctive age-related alteration in the human striate area. Acta neuropathologica *61*, 178-182.

Lisman, J., Yasuda, R., and Raghavachari, S. (2012). Mechanisms of CaMKII action in long-term potentiation. Nat Rev Neurosci *13*, 169-182.

Loewenstein, Y., Kuras, A., and Rumpel, S. (2011). Multiplicative dynamics underlie the emergence of the log-normal distribution of spine sizes in the neocortex in vivo. J Neurosci *31*, 9481-9488.

Lu, C.B., Hamilton, J.B., Powell, A.D., Toescu, E.C., and Vreugdenhil, M. (2011). Effect of ageing on CA3 interneuron sAHP and gamma oscillations is activity-dependent. Neurobiol Aging *32*, 956-965.

Luebke, J.I., and Amatrudo, J.M. (2012). Age-related increase of sI(AHP) in prefrontal pyramidal cells of monkeys: relationship to cognition. Neurobiol Aging *33*, 1085-1095.

Luebke, J.I., and Chang, Y.M. (2007). Effects of aging on the electrophysiological properties of layer 5 pyramidal cells in the monkey prefrontal cortex. Neuroscience *150*, 556-562.

Luebke, J.I., Chang, Y.M., Moore, T.L., and Rosene, D.L. (2004). Normal aging results in decreased synaptic excitation and increased synaptic inhibition of layer 2/3 pyramidal cells in the monkey prefrontal cortex. Neuroscience *125*, 277-288.

Luu, T.T., Pirogovsky, E., and Gilbert, P.E. (2008). Age-related changes in contextual associative learning. Neurobiol Learn Mem *89*, 81-85.

Majewska, A.K., Newton, J.R., and Sur, M. (2006). Remodeling of synaptic structure in sensory cortical areas in vivo. J Neurosci *26*, 3021-3029.

Malinow, R., and Malenka, R.C. (2002). AMPA receptor trafficking and synaptic plasticity. Annual review of neuroscience *25*, 103-126.

Maricich, S.M., Morrison, K.M., Mathes, E.L., and Brewer, B.M. (2012). Rodents rely on Merkel cells for texture discrimination tasks. J Neurosci *32*, 3296-3300.

Marik, S.A., Yamahachi, H., McManus, J.N., Szabo, G., and Gilbert, C.D. (2010). Axonal dynamics of excitatory and inhibitory neurons in somatosensory cortex. PLoS biology *8*, e1000395.

Markham, J.A., and Juraska, J.M. (2002). Aging and sex influence the anatomy of the rat anterior cingulate cortex. Neurobiol Aging *23*, 579-588.

Markham, J.A., McKian, K.P., Stroup, T.S., and Juraska, J.M. (2005). Sexually dimorphic aging of dendritic morphology in CA1 of hippocampus. Hippocampus *15*, 97-103.

Markowska, A.L., Stone, W.S., Ingram, D.K., Reynolds, J., Gold, P.E., Conti, L.H., Pontecorvo, M.J., Wenk, G.L., and Olton, D.S. (1989). Individual differences in aging: behavioral and neurobiological correlates. Neurobiol Aging *10*, 31-43.

Marner, L., Nyengaard, J.R., Tang, Y., and Pakkenberg, B. (2003). Marked loss of myelinated nerve fibers in the human brain with age. The Journal of comparative neurology *462*, 144-152.

Matsuzaki, M., Ellis-Davies, G.C., Nemoto, T., Miyashita, Y., Iino, M., and Kasai, H. (2001). Dendritic spine geometry is critical for AMPA receptor expression in hippocampal CA1 pyramidal neurons. Nature neuroscience *4*, 1086-1092.

Matsuzaki, M., Honkura, N., Ellis-Davies, G.C., and Kasai, H. (2004). Structural basis of long-term potentiation in single dendritic spines. Nature *429*, 761-766.

May, C.P., Hasher, L., and Kane, M.J. (1999). The role of interference in memory span. Mem Cognit *27*, 759-767.

McGuire, B.A., Hornung, J.P., Gilbert, C.D., and Wiesel, T.N. (1984). Patterns of synaptic input to layer 4 of cat striate cortex. J Neurosci *4*, 3021-3033.

Merrill, D.A., Chiba, A.A., and Tuszynski, M.H. (2001). Conservation of neuronal number and size in the entorhinal cortex of behaviorally characterized aged rats. J Comp Neurol *438*, 445-456.

Merrill, D.A., Roberts, J.A., and Tuszynski, M.H. (2000). Conservation of neuron number and size in entorhinal cortex layers II, III, and V/VI of aged primates. J Comp Neurol *422*, 396-401.

Moore, C.I., Browning, M.D., and Rose, G.M. (1993). Hippocampal plasticity induced by primed burst, but not long-term potentiation, stimulation is impaired in area CA1 of aged Fischer 344 rats. Hippocampus *3*, 57-66.

Moore, T.L., Killiany, R.J., Herndon, J.G., Rosene, D.L., and Moss, M.B. (2006). Executive system dysfunction occurs as early as middle-age in the rhesus monkey. Neurobiol Aging *27*, 1484-1493.

Morrison, J.H., and Baxter, M.G. (2012). The ageing cortical synapse: hallmarks and implications for cognitive decline. Nat Rev Neurosci *13*, 240-250.

Moss, M.B., Moore, T.L., Schettler, S.P., Killiany, R., and Rosene, D. (2007). Successful vs. Unsuccessful Aging in the Rhesus Monkey. In Brain Aging: Models, Methods, and Mechanisms, D.R. Riddle, ed. (Boca Raton (FL)).

Mostany, R., Anstey, J.E., Crump, K.L., Maco, B., Knott, G., and Portera-Cailliau, C. (2013). Altered Synaptic Dynamics during Normal Brain Aging. J Neurosci *33*, 4094-4104.

Muir, J.L., Fischer, W., and Bjorklund, A. (1999). Decline in visual attention and spatial memory in aged rats. Neurobiol Aging *20*, 605-615.

Murthy, V.N., Schikorski, T., Stevens, C.F., and Zhu, Y. (2001). Inactivity produces increases in neurotransmitter release and synapse size. Neuron *32*, 673-682.

Nagerl, U.V., and Bonhoeffer, T. (2010). Imaging living synapses at the nanoscale by STED microscopy. J Neurosci *30*, 9341-9346.

Nagerl, U.V., Kostinger, G., Anderson, J.C., Martin, K.A., and Bonhoeffer, T. (2007). Protracted synaptogenesis after activity-dependent spinogenesis in hippocampal neurons. J Neurosci *27*, 8149-8156.

Nakamura, S., Akiguchi, I., Kameyama, M., and Mizuno, N. (1985). Age-related changes of pyramidal cell basal dendrites in layers III and V of human motor cortex: a quantitative Golgi study. Acta Neuropathol *65*, 281-284.

Nimchinsky, E.A., Sabatini, B.L., and Svoboda, K. (2002). Structure and function of dendritic spines. Annu Rev Physiol *64*, 313-353.

Nishiyama, H., Fukaya, M., Watanabe, M., and Linden, D.J. (2007). Axonal motility and its modulation by activity are branch-type specific in the intact adult cerebellum. Neuron *56*, 472-487.

Nolde, S.F., Johnson, M.K., and D'Esposito, M. (1998). Left prefrontal activation during episodic remembering: an event-related fMRI study. Neuroreport *9*, 3509-3514.

Norris, C.M., Korol, D.L., and Foster, T.C. (1996). Increased susceptibility to induction of long-term depression and long-term potentiation reversal during aging. J Neurosci *16*, 5382-5392.

Oberlaender, M., Ramirez, A., and Bruno, R.M. (2012). Sensory experience restructures thalamocortical axons during adulthood. Neuron *74*, 648-655.

Oh, W.C., Hill, T.C., and Zito, K. (2013). Synapse-specific and size-dependent mechanisms of spine structural plasticity accompanying synaptic weakening. Proc Natl Acad Sci U S A *110*, E305-312.

Page, T.L., Einstein, M., Duan, H., He, Y., Flores, T., Rolshud, D., Erwin, J.M., Wearne, S.L., Morrison, J.H., and Hof, P.R. (2002). Morphological alterations in neurons forming corticocortical projections in the neocortex of aged Patas monkeys. Neurosci Lett *317*, 37-41.

Pakkenberg, B., and Gundersen, H.J. (1997). Neocortical neuron number in humans: effect of sex and age. J Comp Neurol *384*, 312-320.

Pakkenberg, B., Pelvig, D., Marner, L., Bundgaard, M.J., Gundersen, H.J., Nyengaard, J.R., and Regeur, L. (2003). Aging and the human neocortex. Exp Gerontol *38*, 95-99.

Park, D.C., Lautenschlager, G., Hedden, T., Davidson, N.S., Smith, A.D., and Smith, P.K. (2002). Models of visuospatial and verbal memory across the adult life span. Psychol Aging *17*, 299-320.

Park, D.C., and Reuter-Lorenz, P. (2009). The adaptive brain: aging and neurocognitive scaffolding. Annu Rev Psychol *60*, 173-196.

Peleg, S., Sananbenesi, F., Zovoilis, A., Burkhardt, S., Bahari-Javan, S., Agis-Balboa, R.C., Cota, P., Wittnam, J.L., Gogol-Doering, A., Opitz, L.*, et al.* (2010). Altered histone acetylation is associated with age-dependent memory impairment in mice. Science *328*, 753-756.

Perez, V.I., Bokov, A., Van Remmen, H., Mele, J., Ran, Q., Ikeno, Y., and Richardson, A. (2009). Is the oxidative stress theory of aging dead? Biochim Biophys Acta *1790*, 1005-1014.

Pestronk, A., Drachman, D.B., and Griffin, J.W. (1980). Effects of aging on nerve sprouting and regeneration. Exp Neurol *70*, 65-82.

Peters, A. (2007). The Effects of Normal Aging on Nerve Fibers and Neuroglia in the Central Nervous System. In Brain Aging: Models, Methods, and Mechanisms, D.R. Riddle, ed. (Boca Raton (FL)).

Peters, A. (2009). The effects of normal aging on myelinated nerve fibers in monkey central nervous system. Front Neuroanat *3*, 11.

Peters, A., Leahu, D., Moss, M.B., and McNally, K.J. (1994). The effects of aging on area 46 of the frontal cortex of the rhesus monkey. Cereb Cortex *4*, 621-635.

Peters, A., Morrison, J.H., Rosene, D.L., and Hyman, B.T. (1998a). Feature article: are neurons lost from the primate cerebral cortex during normal aging? Cereb Cortex *8*, 295-300.

Peters, A., Moss, M.B., and Sethares, C. (2000). Effects of aging on myelinated nerve fibers in monkey primary visual cortex. The Journal of comparative neurology *419*, 364-376.

Peters, A., Sethares, C., and Luebke, J.I. (2008). Synapses are lost during aging in the primate prefrontal cortex. Neuroscience *152*, 970-981.

Peters, A., Sethares, C., and Moss, M.B. (1998b). The effects of aging on layer 1 in area 46 of prefrontal cortex in the rhesus monkey. Cereb Cortex *8*, 671-684.

Pierce, J.P., and Lewin, G.R. (1994). An ultrastructural size principle. Neuroscience *58*, 441-446.

Platano, D., Fattoretti, P., Balietti, M., Bertoni-Freddari, C., and Aicardi, G. (2008). Long-term visual object recognition memory in aged rats. Rejuvenation Res *11*, 333-339.

Portera-Cailliau, C., Weimer, R.M., De Paola, V., Caroni, P., and Svoboda, K. (2005). Diverse modes of axon elaboration in the developing neocortex. PLoS Biol *3*, e272.

Pyapali, G.K., and Turner, D.A. (1996). Increased dendritic extent in hippocampal CA1 neurons from aged F344 rats. Neurobiol Aging *17*, 601-611.

Radley, J.J., Rocher, A.B., Miller, M., Janssen, W.G., Liston, C., Hof, P.R., McEwen, B.S., and Morrison, J.H. (2006). Repeated stress induces dendritic spine loss in the rat medial prefrontal cortex. Cereb Cortex *16*, 313-320.

Rapp, P.R., and Gallagher, M. (1996). Preserved neuron number in the hippocampus of aged rats with spatial learning deficits. Proc Natl Acad Sci U S A *93*, 9926-9930.

Rapp, P.R., Rosenberg, R.A., and Gallagher, M. (1987). An evaluation of spatial information processing in aged rats. Behavioral neuroscience *101*, 3-12.

Rasmussen, T., Schliemann, T., Sorensen, J.C., Zimmer, J., and West, M.J. (1996). Memory impaired aged rats: no loss of principal hippocampal and subicular neurons. Neurobiol Aging *17*, 143-147.

Raz, N., Lindenberger, U., Rodrigue, K.M., Kennedy, K.M., Head, D., Williamson, A., Dahle, C., Gerstorf, D., and Acker, J.D. (2005). Regional brain changes in aging healthy adults: general trends, individual differences and modifiers. Cereb Cortex *15*, 1676-1689.

Ridgway, I.D., Richardson, C.A., and Austad, S.N. (2011). Maximum shell size, growth rate, and maturation age correlate with longevity in bivalve molluscs. J Gerontol A Biol Sci Med Sci *66*, 183-190.

Roberts, T.F., Tschida, K.A., Klein, M.E., and Mooney, R. (2010). Rapid spine stabilization and synaptic enhancement at the onset of behavioural learning. Nature *463*, 948-952.

Rodefer, J.S., and Baxter, M.G. (2007). Neuropsychology of Cognitive Aging in Rodents. In Brain Aging: Models, Methods, and Mechanisms, D.R. Riddle, ed. (Boca Raton (FL)).

Rodefer, J.S., and Nguyen, T.N. (2008). Naltrexone reverses age-induced cognitive deficits in rats. Neurobiol Aging *29*, 309-313.

Rogers, J., Zornetzer, S.F., Bloom, F.E., and Mervis, R.E. (1984). Senescent microstructural changes in rat cerebellum. Brain Res *292*, 23-32.

Rosenzweig, E.S., and Barnes, C.A. (2003). Impact of aging on hippocampal function: plasticity, network dynamics, and cognition. Progress in neurobiology *69*, 143-179.

Sacktor, T.C. (2011). How does PKMzeta maintain long-term memory? Nat Rev Neurosci *12*, 9-15.

Salthouse, T.A. (1996). The processing-speed theory of adult age differences in cognition. Psychol Rev *103*, 403-428.

Sandell, J.H., and Peters, A. (2003). Disrupted myelin and axon loss in the anterior commissure of the aged rhesus monkey. The Journal of comparative neurology *466*, 14-30.

Sanders, M.J. (2011). Context processing in aging: older mice are impaired in renewal of extinguished fear. Exp Aging Res *37*, 572-594.

Scheff, S.W., Bernardo, L.S., and Cotman, C.W. (1978). Decrease in adrenergic axon sprouting in the senescent rat. Science *202*, 775-778.

Scheff, S.W., Price, D.A., Schmitt, F.A., DeKosky, S.T., and Mufson, E.J. (2007). Synaptic alterations in CA1 in mild Alzheimer disease and mild cognitive impairment. Neurology *68*, 1501-1508.

Scheff, S.W., Price, D.A., and Sparks, D.L. (2001). Quantitative assessment of possible age-related change in synaptic numbers in the human frontal cortex. Neurobiol Aging *22*, 355-365.

Scheibel, M.E., Lindsay, R.D., Tomiyasu, U., and Scheibel, A.B. (1975). Progressive dendritic changes in aging human cortex. Exp Neurol *47*, 392-403.

Scheibel, M.E., Lindsay, R.D., Tomiyasu, U., and Scheibel, A.B. (1976). Progressive dendritic changes in the aging human limbic system. Exp Neurol *53*, 420-430.

Schoenbaum, G., Nugent, S., Saddoris, M.P., and Gallagher, M. (2002). Teaching old rats new tricks: age-related impairments in olfactory reversal learning. Neurobiol Aging *23*, 555-564.

Selman, C., Tullet, J.M., Wieser, D., Irvine, E., Lingard, S.J., Choudhury, A.I., Claret, M., Al-Qassab, H., Carmignac, D., Ramadani, F.*, et al.* (2009). Ribosomal protein S6 kinase 1 signaling regulates mammalian life span. Science *326*, 140-144.

Shepherd, G.M., and Harris, K.M. (1998). Three-dimensional structure and composition of CA3-->CA1 axons in rat hippocampal slices: implications for presynaptic connectivity and compartmentalization. J Neurosci *18*, 8300-8310.

Sierra-Mercado, D., Dieguez, D., Jr., and Barea-Rodriguez, E.J. (2008). Brief novelty exposure facilitates dentate gyrus LTP in aged rats. Hippocampus *18*, 835-843.

Slutsky, I., Abumaria, N., Wu, L.J., Huang, C., Zhang, L., Li, B., Zhao, X., Govindarajan, A., Zhao, M.G., Zhuo, M.*, et al.* (2010). Enhancement of learning and memory by elevating brain magnesium. Neuron *65*, 165-177.

Smith, D.E., Rapp, P.R., McKay, H.M., Roberts, J.A., and Tuszynski, M.H. (2004). Memory impairment in aged primates is associated with focal death of cortical neurons and atrophy of subcortical neurons. J Neurosci *24*, 4373-4381.

Smith, T.D., Adams, M.M., Gallagher, M., Morrison, J.H., and Rapp, P.R. (2000). Circuit-specific alterations in hippocampal synaptophysin immunoreactivity predict spatial learning impairment in aged rats. J Neurosci *20*, 6587-6593.

Song, S., Sjostrom, P.J., Reigl, M., Nelson, S., and Chklovskii, D.B. (2005). Highly nonrandom features of synaptic connectivity in local cortical circuits. PLoS Biol *3*, e68.

Stanley, D.P., and Shetty, A.K. (2004). Aging in the rat hippocampus is associated with widespread reductions in the number of glutamate decarboxylase-67 positive interneurons but not interneuron degeneration. J Neurochem *89*, 204-216.

Stettler, D.D., Yamahachi, H., Li, W., Denk, W., and Gilbert, C.D. (2006). Axons and synaptic boutons are highly dynamic in adult visual cortex. Neuron *49*, 877-887.

Svoboda, K. (2004). Do spines and dendrites distribute dye evenly? Trends in neurosciences *27*, 445-446.

Tang, Y., Nyengaard, J.R., Pakkenberg, B., and Gundersen, H.J. (1997). Age-induced white matter changes in the human brain: a stereological investigation. Neurobiol Aging *18*, 609-615.

Tatar, M., Kopelman, A., Epstein, D., Tu, M.P., Yin, C.M., and Garofalo, R.S. (2001). A mutant Drosophila insulin receptor homolog that extends life-span and impairs neuroendocrine function. Science *292*, 107-110.

Thibault, O., and Landfield, P.W. (1996). Increase in single L-type calcium channels in hippocampal neurons during aging. Science *272*, 1017-1020.

Toescu, E.C., and Verkhratsky, A. (2003). Neuronal ageing from an intraneuronal perspective: roles of endoplasmic reticulum and mitochondria. Cell Calcium *34*, 311-323.

Tokuoka, H., and Goda, Y. (2008). Activity-dependent coordination of presynaptic release probability and postsynaptic GluR2 abundance at single synapses. Proc Natl Acad Sci U S A *105*, 14656-14661.

Tombaugh, G.C., Rowe, W.B., Chow, A.R., Michael, T.H., and Rose, G.M. (2002). Theta-frequency synaptic potentiation in CA1 in vitro distinguishes cognitively impaired from unimpaired aged Fischer 344 rats. J Neurosci *22*, 9932-9940.

Tombaugh, G.C., Rowe, W.B., and Rose, G.M. (2005). The slow afterhyperpolarization in hippocampal CA1 neurons covaries with spatial learning ability in aged Fisher 344 rats. J Neurosci *25*, 2609-2616.

Tonkikh, A.A., and Carlen, P.L. (2009). Impaired presynaptic cytosolic and mitochondrial calcium dynamics in aged compared to young adult hippocampal CA1 synapses ameliorated by calcium chelation. Neuroscience *159*, 1300-1308.

Trachtenberg, J.T., Chen, B.E., Knott, G.W., Feng, G., Sanes, J.R., Welker, E., and Svoboda, K. (2002). Long-term in vivo imaging of experience-dependent synaptic plasticity in adult cortex. Nature *420*, 788-794.

Tsang, P.S., and Shaner, T.L. (1998). Age, attention, expertise, and time-sharing performance. Psychol Aging *13*, 323-347.

Tschida, K.A., and Mooney, R. (2012). Deafening drives cell-type-specific changes to dendritic spines in a sensorimotor nucleus important to learned vocalizations. Neuron *73*, 1028-1039.

Turner, A.M., and Greenough, W.T. (1985). Differential rearing effects on rat visual cortex synapses. I. Synaptic and neuronal density and synapses per neuron. Brain Res *329*, 195-203.

Uemura, E. (1980). Age-related changes in prefrontal cortex of Macaca mulatta: synaptic density. Exp Neurol *69*, 164-172.

Uemura, E. (1985). Age-related changes in the subiculum of Macaca mulatta: synaptic density. Exp Neurol *87*, 403-411.

Uylings, H.B., and de Brabander, J.M. (2002). Neuronal changes in normal human aging and Alzheimer's disease. Brain Cogn *49*, 268-276.

Vela, J., Gutierrez, A., Vitorica, J., and Ruano, D. (2003). Rat hippocampal GABAergic molecular markers are differentially affected by ageing. J Neurochem *85*, 368-377.

Veng, L.M., Mesches, M.H., and Browning, M.D. (2003). Age-related working memory impairment is correlated with increases in the L-type calcium channel protein alpha1D (Cav1.3) in area CA1 of the hippocampus and both are ameliorated by chronic nimodipine treatment. Brain research Molecular brain research *110*, 193-202.

Verhaeghen, P., and Cerella, J. (2002). Aging, executive control, and attention: a review of meta-analyses. Neuroscience and biobehavioral reviews *26*, 849-857.

Vogel, R.W., Ewers, M., Ross, C., Gould, T.J., and Woodruff-Pak, D.S. (2002). Age-related impairment in the 250-millisecond delay eyeblink classical conditioning procedure in C57BL/6 mice. Learning & memory *9*, 321-336.

von Heimendahl, M., Itskov, P.M., Arabzadeh, E., and Diamond, M.E. (2007). Neuronal activity in rat barrel cortex underlying texture discrimination. PLoS biology *5*, e305.

Wager, T.D., and Smith, E.E. (2003). Neuroimaging studies of working memory: a meta-analysis. Cogn Affect Behav Neurosci *3*, 255-274.

Wallace, M., Frankfurt, M., Arellanos, A., Inagaki, T., and Luine, V. (2007). Impaired recognition memory and decreased prefrontal cortex spine density in aged female rats. Ann N Y Acad Sci *1097*, 54-57.

Wang, D.S., Bennett, D.A., Mufson, E.J., Mattila, P., Cochran, E., and Dickson, D.W. (2004). Contribution of changes in ubiquitin and myelin basic protein to age-related cognitive decline. Neurosci Res *48*, 93-100.

Wang, M., Gamo, N.J., Yang, Y., Jin, L.E., Wang, X.J., Laubach, M., Mazer, J.A., Lee, D., and Arnsten, A.F. (2011). Neuronal basis of age-related working memory decline. Nature *476*, 210-213.

Wang, S., and Albers, K.M. (2009). Behavioral and cellular level changes in the aging somatosensory system. Annals of the New York Academy of Sciences *1170*, 745-749.

Wang, X., and Michaelis, E.K. (2010). Selective neuronal vulnerability to oxidative stress in the brain. Front Aging Neurosci *2*, 12.

Weiss, C., and Thompson, R.F. (1991). The effects of age on eyeblink conditioning in the freely moving Fischer-344 rat. Neurobiol Aging *12*, 249-254.

West, M.J. (1993). New stereological methods for counting neurons. Neurobiol Aging *14*, 275-285.

West, M.J., Coleman, P.D., Flood, D.G., and Troncoso, J.C. (1994). Differences in the pattern of hippocampal neuronal loss in normal ageing and Alzheimer's disease. Lancet *344*, 769-772.

Williams, G.C. (1957). Pleiotropy, natural selection, and the evolution of senescence. Evolution *11*, 398-411.

Wolfe, J.W., and Butterworth, J.F. (2011). Local anesthetic systemic toxicity: update on mechanisms and treatment. Curr Opin Anaesthesiol *24*, 561-566.

Wu, H.P., Ioffe, J.C., Iverson, M.M., Boon, J.M., and Dyck, R.H. (2013). Novel, whisker-dependent texture discrimination task for mice. Behav Brain Res *237*, 238-242.

Xu, H.T., Pan, F., Yang, G., and Gan, W.B. (2007). Choice of cranial window type for in vivo imaging affects dendritic spine turnover in the cortex. Nature neuroscience *10*, 549-551.

Xu, T., Yu, X., Perlik, A.J., Tobin, W.F., Zweig, J.A., Tennant, K., Jones, T., and Zuo, Y. (2009). Rapid formation and selective stabilization of synapses for enduring motor memories. Nature *462*, 915-919.

Yamagata, Y., Kobayashi, S., Umeda, T., Inoue, A., Sakagami, H., Fukaya, M., Watanabe, M., Hatanaka, N., Totsuka, M., Yagi, T.*, et al.* (2009). Kinase-dead knock-in mouse reveals an essential role of kinase activity of Ca2+/calmodulin-dependent protein kinase IIalpha in dendritic spine enlargement, long-term potentiation, and learning. J Neurosci *29*, 7607-7618.

Yamahachi, H., Marik, S.A., McManus, J.N., Denk, W., and Gilbert, C.D. (2009). Rapid axonal sprouting and pruning accompany functional reorganization in primary visual cortex. Neuron *64*, 719-729.

Yang, G., Pan, F., and Gan, W.B. (2009). Stably maintained dendritic spines are associated with lifelong memories. Nature *462*, 920-924.

Yang, G., Pan, F., Parkhurst, C.N., Grutzendler, J., and Gan, W.B. (2010). Thinned-skull cranial window technique for long-term imaging of the cortex in live mice. Nat Protoc *5*, 201-208.

Yang, Z., Krause, M., Rao, G., McNaughton, B.L., and Barnes, C.A. (2008). Synaptic commitment: developmentally regulated reciprocal changes in hippocampal granule cell NMDA and AMPA receptors over the lifespan. Journal of neurophysiology *99*, 2760-2768.

Yankner, B.A., Lu, T., and Loerch, P. (2008). The aging brain. Annu Rev Pathol *3*, 41-66.

Yeoman, M., Scutt, G., and Faragher, R. (2012). Insights into CNS ageing from animal models of senescence. Nat Rev Neurosci *13*, 435-445.

Yuste, R., and Bonhoeffer, T. (2001). Morphological changes in dendritic spines associated with long-term synaptic plasticity. Annu Rev Neurosci *24*, 1071-1089.

Zito, K., Scheuss, V., Knott, G., Hill, T., and Svoboda, K. (2009). Rapid functional maturation of nascent dendritic spines. Neuron *61*, 247-258.

Zuo, Y., Yang, G., Kwon, E., and Gan, W.B. (2005). Long-term sensory deprivation prevents dendritic spine loss in primary somatosensory cortex. Nature *436*, 261-265.

Acknowledgments

The submission of this thesis marks the completion of an important stage of my life. It has been a challenging and fun ride, with ups and downs, which will leave an invaluable trace on my formation but also on my experience and personal memories. I see this as an opportunity to look back and think of the people which have directly or indirectly shared this path with me.

I'd like to thank my PhD supervisor Vincenzo De Paola for wanting me in his lab and for giving me the opportunity to see neurons in their natural environment. With both of us on the learning curve, as a student and as a supervisor respectively, I believe the outcome was very positive.

I'd like to thank Mark Ungless as a mentor for showing constant interest in my work, for being supportive and showing me the good side of things when my view was negative.

Also thanks to our collaborators Sen Song and Graham Knott for their contribution and unique expertise.

Thanks to Valentina F. for introducing me to animal behaviour experiments and for her advice. Thanks to Hamlata for all her help at the start of my PhD. Thanks to Dawn and Graham that offered to read and correct this thesis.

Thanks to the people in the Neuroplasticity lab for making it fun and so much easier: Hamlata, Valentina F., Lieven, Graham, Dawn, Peter, Lucien. Thanks for all the lunch/coffee breaks talking about science, the gossip, the non-sense, the swearing, the facts of the day and all the rest. Thanks for the great time spent together at the Friday drinks, the Christmas parties, the pub quizzes and so on… Most of all, thanks for having a lough every day.

Thanks to Richard and Christine for being such welcoming and supportive friends, for making us feel at home even though it was far.

It is hard to describe how lucky I am to share my life with Vale. Thank you for being at my side, for your immense support, for putting up with me and making me a better person.

Without my family none of what I have achieved would have been possible. Thanks to my little sister for all her affection and for showing great strength. Thanks to my parents for the opportunities they have gifted me with. Thanks to my dad for teaching me to be curious, critical and doubtful. For being the best role model possible, for your hard work for your family and friends. For supporting my choices even though you missed me. Sei forte babbo!

Thanks to my mum, to whom I'd like to dedicate this work. Ten years have gone since you left us but your memory is still alive as is your smile in my mind. You give me strength and motivation every day.